**BiGART 2025** - Biology-Guided Adaptive Radiotherapy

**25th Acta Oncologia symposium**

acta oncologica

**Aarhus, Denmark June 17-18 2025**

# BiGART 2025

## Programme & abstract book

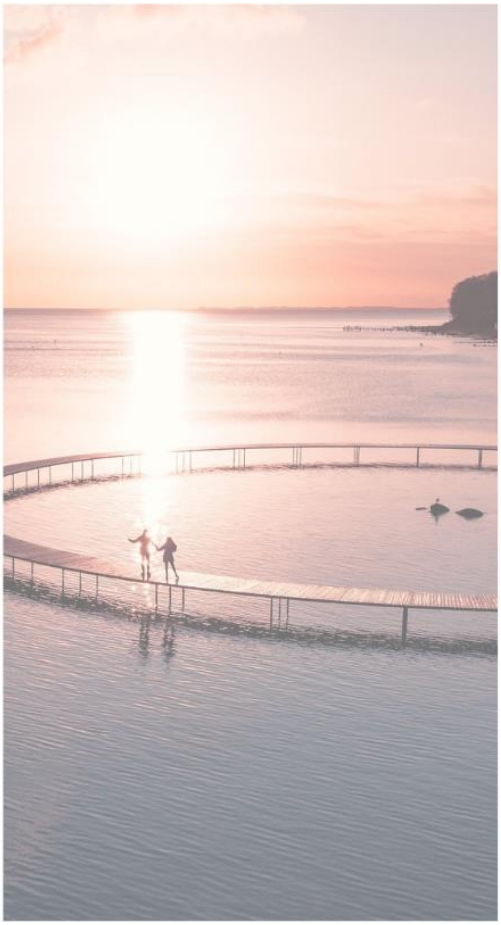

Danish Cancer Society

# WELCOME TO AARHUS FOR BiGART 2025

Welcome to the 25th Acta Oncologica Symposium: The BiGART 2025 conference on Biology-Guided Adaptive Radiotherapy.

We are pleased to welcome the radiotherapy community for a diverse and dynamic conference programme, and we are looking forward to meaningful discussions across a wide range of topics.

A new initiative this year is the 'pitch your study'-session that aims to showcase upcoming projects and connect with potential collaborators on advancing research projects.

In addition to our Nordic and international esteemed invited speakers, we are proud to present a range of oral- and poster presentations from abstracts. The abstract review committee were impressed with the high quality of the submitted abstracts.

With special appreciation, we thank the Acta Oncologica BiGART special issue editors, Jens Overgaard and Morten Høyer. The special issue will be another significant collection of papers.

**Thematic sessions**

Biology-guided and adaptive radiotherapy anno 2025 ▪ Prediction of toxicity and morbidity ▪ Artificial intelligence in radiotherapy ▪ Reirradiation – possibilities and pitfalls ▪ Pitch your study (upcoming prospective studies) ▪ Poster discussion ▪ Late effects in particle therapy of CNS tumors ▪ Emerging therapies ▪ Biology and clinical applications ▪ Harnessing grand-scale data sets

**Invited speakers**

Matthias Guckenberger ▪ Per Karlsson ▪ Trine Tramm ▪ Barbara Jereczek-Fossa ▪ Marianne Guren ▪ Ye Zhang ▪ Søren M. Bentzen ▪ Ane Appelt ▪ Jean-Michel Hannoun-Levi ▪ Anna Embring ▪ Armin Lühr ▪ Arturs Meijers ▪ Anne Vestergaard ▪ Hiske van der Weide ▪ Brita Singers Sørensen ▪ Betina Børresen ▪ Pierre Blanchard ▪ Randi Syljuåsen

We would like to extend our thanks to speakers, poster presenters, local helpers, and all Danish, Nordic and international colleagues and friends contributing to the conference. A special thank you for the support to Acta Oncologica and the Danish Cancer Society.

**The organising committee,**

Jesper Grau Eriksen, Birgitte Offersen & Karen-Lise Garm Spindler

# PROGRAMME

## Tuesday June 17

**08:00 Registration and breakfast**

**08:30 Welcome**

- Karen-Lise Spindler, Birgitte Offersen, Jesper Grau Eriksen

**Opening keynote lecture**

- 08:35 **Matthias Guckenberger**, *Zürich, Switzerland, ESTRO president*: Clinical radiotherapy trials in the future

**08:55 Session 1: Biology-guided and adaptive radiotherapy anno 2025**
Chair: **Birgitte Offersen**, *Aarhus, Denmark*

Invited speakers

- 08:55 **Per Karlsson**, *Gothenburg, Sweden*: Gene expression profiles and breast cancer radiation therapy
- 09:15 **Trine Tramm**, *Aarhus, Denmark*: Tumor infiltrating lymphocytes and breast cancer radiation therapy

Oral presentations

- 09:35 **Jens Overgaard**, *Aarhus, Denmark*: Subsite variation of HPV-related p16-expression in oropharynx cancer: Evaluation of frequency and prognostic impact in 8557 DAHANCA patients
- 09:45 **Karina Lindberg Gotlieb**, *Odense, Denmark*: Clinical Study of VMAT vs. 3DCRT for Breast Cancer with Lymph Node Involvement: Better Coverage, Faster Treatment, and No Increased Contra-Lateral Organ Dose
- 09:55 **Anne Bisgaard**, *Odense, Denmark*: Tracking changes in diffusion MRI for short course radiotherapy in rectal cancer: a multi-center study
- 10:05 **Camilla Skinnerup Byskov**, *Aarhus, Denmark*: Adaptive Radiotherapy and Quality Assurance in the European randomised phase III PROTECT trial for oesophageal cancer patients

**10:15 Coffee break**

**10:45 Session 2: Prediction of toxicity and morbidity**
Chair: **Marianne Guren**, *Oslo, Norway*

Invited speakers

- 10:45 **Barbara Alicja Jereczek-Fossa**, *Milan, Italy*, ESTRO president-elect: Predicting and Preventing Toxicity in Pelvic Radiotherapy: AI, Microbiome, Radiomics, and More
- 11:05 **Marianne Guren**, *Oslo, Norway*: Personalizing radiotherapy to prevent pelvic toxicity
- 11:25 **Karen-Lise Spindler**, *Aarhus, Denmark*: Considering new organs at risk in pelvic radiotherapy

Oral presentations

- 11:40 **Johanne Steffensen**, *Aarhus Denmark*: Impact of radiotherapy on vaginal and sexual health in women with anal cancer: A prospective Danish cohort analysis
- 11:50 **Line Schack**, *Aarhus, Denmark*: Associations between SNPs and Radiation Induced Fibrosis in Breast Cancer Patients: Results from a Genome-Wide Association Study

**12:10 Lunch**

**13:10 Session 3: Artificial intelligence in radiotherapy**
Chair: **Christian Rønn Hansen**, *Odense, Denmark*

Invited speakers

- 13:10 **Ye Zhang**, *Villigen, Switzerland*: Automation in Radiotherapy – where are we going?

Oral presentations

- 13:30 **Lise Thorsen**, *Aarhus Denmark*: In-depth analysis of failure rates and -modes in auto-segmentation of the esophagus in patients treated for lung cancer
- 13:40 **David G. Kovacs**, *Copenhagen, Denmark*: External Validation of an Automated Deep Learning-Based Delta 18F-FDG PET/CT Biomarker for Loco-Regional Control Probability Stratification
- 13:50 **Christian Rønn Hansen**, *Odense, Denmark*: Exploring the performance of dose prediction with deep learning for head and neck cancer on a multi-centre clinical dataset
- 14:00 **Mathis Rasmussen**, *Aarhus Denmark*: First-in-world demonstration of benefit of AI assisted head and neck cancer target contouring in a prospective blinded randomized clinical trial

**14:15 Coffee break**

**14:45 Session 4: Reirradiation – possibilities and pitfalls**
Chair: **Lone Hoffman**, *Aarhus, Denmark*

Invited speakers

- 14:45 **Søren M. Bentzen**, *Maryland, US*: Radiobiology of reirradiation
- 15:05 **Ane Appelt**, *Copenhagen, Denmark*: Dealing with dose accumulation
- 15:25 **Jean-Michel Hannoun-Levi**, *Nice, France*: Reirradiation, current status and future perspectives
- 15:45 **Anna Embring**, *Stockholm, Sweden*: Reirradiation in Paediatric CNS Tumours: Outcome After Implementing National Guidelines

Oral presentations

- 16:00 **Morten Nielsen**, *Odense, Denmark*: A comprehensive national audit of radiotherapy retreatment numbers, sites and indications
- 16:10 **Christina Glismand Truelsen**, *Aarhus, Denmark*: Acute Toxicity and Quality of Life in the ReRad II Trial on Dose-Escalated Proton Reirradiation for Locally Recurrent Rectal Cancer

**16:20 Session 5: Pitch your study (upcoming prospective studies)**
Chair: **Karen-Lise Garm Spindler**, *Aarhus, Denmark*

- 16:20 **Jean-Michel Hannoun-Levi**, *Nice, France*: The VENUS trial
- 16:27 **Einar Dale**, *Oslo, Norway*: RAdiotherapy with FDG-PET guided Dose-PAINTing compared with standard radiotherapy for primary head and neck cancer-3 (RADPAINT-3) – Randomized, multi-center phase II trial
- 16:34 **Ruta Zukauskaite**, *Odense, Denmark*: DAHANCA 41: A national randomised trial using 0 vs 5 millimetres high-dose CTV margin for primary radiotherapy of Head and Neck Squamous Cell Carcinomas
- 16:41 **Uffe Bernchou**, *Odense, Denmark*: ERADICATE: A randomised trial to test Early magnetic resonance imaging-guided RADIotherapy ablation of loCAlly advanced pancreaTic cancer
- 16:48 **Sara Linde**, *Aarhus, Denmark*: Pre-trial quality assurance and design of the NIELS trial: A phase III study of dose-escalated radiotherapy in patients with small cell lung cancer

**17:00 Poster discussion and refreshments**

**18:00 End of meeting, day 1**

**19:00 Museum visit, Conference dinner and networking – ARoS art museum**

## Wednesday June 18

**08:00 Session 6: Late effects in particle therapy of CNS tumors**
Chair: **Morten Høyer**, *Aarhus, Denmark*

Invited speakers

- 08:00 **Armin Lühr**, *Dortmund, Germany*: Beyond dose in proton therapy
- 08:20 **Arturs Meijers**, *Villigen, Switzerland*: Dose rate as predictor for brain damage
- 08:40 **Hiske van der Weide**, *Groningen, the Netherlands*: Changes in the brain after proton therapy
- 09:00 **Anne Vestergaard**, *Aarhus, Denmark*: Brain image change analysis in a Danish proton treated cohort

Oral presentations

- 09:15 **Laura Toussaint**, *Aarhus, Denmark*: Impact of radiation dose on neurocognitive function and quality of life in longterm childhood brain tumor survivors
- 09:25 **Robin Hegering**, *Dortmund, Germany*: Spatial distribution of astrocytes as a late response to partial-brain proton irradiation in mice at different doses

**9:40 Coffee break**

**10:10 Session 7: Emerging therapies**
Chair: **Cai Grau**, *Aarhus, Denmark*

Invited speakers

- 10:10 **Brita Singers Sørensen**, *Aarhus Denmark*: FLASH – Which factors matter?
- 10:30 **Betina Børresen**, *Copenhagen/Lund, Denmark/Sweden*: The canine cancer patient in FLASH research

Oral presentations

- 10:50 **Niels Bassler**, *Aarhus, Denmark*: Proton Minibeam Radiotherapy - Preclinical Research at DCPT
- 11:05 **Eirik Malinen**, *Oslo, Norway*: Integrating 2D dosimetry and cell survival analysis to improve local effect predictions in spatially fractionated radiotherapy
- 11:20 **Jinyan Duan**, *Bristol, UK*: A Geant4 simulation of DNA Damage in BNCT with ongoing lithium ion studies
- 11:35 **Tanja Mälkiä**, *Helsinki, Finland*: A retrospective study of oral mucosa dose relation to grade 3 oral mucositis in locally recurrent inoperable head and neck carcinoma patients treated with reactor-based BNCT

**12:00 Lunch**

**13:00 Session 8: Biology and clinical applications**
Chair: **Brita Singers Sørensen**, *Aarhus, Denmark*

Invited speakers

- 13:00 **Randi Syljuåsen**, *Oslo, Norway*: Radiation-Induced DNA Damage and Immune Signaling: Mechanisms and Therapeutic Opportunities
- 13:20 **Pierre Blanchard**, *Paris, France*: ctDNA guided management of head & neck carcinoma

Oral presentations

- 13:40 **Anne Vittrup Jakobsen**, *Aarhus, Denmark*: The prognostic value of cell-free DNA kinetics during chemoradiotherapy in squamous cell carcinomas of the anus
- 13:50 **Cathrine Bang Overgaard**, *Aarhus, Denmark*: Highlighting proton RBE Complexities: RBE changes with biological endpoint, dose fractionation, and SOBP position in a murine leg model
- 14:00 **Inga Solgård Juvkam**, *Oslo Norway*: Cellular responses in murine salivary glands to fractionated irradiation: Implications for fibrosis and hyposalivation
- 14:10 **Ingerid Skjei Knudtsen***, Trondheim, Norway*: [68Ga]Ga-PSMA-11 vs [18F]F-PSMA-1007 PET/MRI of recurrent prostate cancer: detection rates at different PSA-levels and implications for salvage radiotherapy

**14:25 Session 9: Harnessing grand-scale data sets**
Chair: **Stine Korreman**, *Aarhus, Denmark*

Oral presentations

- 14:25 **Azadeh Abravan***, Manchester, UK*: Seasons, socioeconomics, comorbidities, and stages: Unraveling the factors correlating with diagnostic intervals in cancer care
- 14:35 **Sarah Stougaard**, *Odense, Denmark*: Impact of GTV-CTV Margin and Other Predictors on Radiation-Induced Dysphagia in Head and Neck Cancer Patients
- 14:45 **Kristine Wiborg Høgsbjerg**, *Aarhus, Denmark*: Beyond the First Cut - A Comparison of Breast Induration in Breast Cancer Patients with and without Repeat Surgery Based on DBCG Data
- 14:55 **Anders W. Mølby Nielsen**, *Aarhus, Denmark*: Local recurrence with and without a tumour-bed boost: a post-hoc analysis of the DBCG IMN2 study
- 15:05 **Mette Skovhus Thomsen**, *Aarhus, Denmark*: Quality assessment of 2705 treatment plans in the randomised Danish Breast Cancer Group Skagen trial 1

**15:30 Closing session – prizes and farewell**

- Karen-Lise Spindler, Birgitte Offersen, Jesper Grau Eriksen

# ABSTRACTS

## Poster discussion groups

### 1-8: Dosimetry and reirradiation

*Chair: Jean-Michel Hannoun-Levi*

Dosimetry

1. **Jenna Tarvonen**, *Helsinki, Finland*: Paraffin wax as a bolus material in accelerator-based boron neutron capture therapy
2. **Anna Mann Nielsen**, *Herlev, Denmark*: Dosimetric impact of esophageal inter-fraction motion in esophagus-sparing radiotherapy for metastatic spinal cord compression

Reirradiation

3. **Siri Grøndahl**, *Aarhus, Denmark*: Decision Support Model for referral of patients with glioma to proton therapy
4. **Maria Fuglsang Jensen**, *Aarhus, Denmark*: Proton versus photon treatment planning in the Scandinavian CURE Lung trial for reirradiation of thoracic tumours
5. **Lone Hoffmann**, *Aarhus, Denmark*: Intercentre reirradiation treatment planning consistency: Pre-trial QA in the CURE Lung trials for recurrent or new thoracic cancers
6. **Laura Kaplan**, *Næstved, Denmark*: Dose accumulation for reirradiation: a national study of inter-center variation across eight treatment sites
7. **Stine Overvad Fredslund**, *Aarhus, Denmark*: CURE Lung: CUratively intended thoracic REirradiation. An observational study of curative intended reirradiation of thoracic tumours including lung-cancer recurrences, solitary lung metastases, or new primary lung cancer in the thorax
8. **Laura P. Kaplan**, *Næstved, Denmark*: Clinical workflow for reirradiation: National consensus recommendations on imaging, treatment planning, dose accumulation, and treatment delivery

### 9-17: Artificial intelligence in radiotherapy

*Chair: Stine Korreman*

9. **Johan Martin Søbstad**, *Bergen, Norway*: Time efficiency, geometric accuracy, and clinical impact of AI-assisted contouring in head and neck cancer radiotherapy
10. **Henrik Dahl Nissen**, *Vejle, Denmark*: The Influence of AI-Assisted Delineation on Final Delineations of Targets and Organs at Risk Over Time
11. **Anders Traberg Hansen**, *Aarhus, Denmark*: Application of a Neural Network for Predicting Stereotactic Radiotherapy Field Orientations
12. **Jesper Kallehauge**, *Aarhus, Denmark*: Uncertainty-Aware Deep Learning-Based Auto-Segmentation of Glioblastoma Using Conformal Prediction
13. **Morten Sahlertz**, *Aarhus, Denmark*: Towards objective cosmetic outcome self-evaluation: machine-learning on photographic data from breast-conserving treatment
14. **Kristoffer Moos**, *Aarhus, Denmark*: Rethinking the Elective Target Volume in Patients with Oropharyngeal Cancer

15. **Maja Vestmø Maraldo**, *Copenhagen, Denmark*: Attitudes towards AI-generated risk prediction in patients with early breast cancer: an international multi-center survey
16. **Lise Thorsen**, *Aarhus, Denmark*: Monitoring the performance of AI segmentation of organ at risk in clinical practice at the Department of Oncology at Aarhus University Hospital
17. **Emilie Helgesen Karlsson**, *Odense, Denmark*: Diffusion MRI for Enhanced Tumour Delineation and Outcome Prediction in Pancreatic Cancer Using Artificial Intelligence

**18-26: Biology and clinical applications**
*Chair: Pierre Blanchard*

18. **Hild Milde Bekkevoll**, *Trondheim, Norway*: Mechanisms of Radiation-Induced Bone Damage: In Vitro Studies
19. **Stine Vestergaard Eriksen**, *Vejle, Denmark*: Natural killer cell activity in patients treated with curatively intended radiotherapy for prostate cancer: An observational study
20. **Jens Edmund**, *Herlev, Denmark*: Spatial correlation of FAZA PET and FDG PET for head and neck cancer: a search for a more accessible way to image hypoxia
21. **Folefac C. Asonganyi**, *Aarhus, Denmark*: Preclinical study of reirradiation with hyperthermia in recurrent murine tumors
22. **Emil Leth Villumsen**, *Aarhus, Denmark*: The CAM Model: A Novel Preclinical Platform for Proton Radiotherapy and Nuclear Imaging in Oncology
23. **Jacob Kinggaard Lilja-Fischer**, *Aarhus, Denmark*: Mutational profile of oropharyngeal cancer in relation to HPV, tobacco smoking and prognosis with validation in the DAHANCA 19 randomized trial
24. **Morten Busk**, *Aarhus, Denmark*: Dual-tracer autoradigraphy in orthotopic tumor models: Towards personalized PET-guided therapy
25. **Manish Kakar**, *Oslo, Norway*: Vision transformers may enable early detection of radiation-induced toxicity in submandibular glands from a murine model
26. **Bao Ngoc Huynh**, *Oslo, Norway*: Detecting Early Toxicity in a Murine Head and Neck Model Using Explainable CNNs

**27-35: Clinical 1**
*Chair: Jens Overgaard*

27. **Josef Khalid**, *Aarhus, Denmark*: Squamous cell carcinoma in the oral cavity – need for risk stratification of the neck?
28. **Maiken M. Hjelt**, *Aarhus, Denmark*: Trends in feeding tube insertion and weight loss over time in patients with Head and Neck Cancer undergoing curative (chemo)radiotherapy
29. **Sara Volf Jensen**, *Aarhus, Denmark*: Oral Hygiene Habits and Fluoride Levels after Head and Neck Radiotherapy: An Exploratory Clinical Study
30. **Eva Onjukka**, *Stockholm, Sweden*: The effect of evolving clinical practice in head and neck radiotherapy
31. **Anna Embring**, *Stockholm, Sweden*: Radiotherapy in children treated for neuroblastoma: comparative photon/proton treatment plans and side effects
32. **Eva Onjukka**, *Stockholm, Sweden*: How to account for temporal patterns of dysphagia scores in a real-world dataset

33. **Daniella Elisabet Østergaard**, *Copenhagen, Denmark*: Real-world experience of pediatric radiotherapy over two decades (to guide future treatments)
34. **Lars Ulrik Fokdal**, *Vejle, Denmark*: Survival prediction in cancer patients receiving whole brain radiotherapy for brain metastases
35. **Camilla Kronborg**, *Aarhus, Denmark*: Sexual Function-Related Organs at Risk in Rectal Cancer: Opportunities for Sparing in Radiotherapy Planning

**36-44: Clinical 2**

*Chair: Cai Grau*

36. **Mai Lykkegaard Ehmsen**, *Aarhus, Denmark*: Dosimetry audits as part of the radiotherapy quality assurance (RTQA) program in the PROTECT-trial
37. **Malthe Fiil**, *Aarhus, Denmark*: The value of magnetic resonance imaging in the response evaluation of primary radiotherapy for squamous cell carcinomas of the oral cavity, pharynx and larynx
38. **Hanna Rahbek Mortensen**, *Aarhus, Denmark*: Real world survival and morbidity after concurrent chemotherapy and radiotherapy in patients with gastroesophageal cancer
39. **Kristine Wiborg Høgsbjerg**, *Aarhus, Denmark*: Patient Perspectives on Participation in the DBCG Proton Trial: A Qualitative Research Study
40. **Sara Linde**, *Aarhus, Denmark*: Role of prophylactic cranial irradiation in patients with limited disease small cell lung cancer: a Danish single institution cohort
41. **Maja Bendtsen Sharma**, *Aarhus, Denmark*: Patient reported respiratory symptoms 10 years after loco-regional breast cancer radiotherapy: Look for other causes than radiotherapy
42. **Anne Wilhøft Kristensen**, *Aarhus, Denmark*: Factors Influencing Participation in a Proton Therapy Clinical Trial Among Patients with Pharyngeal and Laryngeal Cancer: A Cross-Sectional Study
43. **Oscar N. Brændstrup**, *Aarhus, Denmark*: Cosmetic outcome after kilovoltage therapy of facial basal cell carcinoma: A Danish national prospective study of 932 patients
44. **Katrine Smedegaard Storm**, *Herlev, Denmark*: Bowel delineation methods and predictors of acute and late diarrhea in radiotherapy for anal cancer

**45-52: Adaptive radiotherapy 1**

*Chair: Ane Appelt*

45. **Trine Omand Kirkegaard Sørensen**, *Aalborg, Denmark*: Reducing preposition variations and monitor intrafraction movement with surface-guided radiation therapy for breast cancer patients
46. **Simon Nyberg Thomsen**, *Aarhus, Denmark*: The necessity of managing intra-fractional motion in stereotactic radiotherapy for central lung lesions
47. **Kristine Wiborg Høgsbjerg**, *Aarhus, Denmark*: Increasing Stability of Chest Wall Position During Deep-Inspiration Breath-Hold Under Breast Cancer Radiotherapy
48. **Marjolein Heidotting**, *Aarhus, Denmark*: Post-treatment analysis of delivered dose in interstitial pulsed dose rate brachytherapy boosts of gynaecological cancers
49. **Per Poulsen**, *Aarhus, Denmark*: Position errors and drift motion of mediastinal lymph nodes during DIBH lung cancer radiotherapy

50. **Jolanta Hansen**, *Aarhus, Denmark*: Preliminary studies of VMAT vs. RAD dose planning for high-risk breast cancer
51. **Karolina Klucznik**, *Aarhus, Denmark*: First clinical motion-including prostate and bladder dose reconstruction in real-time during prostate SBRT delivery
52. **Fardous Reaz**, *Aarhus, Denmark*: An Assessment of the SIRMIO Beamline's Feasibility for pMBRT Experiments with Heterogeneous and Homogeneous Target Doses

**53-59: Adaptive radiotherapy 2**
*Chair: Eirik Malinen*

53. **Katia Parodi**, *Munich, Germany*: First in-vivo application of the SIRMIO platform for precision, image-guided small animal IMPT proton irradiation
54. **Ruta Zukauskaite**, *Odense, Denmark*: Burden of dysphagia after changes in high-dose CTV margins for head and neck cancer patients
55. **Christian Rønn Hansen**, *Odense, Denmark*: Impact of GTV-to-CTV margin reduction on late toxicity in bilateral oropharyngeal radiotherapy: A treatment planning study
56. **Faisal Mahmood**, *Odense, Denmark*: Impact of Low-Dose Contrast-Enhanced MRI for Glioblastoma Delineation in Adaptive Radiotherapy
57. **Eirik Malinen**, *Oslo, Norway*: Partial tumor boosting in definitive radiotherapy of soft tissue sarcoma
58. **Lisette Juul Sandt**, *Herlev, Denmark*: Simulation-free online adaptive radiotherapy for patients with metastatic spinal cord compression – a feasibility study
59. **Martin Nielsen**, *Aalborg, Denmark*: Correction of IGRT and Intra-fraction movement using ExacTrac Dynamic for Head and Neck Cancer Patients

**60-65: Particle Therapy 1**
*Chair: Morten Høyer*

60. **Sarah Eckholdt Jensen**, *Aarhus, Denmark*: Dosimetric Impact of Respiratory and Anatomical Changes in Proton vs. Photon Therapy: Insights from the European PROTECT Trial on Locally Advanced Esophageal Cancer
61. **Stine Elleberg Petersen**, *Aarhus, Denmark*: Shortening proton therapy treatment time of high-risk prostate cancer patients using laxatives and CBCT guidance
62. **Liliana Stolarczyk**, *Aarhus, Denmark*: Measurement-less patient-specific QA in proton therapy: DCPT experience
63. **Lasse Bassermann**, *Aarhus, Denmark*: Quantification of proton stopping-power ratios for photon-counting computed tomography
64. **Maria Christiane Warncke Heisel**, *Aarhus, Denmark*: The impact of anatomical variations and RBE uncertainties on proton therapy dose delivery within a randomized clinical trial for high-risk prostate cancer
65. **Fardous Reaz**, *Aarhus, Denmark*: Micro-dosimetric measurement of secondary particles generated in bolus and collimator for passive scattering systems in carbon ion therapy

**66-71: Particle Therapy 2**
*Chair: Armin Lühr*

66. **Kyriakos Fotiou**, *Aarhus, Denmark*: Quantifying specific proton range uncertainty for pediatric cancer patients
67. **Ivanka Sojat Tarp**, *Aarhus, Denmark*: Evaluating stopping-power ratio accuracy for proton therapy planning of brain cancer patients applying two dual-energy CT approaches, including metal implant considerations
68. **Anne Vestergaard**, *Aarhus, Denmark*: Proton treatment planning guidelines to reduce radiation-induced image changes in gliomas
69. **Heidi S. Rønde**, *Aarhus, Denmark*: Clinical implementation of Intensity Modulated Proton Therapy (IMPT) for testicular seminoma – result for treatment of the first 30 patients
70. **Ludvig Muren**, *Aarhus, Denmark*: Linear energy transfer inclusive normal tissue complication probability modelling for late rectal and urinary morbidity following proton therapy
71. **Anne Haahr Andresen**, *Aarhus, Denmark*: 3D Swin Transformer for Patient-Specific Proton Dose Prediction of Brain Cancer Patients

**72-79: FLASH & imaging**
*Chair: Brita Singers Sørensen*

<u>FLASH</u>

72. **Priyanshu M. Sinha**, *Aarhus, Denmark*: Determining the effects of hyperthermia on the tumor and acute normal tissue response of electron FLASH radiotherapy
73. **Line Kristensen**, *Aarhus, Denmark*: Fractionation reduces FLASH-sparing in an acute skin murine model
74. **Line Kristensen**, *Aarhus, Denmark*: Mild hypoxia reduces FLASH skin-sparing in a murine model
75. **Anna Holtz Hansen**, *Aarhus, Denmark*: How is the FLASH effect influenced by oxygen deprivation in a murine model?

<u>Imaging</u>

76. **Cecilie Valet Henneberg**, *Herlev, Denmark*: A Quantitative Approach to Image Quality Assessment for Delineation in Radiotherapy
77. **Mathias Dreyer Teller**, *Herlev, Denmark*: A prospective observational study on the clinical utility of photon-counting and dual-energy CT for prostate cancer delineation
78. **Hella Maria Brøgger Sand**, *Aalborg, Denmark*: Accurate Dose Calculation in Combined Single- and Dual-Energy CT Workflows in Radiotherapy
79. **Johanna Austrheim Hundvin**, *Bergen, Norway*: Influence of b-value combination in quantitative diffusion weighted MRI of rectal cancer

**POSTER GROUPS**

- 1-2: Dosimetry
- 3-8: Reirradiation
- 9-17: Artificial intelligence in radiotherapy
- 18-26: Biology and clinical applications
- 27-35: Clinical 1
- 35-44: Clinical 2
- 45-52: Adaptive radiotherapy 1
- 53-59: Adaptive radiotherapy 2
- 60-65: Particle Therapy 1
- 66-71: Particle Therapy 2
- 72-75: FLASH
- 76-79: Imaging

# Abstracts session 1: Biology-guided and adaptive radiotherapy anno 2025

**Subsite variation of HPV-related p16-expression in oropharynx cancer:**

**Evaluation of frequency and prognostic impact in 8557 DAHANCA patients**

*Authors:*

Lassen P MD[1,3], Alsner J MSc[1], Plaschke CC MD[2], Maare C MD[3], Primdahl H MD[4], Johansen J MD[5], Andersen M MD[6], Farhadi M MD[7] and Overgaard J MD[1]

On behalf of The Danish Head and Neck Cancer Group – DAHANCA

*Affiliations:*

[1]Department of Experimental Clinical Oncology, Aarhus University Hospital, Palle Juul Jensens Blvd [35,] 8200 Aarhus N, Denmark

[2]Department of Oncology, Copenhagen University Hospital, Rigshospitalet, Blegdamsvej 9, 2100 Copenhagen, Denmark

[3]Department of Oncology, Herlev Hospital, Copenhagen University, Borgmester Ib Juuls Vej 1, 2730 Herlev, Denmark

[4]Department of Oncology, Aarhus University Hospital, Palle Juul Jensens Blvd 35, 8200 Aarhus N, Denmark

[5]Department of Oncology, Odense University Hospital, J. B. Winsløws Vej 4, 5000 Odense, Denmark

[6]Department of Oncology, Aalborg University Hospital, Hobrovej 18-22, 9000 Aalborg, Denmark

[7]Department of Oncology, Næstved Hospital, Ringstedgade 61, 4700 Næstved, Zealand, Denmark

*Corresponding author:*

Pernille Lassen MD
Department of Experimental Clinical Oncology,
Aarhus University Hospital, Palle Juul Jensens Blvd 35, 8200 Aarhus N, Denmark
email: pernille@oncology.au.dk

**Introduction:**

Separate staging criteria based on p16-expression is implemented in the TNM8 classification of oropharyngeal carcinoma (OPSCC). However, recent data indicates significant oropharyngeal subsite differences in both the frequency of HPV-relation and the survival probability. Based on this complete, nationwide cohort study with prospectively collected data on consecutive patients collected over 35 years, we provide a detailed description of the subsite variation in OPSCC including an evaluation of the impact p16-expression on outcome.

**Material/ methods:**

For the present study, patients living in Denmark and referred for treatment of biopsy proven stage I-IV OPSCC diagnosed between 1986-2020 were identified in the DAHANCA database. HPV-association was determined by p16-status. Oropharyngeal subsite classification is registered in the DAHANCA database by the surgeon performing the diagnostic biopsy according to the TNM subsite classification. Tumors were subsequently grouped into “tonsil/base of tongue (BOT)”, “neighboring subsites” (tonsillar fossa & arch of the palate, glossotonsilar sulci and vallecula) and “distant subsites” (inferior surface of the soft palate, posterior wall and uvula).

**Results:**

A total of 8557 patients were identified with 5794 (68%) of tumors originating in “tonsil/BOT”, 1920 (22%) in “neighboring subsites” and 802 (10%) in “distant subsites”. Among tumors with known p16-status, a marked increase in the frequency of p16-positivity was seen in “tonsil/ BOT” tumors, from around 10-15% in the beginning of the study-period to reach approximately 75% in 2016-2020, **Figure 1A**. For tumors originating in “neighboring subsites” an increase in the proportion of p16-positivity was also evident but less pronounced (from 10-15% to 30-50%),

whereas in “distant subsites” the percentage of p16-positive tumors remained low and stable over time (5-15%). **Figure 1B** demonstrates the 5-year risk of loco-regional failure according to subsite and p16-status in patients treated with curative intent (N=3327). The favorable prognostic impact of p16-positivity was confirmed only in “tonsil/BOT” and “neighboring subsites”, whereas tumors arising in “distant subsites” had a poorer outcome whether p16-positive or p16-negative.

**Conclusions:**

“Tonsil/BOT” tumors were much more common than other OPSCC, and the frequency of p16-expression and lack of prognostic impact seen in tumors arising in the “distant subsites” is comparable to that of non-oropharyngeal HNSCC. This indicates that grouping all p16-positive OPSCC as one entity for staging and prognostication, as currently done in TNM8, is probably too simple as it does not accurately depict the differences in biology and the consequent treatment response of the tumors.

**Figure 1A.** Frequency of tumor p16-status (positive, negative, unknown) by subsite in 5-year periods from 1986-2020.

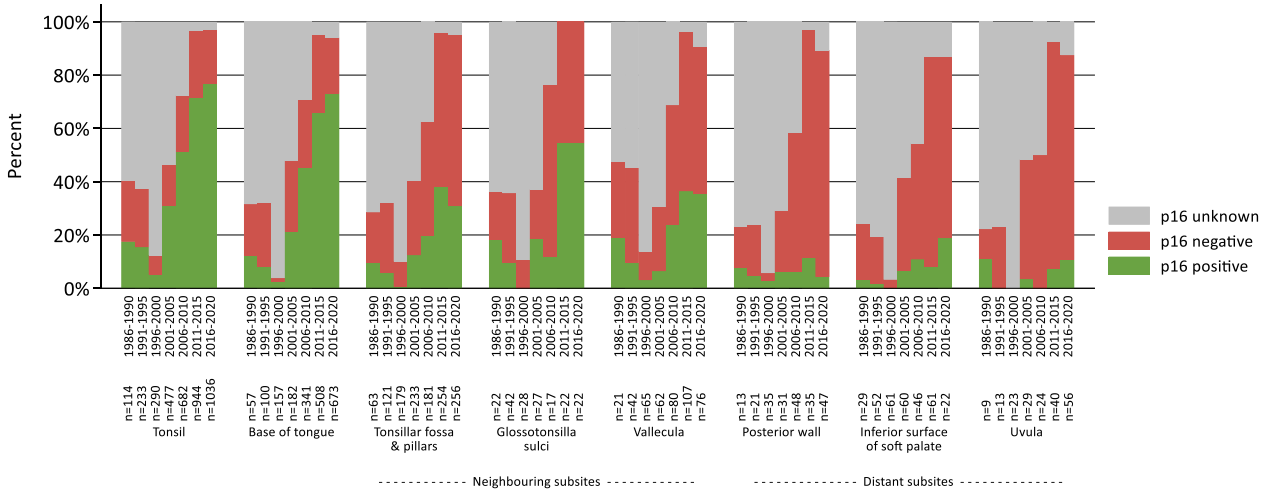


**Figure 1B.** 5-year risk of loco-regional failure in patients treated with curative intent (N=3327) stratified by oropharyngeal subsite and tumor p16-status.

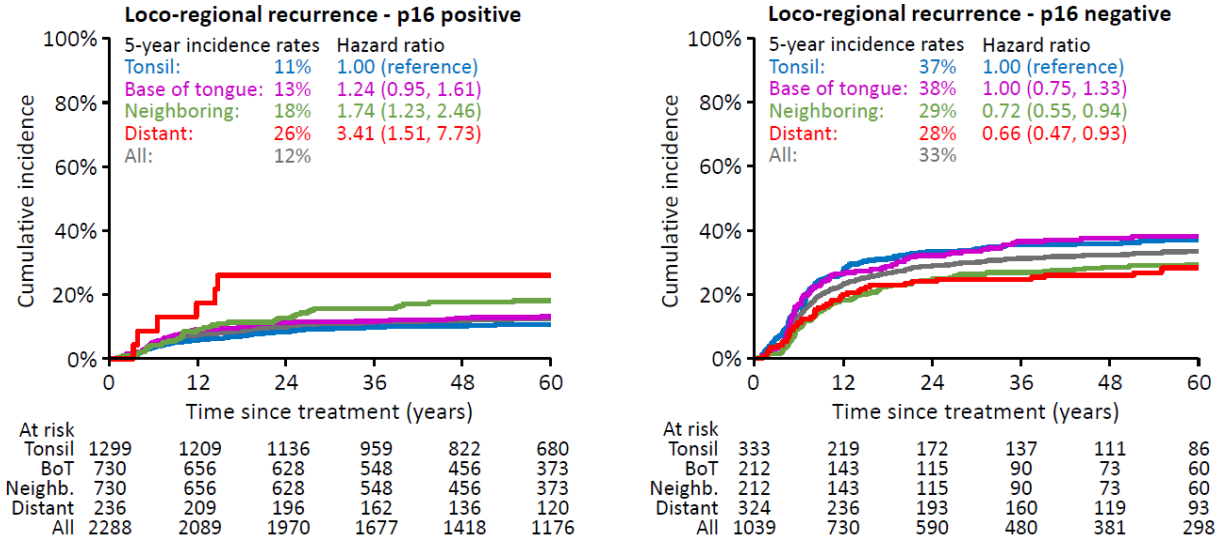

# Clinical Study of VMAT vs. 3DCRT for Breast Cancer with Lymph Node Involvement: Better Coverage, Faster Treatment, and No Increased Contra-Lateral Organ Dose

Karina Lindberg Gottlieb[1], Kenni Højsgaard Engstrøm[1], Irene Hazell[1], Lars Johnsen[1], Martin Kjellgren[1], Mette Holck Nielsen[2], Carsten Brink[1] and Ebbe Laugaard Lorenzen[1]

1. Laboratory of Radiation Physics, Department of Oncology, Odense University Hospital, DK-5000 Odense, Denmark
2. Department of Oncology, Odense University Hospital, DK-5000 Odense, Denmark

Contacting author: Karina Lindberg Gottlieb, karina.lindberg@rsyd.dk

## Introduction

Lymph node coverage, particularly of the internal mammary nodes (IMN), is crucial in breast cancer radiotherapy, supported by clinical evidence[1]. Volumetric Modulated Arc Therapy (VMAT) has shown advantages over 3D Conformal Radiotherapy (3DCRT) in planning studies for breast cancer treatments involving lymph nodes, including IMN[2]. However, several studies have indicated that VMAT can result in an increased low-dose exposure to both contralateral and ipsilateral organs. Despite these findings, there is limited clinical data directly comparing VMAT and 3DCRT. This study aims to evaluate clinical data, including target coverage, treatment time, and doses to organs at risk (OARs) for patients treated with either technique.

## Materials and Methods

In a clinical study, VMAT was introduced for locoregional breast cancer radiotherapy, including IMN, at our institution in June 2023, following a pilot study[2]. The study included 203 patients: 106 received 3DCRT (June 2022-May 2023) and 97 received VMAT (June 2023-May 2024). Of these, 174 were treated with gating (92 in the 3DCRT group and 82 in the VMAT group). Target volume and OAR contouring followed ESTRO guidelines[3]. Treatment planning used Pinnacle with auto-planning, a 10mm skin-flash, and Elekta linacs for delivery. Daily IGRT with CBCT was performed for all patients, and in the VMAT group, plans were recalculated if external contour variations exceeded 8 mm to check the robustness of the VMAT plan. Treatment times, recorded in MOSAIQ, were measured from beam-on to beam-off. All patients received 40 Gy in 15 fractions, with 2 and 1 in the 3DCRT group receiving a final boost and a simultaneous boost respectively, and 2 patients in the VMAT group receiving a simultaneous integrated boost. The 3DCRT utilized a tangential field-in-field technique, while VMAT used a two-arc "butterfly" technique.

## Results

Treatment times were significantly shorter for VMAT: median 4.0 minutes (IQR 3.6–4.6 min) compared to 6.6 minutes (IQR 5.9–9.0 min) for 3DCRT ($p < 0.001$). Coverage of CTVp_breast/CTVp_chest was similar between the two techniques, but VMAT provided better coverage of lymph node regions. Doses to OARs were comparable between both groups (Figure 1).

## Conclusions

To our knowledge, this is the first large clinical study directly comparing VMAT and 3DCRT for breast cancer patients. The significant reduction in treatment time with VMAT, especially in patients requiring longer treatments, improves patient comfort and treatment precision. Importantly, this study demonstrates that VMAT can be performed without the increased low-dose exposure to the contra-lateral OAR commonly associated with the technique.

**References**

1. Thorsen, L.B.J., J. Overgaard, L.W. Matthiessen, et al. "Internal Mammary Node Irradiation in Patients With Node-Positive Early Breast Cancer: Fifteen-Year Results From the Danish Breast Cancer Group Internal Mammary Node Study." *J Clin Oncol*, April 8, 2022. https://doi.org/10.1200/JCO.22.00044.

2. Engstrøm, K.H., C. Brink, M.H. Nielsen, et al. "Automatic Treatment Planning of VMAT for Left-Sided Breast Cancer with Lymph Nodes." *Acta Oncol* 60, no. 11 (2021): 1425–31. https://doi.org/10.1080/0284186X.2021.1983209.

3. Offersen, B.V., L.J. Boersma, C. Kirkove, et al. "ESTRO Guideline on Target Volume Delineation for Elective Radiation Therapy of Early Stage Breast Cancer." *Radiother Oncol* 114, no. 1 (2015): 3–10. https://doi.org/10.1016/j.radonc.2014.11.030.

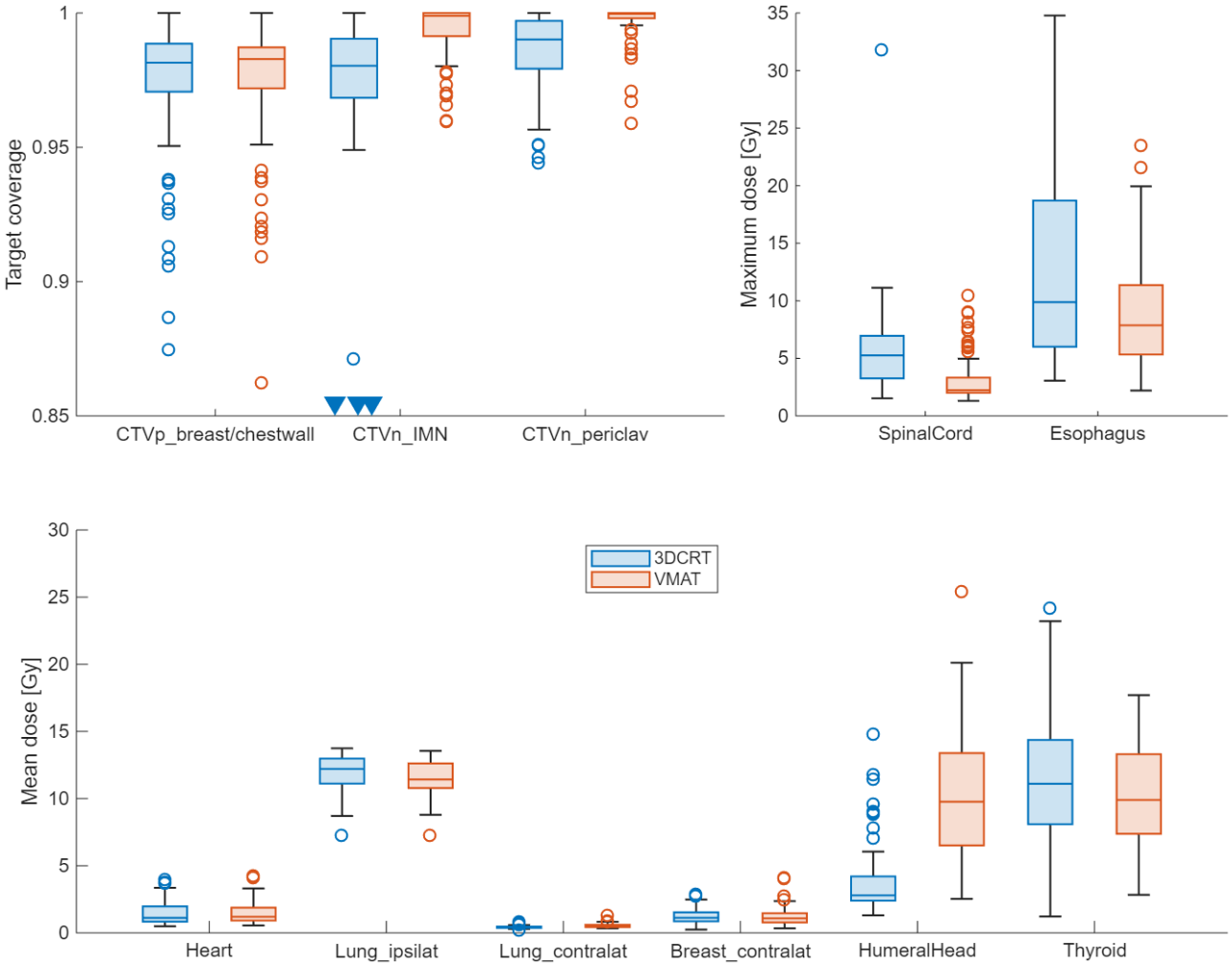


Figure 1: Boxplot of dose-volume metrics for patients treated within the two groups (3DCRT vs. VMAT).

**Tracking changes in diffusion MRI for short course radiotherapy in rectal cancer: a multi-center study**

**Authors:**

Anne L. H. Bisgaard[1] Chavelli M. Kensen[2] Marielle E.P. Phillippens[3] Martijn P.W. Intven[3] G.J. Meijer[3] Corrie A.M. Marijnen[2] Uulke A. van der Heide[2] Erik van der Bijl[4] Pètra Braam[4] Petra J. van Houdt[2] Faisal Mahmood[1,5]

Corresponding author: Anne L.H. Bisgaard, anne.bisgaard@rsyd.dk

**Affiliations:**

[1]Laboratory of Radiation Physics, Odense University Hospital, Odense, Denmark
[2]Department of Radiation Oncology, The Netherlands Cancer Institute, Amsterdam, The Netherlands
[3]Department of Radiotherapy, University Medical Hospital Utrecht, Utrecht, The Netherlands
[4]Department of Radiation Oncology, Radboud University Medical Center, Nijmegen, The Netherlands
[5]Department of Clinical Research, University of Southern Denmark, Odense, Denmark

## Introduction

The apparent diffusion coefficient (ADC) derived from diffusion-weighted MRI (DWI) is a potential biomarker for predicting response to neoadjuvant radiotherapy in rectal cancer, enabling personalized treatment. This study aims to determine whether longitudinal changes in DWI parameters can be detected during short-course radiotherapy in a multi-centre cohort of patients with rectal cancer treated on a 1.5T MRI-linac.

## Materials and methods

This retrospective study included patients with rectal cancer across three centres who received radiotherapy on the MRI-Linac. All patients were enrolled in the ongoing MOMENTUM trial (clinicaltrials.gov, NCT04075305 [1]). In total, 200 patients were evaluated with respect to tumour characteristics and treatments. Patients with primary tumours who received short course radiotherapy (5 fractions of 5Gy) with at least 2 fractions on the MRI-Linac, and no other treatment prior to this, were selected for further analysis (n=141).

GTVs were rigidly propagated from pre-treatment T2-weighted MRI to DWI for each treatment fraction. Within a 5 mm margin around the GTV, a region of interest (ROI) was defined on the high b-value DWI image using a threshold-based delineation tool [2]. ADC voxel-values were extracted within this ROI using b-values in the range [100, 800] s/mm$^2$. For each patient, median ADC values within the ROI were reported and the ADC time-trend across fractions was extracted using linear fitting. Acquisition-related ADC variation

was addressed by grouping sequences according to scan parameters and applying median scaling of ADC histograms from all tumour voxel-values between the groups [3].

**Results**

Seven DWI sequences were identified across centers and grouped into 4 groups. The median ADC values were 1.13, 1.19, 1.07 and 1.16 $mm^2/s$ for group 1-4, respectively. Relatively small scaling factors (range: 0.98-1.09) were needed to account for this variation. The median (range) ADC change during radiotherapy was 19.8% (-23.7%-102.7%) (Figure 1).

**Conclusion**

The sequence-related ADC variation was relatively small, demonstrating feasibility of multi-centre investigations of MRI-Linac-based DWI. We observed ADC changes during treatment larger than a repeatability coefficient of 17% reported in other studies on the 1.5T MRI-Linac [4], suggesting that longitudinal DWI can reflect radiotherapy-induced changes. These findings encourage future multi-centre studies linking ADC to clinical outcomes in rectal cancer.

**References**


1. de Mol van Otterloo SR et al. Front Oncol. 2020;10.
2. Bisgaard ALH et al. Phys Imaging Radiat Oncol. 2022;21:146–52.
3. Fernandez Salamanca M et al. Front Oncol. 2024;14:1–7.
4. Eijkelenkamp H et al. Phys Imaging Radiat Oncol. 2025;33:0–3.


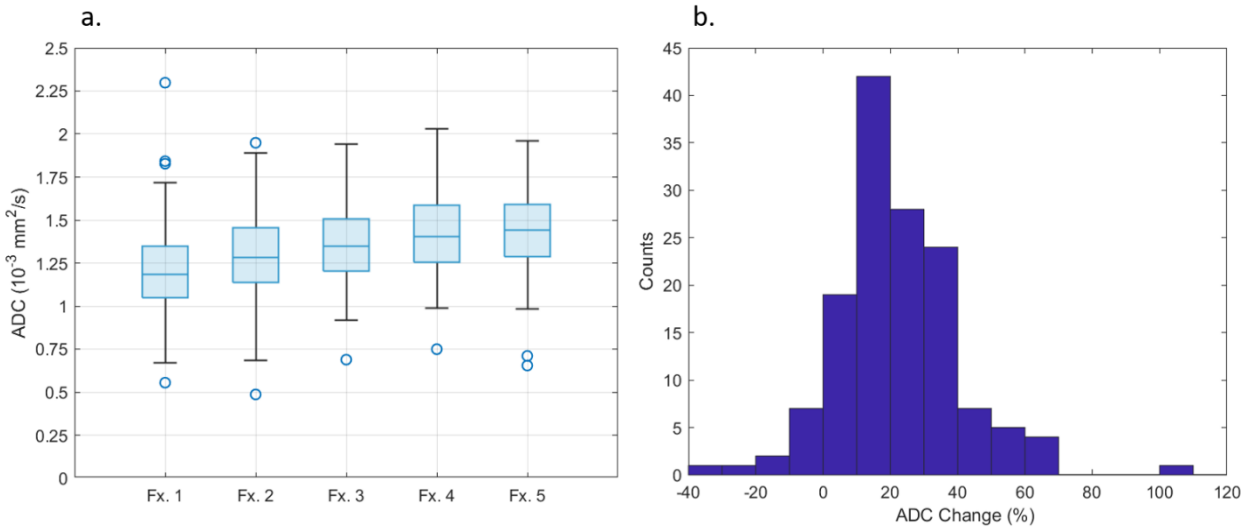


*Figure 1: Boxplot showing the median apparent diffusion coefficient (ADC) values for all patients and fractions (a) and distribution of ADC changes (%) between fraction 1 and 5 ((fraction5-fraction1)/fraction1) for all patients (b). For each patient, the ADC change was calculated based on regression constants from a linear fit to the ADC as a function of fraction no. The figure shows ADC values after median scaling between DWI sequences.*

**Adaptive Radiotherapy and Quality Assurance in the European randomised phase III PROTECT trial for oesophageal cancer patients**

Byskov CS[1], Ehmsen ML[2], Jensen MF[2], Mortensen, HR[2], Nordsmark M[1], Defraene G[3], Haustermans K[3,4], Populaire P[3,4], Weber D[5], Meijers A[5], Balermpas P[6], Fabiano S[6], Hoffmann L[1,7]

[1]Dept of Oncology, Aarhus University Hospital, Aarhus, Denmark

[2]Danish Centre for Particle Therapy, Aarhus University Hospital, Aarhus, Denmark

[3]KU Leuven – University of Leuven – Dept of Oncology –Laboratory of Experimental Radiotherapy, Leuven, Belgium

[4]Dept of Radiation Oncology, University Hospitals Leuven, Leuven, Belgium

[5]Paul Scherrer Institute, Villigen, Switzerland

[6]University Hospital Zurich, Zurich, Switzerland

[7]Dept of Clinical Medicine, Aarhus University, Aarhus, Denmark

**Introduction:** The European randomised phase III-trial, PROTECT, evaluates clinical outcomes of proton therapy (PT) versus photon therapy (XT) in oesophageal cancer patients receiving chemoradiotherapy followed by surgery. To ensure treatment accuracy and maintain the highest trial standards, a comprehensive radiotherapy quality assurance (RTQA) programme, including adaptive radiotherapy strategies, has been implemented. This study presents the first results from the on-trial RTQA programme, with a focus on clinical plan adaptations.

**Materials and Methods:** On-trial RTQA includes individual case reviews (ICR) for the first two patients and every fifth patient per site. Additionally, mandatory weekly four-dimensional computed tomography (4D-CT) surveillance scans are conducted for at least the first eight patients at each site to monitor anatomical changes and inform potential plan adaptations. Surveillance scans may be replaced by implementation of cone-beam CT-based triggering of adaptations or less frequent imaging based on a validation study.

**Results:** Four sites actively include patients, with a total of 67 patients enrolled. ICR was completed for 22 patients, revealing six major and 11 minor variations in target and organ-at-risk (OAR) delineation, while six cases had no variations. Most major deviations were in early cases and changes were implemented prior to treatment initiation. Treatment plan reviews identified one major and four minor variations. No plans required re-optimisation before treatment initiation.

In total, 29 of 62 (47%) fully treated patients required adaptive replanning of the treatment plan (11 PT, 18 XT) during the treatment course of 28 or 23 fractions. For one XT patient, three plan adaptations were required, for nine patients, two adaptations were required (3 PT, 6 XT) and for 19 patients one plan adaptation was performed (8 PT, 11 XT). The main reason for plan adaptations was inadequate coverage of the internal clinical target volume (27 cases, 8 PT, 19 XT) (Figure 1) caused by changes of the diaphragm position and the target volume. The maximum dose to organs at risk were exceeded for 11 plans (3 PT, 8 XT). One PT patient was replanned due to pneumonia and one XT replan was due to suboptimal 4D-CT imaging at planning CT.

**Conclusions:** A comprehensive RTQA programme was implemented for the PROTECT trial. While target delineation remains a key source of major variations (27%), treatment plan robustness was

generally maintained. However, 47% of patients required replanning due to anatomical changes, emphasizing the necessity of systematic imaging surveillance and proactive adaptive radiotherapy protocols to ensure optimal treatment delivery.

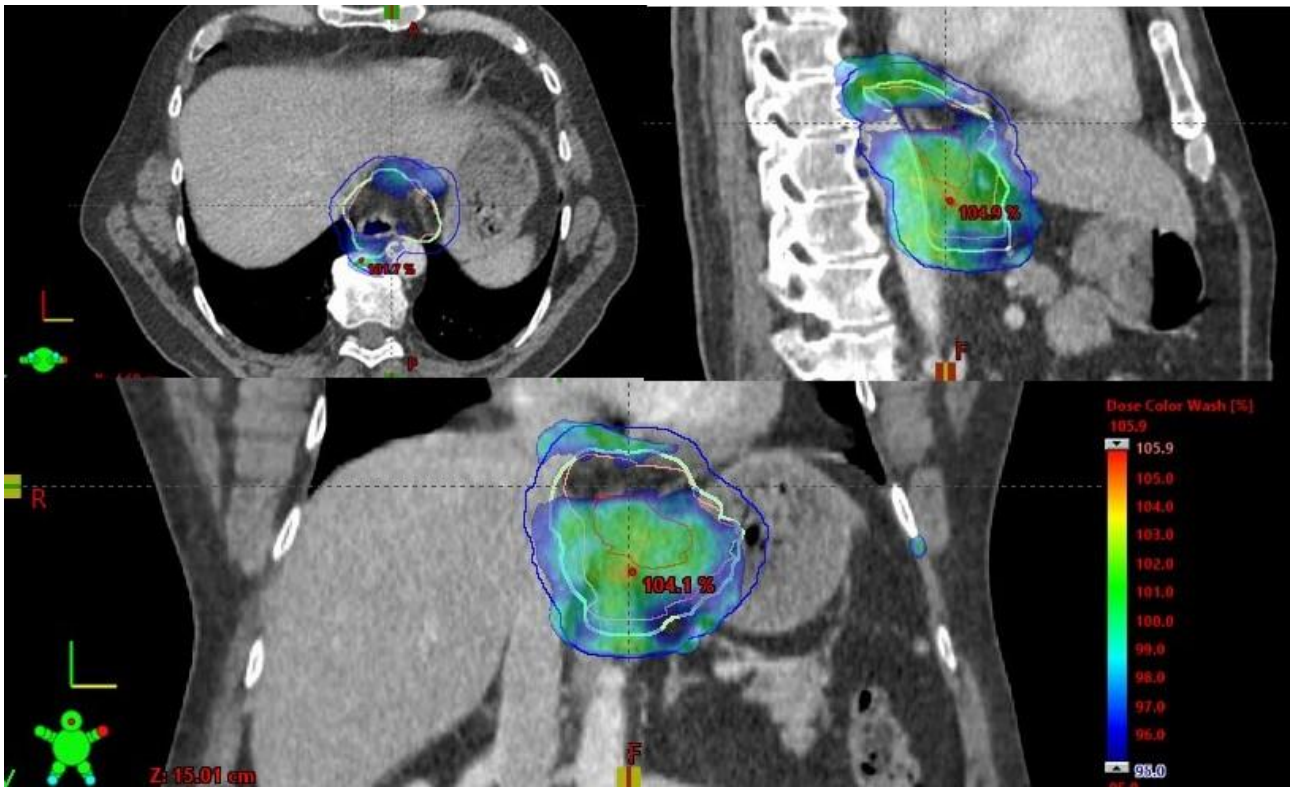


Figure 1 Example of a patient with insufficient coverage of the internal clinical target volume (light green) observed on the first weekly surveillance 4D-CT scan.

# Abstracts session 2: Prediction of toxicity and morbidity

# Impact of radiotherapy on vaginal and sexual health in women with anal cancer: A prospective Danish cohort analysis

Johanne H. Steffensen [1,2], Eva Serup-Hansen[3], Camilla J.S. Kronborg [2,5], Karen-Lise G. Spindler[1,4]

[1]Department of Experimental Clinical Oncology, Aarhus University Hospital, Aarhus, Denmark [2]Department of Clinical Medicine, Aarhus University, Aarhus, Denmark, [3]Department of Oncology, Copenhagen University Hospital – Herlev and Gentofte, Denmark, [4]Department of Oncology, Aarhus University Hospital, Aarhus, Denmark, [5]Danish Centre for Particle Therapy, Aarhus University Hospital, Aarhus, Denmark

**Introduction** Women undergoing pelvic radiotherapy (RT) for anal cancer (AC) frequently experience long-term vaginal and sexual complications, yet dedicated research on this group remains limited. This study investigates the prevalence and progression of these late effects in a national Danish cohort.

**Materials and Methods** This sub-study used data from the DACG-I prospective cohort (NTC 05570279), including women with AC treated with curative RT from 2015 to 2020. Vaginal and sexual health outcomes were evaluated at baseline and at 1, 3, and 5 years using the NCI-CTCAE v4.0 and the EORTC Quality of Life Questionnaire CX24. Descriptive statistics summarized patient characteristics and prevalence, while longitudinal symptom trajectories were analyzed using the Wilcoxon signed-rank test.

**Results** A total of 221 women were included before treatment. Follow-up data were available for 213 at 1 year, 188 at 3 years, and 132 at 5 years. The mean enrollment age was 62.2 years. The radiation dose to the primary tumor and involved nodes varied, with 25% receiving 60 Gy, 69% receiving 64 Gy, and 6% receiving ≤54 Gy, delivered in 27-32 fractions. Elective lymph nodes received 48-51.2 Gy. Attrition was mainly due to mortality (n=32) and withdrawal (n=14), while 44 participants had not yet completed the 5-year follow-up. Among those remaining, patient-reported outcome (PRO) completion rates ranged from 82.4% to 95.5%.

The percentage of women reporting grade ≥2 vaginal dryness increased from 4.8% before RT to 9.9% at 1 year (p=0.018), then stabilized at 11.4% by 5 years. Vaginal pain reports rose from 1.0% pre-treatment to 4.1% at 1 year (p=0.005), with no significant changes thereafter. Reported vaginal irritation, measured with EORTC-CX24, rose from 8.8% at baseline to 12.7% after 1 year (p=0.008) before leveling off.

Seventy-two percent of participants were sexually inactive before treatment, maintaining at 71% by 5 years. Among sexually active women, enjoyment dropped from 73.8% pre-treatment to 48.7% at 1 year, improving slightly to 53.6% at 5 years. Grade ≥2 vaginal symptoms affected 42% of sexually active women, with a significant rise at 1 year that persisted over time.

**Conclusion** This study provides a comprehensive evaluation of long-term vaginal and sexual health outcomes in women treated with RT for AC. The results highlight the persistence of these complications and underscore the need for targeted interventions. Future research should prioritize strategies to mitigate radiation-induced toxicities, explore dose-response effects, and assess interventions to enhance long-term sexual well-being.

**Associations between SNPs and Radiation Induced Fibrosis in Breast Cancer Patients: Results from a Genome-Wide Association Study**

Line M H Schack[1,4], Thomas Damm Als[2], Leila Dorling[3], Laura Fachal[3], Craig Luccarini[3], Alison M Dunning[3], Jens Overgaard[1], Birgitte V Offersen[1,4], Christian Nicolaj Andreassen[1,4], Jan Alsner[1], on behalf of the Danish Breast Cancer Group (DBCG)

1 Department of Experimental Clinical Oncology, Aarhus University Hospital, Denmark
2 Department of Molecular Medicine (MOMA), Aarhus University Hospital, Denmark
3 Centre for Cancer Genetic Epidemiology, Department of Oncology, University of Cambridge, United Kingdom
4 Department of Oncology, Aarhus University Hospital, Denmark

*Running title*
GWAS of radiotherapy induced morbidity in breast cancer

*Corresponding author*
Line M H Schack
Department of Experimental Clinical Oncology and Department of Oncology,
Aarhus University Hospital
Palle Juul-Jensens Boulevard 99
DK-8200 Aarhus N
Tel: +45 7845 4973
Email: schack@oncology.au.dk

**Introduction**

Radiation-induced fibrosis affects women having undergone post-lumpectomy radiotherapy to a varying degree. Publications have identified Single Nucleotide Polymorphisms (SNPs) associated with fibrosis after radiotherapy in breast cancer patients. We aimed to identify new genetic variants in a cohort of early breast cancer patients representing two cohorts treated within the Danish Breast Cancer Group protocols.

**Materials and methods**

The analysis included 933 patients treated with lumpectomy and adjuvant radiotherapy in the DBCG trials hypo- versus normofractionated radiotherapy trial, DBCG-HYPO, and the DBCG partial versus whole breast irradiation trial, DBCG-PBI.

Samples were genotyped using the Illumina Infinium OncoArray Bead Chip. Associations between common genetic variants and fibrosis grade 2 or 3 (LENT-SOMA) in a per-risk allele log-additive genetic model were tested in an exploratory genome-wide association study (GWAS). A genome-wide significance cut-off of $p<5{\cdot}10^{-8}$ was applied.

**Results**

An association reaching a p-value = $5.90{\cdot}10^{-8}$ after removal of principal component outliers was identified in a locus on chromosome 10. The strongest association was represented by the SNP rs75542274.

**Conclusion**

An exploratory GWAS identified a locus on chromosome 10 reaching a near-significant association with radiation-induced fibrosis. This finding must be tested in independent studies or in meta-analysis.

**Figure**

Manhattan plot after removal of PCA outliers and adjusted for covariates. X-axis representing chromosomes 1-23, Y-axis representing the negative log(10) of p-values, red line is genome-wide significance cut-off of $p<5{\cdot}10^{-8}$.

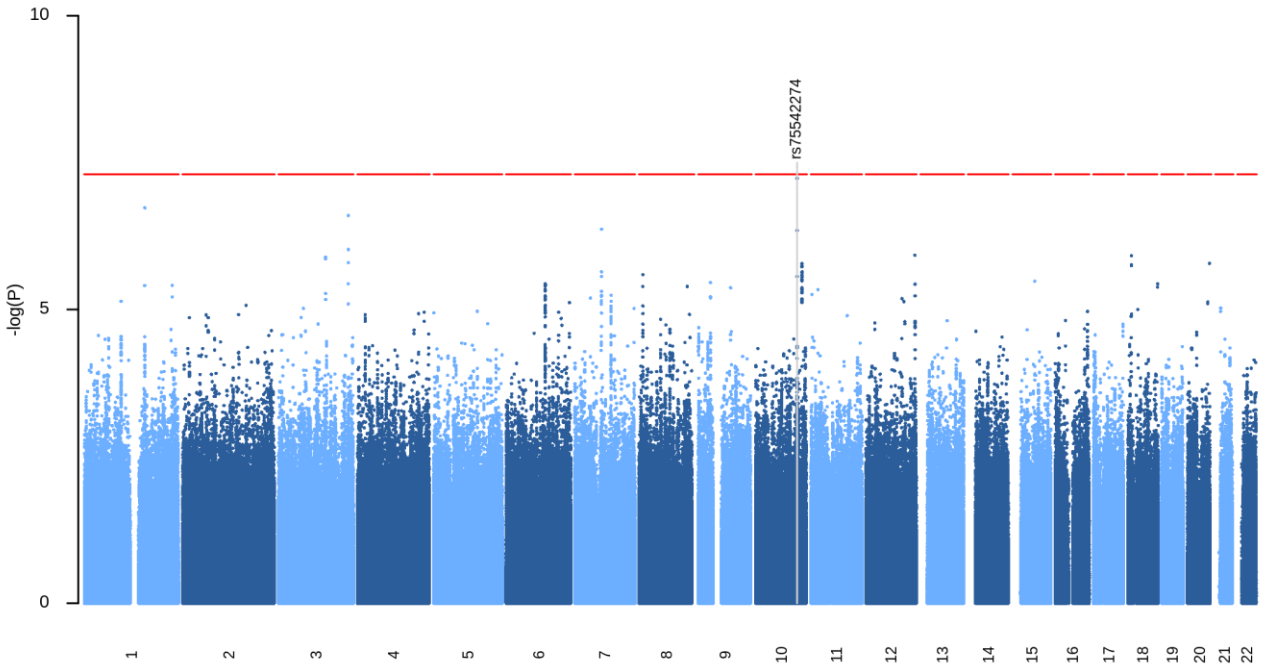
10
5
0
-log(P)
rs75542274
1
2
3
4
5
6
7
8
9
10
11
12
13
14
15
16
17
18
19
20
21
22

# Abstracts session 3: Artificial intelligence in radiotherapy

# In-depth analysis of failure rates and -modes in auto-segmentation of the esophagus in patients treated for lung cancer

Lise Bech Jellesmark Thorsen[1,2], Marianne Marquard Knap[1], Tine Bisballe Nyeng[1], Torben Aagaard[1], Ditte Sloth Møller[1,2], Anne Ivalu Sander Holm[1]

Presenting Author: Lise Bech Jellesmark Thorsen, Department of Oncology, Aarhus University Hospital. e-mail: liseb@oncology.au.dk.

1) Department of Oncology, Aarhus University Hospital, Aarhus, Denmark
2) Department of Clinical Medicine, Aarhus University, Aarhus, Denmark

**Introduction**: Routine use of AI-based tools for auto-segmentation of organs at risk (OAR) in radiation therapy (RT) must be monitored to identify causes of failure and possible areas of improvement. AI-tools may be failure-prone when applied in patient populations different from those used to develop the tool, i.e. if data bias is present. We report a detailed analysis of failure rates and modes for automated delineation of the esophagus in patients with lung cancer.

**Materials and Methods**: A bespoke AI-solution (b-AI) for auto-segmentation of thoracic OAR was developed in-house on contrast-enhanced (CE) 4D-CT-scans from patients treated with lung cancer. For 20 consecutive months starting in June 2023, thoracic OAR were auto-segmented using this b-AI in all patients treated with RT for lung cancer at Aarhus University Hospital. Long-course RT was planned on CE 4D-CT-scans, whereas stereotactic RT was mainly planned on non-CE 4D-CT-scans. Uncorrected and corrected b-AI contours were saved and compared for monitoring. Esophageal outliers were defined as having 2mm Surface Dice Similarity Coefficient (SDSC)< 0.8 and/or mean Hausdorff Distance> 2mm. Two oncologists reviewed all outlier cases to assess failure modes, b-AI failure characteristics and associated traits of anatomical anomalies. Chi-squared or Fisher's exact test were applied to assess differences in frequencies between CE- versus non-CE contours.

**Results**: Among 402 consecutive patients, 53 outliers (13.1%) were confirmed as failures (table 1). More failures occurred in non-CE vs. CE planning CT scans (p=0.00001). In all CE scans an obvious failure mode was determined, whereas this was the case in only 52% of non-CE scans. The dominant failure-mode overall (n=26) was abnormal anatomy, mainly presenting as aberrant esophageal dimensions or trajectory. Three cases of abnormal anatomy were due to prior esophageal or pulmonary surgery, and eight additional cases were due to gross hiatal herniation. There were no significant differences in AI-failure characteristics or anatomical failure causes between scan types. Most AI-failure characteristics would be reflected in the cranio-caudal extent of the esophageal contour, suggesting that simple thresholds for esophageal dimensions could be utilized to flag possible failures up-front.

**Conclusion**: While the CE-scan-based b-AI performed well for esophageal contouring in CE scans, performance in non-CE scans was worse, and less predictable, demonstrating clinical importance of data bias in application of AI-tools. Anatomical failure characteristics suggested that cases at high risk of failure could be identified up-front and that development of quantitative thresholds for flagging failures before undertaking corrections may be possible.

| | Lung (contrast-enhanced) | | SRT (non-contrast-enhanced) | | |
|---|---|---|---|---|---|
| | N | % | N | % | p for difference |
| No. patients | 197 | | 205 | | p=0.00001 |
| No. failures | 11 | 5.6 | 42 | 20.5 | |
| **Failure mode** | | | | | p=0.001 |
| Tumor anatomy | 1 | 0.5 | 1 | 0.5 | |
| Setup position | 3 | 1.5 | 1 | 0.5 | |
| Image artefacts | 0 | 0.0 | 1 | 0.5 | |
| Unknown | 0 | 0.0 | 20 | 9.8 | |
| Abnormal anatomy | 7 | 3.6 | 19 | 9.3 | |
| **Main AI failure characteristic** | | | | | p=0.19 |
| Ends too cranial | 9 | 81.8 | 29 | 69.0 | |
| Starts too caudal | 0 | 0.0 | 9 | 21.4 | |
| Starts too caudal and ends too cranial | 1 | 9.1 | 3 | 7.1 | |
| Tumor-involved esophagus | 1 | 9.1 | 1 | 2.4 | |
| **Main anatomical failure cause** | | | | | p=0.17 |
| Esophagus abnormal | 6 | 85.7 | 9 | 47.4 | |
| Lung/pleura abnormal | 1 | 14.3 | 4 | 21.1 | |
| Narrow mediastinum | 0 | 0.0 | 6 | 31.6 | |

Table 1: Frequencies of failure modes, characteristics of AI failures and the main anatomical causes of failure in esophageal auto-segmentation on contrast- vs. non-contrast enhanced CT scans as identified by two oncologists. P values calculated using chi-squared (first row) or Fisher's exact test as appropriate depending on no. of observations.

# External Validation of an Automated Deep Learning-Based Delta 18F-FDG PET/CT Biomarker for Loco-Regional Control Probability Stratification

## Authors

David G. Kovacs, MSc[1,2,*]
Marianne Aznar[3,4]
Marcel van Herk[3,4]
Iskandar Mohamed[4]
James Price[4]
Claes N. Ladefoged[1,5]
Barbara M. Fischer[1,2]
Flemming L. Andersen[1,2]
Andrew McPartlin[6]
Eliana M. Vasquez Osorio[3,4]
Azadeh Abravan[3,4]

[1] Department of Clinical Physiology and Nuclear Medicine, Rigshospitalet, University of Copenhagen, Copenhagen, Denmark

[2] Department of Clinical Medicine, Faculty of Health and Medical Sciences, Copenhagen, Denmark

[3] Division of Cancer Sciences, University of Manchester, Manchester, the United Kingdom of Great Britain and Northern Ireland

[4] The Christie NHS Foundation Trust, Manchester, the United Kingdom of Great Britain and Northern Ireland

[5] Department of Applied Mathematics and Computer Science, Technical University of Denmark, Lyngby, Denmark

[6] Princess Margaret Cancer Centre, Toronto, Canada

***** Corresponding author: david.gergely.kovacs.petersen@regionh.dk

## Introduction

Delta-biomarkers, which capture changes in biomarker signals over time, have the potential to guide treatment follow-up decisions but traditionally require intensive manual segmentation and/or image registration. This study evaluates an externally developed deep learning algorithm for the automated delineation of 18F-FDG-avid tumour volumes, calculates their change after treatment (ΔPET-GTV, [$cm^3$]), and assesses its ability to stratify patients by loco-regional control probability.

## Materials and methods

A deep learning algorithm, trained for PET-GTV delineation at Copenhagen University Hospital, Rigshospitalet, DK, was installed at the University of Manchester and used to segment pre- and post-radiotherapy 18F-FDG PET/CT scans from 50 head and neck cancer patients treated at The Christie NHS Foundation Trust with radical radiotherapy. The model, trained on pre-treatment scans alone, was applied to both time points without requiring image registration or volume propagation. Tumour volumes from these delineations were used to compute ΔPET-GTV, representing the absolute change in tumour volumes between scans. Patients were stratified by the median ΔPET-GTV, and Kaplan-Meier analysis with a log-rank test assessed differences in loco-regional control probability between groups. A secondary analysis involved qualitative physician assessment of AI-generated PET-GTVs for use in radiotherapy planning using a four-point Likert scale.

## Results

Only one of nine loco-regional failure events occurred in the high ΔPET-GTV group. After one year, the probability of loco-regional control was 94.1% [95% CI: 83.6–100%] in the high ΔPET-GTV group compared to 53.6% [95% CI: 32.2–89.1%] in the low ΔPET-GTV group ($p = 0.02$) (based on the log-rank test, Figure 1). These findings suggest that AI-based tumour volume assessment enables robust patient stratification and may replace manual approaches. Physician ratings showed that AI-gener-ated tumour volumes were acceptable or better for radiotherapy planning in 77% of cases, though they were generally smaller and included fewer nodes, potentially affecting dose distribution in 56% of cases. In two patients, AI correctly identified oropharyngeal tumours that were clinically unknown at the time of scanning but later confirmed by biopsy.

## Conclusions

Deep learning-based PET-GTV delineation can generate physiologically meaningful tumour volumes, and these can be used to compute volume changes (ΔPET-GTV) automatically. These findings suggest that a fully automated ΔPET-GTV pipeline could be used for patient risk stratification and to identify patients who may benefit from closer post-treatment follow-up. This approach is feasible with the tested tools and eliminates the need for manual segmentation and registration, making it a practical tool for clinical decision-making.

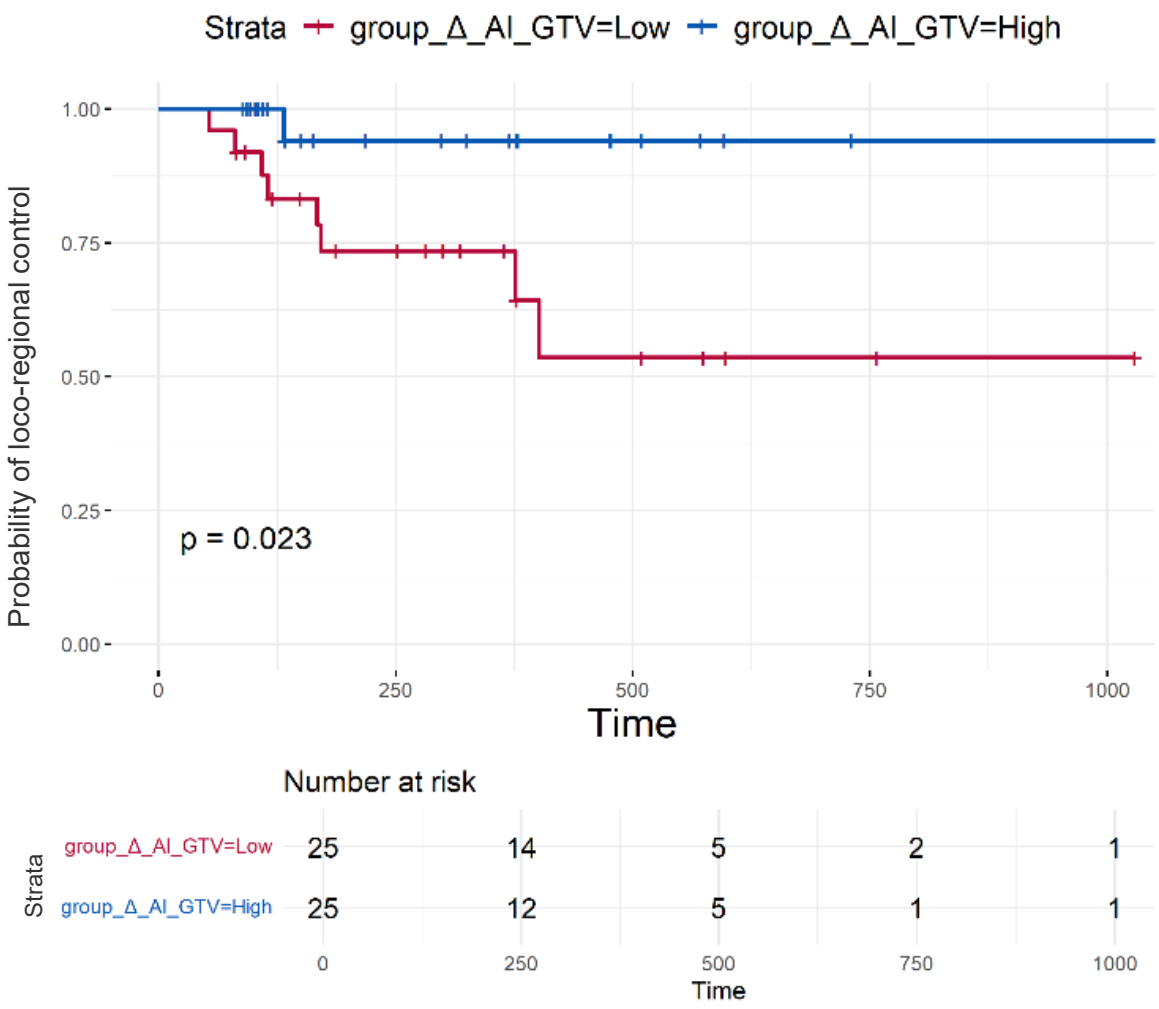


**Figure 1:** Kaplan-Meier survival curves comparing loco-regional control probability between high and low ΔPET-GTV [$cm^3$] groups. Time is given in days. Patients with a higher ΔPET-GTV, likely reflecting a stronger treatment response, had a significantly better prognosis (p = 0.02). The externally validated AI model automatically delineated FDG-avid tumour volumes from pre-and post-treatment 18F-FDG PET/CT scans. This pipeline allows fully automated risk stratification without manual segmentation or registration and may help guide personalized follow-up strategies.

**Exploring the performance of dose prediction with deep learning for head and neck cancer on a multi-centre clinical dataset**

Author information:

Camilla Panduro Nielsen (1,2), Margerie Huet-Dastarac (3), John A. Lee (3), Edmond Sterpin (3,4), Ruta Zukauskaite (5), Jørgen Johansen (5,6), Simon Long Krogh (1), Maximilian Lukas Konrad (1,2), Kenneth Jensen (6), Jeppe Friborg (7), Jeanette Frieda Aviaya Sommer (1), Sarah Stougaard (1,2), Jens Overgaard (8), Kasper Toustrup (8), Camilla Kjaer Lonkvist (9), Patrik Sibolt (9), Bob Smulders (6,7), Mohammad Farhadi (10), Laura Patricia Kaplan (10), Anne Ivalu Sander Holm (11), Rasmus Kjeldsen (12), Martin Skovmos Nielsen (12), Ebbe Laugaard Lorenzen (1,2), Carsten Brink (1,2), Ana Maria Barragán-Montero (3), Christian Rønn Hansen (1,2,6)

1 Laboratory of Radiation Physics, Department of Oncology, Odense University Hospital, Denmark;
2 Institute of Clinical Research, University of Southern Denmark, Denmark;
3 Molecular Imaging, Radiotherapy and Oncology, Institut de Recherche Expérimentale et Clinique, UCLouvain, Belgium;
4 Department of Oncology, Laboratory of Experimental Radiotherapy, KU Leuven, Belgium;
5 Department of Oncology, Odense University Hospital, Denmark;
6 Danish Centre for Particle Therapy, Aarhus University Hospital, Denmark
7 Department of Oncology, Rigshospitalet, University Hospital of Copenhagen, Denmark;
8 Department of Experimental Clinical Oncology, Aarhus University Hospital, Denmark;
9 Department of Oncology, University Hospital Herlev, Denmark;
10 Department of Oncology and Palliative Units, Zealand University Hospital, Næstved, Denmark;
11 Department of Oncology, Aarhus University Hospital, Denmark;
12 Department of Oncology, Aalborg University Hospital, Aalborg, Denmark

Corresponding author: Christian Rønn Hansen, Christian.roenn@rsyd.dk

**Introduction**

Radiotherapy (RT) for advanced head and neck (H&N) cancer is complex due to close proximity of tumour and healthy tissue volumes to each other. Dose prediction with deep learning shows promise in generating clinically comparable dose distributions, potentially making it valuable for RT plan optimization, quality assurance (QA), and modality treatment, e.g., proton RT or Image-Guided Adaptive RT, based on NTCP reduction. However, generalizability beyond the context of training and test data remains a challenge. This study aimed to develop a dose prediction model for loco-regionally advanced H&N cancer and evaluate its performance on a large clinical multi-centre cohort.

**Materials and Methods**

A hierarchically densely connected U-Net was trained on data from 430 H&N cancer patients treated with photon RT (66 or 68 Gy) at Odense University Hospital (2020–2023), following DAHANCA guidelines. The dataset was split into 90% for training/validation and 10% for testing. Inputs included CT scans, prescription dose, and contours of PTVs and OARs, while dose distributions were provided only during training. Predicted doses were normalized to ensure PTV1 mean dose ($D_{mean}$) matched the prescription dose.

The model was further validated on a national cohort of 605 H&N patients (DAHANCA cohort) treated at six Danish centres (2016–2023) to assess generalisability. Performance was evaluated by comparing dose metrics and voxel-wise dose values between predicted and clinically applied dose distributions and by global 3D gamma analysis (criteria: 3% dose difference, 3 mm distance, 0.5 voxel step size).

**Results**

The median $D_{mean}$ difference between predicted and clinically applied dose distributions on the test dataset was 0.5% of clinically applied dose [0.3, 0.7] (interquartile range) for all PTVs, compared to 0.3% [-0.10, 0.7] in the DAHANCA cohort. The median $D_{mean}$ difference for OARs was 0.7% of prescription dose [-0.7, 2.9] for the test dataset and 1.4% [-0.7, 5.3] for the DAHANCA cohort, figure 1.

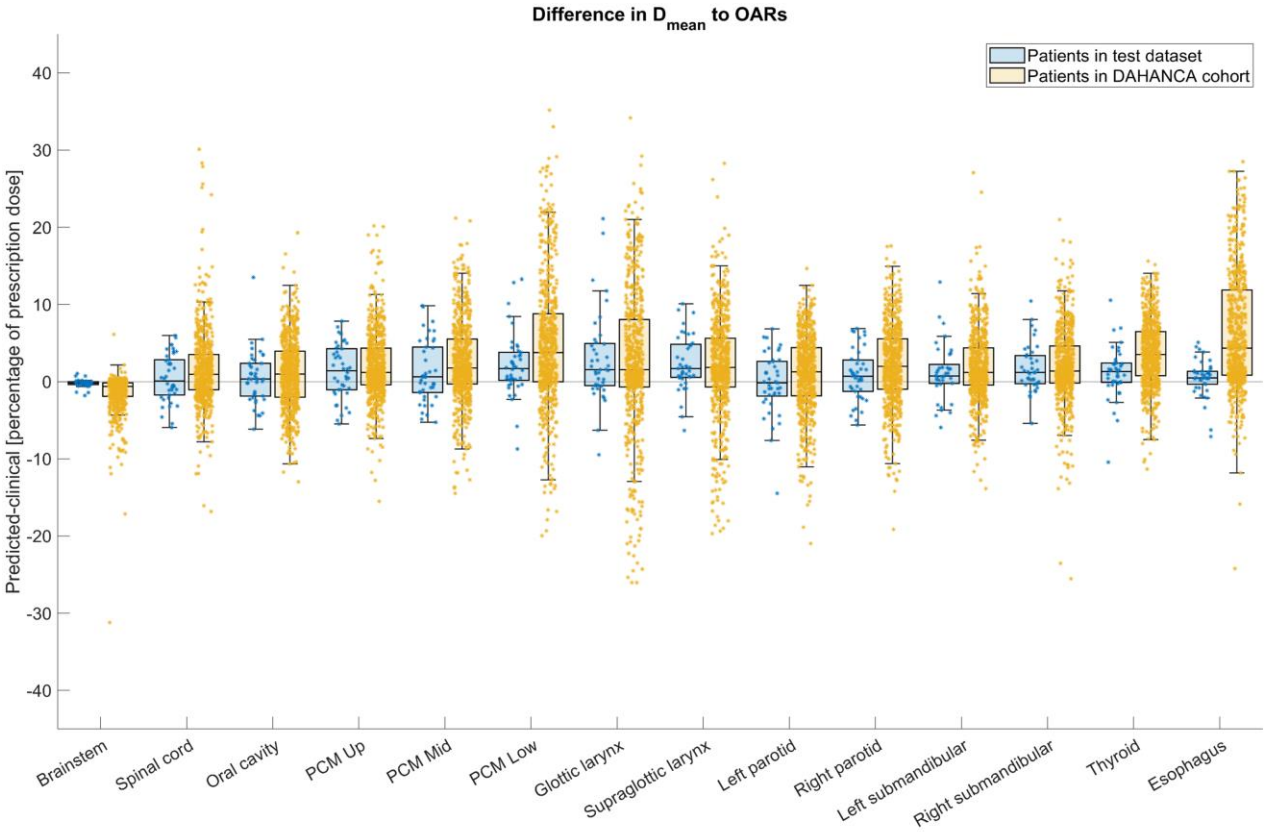


Figure 1 - Boxplot with individual patient samples overlaid showing the difference in $D_{mean}$ to OARs between predicted and clinically applied dose distributions in percentage of prescription dose in the test dataset and the DAHANCA cohort.

The voxel-wise comparison showed a mean difference of 0.03 Gy (95% confidence interval ± 4.7 Gy) for the test dataset and 0.2 Gy ± 5.4 Gy for the DAHANCA cohort.

The median gamma pass rate was 92.4% [91.5, 93.6] for the test dataset and 94.3% [92.7, 95.6] for the DAHANCA cohort.

**Conclusions**

The model performed well, and dose distribution was similar in both the single-centre and the larger multi-centre datasets. Leveraging dose prediction to guide plan optimization could pave the way for automated QA of individual patient treatment plans, potentially ensuring consistently high-quality RT for all patients in the future.

**First-in-world demonstration of benefit of AI assisted head and neck cancer target contouring in a prospective blinded randomized clinical trial**

Mathis E Rasmussen[1,4], Jintao Ren[1,2], Jasper A Nijkamp[1,2], Anne IS Holm[3], Kristoffer Moos[1,2], Kim M Hochreuter[1], Hanne Primdahl[3], Nicolaj Andreassen[3], Kasper Toustrup[3], Line MH Schack[3], Jesper G Eriksen[4], Stine S Korreman[1,2]

[1]Danish Center for Particle Therapy, Aarhus University Hospital, Aarhus, Denmark. [2]Department of Clinical Medicine, Aarhus University, Aarhus, Denmark. [3]Department of Oncology, Aarhus University Hospital, Aarhus, Denmark. [4]Department of Experimental Clinical Oncology, Aarhus University Hospital, Aarhus, Denmark

**Introduction**

This prospective randomized clinical trial aimed to demonstrate that the quality of AI-assisted GTV contouring in head and neck cancer is on par with manual contouring, through review and approval by a blinded multidisciplinary expert panel.

**Material and methods**

The study included 85 consecutive patients with oral cavity, oro-/hypo-pharynx or supra-glottic larynx cancers from Sept-2023 to Jan-2025.

In our institution, target contours generated by the delineating oncologist are routinely edited and approved at a target conference including a senior oncologist, a radiologist and a nuclear-medicine physician. The magnitude of changes performed to the target structures during target conference was the primary study endpoint.

Patients were randomized after informed consent to the control arm (manual contouring) or the intervention arm (AI-assisted contouring). A refined version of a published nnUNet-based model [1] was used for predicting AI-contours, which were imported into the treatment planning system (TPS), using the RadDeploy framework [2].

The target conference was blinded to the origin of contours (control/intervention arm). Changes were measured using Dice score (DSC), surface Dice 1mm tolerance (sDSC), and normalized added path length (APL). Primary tumour (GTV-T) and nodal volumes (GTV-N) were analysed separately.

The study aimed for non-inferiority with a margin of 10% for DSC and sDSC. Confidence intervals (CI, 95%) were calculated using bootstrapping (9999 iterations). Mann-Whitney-U test was further performed, using 0.05 as significance threshold.

**Results**

Two patients did not fulfill inclusion criteria, leaving 83 patients for analysis, with 41/42 in control/intervention arm. Patient characteristics were balanced between the two groups.

For both GTV-T and GTV-N, changes performed at target conference in the intervention (AI-assisted) arm were well within the inferiority margin with respect to the (manual) control arm, confirming the non-inferiority hypothesis. All results are illustrated in figure 1.

For GTV-T, there was a clear tendency for the spread of changes over the population to be smaller in the intervention arm than in the control arm, with fewer cases of large changes, for all metrics.

For GTV-N, the intervention arm and control arm were more similar with a slight tendency for larger changes in the intervention arm for APL.

**Conclusion**

AI assistance was shown to be a useful tool for GTV contouring for head and neck cancer in clinical practice with performance at least as good as manual contouring. This result paves the way for including AI assistance in standard clinical routine in the future to reduce manual workload.

**References**

[1] Jintao Ren, Jesper G Eriksen, Jasper A Nijkamp and Stine Korreman, ”Comparing different CT, PET and MRI multi-modality image combinations for deep learning-based head and neck tumor segmentation”, Acta Oncologica 60(11):1399-1406, doi: 10.1080/0284186X.2021.1949034, 2021.

[2] Mathis Ersted Rasmussen, Casper Dueholm Vestergaard, Jesper Folsted Kallehauge, Jintao Ren, Maiken Haislund Guldberg, Ole Nørrevang, Ulrik Vindelev Elvstrøm, and Stine Sofia Korreman, ”RadDeploy: A framework for integrating in-house developed models seamlessly into radiotherapy workflows”, Physics in Imaging and Radiation Oncology 31:100607, doi: 10.1016/j.phro.2024.100607, 2024.

Figure 1: Left column results for GTV-T; right column results for GTV-N. The three rows from top to bottom show DSC, sDSC, and APL. Inferiority margin comparison is shown for DSC and sDSC, and p-values are stated for all group comparisons.

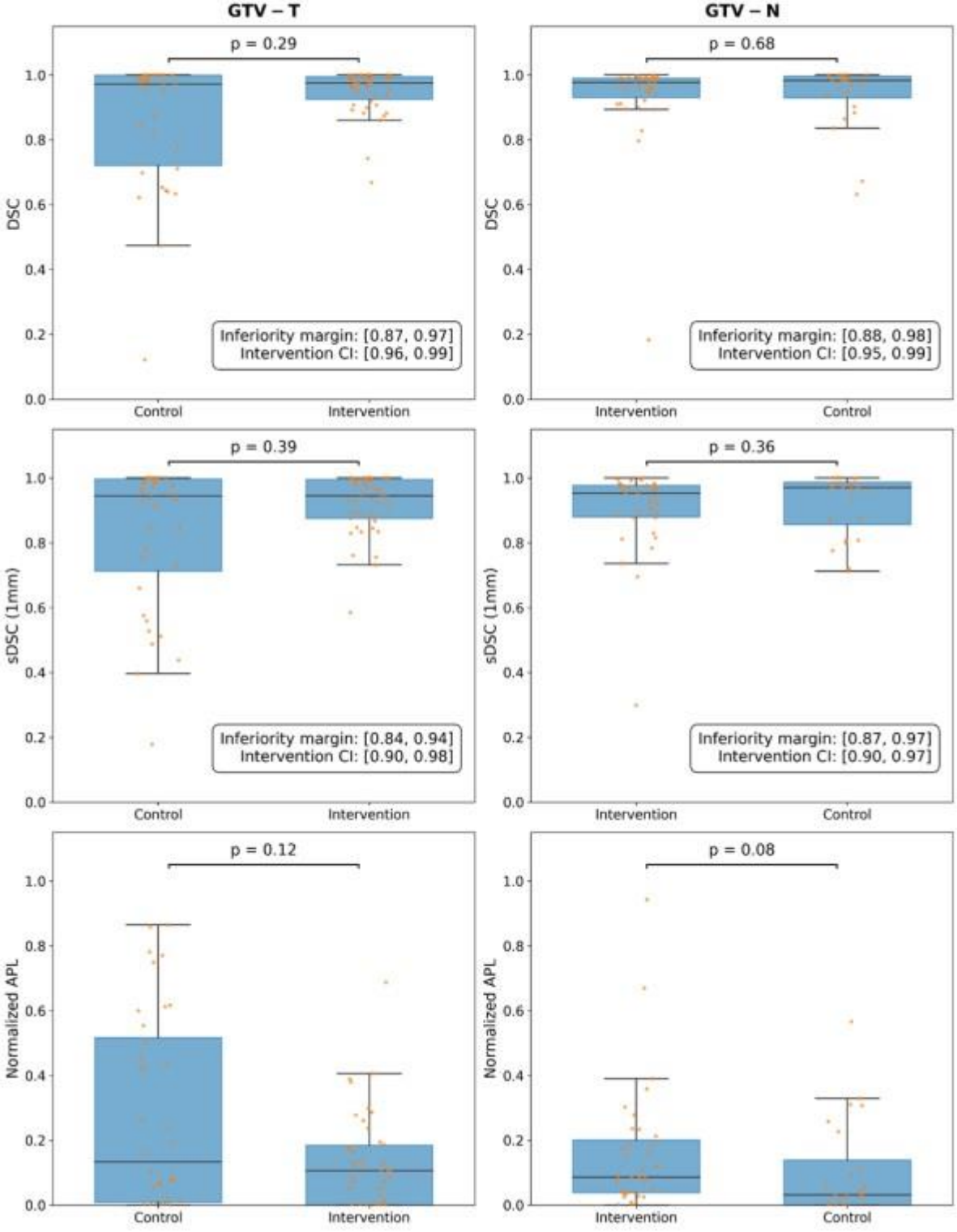

# Abstracts session 4:
# Reirradiation - possibilities and pitfalls

**A comprehensive national audit of radiotherapy retreatment numbers, sites and indications**

Morten Nielsen[1], Vibeke Nordmark Hansen[2,3],Laura Patricia Kaplan[4], Mai-Britt Linaa[5], Mikkel Drøgemüller Lund[6], Martin Skovmos Nielsen[7,8], Wiviann Ottosson[9], Cécile Peucelle[2], Laura Ann Rechner[9], Heidi S. Rønde[10], Tine Schytte[1,11], Weronika Maria Szejniuk[7,8], Rebecca Jean Tobin[2], Lone Hoffmann[5,12,*], Ane Appelt[13,*]

1) Department of Oncology, Odense University Hospital, Odense, Denmark
2) Department of Oncology, Centre for Cancer and Organ Diseases, Copenhagen University Hospital - Rigshospitalet, Copenhagen, Denmark
3) Royal Marsden NHS Foundation Trust, Sutton, Surrey, UK
4) Department of Oncology and Palliative Units, Zealand University Hospital, Næstved, Denmark
5) Department of Oncology, Aarhus University Hospital, Aarhus, Denmark
6) Department of Oncology, Vejle Hospital, University Hospital of Southern Denmark, Vejle, Denmark
7) Department of Oncology & Clinical Cancer Research Center, Aalborg University Hospital, Aalborg, Denmark
8) Department of Clinical Medicine, Aalborg University, Aalborg, Denmark
9) Department of Oncology, Radiotherapy Research Unit, Copenhagen University Hospital - Herlev and Gentofte, Herlev, Denmark
10) Danish Centre for Particle Therapy, Aarhus University Hospital, Denmark
11) Department of Clinical Research, University of Southern Denmark, Odense, Denmark
12) Department of Clinical Medicine, Aarhus University, Aarhus, Denmark
13) Leeds Institute of Medical Research, University of Leeds, UK

*) Shared last authorship

## Introduction

The number of retreated and reirradiated patients is increasing nationally and internationally. As a precursor to a prospective national Danish reirradiation registry, a comprehensive national audit of reirradiation courses in 2023 was performed, with an analysis of changes relative to preceding years.

## Materials and methods

Radiotherapy retreatment courses in 2023 were audited by all (eight) radiotherapy centers in Denmark. Furthermore, six centers extended the evaluation to include 2021-22, and two centers included 2014, 2015, 2017, and 2019. Reirradiation courses were classified as Type 1 (ie. overlap between irradiated volumes) and Type 2 (ie. concern for accumulated doses) [1]. One center identified and annotated reirradiations prospectively to facilitate subsequent retrieval, while the other seven retrospectively extracted data from Record & Verify and treatment planning systems, combined with manual evaluation. Treatments were stratified into curative/ablative treatments and palliative treatments by prescription dose, with prescriptions up to 30 Gy/10 fractions (F) (ie. 32.5 Gy EQD2 with $\alpha/\beta = 10$ Gy) assumed palliative except for specific cases (eg. lymphomas and preoperative rectum cancer). Stereotactic radiotherapy in oligometastatic disease is considered curative/ablative.

## Results

The total number of radiotherapy patients at all Danish centers in 2023 was 17,873. Of these, 2,829 received at least one retreatment course, of which 1,316 represented reirradiation type 1 or type 2; 907 with curative intent and 518 with palliative intent.

From 2014 to 2023 the number of retreated patients and the fraction of all treated patients they constitute, as well as the number of palliative and curative reirradiation treatment plans, generally increased (Figure 1).

The audit found large variation in the dose prescriptions and fractionation numbers used for reirradiation (176 different dose prescriptions), with smaller variation for palliative (58 different prescriptions) than for curative/ablative regimes (140 different prescriptions). Certain prescriptions were widely used such as 8 Gy/1 F, 20 Gy/4 F, 30 Gy/10 F in palliative reirradiations; 20 Gy/1 F or 27 Gy/3 F in brain stereotactic reirradiations; 45 Gy /3 F in stereotactic oligometastatic lung reirradiations; and a variety of curative treatments to full definitive doses adhering to national guidelines or trials.

Palliative type 1/type 2 reirradiations were primarily thoracic (26%), spine (22%) and abdominal/pelvic (22%) and curative/ablative type 1/type 2 reirradiations were primarily breast (23%), lung stereotactic treatments (22%) and brain stereotactic treatments (14%).

## Conclusions

An increasing number of patients are receiving reirradiation in Denmark over the years. For reirradiation, dose prescription and fractionation schemes vary widely.

Figure 1:

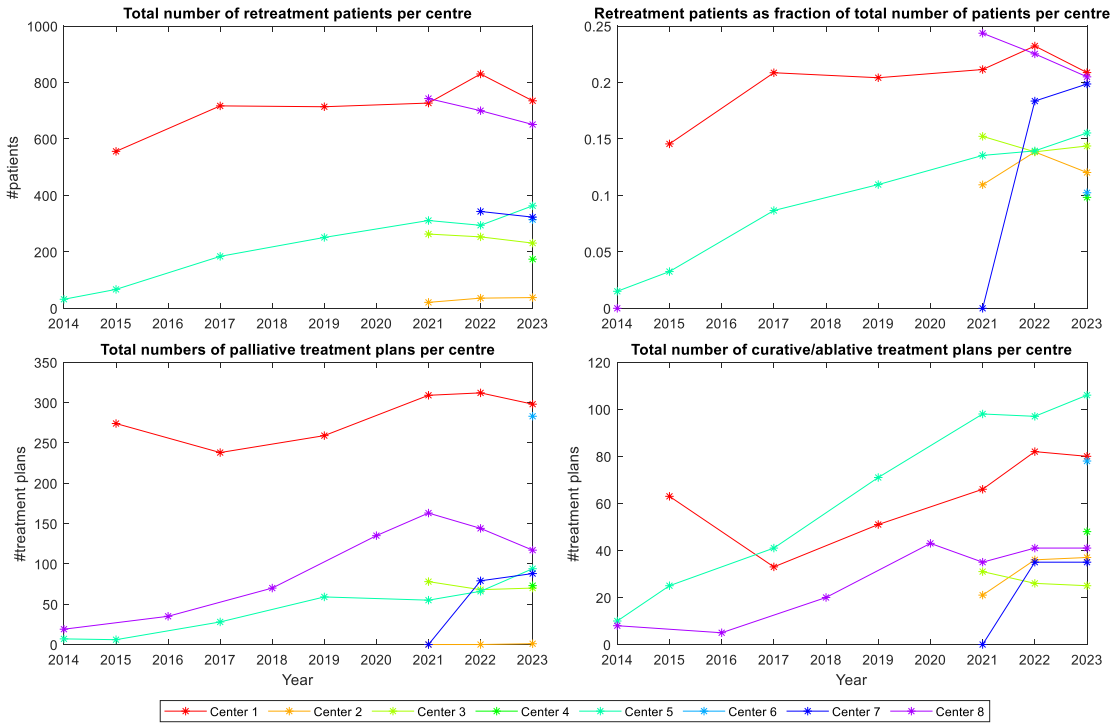


Figure text:

The graphs show for each year and each radiotherapy center, the total number of retreated patients, the number of patients receiving retreatment divided by the total number of patients, as well as the number of palliative and curative treatment plans delivered as type 1 or type 2 reirradiations.

Reference:

[1] Andratschke et al. European Society for Radiotherapy and Oncology and European Organisation for Research and Treatment of Cancer consensus on re-irradiation: definition, reporting, and clinical decision making. Lancet Oncol. 2022 Oct;23(10):e469-e478.

# Acute toxicity and Quality of Life in the ReRad II trial on dose-escalated proton reirradiation for locally recurrent rectal cancer


## Authors and affiliations

Truelsen C.G[a,b,c], Rønde H.S[a], Kallehauge J.F[a,c], Szpejewska J.E.[d], Bahij R[e], Diness L. V.[f], Bjerregaard J.K.[g], Poulsen L.Ø[h], Havelund B.M[i], Pedersen B.G[c,j], Iversen L.H[c,k], Spindler K.G[b,c], Kronborg C.S[a,c]

a. Danish Centre for Particle Therapy, Aarhus University Hospital, Aarhus, Denmark
b. Department of Oncology, Aarhus University Hospital, Aarhus, Denmark
c. Department of Clinical Medicine, Aarhus University, Aarhus, Denmark
d. Næstved, Department of Oncology, Zealand University Hospital, Næstved, Denmark
e. Department of Oncology, Odense University Hospital, Odense, Denmark
f. Department of Oncology, Copenhagen University Hospital - Herlev and Gentofte, Herlev, Denmark
g. Department of Oncology, Copenhagen University Hospital - Rigshospitalet, Copenhagen, Denmark
h. Department of Oncology, Aalborg University Hospital, Aalborg, Denmark
i. Department of Oncology, University Hospital of Southern Denmark, Lillebaelt Hospital, Vejle, Denmark
j. Department of Radiology, Aarhus University Hospital, Aarhus, Denmark
k. Department of Gastrointestinal Surgery, Aalborg University Hospital, Aalborg, Denmark

**Email-addresses of first author**:
Truelsen C.G: chtrue@rm.dk

**Background**:

Locally recurrent rectal cancer (LRRC) in previously irradiated patients presents a clinical challenge due to limited treatment options and the risk of cumulative toxicity. Intensity-Modulated Proton Therapy (IMPT) allows for dose escalation, which may improve tumour control while reducing dose exposure to surrounding organs at risk (OARs). However, prospective data on toxicity as well as patient-reported outcomes (PROs) and quality of life (QoL) in this setting remain limited.

**Materials and Methods**:

A planned interim analysis of the prospective phase II trial, ReRad II (ClinicalTrials.gov ID NCT04695782), evaluates acute toxicity and PROs in the initial 25 patients treated with dose-escalated IMPT for LRRC. Patients received 55 Gy (RBE) in 44 fractions (neoadjuvant) or 57.5–65 Gy (RBE) in 46–52 fractions (definitive). The clinical target volume (CTV) encompassed the gross tumour volume (GTV) with a 1 cm isotropic margin, adjusted for anatomical barriers. Acute toxicity was graded according to NCI-CTCAE v5.0, and dosimetric parameters were correlated with toxicity outcomes. PROs were evaluated by linear mixed model analysis using EORTC QLQ-C30 and QLQ-CR29 completed at pretreatment, during treatment, and at 3 months follow-up. PRO completion rates ranged from 100 % to 79 %.

**Results**:

In 25 patients, 49 GTVs were delineated, forming 29 CTVs. The median reirradiated CTV volume was 84.2 cm3 (range: 14.6-586.9). Bladder, bowel bag, and bowel loops had median $D_{mean}$ values of 7.5, 1.8, and 11.5 Gy(Relative biological effectiveness(RBE)), with $D_{0.03cc}$ of 58.1, 59.9, and 59.3 Gy(RBE), respectively, reflecting proximity to the target. Treatment-related acute toxicity of grade ≥3 (ileus) was reported in 2/25 patients, both with pre-existing ileus episodes. Urinary retention was significantly associated with bladder $D_{0.03cc(Gy)}$ ($p = 0.048$), whereas bowel dose parameters were not predictive of toxicity. PROs demonstrated stable global health status (pretreatment (PT): mean 68.3 [95% CI: 61.2–75.5], post-radiotherapy: mean 71.1 [95% CI: 65.6–76.6], three months post-treatment: mean 65.0 [95% CI: 59.0–71.0]). Other functional scores remained unchanged, while significant improvement was reported for emotional and cognitive functioning, presented in Figure 1.

**Conclusion**:

This planned interim analysis supports the continuation of the trial, demonstrating that dose-escalated proton reirradiation for LRRC is feasible with a manageable acute toxicity profile and preserved patient-reported QoL. This dataset represents the largest prospective study conducted on proton reirradiation for LRRC. Ongoing trial recruitment and further follow-up will provide long-term toxicity and local control outcomes, guiding future treatment strategies.

Figure 1: EORTC QLQ-C30 functional (A) and symptom (B) scales estimated using a linear mixed model analysis, reported as predicted mean scores with 95% confidence intervals. Higher functional scores signify better functioning, whereas higher symptom scores indicate a greater severity of symptom burden.

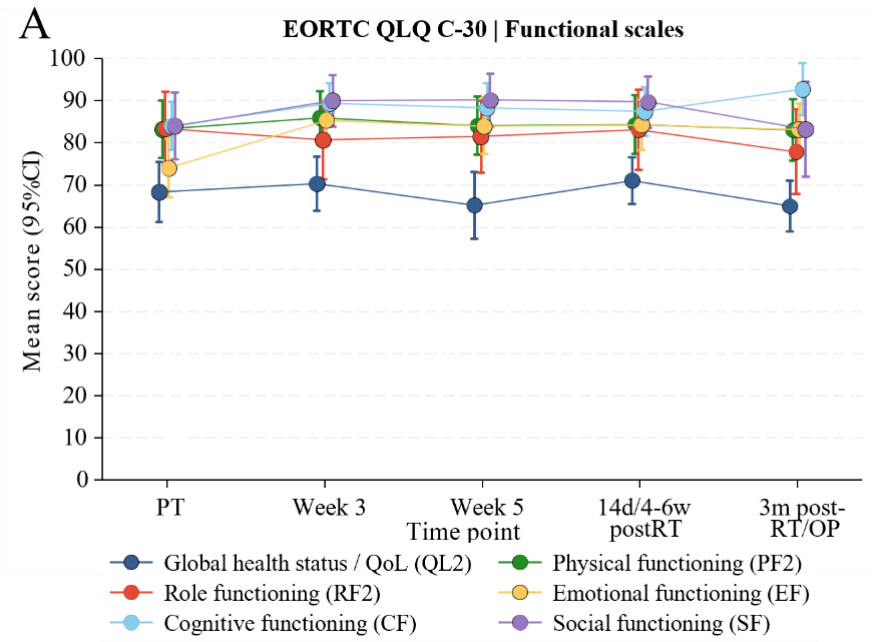


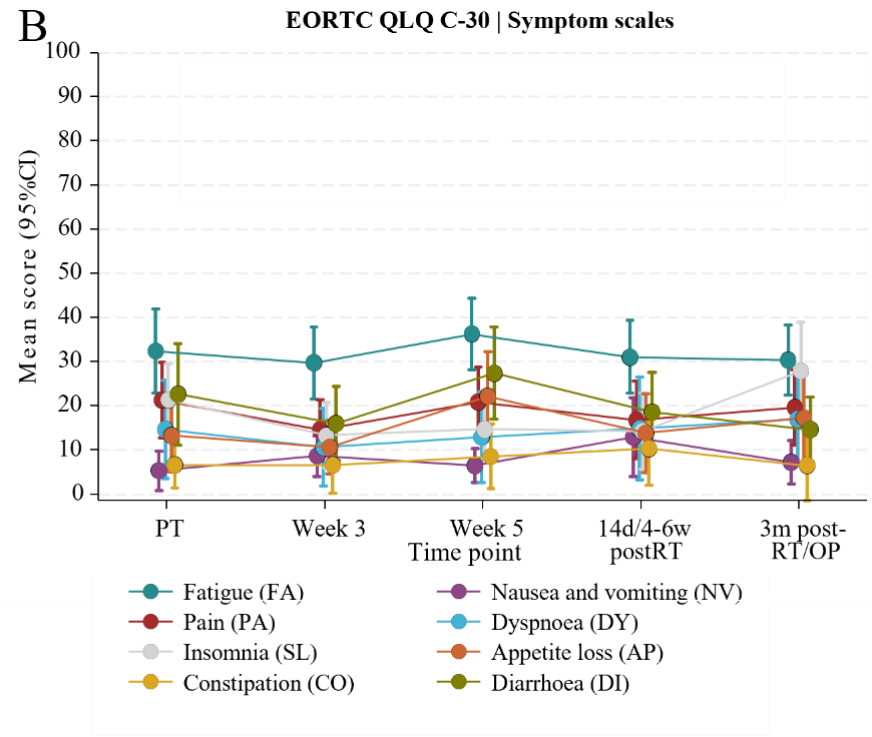

# Abstracts session 5:
# Pitch your study (upcoming prospective studies)

**Management of second ipsilateral breast tumor event: An advocacy for a randomized trial**

Jean-Michel Hannoun-Levi
jean-michel.hannoun-levi@nice.unicancer.fr

J.-M. Hannoun-Lévi (a), A. Savignoni (b), J.-G. Féron (c), C. Malhaire (d), C. Ezzili (e), A. Brédart (f), P. Loap (g), Y. Kirova (g)

a) Department of Radiation Oncology, centre Antoine-Lacassagne, université Côte d'Azur, Nice, France
b) Department of Biostatistics, institut Curie, Paris, France
c) Department of Breast Surgery, institut Curie, Paris, France
d) Department of Medical Imaging, institut Curie, Paris, France
e) Department of Clinical Research, institut Curie, Paris, France
f) Psycho-Oncology Unit, institut Curie, Paris, France
g) Department of Radiation Oncology, institut Curie, Paris, France

For a second ipsilateral breast tumor event, salvage mastectomy is the standard of care while second conservative treatment is a possible option. However, level 1 proofs are missing, leading to perform salvage mastectomy for patients who could receive second conservative treatment and consequently avoid psychological/quality of life salvage mastectomy deleterious impacts. A phase 3 randomized trial comparing salvage mastectomy to second conservative treatment is needed. Here we discuss what would be to us the optimal design of such trial to confirm the non-inferiority between the two salvage options, with a focus on methodological aspects in terms of patient characteristics and statistical issues.

**RAdiotherapy with FDG-PET guided Dose-PAINTing compared with standard radiotherapy for primary head and neck cancer-3 (RADPAINT-3) â€“ Randomized, multi-center phase II trial**

Dale Einar (1), Amdal Cecilie D (1), Furre Torbjørn (2), Thomassen Solveig U (1), Tulipan Andreas J (3, 4), Hellebust Taran P (2), Eide Hanne A (1), Bratland Åse (1), Alsaker Mirjam D (5), Brydøy Marianne (6), Lyng Heidi (7, 8), Malinen Eirik (7, 8)

(1) Dept of Oncology, Oslo University Hospital (OUS), Oslo, Norway, (2) Dept of Medical Physics, OUS, Oslo, Norway, (3) Dept of Radiology and Nuclear Medicine, OUS, Oslo, Norway, Dept of Radiology, (4) Nuclear medicine/PET-centre, Haukeland University Hospital, Bergen, Norway (5) Dept of Oncology, Haukeland University Hospital, Bergen, Norway, (6) Dept of Oncology, St Olavs Hospital, Trondheim, Norway, (7) Institute for Radiation Research, OUS, Oslo, Norway, (8) Dept of Physics, University of Oslo, Oslo, Norway

**Presenting author:** Einar Dale, eindal@ous-hf.no

**Introduction**: Dose painting of radioresistant tumor regions can increase the chance of cure with minimized radiation-induced toxicity for head and neck cancer (HNC) patients with poor prognosis. The objective of the RADPAINT-3 trial is to investigate whether dose painting is safe compared to standard radiotherapy (RT).

**Methods:** RADPAINT-3 (NCT06297902) is a randomized, non-inferiority, multi-center phase II study, initiated at Oslo University Hospital, accruing from August 2024. The main inclusion criterion is patients with HPV-unrelated HNC with poor prognosis. The primary endpoint is frequency of grade ≥ 3 (CTCAE v5.0) mucosal ulcers one year after treatment. The expected inclusion period is three years, total study duration is six years and planned inclusion number is 100 patients. The collaborating sites are Haukeland University Hospital (Bergen) and St Olavs Hospital (Trondheim). Patients will be randomized 1:1 to either standard RT (2 Gy x 34) or dose painting (Figure 1). All patients will have FDG-PET/CT prior to RT. In the experimental arm, we will escalate the dose to the FDG-avid, hypermetabolic part of the tumor (maximum point dose 83.3 Gy). Dose painting will be applied to these regions during the first half of the fractionated treatment (17 of 34 fractions). We will select patients for proton therapy after comparative treatment planning, proton vs photon. If the calculated reduction in normal tissue complication probability (NTCP of dysphagia and xerostomia, grade ≥ 2) is larger than 10%, the patient will be offered proton therapy, either as dose-painting or standard RT. The RADPAINT-3 trial includes translational research, where we aim to elucidate underlying mechanisms related to the RT effect by investigating cytokine levels in repetitive blood samples to potentially predict tumor response and toxicity.

**Results:** As of March 2025, 20 patients have been enrolled. Nineteen patients received treatment as per protocol, while one withdrew consent before treatment.

**Discussion:** The ultimate aim is to optimize the balance between disease control and toxicity for a high-risk group of patients with HNC. If RADPAINT-3 shows that there is no excess toxicity, we will continue the study with local control at 1 year after RT as the new primary endpoint. Power analysis show that we will need in total 182 evaluable patients. The translational research will then be extended to investigate gene expression data from pre-therapy routine tumor biopsies and correlate this with the analysis of blood samples and tumor control.

**Figure 1**

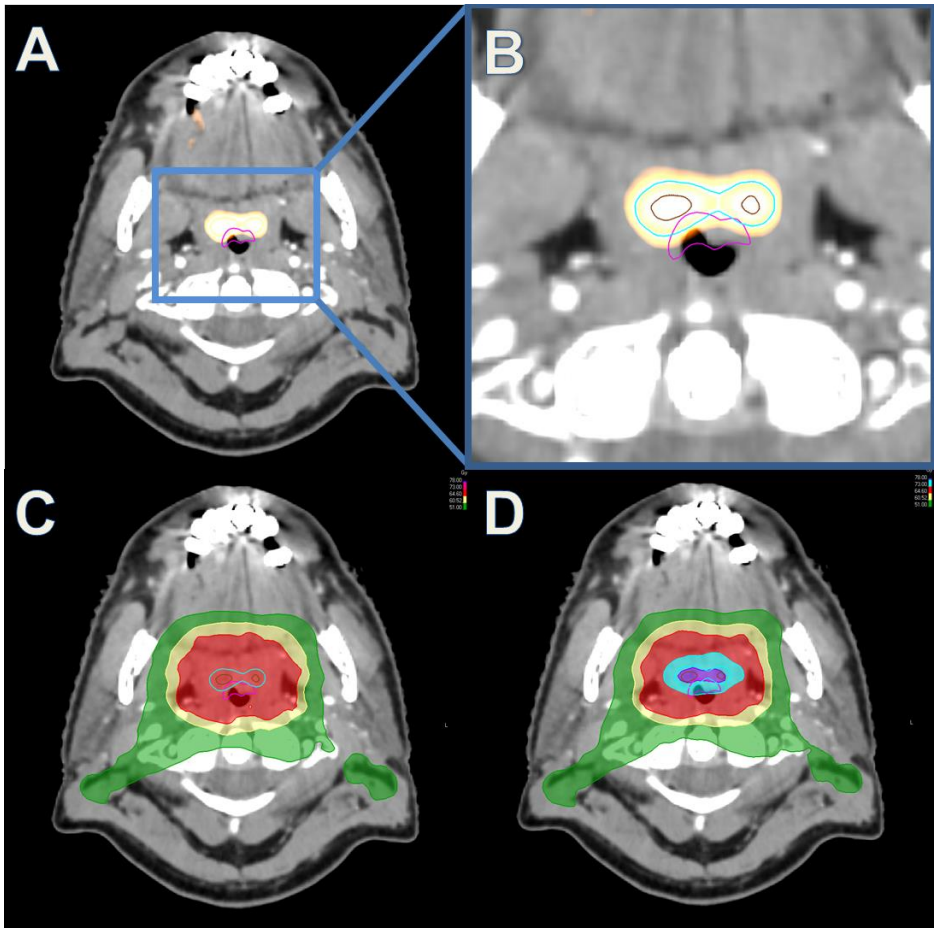


(A) FDG/PET CT showing the high uptake region of the primary tumor (stage T2 N0 M0, HPV negative tonsillar carcinoma). (B) Delineations; Cyan; Prescription volume PV33, Brown; PV66 (C) Dose distribution of a standard plan. Green isodose ; 54 Gy. Yellow isodose; 64 Gy. Red isodose; 68 Gy. (D) Dose distribution from the dose painting plan. In addition to the standard isodoses the cyan isodose; 73.1 Gy and the purple isodose; 78.2 Gy.

# DAHANCA 41: A national randomised trial using 0 vs 5 millimetres high-dose CTV margin for primary radiotherapy of Head and Neck Squamous Cell Carcinomas

Ruta Zukauskaite[1], Jesper Grau Eriksen[2], Anne Ivalu Holm[3], Mogens Bernsdorf[4], Bob Smulders[4], Mohammad Farhadi[5], Eva Samsøe[5], Camilla Kjaer Lonkvist[6], Patrik Sibolt[6], Maria Andersen[7], Martin Skovmos Nielsen[7], Cai Grau[8], Jens Overgaard[2], Christian Rønn Hansen[8,9,10]

Affiliations

1) Department of Oncology, Odense University Hospital, Odense, Denmark;

2) Department of Experimental Clinical Oncology, Aarhus University Hospital, Aarhus, Denmark;

3) Department of Oncology, Aarhus University Hospital, Denmark;

4) Department of Clinical Oncology, Rigshospitalet, Denmark;

5) Zealand University Hospital, Department of Oncology, Næstved, Denmark;

6) Department of Oncology, Herlev and Gentofte Hospital, University of Copenhagen, Herlev, Denmark

7) Department of Oncology, Aalborg University Hospital, Denmark

8) Danish Centre for Particle Therapy, Aarhus University Hospital, Aarhus, Denmark

9) Odense University Hospital, Laboratory of Radiation Physics, Odense, Denmark;

10) University of Southern Denmark, Department of Clinical Research, Odense, Denmark

**Background**

Primary radiotherapy is a cornerstone in the treatment of head and neck squamous cell carcinoma (HNSCC), with clinical target volume (CTV) margins traditionally added to the gross tumour volume (GTV) to account for microscopic spread. The standard 5 mm high-dose CTV margin has been widely adopted but is based on consensus rather than prospective evidence. Retrospective analyses suggest that most recurrences occur within the GTV, independent of CTV margins and that reducing margins may lower toxicity without compromising local control. DAHANCA 41 is a prospective, multicenter, randomised non-inferiority trial designed to test whether omitting the high-dose CTV margin (0 mm) can maintain tumour control while reducing radiation-related toxicity.

**Methods**

This phase III trial will randomise approximately 1,600 patients 1:1 to receive definitive radiotherapy with either a 0 mm (GTV=CTV1) or 5 mm (GTV+5 mm=CTV1) high-dose margin. All other treatment aspects, including elective nodal irradiation and systemic therapy, follow standard DAHANCA guidelines. The primary endpoint is 3-year loco-regional control, with non-inferiority defined by a threshold of 5%. Secondary endpoints include acute and late toxicity, patient-reported outcomes (PROs), disease-free survival, and overall survival. Acute toxicity will be assessed using standardised DAHANCA clinician-rated forms and PROs at treatment end and post-treatment (weeks 2 and 8). Late morbidity and functional outcomes will be evaluated at regular intervals up to 10 years. Radiotherapy quality assurance is ensured through centralised review and adherence to DAHANCA contouring guidelines.

**Discussion**

If proven non-inferior, a 0 mm CTV margin could become the new standard for HNSCC radiotherapy, potentially reducing swallowing dysfunction, xerostomia, and overall treatment burden without compromising tumour control. This study presents a unique opportunity to refine treatment strategies, enhancing oncologic efficacy and quality of life. DAHANCA 41 is open for international participation, and accredited centres are invited to join. The collaboration will ensure robust, practice-changing data applicable across multiple treatment settings. By participating, centres contribute to advancing head and neck cancer care, gaining early experience with a potentially paradigm-shifting radiotherapy approach.

**ERADICATE: A randomised trial to test Early magnetic resonance imaging-guided RADIotherapy ablation of loCAlly advanced pancreaTic cancEr**

Uffe Bernchou[1,2], Rana Bahij[3], Mathilde Weisz Ejlsmark[2,3], Faisal Mahmood[1,2], Anders Bertelsen[1], Carsten Brink[1,2], Tine Schytte[2,3], and Per Pfeiffer[2,3]

1 Laboratory of Radiation Physics, Department of Oncology, Odense University Hospital, Odense, Denmark.

2 Department of Clinical Research, University of Southern Denmark, Odense, Denmark

3 Department of Oncology, Odense University Hospital, Odense, Denmark.

**Introduction**

Current management of locally advanced pancreatic cancer (LAPC) involves up to six months of chemotherapy, possibly followed by chemoradiation if resectability is not achieved. This regimen was developed in an era when radiotherapy (RT) was delivered in five to six weeks. However, ablative magnetic resonance image-guided RT (MRIgRT) prescribed in five fractions has shown to be safe and effective in LAPC and could be delivered up-front without noteworthy delay of the chemotherapy. The only evidence for up-front ablative RT in pancreatic cancer comes from a retrospective analysis of early-stage, medically inoperable patients, showing longer overall survival compared to induction chemotherapy followed by RT (Zhu X et al. Cancer Manag Res. 2018;10:1295-304). Up-front ablative RT followed by chemotherapy has not been attempted in LAPC, and we therefore propose the ERADICATE trial to test this approach.

**Materials and methods**

ERADICATE is a randomized, phase II trial, with a pick-the-winner design. Patients will be staged at multidisciplinary tumour boards and immediately randomized 1:1 between two arms. The standard arm comprises chemotherapy potentially followed by MRIgRT. The experimental arm comprises MRIgRT within three weeks of randomization, followed by chemotherapy starting no later than week four (see figure 1). Resection followed by adjuvant chemotherapy will be performed in either arm at any stage if possible.

The primary endpoint is overall survival. Secondary endpoints include health-related quality of life, patient-reported symptoms, time to locoregional failure, time to distant metastases, and clinician-reported toxicity. The sample size calculation assumes a 30% and 40% two-year survival rate for the standard and experimental arm, respectively. By including a total of 128 patients (containing a 5% loss to follow-up), the study will pick the "correct" winner arm with a likelihood of 90% in case a survival difference of at least 10% at two years is present in nature.

**Results**

A protocol draft is currently being discussed among MRI-linac centres, and we invite all centres to participate. At Odense University Hospital, we are testing up-front ablative MRIgRT in patients with LAPC in a pilot study to ensure that chemotherapy supplied immediately after ablative RT does not induce unexpected toxicity.

**Conclusion**

Recent studies indicate that treating LAPC using ablative MRIgRT after induction chemotherapy is safe and can be delivered in only 1-2 weeks. We will test the use of up-front ablative MRIgRT for early local control of the primary tumour in newly diagnosed patients followed by chemotherapy in the randomized trial ERADICATE.

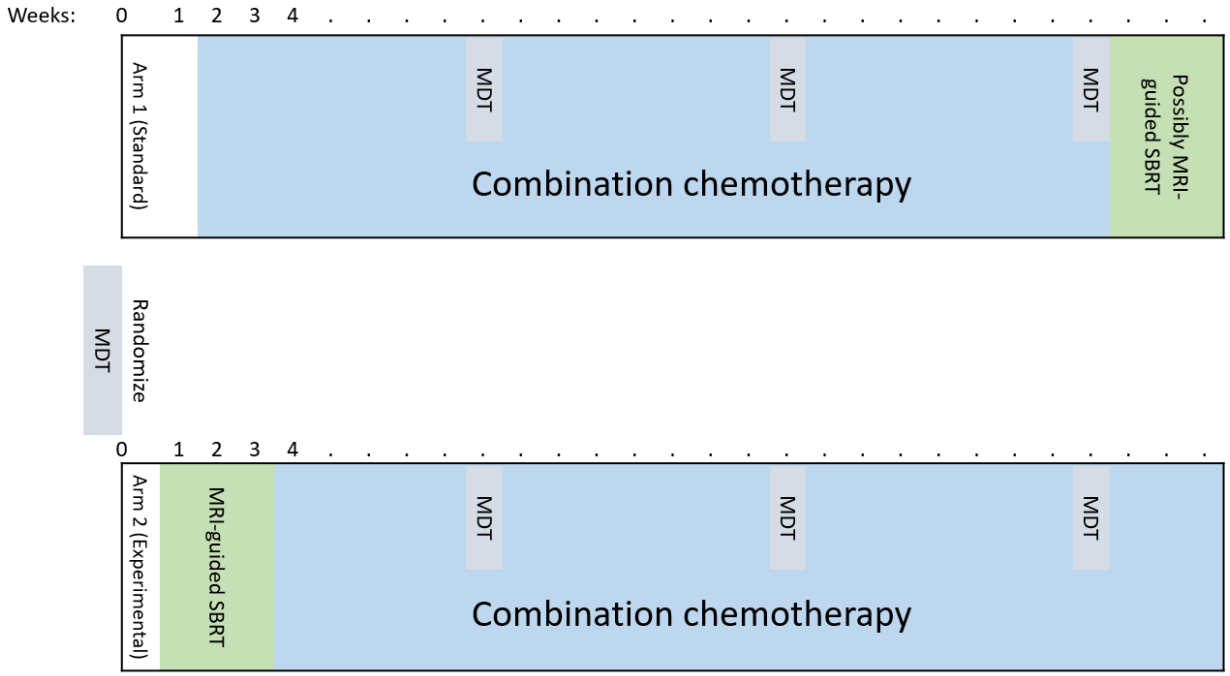


Figure 1: Study outline. The local guidelines determine the timing and frequency of MDTs.

# Pre-trial quality assurance and design of the NIELS trial: A phase III study of dose-escalated radiotherapy in patients with small cell lung cancer

**Author information:** Sara Linde[1,2], sarlin@rm.dk

Sara Linde [1,2], Ditte S. Møller [1,2], Mai-Britt Linaa [1], Ane Appelt [3], Erik Almhagen [4,5], Kenneth F. Hofland [6], Marianne M. Knap [1], Charlotte Kristiansen [7], Lotte H. Land [8,9], Christina Larsen [10], Nina Levin [11,12], Karin Lindberg [4,13], Mikkel D. Lund [7], Lars Merring-Mikkelsen [14], Tine B. Nielsen [15], Wiviann Ottosson [10], Gitte F. Persson [10,16], Hella M.B. Sand [14], Morten H. Suppli [17], Fernanda Villegas [4,5], Hjørdis H. Schmidt [1], Weronika M. Szejniuk [18,19], Lone Hoffmann[1,2]

[1]Department of Oncology, Aarhus University Hospital, Aarhus, Denmark
[2]Department of Clinical Medicine, Aarhus University, Aarhus, Denmark
[3]Leeds Institute of Medical Research, University of Leeds, Leeds, UK
[4]Department of Oncology-Pathology, Karolinska Institutet, Stockholm, Sweden
[5]Nuclear Medicine and Medical Physics, Karolinska University Hospital, Stockholm, Sweden
[6]Department of Oncology, Zealand University Hospital, Næstved, Denmark
[7]Department of Oncology, Vejle Hospital, University Hospital of Southern Denmark, Vejle, Denmark [8]Department of Oncology, Odense University Hospital, Odense, Denmark
[9]Department of Clinical Research, University of Southern Denmark, Odense, Denmark
[10]Department of Oncology, Copenhagen University Hospital – Herlev and Gentofte, Herlev, Denmark
[11]Department of Clinical and Molecular Medicine, Norwegian University of Science and Technology, NTNU, Trondheim, Norway
[12]Department of Oncology, St. Olavs Hospital, Trondheim, Norway
[13]Centre of Pulmonary Oncology, HHLH-section, Karolinska University Hospital, Stockholm, Sweden
[14]Department of Oncology, Aalborg University Hospital, Aalborg, Denmark
[15]Laboratory of Radiation Physics, Department of Oncology, Odense University Hospital, Odense, Denmark
[16]Department of Clinical Medicine, Copenhagen University, Copenhagen, Denmark
[17]Department of Oncology, Zealand University Hospital, Næstved, Denmark
[18]Department of Oncology & Clinical Cancer Research Center, Aalborg University Hospital, Aalborg, Denmark
[19]Department of Clinical Medicine, Aalborg University, Aalborg, Denmark

## Introduction

The Nordic trial of Inhomogeneous dose Escalated radiotherapy for patients with Limited disease Small cell lung cancer (NIELS) will investigate if dose-escalation (as high as possible up to a mean dose of 80Gy in 40 fractions (fx), twice daily delivered (BID)), will improve survival for patients with limited disease small cell lung cancer (LD-SCLC). Because dose-escalation is potentially harmful, robust pre-trial radiotherapy quality assurance (QA) is essential. The pre-trial QA study aimed to examine the feasibility of the planned dose-escalation in the NIELS trial in a multicenter setting.

## Materials and Methods

To be eligible for the NIELS trial, patients with LD-SCLC must be candidates for the current Nordic standard radiotherapy treatment of 60Gy/40fx BID. When included in the primary

cohort, patients will be randomized between current standard treatment and the experimental inhomogeneously dose-escalated treatment up to 80Gy/40fx BID, Figure 1. Seven Nordic centers participated in the pre-trial QA of the dose-planning approach. Five cases were distributed with target and organs at risk (OAR) delineations. All centers created a standard dose plan and an escalated dose plan for all five cases. Achievable dose-escalation was examined, and doses to OAR were compared using a random effects generalized linear model, with case and radiotherapy center as random effects.

**Results**

All primary tumors (GTVp) and involved lymph nodes (GTVn) could be escalated beyond standard dose; the escalation-level was limited by proximity to OAR, especially for GTVn. The median of the escalated mean dose [minimum-maximum] was 79.6Gy [76.9-81.0] and 75.8Gy [68.3-81.1] for GTVp and GTVn, respectively. There were three separate breaches of mandatory constraints for OAR, all on escalated plans. The median mean lung dose (MLD) was 13.4Gy [6.9-17.0] for standard plans and 14.1Gy [7.0-17.6] for escalated plans. The pair-wise median difference was 0.3Gy, and the difference in MLD was statistically significant
($p=0.013$), though clinically small. There were no other statistically significant differences in doses to OAR between the standard and escalated plans.

**Conclusion**

This pre-trial QA study found that inhomogeneous dose-escalation up to 80Gy/40fx BID was feasible while respecting mandatory dose constraints for OAR. Only small OAR dose differences were found between standard and escalated plans, and based on this, minimum excess toxicity for the experimental arm is expected for the NIELS trial.

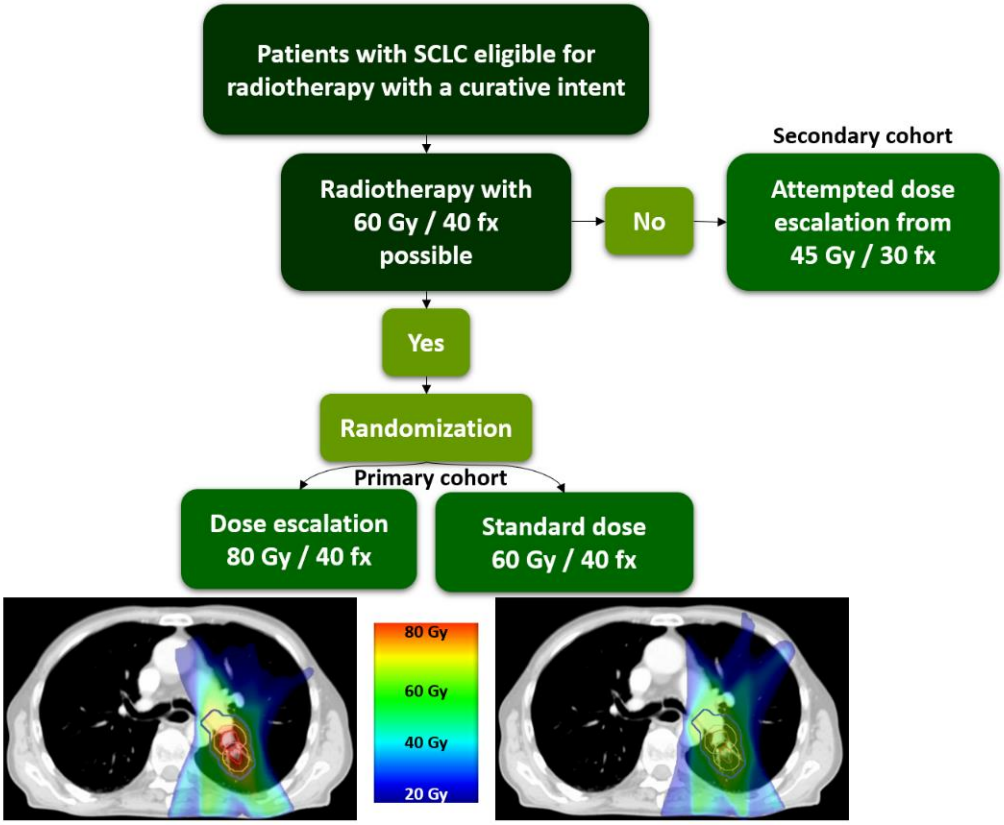


**Figure 1**. NIELS trial design. If standard treatment of 60Gy/40fx BID is possible within OAR constraints, patients are randomized 1:1 between dose-escalation (experimental arm) and standard dose (standard arm). If standard treatment is not possible, patients are enrolled in a secondary cohort, where dose-escalation is attempted as high as possible from 45Gy/30fx BID. At the lower pane, the dose distribution in dose color wash is shown on the CT scan for the escalated and the standard plan - Delineation of GTVs (red), CTV (orange), and PTV (blue) is shown.

# Abstracts session 6:
# Late effects in particle therapy of CNS tumors

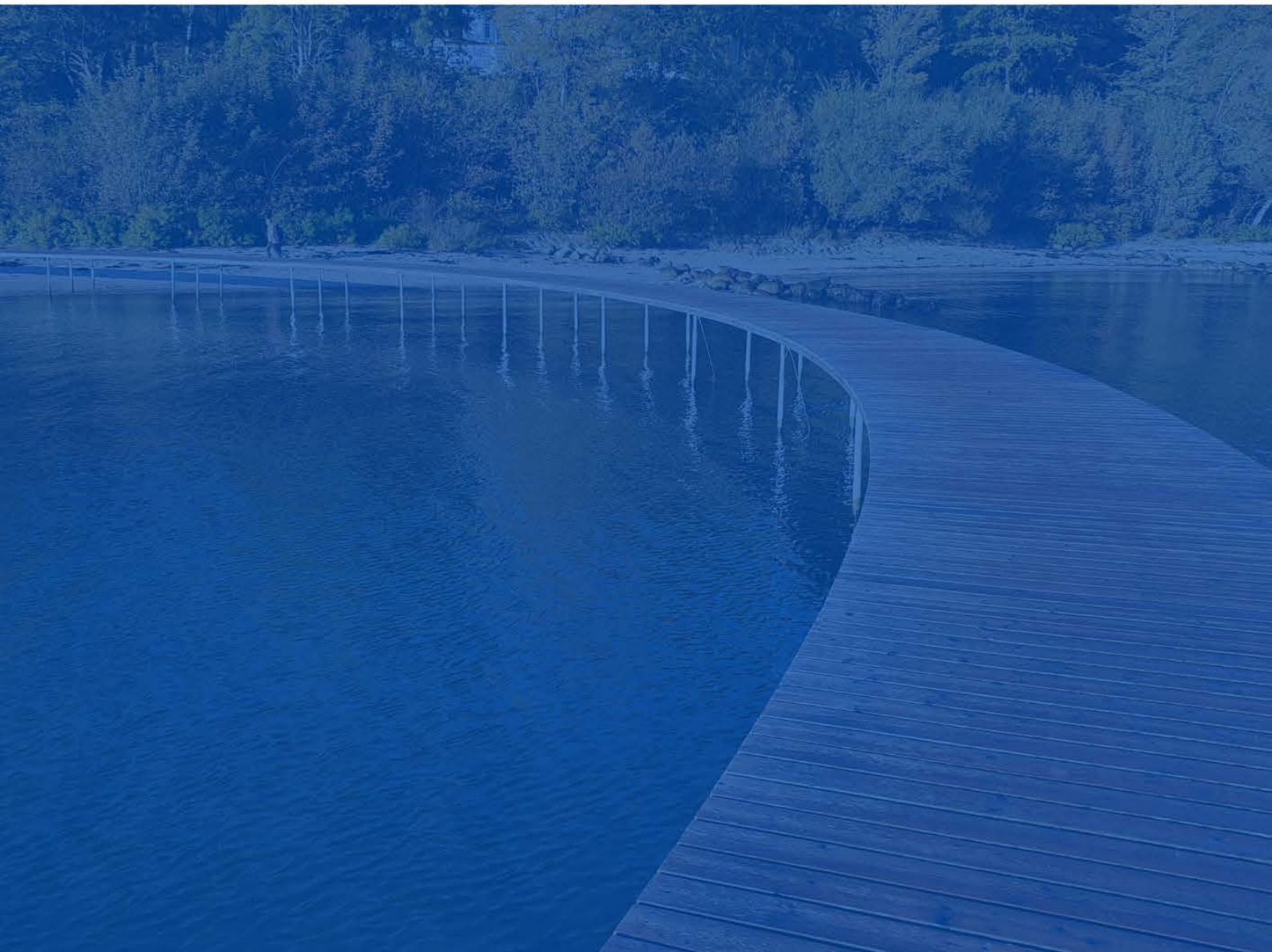

**Impact of radiation dose on neurocognitive function and quality of life in long-term childhood brain tumor survivors**

Laura Toussaint[1,2,*], Anne Sophie Lind Helligsø[3], Ali Amidi[4], Rikke Hedegaard Dahlrot[5,6], Louise Tram Henriksen[3], Maja Vestmø Maraldo[7,8], Ludvig Paul Muren[1,2], Martin Skovmos Nielsen[9], Anouk Trip[1], Lisa Maria Wu[3,10], Yasmin Lassen-Ramshad[1]

1. *Danish Centre for Particle Therapy, Aarhus University Hospital, Aarhus, Denmark*
2. *Department of Clinical Medicine, Aarhus University, Aarhus, Denmark*
3. *Department of Pediatrics and Adolescent Medicine, Aarhus University Hospital, Aarhus, Denmark*
4. *Unit for Psychooncology & Health Psychology, Department of Psychology and Behavioral Sciences, Aarhus University, Aarhus, Denmark*
5. *Department of Oncology, Odense University Hospital, Odense, Denmark*
6. *Department of Clinical Research, University of Southern Denmark, Denmark*
7. *Department of Oncology, Copenhagen University Hospital - Rigshospitalet, Copenhagen, Denmark*
8. *Department of Clinical Medicine, University of Copenhagen, Copenhagen, Denmark*
9. *Department of Oncology, Aalborg University Hospital and Clinical Cancer Research Center, Aalborg, Denmark*
10. *Department of Psychology, Reykjavik University, Reykjavik, Iceland*

**contact email: lautou@rm.dk*

**Introduction:** Long-term survivors of a childhood brain tumor are at risk of developing late effects such as neurocognitive impairment, potentially impacting their quality of life (QoL). Patients treated with radiotherapy (RT) often exhibit neurocognitive impairment in some domains and report a lower overall QoL later in life. However, RT dose-effect relationships for specific subareas of the brain remain to be unraveled. The aim of this study was, therefore, to explore the potential impact of RT dose to organs at risk (OARs) on neurocognitive function and QoL in a nationwide cohort of long-term childhood brain tumor survivors.

**Material and methods:** For a total of 132 childhood brain tumor survivors diagnosed from 2001 - 2017 at all four Danish RT centers admitting children, neurocognitive assessments and QoL data were collected at least 5-years post-diagnosis. Of the total cohort, 17 patients were excluded due to non-retrievability of RT-plans, 29 for incomplete neurocognitive assessment, and 8 for incomplete QoL questionnaires. Neurocognitive scores were therefore analyzed for 86 patients (61 non-RT/25 RT) and QoL scores for 107 (79 non-RT/28 RT). Two-sided Mann Whitney U-tests were used to compare neurocognitive and QoL outcome between non-RT and RT groups. If significant differences were identified, OAR-specific linear regression models with backward selection were performed to evaluate dose effects while adjusting for potential confounders, including whole-brain irradiation, age at treatment, sex, chemotherapy, surgery, hydrocephalus and time since diagnosis. The tested dose metrics were mean dose (Dmean) to the brain,

supratentorial brain, cerebellum, brainstem, pituitary gland, hippocampus (left/right) and temporal lobe (left/right), as well as the volume of hippocampus (left/right) receiving 40 Gy (V40Gy) and the volume of brain receiving 30 Gy (V30Gy). The final predictive model was refined using robust linear regression with bootstrapping (1000 samples) to estimate the 95% confidence intervals, reducing reliance on normality assumptions.

**Results:** No statistically significant differences were observed between no-RT and RT groups on any of the neurocognitive test scores. However, QoL analysis showed that RT-treated patients had significantly lower scores in physical and social functioning (Table 1):

*Physical Functioning = 93.3 (90.7, 95.4) + -0.3 (-0.5, -0.1) x Pituitary Dmean*

*Social Functioning = 86.3 (80.3, 97.1) + -0.4 (-0.9, -0.1) x Left Hippocampus Dmean + 9.8 (1.3, 15.9) x Male(Yes=1/No=0) + 7.4 (-3.9, 22.9) x chemotherapy(Yes=1/No=0)*

**Conclusion:** These findings indicate that RT dose effects, particularly in the pituitary and left hippocampus, may contribute to reduced QoL in childhood brain tumor survivors.

*Table 1: Median [range] z-scores of neurocognitive outcomes/scores from the QoL questionnaires for survivors treated without vs. with radiotherapy. The p-values correspond to the Mann Whitney U-test. For all items, a higher score represents better functioning. Abbreviations: RT radiotherapy, TMT Trail Making Test, CCPT Conners' Continuous Performance Test, HVLT-R Hopkins Verbal Learning Test-Revised, COWAT Controlled Oral Word Association Test, QoL quality of life.*

| Domain | Test | No-RT | RT | p-value |
|---|---|---|---|---|
| **Processing speed** | **TMT-A** | -0.5 [-3.9 – 1.2] | -0.3 [-9.9 – 1.4] | 0.58 |
| | **Coding** | -0.7 [-3 – 1.3] | 0 [-3 – 15.3] | 0.20 |
| **Sustained attention** | **CCPT detectability** | -0.6 [-2.8 – 1.1] | -0.7 [-3.3 – 4.5] | 0.99 |
| | **CCPT omission** | -0.2 [-4 – 0.7] | -0.3 [-4 – 0.7] | 0.59 |
| | **CCPT commission** | 0.1 [-2 – 1.2] | -0.3 [-3.2 – 1.9] | 0.28 |
| **Attention and working memory** | **Digit span** | -0.7 [-1.7 – 1.7] | -0.3 [-2.7 – 2.3] | 0.20 |
| **Verbal learning and memory** | **HVLT-R total** | -1.5 [-3 – 1] | -0.8 [-3 – 1.4] | 0.30 |
| | **HVLT-R delayed** | -2.2 [-3 – 1.3] | -1.5 [-3 – 1] | 0.27 |
| | **HVLT-R retention** | -1.4 [-3 – 1.7] | -1.3 [-3 – 1.2] | 0.97 |
| **Verbal fluency** | **COWAT letter S** | 0 [-1.5 – 10.2] | 0 [-2.2 – 2.4] | 0.35 |
| | **COWAT Animals** | 0 [-2.5 – 1.8] | 0 [-2.1 – 3.4] | 0.93 |
| **Executive function** | **TMT-B** | -0.4 [-12.2 – 1.6] | -0.5 [-20 – 2.1] | 0.62 |
| **EORTC QLQ C30 questionnaires** | **Global QoL** | 75 [25 – 100] | 83.3 [41.7 – 100] | 0.21 |
| | **Physical functioning** | 93.3 [33.3 – 100] | 86.7 [33.3– 100] | <0.01* |
| | **Role functioning** | 100 [0 – 100] | 100 [33.3 – 100] | 0.39 |
| | **Emotional functioning** | 83.3 [25 – 100] | 91.7 [8.3 – 100] | 0.79 |
| | **Cognitive functioning** | 83.3 [0 – 100] | 83.3 [0 – 100] | 0.61 |
| | **Social functioning** | 100 [16.7 – 100] | 83.3 [0 – 100] | <0.01* |

# Spatial distribution of astrocytes as a late response to partial-brain proton irradiation in mice at different doses

Robin Hegering [1], Sindi Nexhipi [2,3], Antje Dietrich [2,3] and Armin Lühr [1]

[1] Department of Physics, TU Dortmund University, Dortmund, Germany
[2] OncoRay – National Center for Radiation Research in Oncology, Faculty of Medicine and University Hospital Carl Gustav Carus, Technische Universität Dresden, Helmholtz-Zentrum Dresden-Rossendorf, Germany
[3] German Cancer Consortium (DKTK), Partner Site Dresden, and German Cancer Research Center (DKFZ), Heidelberg, Germany

**Introduction:** In recent years, several clinical studies have reported unexpected late radiation-induced side effects in healthy brain tissue after proton therapy. There is speculation that a disruption of the blood-brain barrier (BBB) promotes the development of side effects, with astrocytes being one of the integral functional elements of the BBB. To investigate the brain's response to proton radiation, a preclinical mouse model was established at the University Proton Therapy Dresden. Based on data from this experiment, the impact of dose on the spatial distribution and number of astrocytes within the brain was examined.

**Methods:** Mice were irradiated with collimated (4 mm) proton beams, targeting the right hippocampus and stopping in the right hemisphere. After six months, they were sacrificed and the excised brains were axially cut and stained for glial acidic fibrillary protein (GFAP) to detect astrocytes (Fig. 1A). For mice irradiated with doses prescribed to the right hippocampus of 45 Gy, 65 Gy, 85 Gy, and 0 Gy (control), three mid-brain slices including the hippocampal region were considered. A pipeline was established to segment astrocytes after background subtraction and applying a threshold with ImageJ. For each segmented object, the centroid coordinates were calculated and counted within tiles of 100 µm × 100 µm. For statistical analysis, two rectangular regions of interest (ROIs) were defined centered along the beam axis (Fig. 1B,C): one in the right hemisphere (containing the high-dose region) and one in the left hemisphere (corresponding contralateral region).

**Results:** The astrocyte distribution within the 0 Gy control was highly symmetric in both hemispheres, mainly following anatomical structures (Fig. 1C). In contrast, a clear pattern of increased astrocyte numbers on the irradiated (right) side was apparent for all dose groups, roughly following the shape of the dose distribution (Fig. 1B, for 65 Gy-irradiated slice). The mean number of astrocytes per tile in the ROI on the right hemisphere increased linearly with prescribed dose (Fig. 1D). On the contralateral hemisphere, it was significantly lower, yet elevated in comparison to the 0 Gy control. Besides dose, the cerebral cortex showed much lower astrocyte counts, with rapid increase towards the thalamus at the anatomical boundary (Fig. 1E).

**Conclusion:** Histological sections of mouse brains whose right hippocampus had been irradiated with protons showed a clear dose-dependent increase in astrocytes in irradiated areas. Combined with other findings from this dataset, an improved understanding of the BBB's role in modulating radiation-induced side effects is expected.

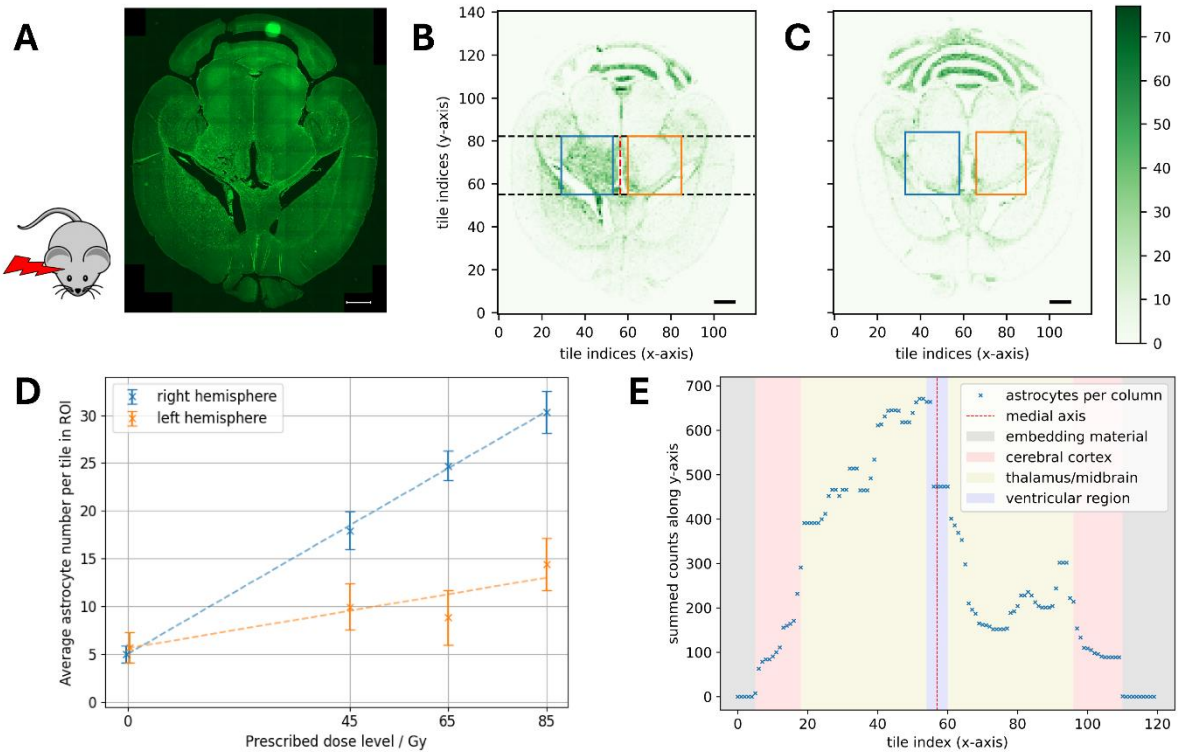


**Figure 1:** Spatial astrocyte distribution in mouse brain slices. Scale bars: 1 mm. **(A)** Raw microscopic image of glial acidic fibrillary protein (GFAP) staining on a 65 Gy mid-brain slice. **(B)** Number of astrocytes within 100 µm x 100 µm tiles for this 65 Gy slice with rectangular regions of interest (ROIs) in right (blue) and left (orange) hemispheres. **(C)** Analog to B for a 0 Gy control slice. **(D)** Mean astrocyte number per tile within ROI of right and left hemisphere, averaged over three slices per mouse. Dashed lines to guide the eye. **(E)** Astrocyte number along the beam axis (summed between black lines in B). Background color indicates anatomical region.

# Abstracts session 7:
# Emerging therapies

**Safety and efficacy of a hypofractionated FLASH protocol for treating dogs with spontaneous malignant tumors**

Presenting author:
Betina Børresen: bb@sund.ku.dk
Department of Veterinary Clinical Sciences, University of Copenhagen, Frederiksberg, Denmark

Authors: Betina Børresen[1], Bolette W. Gjaldbaek[1], Emilie S. Wismann[1], Maja L. Arendt[1], Filip Hörberger[2], Liliana Lemos da Silva[2], Pontus Wahlqvist[3], Anne R. Krogh[1], Anna V. Müller[1], Sven Bäck[3], Per Munck af Rosenschöld[2,3], Crister Ceberg[2], Kristoffer Petersson[3,4]

Affiliations:
[1] Department of Veterinary Clinical Sciences, University of Copenhagen, Frederiksberg, Denmark
[2] Medical Radiation Physics, Department of Clinical Sciences, Lund University, Lund, Sweden, [3] Radiation Physics, Department of Hematology, Oncology and Radiation Physics, Skåne University Hospital, Lund, Sweden,
[4] Department of Oncology, University of Oxford, Oxford, United Kingdom.

## Background and aims
Previous work in veterinary cancer patients has shown that >30Gy single-fraction FLASH radiotherapy carries a risk of inducing severe late adverse effects. Hypofractionated FLASH treatment warrants exploration as it could enable higher treatment doses for improved tumor control, while decreasing the risk of late toxicity. Accordingly, the aims of this study were to validate hypofractionated FLASH in canine cancer patients and to decide on a safe and effective treatment schedule.

## Methods
Dogs with solid malignant tumors were included if the owners decided against other types of therapy. A dose-escalation protocol was applied, starting from 32Gy 10MeV electron FLASH delivered in 4 weekly 8Gy fractions (overall treatment time: 22 days). At least 3 dogs were treated at each dose level prior to escalation in 2Gy/fraction increments. Efficacy and toxicity were evaluated using the veterinary RECIST and VRTOG criteria during a planned 12-month follow up period. Following evaluation of results from the weekly 4-fraction protocol, a revised protocol was designed with 3 biweekly fractions (overall treatment time: 8 days), starting with 10Gy/fraction.

## Results
From September 2023 to February 2025, a total of 26 dogs with a total of 30 targets were treated. Four of the 30 targets were microscopic residual disease following surgery, two targets were metastatic lymph nodes, and the remaining 24 targets were macroscopic tumors. The tumor types were nine mast cell tumors, six soft tissue sarcomas, six squamous cell carcinomas, six oral malignant melanomas and one epitheliotropic lymphoma. Nine

targets (8 dogs) were treated with 4x8Gy, 14 targets (13 dogs) were treated with 4x10Gy, four targets (3 dogs) were treated with 4x12Gy, and 3 targets (2 dogs) were treated with biweekly 3x10Gy. In terms of safety, the 4x8Gy protocol was well-tolerated, however high grade acute toxicity was observed for 4x10-12Gy, which led to termination of this protocol and adjustment to the 3-fraction protocol. The 4x8Gy protocol had only short-term efficacy for macroscopic tumors, however long-term clinical benefit was observed for the 4x10-12Gy protocols. Initial data suggests that the accelerated 3-fraction protocol is safe in the early post-treatment setting.

## Conclusions

Following this study, it remains undetermined what the optimal hypofractionated protocol is, as the weekly 4-fraction dose-escalation arm had to be terminated due to unacceptable toxicity at the high dose range. Additional patients will have to be included in the biweekly 3-fraction treatment arm before conclusions can be drawn regarding this schedule.

**Proton Minibeam Radiotherapy - Preclinical Research at DCPT**

Fardous Reaz [1,2], Line Kristensen[1,2,3], Erik Traneus[4], Brita Singers Sørensen[2,3], and Niels Bassler[1,2]

1. Department of Clinical Medicine, Aarhus University, Denmark.
2. Danish Centre for Particle Therapy, Aarhus, Demark.
3. Department of Oncology, Aarhus University, Denmark.
4. RaySearch Laboratories, Stockholm, Sweden.

Spatially fractionated radiotherapy with millimeter-sized proton beams (pMBRT) have in preclinical studies shown potential for effective tumor treatment while sparing normal tissues. Clinical translation requires quantification and unambiguous comparison against conventional radiotherapy. At DCPT we have constructed a mini-beam collimation system with the aim to obtain dose tumor control (TCP) and normal tissue complication (NTCP) dose-response curves to quantify the increase in the therapeutic window.

We compare pMBRT to conventional proton therapy for uniform target dose. Our arrangement was derived from an established mouse irradiation setup. A tuned multi-slit collimator (2.25 mm slit period, with 1 mm apertures) with a proton treatment plan delivered a uniform dose to a PTV, but with alternating dose-peaks and -valleys in the entrance. The right hind legs of female C3H/ HeNRj mice were irradiated at the highest dose contrast (peak-to-valley dose ratio = 7.5) at the entrance and tumor bearing CDF1 mice at PTV. The acute skin toxicity and tumor volume were recorded using a well-accepted scoring system. Dose-response curves were obtained as a function of the PTV dose. Tumor bearing mice were irradiated in the homogenous PTV to prove TCP equivalence.

pMBRT demonstrated a significantly reduced normal tissue sparing compared to conventional irradiation, see figure 1. No higher toxicity levels were observed for pMBRT, a common occurrence in conventional modality for the same PTV dose. The estimated grid factor of at least < 0.65 (toxicity Score 1.5) and < 0.7 (Score 2.5) supports the enhanced tissue-sparing of pMBRT while delivering the same target dose. Similar tumor responses were observed for conventional and pMBRT.

We demonstrate a simple method, where gains in the therapeutic window can directly be established from PTV dose, instead of relying on average dose or EUD in the heterogenous dose environment. The study underscores pMBRT's potential to spare healthy tissue while obtaining a similar tumor dose, in a new way. These promising results support the broader clinical implementation of pMBRT.

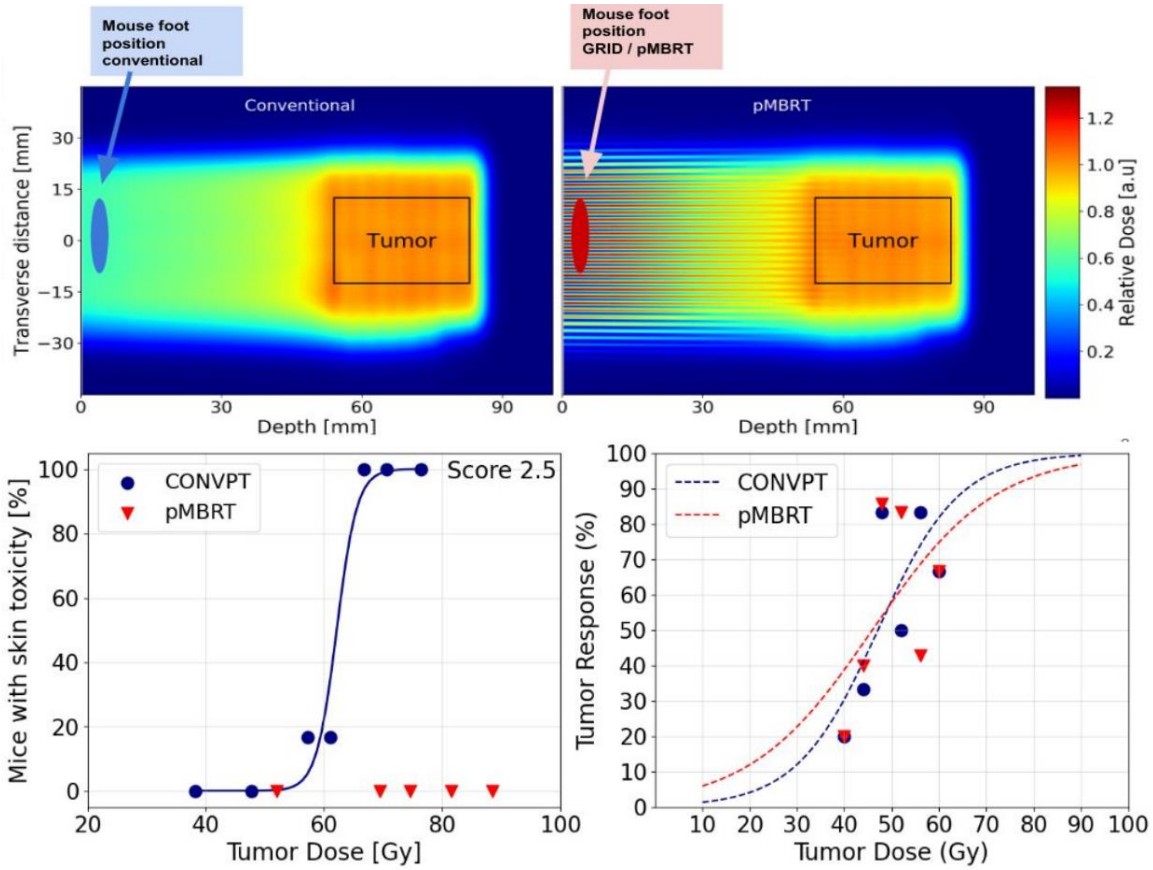


**Fig 1:** The spatially fractionated dose distribution of pMBRT (top right) significantly reduces the occurrence of skin toxicity in irradiated mice, with no incidence of higher-level toxicity within the administered dose range: NTCP data outside the PTV shown to the lower left for acute score 2.5. TCP data to the lower right, showing a similar tumor response is observed for both pMBRT and conventional proton therapy in the PTV.

**Integrating 2D dosimetry and cell survival analysis to improve local effect predictions in spatially fractionated radiotherapy**

Delmon Arous[1,2*], Jacob Larsen Lie[1], Nina Jeppesen Edin[1], and Eirik Malinen[1,3†]
*1: Department of Physics, University of Oslo, Norway*

*2: Department of Medical Physics, Oslo University Hospital, Norway*

*3: Department of Radiation Biology, Oslo University Hospital, Norway*

**Presenting author*

† eirik.malinen@fys.uio.no

## Introduction

Spatially fractionated radiotherapy (SFRT) is a method that applies heterogeneous radiation dose distributions, typically with alternating high- and low-dose regions, to exploit differential tumor and normal tissue responses and thereby enhance therapeutic efficacy. Yet, robust methods for accurately analyzing and predicting local cell survival following SFRT *in vitro* remain limited. This study proposes a novel methodology that integrates spatial dosimetry with colony formation assessment and modelling to better predict SFRT-induced cell responses.

## Materials and Methods

A549 lung cancer cells were irradiated with 220 kV X-rays under three different field conditions: open, striped, and dotted radiation patterns (Figure 1). Colony formation was assessed using image segmentation to identify cell colony (CC) centroids in scanned images of cell culture flasks. Dose distributions in 2D were mapped with radiochromic film dosimetry. Digital images containing CC locations and dose maps were divided into 1 mm² quadrats for analysis. A Poisson regression model was fitted to colony counts per quadrat, incorporating the linear-quadratic (LQ) model parameters $\alpha$ and $\beta$. A modified LQ (MLQ) model was introduced by including an additional interaction term between the radiation dose and the distance $d$ from a colony to the nearest peak dose region, characterized by the fit parameter $\delta$.

## Results

The proposed methodology was successfully implemented (Figure 1). Fitting the LQ model across all quadrats and radiation patterns yielded $\alpha$ = 0.254 $Gy^{-1}$ and $\beta$ = 0.039 $Gy^{-2}$, whereas the MLQ model provided $\alpha$ = 0.249 $Gy^{-1}$, $\beta$ = 0.032 $Gy^{-2}$, and $\delta$ = −0.040 $Gy^{-1}cm^{-1}$. Uncertainty in all

parameters was consistently below 0.5%. The MLQ model demonstrated slightly lower fitting errors than the standard LQ model, suggesting improved predictive accuracy.

## Conclusions

This study successfully developed a novel analysis pipeline for 2D localization of CCs and SFRT survival modeling *in vitro*. The results indicate that, in addition to the delivered radiation dose, the distance to the peak dose regions is a significant factor influencing local SFRT effects. Incorporating a spatial factor through a MLQ model may enhance the understanding of SFRT-induced cell survival and improve predictive models for radiotherapy outcomes.

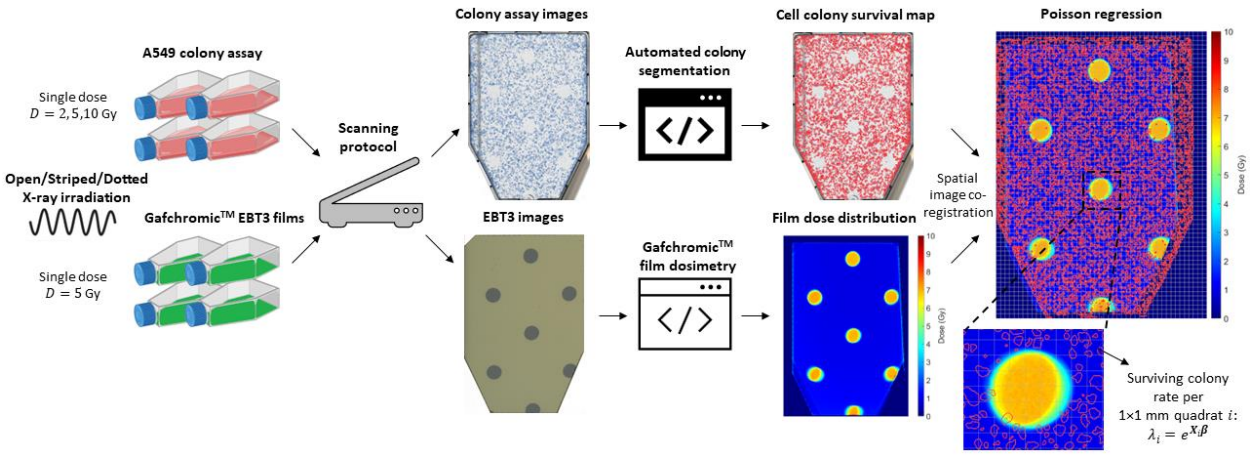


***Figure 1**: Graphical abstract demonstrating the developed methodology.*

# A Geant4 simulation of DNA Damage in BNCT with ongoing lithium ion studies

J Duan*[1], C De Sio[1], L Ballisat[1], S Guatelli[2], L Abu Sabah[1], L Beck[1], A Rosenfeld[1], D Sakata[3], Y Shi[1], and J Velthuis[1]

[1]School of Physics, University of Bristol, Bristol, UK

[2]Centre For Medical Radiation Physics, University of Wollongong, Wollongong, Australia

[3]School of Allied Health Sciences, Osaka University, Osaka, Japan

## Introduction

Boron Neutron Capture Therapy (BNCT) is a novel cancer treatment that utilizes neutron capture reactions of $^{10}B$ to generate high-LET particles, α particles and lithium ions, to induce lethal damage to cancer cells. BNCT is gathering a lot of attention as clinical results show that BNCT is a very effective treatment, see e.g. [1, 2, 3]. A key step in developing a fundamental understanding of the treatment are modelling studies, see e.g. [4, 5, 6]. The α particle contribution to DNA damage is well understood, while there is significant variation in the biological effects of lithium ions produced on the outside of the cell. This is mainly due to different charge state models for the lithium ions, resulting in different ranges and thus different amounts of DNA damage.

*Email: zh21940@bristol.ac.uk

## Materials and methods

DNA damage is simulated using Geant4 11.1.1 and Geant4-DNA. There are two main reactions

$$^{10}B + n \rightarrow {}^{7}Li + \alpha + \gamma \quad (93.57\%) \quad E_{\alpha_{high}} = 1.4717\ \text{MeV} \quad E_{Li} = 0.8320\ \text{MeV} \quad (1)$$

$$^{10}B + n \rightarrow {}^{7}Li + \alpha \quad (6.32\%) \quad E_{\alpha_{low}} = 1.7772\ \text{MeV} \quad E_{Li} = 1.0143\ \text{MeV} \quad (2)$$

For direct damage, energy deposits are scored up to a radius of 0.35 nm from the sugar-phosphate group centre. A linear damage model is used to evaluate the direct damage in the range 5–37.5 eV. For indirect damage, OH radicals are tracked until 5 ns and are re-moved from the simulation if more than 9 nm from the DNA. The chemistry model used was G4EmDNAChemistry option3. A 40.5% probability is used to determine whether an OH radical causes an indirect strand break.

## Results

Lithium ions deposit energy over a more limited range, about 4 µm, compared to α parti-cles, 8-10 µm. For a spherical cell with a 5 µm radius and a nucleus with a 3 µm radius, the number of single strand breaks for α's originating at the edge of the cell is approximately 15.7% lower than for $\alpha_{low}$'s originating at the edge of the nucleus and 6.1% for $\alpha_{high}$. The number of double strand breaks (DSBs) for α's originating at the edge of the cell is approx-imately 7.9% higher for $\alpha_{high}$'s and 6.5% lower for $\alpha_{low}$'s compared to α's originating at the edge of the nucleus. This is due to the location of their Bragg peaks. Due to the limited range of both α's and lithium ions, cells on the diagonal of a 3 × 3 × 3 cluster only show 5.3% of the DSBs. A newly integrated effective charge calculation and charge exchange model[4] further improves the lithium ion track structure simulations. New results will be presented.

References


[1] N. Hu et al. *Scientific Reports*, 12(1):13778, August 12 2022.

[2] K. Hirose and M. Sato. *Int J Radiat Oncol Biol Phys.*, 120(3):796–804, Nov 2024.

[3] T. Kashihara et al. *Radiotherapy and Oncology*, 202:110607, 2025.

[4] Naoki D-Kondo et al. *Physics in Medicine & Biology*, 69(14):145016, jul 2024.

[5] Y. Han et al. *Physics in Medicine & Biology*, 68(17):175028, aug 2023.

[6] T. Sato et al. *Sci Rep 8, 98*, 2018.

Author information:

Tanja Mälkiä
tanja.malkia@hus.fi
Department of Radiation Oncology, Helsinki University Hospital Comprehensive Cancer Center and University of Helsinki, Helsinki, Finland

Hanna Koivunoro
Department of Radiation Oncology, Helsinki University Hospital Comprehensive Cancer Center and University of Helsinki, Helsinki, Finland
Neutron Therapeutics Finland Oy, Helsinki, Finland

Tiina Seppälä
Department of Radiation Oncology, Helsinki University Hospital Comprehensive Cancer Center and University of Helsinki, Helsinki, Finland

Leena Kankaanranta
Department of Radiation Oncology, Helsinki University Hospital Comprehensive Cancer Center and University of Helsinki, Helsinki, Finland

Liisa Porra
Department of Radiation Oncology, Helsinki University Hospital Comprehensive Cancer Center and University of Helsinki, Helsinki, Finland

Anu Anttonen
Department of Radiation Oncology, Helsinki University Hospital Comprehensive Cancer Center and University of Helsinki, Helsinki, Finland

Mikko Tenhunen
Department of Radiation Oncology, Helsinki University Hospital Comprehensive Cancer Center and University of Helsinki, Helsinki, Finland

Heikki Joensuu
Department of Radiation Oncology, Helsinki University Hospital Comprehensive Cancer Center and University of Helsinki, Helsinki, Finland

**A retrospective study of oral mucosa dose relation to grade 3 oral mucositis in locally recurrent inoperable head and neck carcinoma patients treated with reactor-based BNCT**

## Introduction

Despite advanced multimodal primary head and neck (HN) carcinoma treatments, the risk of local recurrence rate varies 15-50% in advanced cases (1,2). The prognosis after recurrence is poor and remains a therapeutic challenge (3,4).

Boron neutron capture therapy (BNCT) is a biologically targeted radiotherapy based on the neutron capture reaction of boron carrier and thermal neutrons in tumor cells (5). The radiobiologically effective dose of BNCT is expressed as the sum of four dose components (boron, nitrogen capture, fast neutron and photon dose) each multiplied by relative/compound biological effectiveness (RBE/CBE) factors (6).

In clinical studies, BNCT has been used to treat locally recurrent HN carcinomas with high response rates (65-81%) (7,8). In Finland, up to 54% HN carcinoma patients developed grade 3 oral mucositis (OM) after BNCT treatment (9).

A new era of BNCT treatment using accelerator-based BNCT has started. We evaluated the reasons for the high prevalence of severe OM within the Finnish HN patient cohort to improve future treatments with accelerator-based BNCT.

## Materials and methods

N=92 patients with locally recurrent inoperable HN carcinoma were treated with reactor-based BNCT in Finland between 2003 and 2012. The maximum radiobiologically effective dose to the oral mucosa was defined. The oral mucosa dose was calculated using the skin nitrogen concentration (4.2%), because the elemental composition of the oral mucosa is unknown.

A sigmoidal Normal Tissue Complication Probability (NTCP) model was created by arranging the patients into four groups based on the mucosal dose magnitude. The probability for grade 3 OM was calculated for each dose group based on the observed responses.

The relation between severe OM and various parameters including patient group, tumor properties, previous treatments, boron infusion and BNCT irradiation were analyzed with a t-independent test and logistic regression.

**Results**

Grade 3 OM was observed in 42% patients after the first BNCT treatment.

The prevalence of OM increased when the maximum dose to the oral mucosa increased (figure 1). From the sigmoidal NTCP curve we estimated D50%=13.5Gy(W) (maximum dose) for grade 3 OM. 3D dose distributions could not be calculated from retrospective material.

The other parameters did not correlate with the prevalence of severe OM.

Figure 1.

$$NTCP = \frac{1}{1+\left(D_{50}/D\right)^{k}}$$

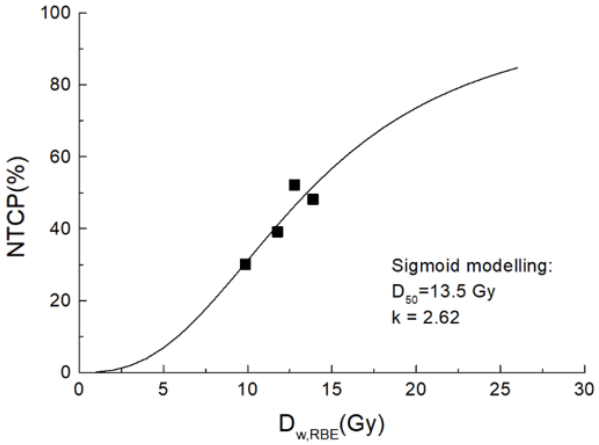


Conclusions

The prevalence of grade 3 OM increased when the maximum dose to the oral mucosa increased.

More comprehensive information about dose distribution in the oral cavity, patient-specific factors (smoking, alcohol consumption) and mucosal radiosensitivity could provide more information about the causes of severe OM.

References:


1. Argiris A, Karamouzis MV, Raben D, Ferris RL. Head and neck cancer. Lancet. 2008 May 17;371(9625):1695-709. doi: 10.1016/S0140-6736(08)60728-X.
2. Rettig EM, D'Souza G. Epidemiology of Head and Neck Cancer. Surg Oncol Clin N Am. 2015 Jul;24(3):379-96. doi: 10.1016/j.soc.2015.03.001.
3. Vargo JA, Ward MC, Caudell JJ, Riaz N, Dunlap NE, Isrow D et al. A multi-institutional comparison of SBRT and IMRT for definitive reirradiation of recurrent or second primary head and neck cancer. Int J Radiat Oncol Biol Phys. 2018 Mar 1;100(3):595-605. doi: 10.1016/j.ijrobp.2017.04.017.
4. Ward MC, Riaz N, Caudell JJ, Dunlap NE, Isrow D, Zakem SJ, et al. Refining patient selection for reirradiation of head and neck squamous carcinoma in the IMRT era: a multi-institution cohort study by the MIRI collaborative. Int J Radiat Oncol Biol Phys. 2018 Mar 1;100(3):586-594. doi: 10.1016/j.ijrobp.2017.06.012.
5. Barth RF, Coderre JA, Vicente MG, Blue TE. Boron neutron capture therapy of cancer: Current status and future prospects. Clin Cancer Res. 2005 Jun 1;11(11):3987-4002. doi: 10.1158/1078-0432.CCR-05-0035.
6. Coderre JA, Morris GM. The radiation biology of boron neutron capture therapy. Radiat Res. 1999 Jan;151(1):1-18.
7. Takeno S, Yoshino Y, Aihara T, Higashino M, Kanai Y, Hu N et al. Preliminary outcomes of boron neutron capture therapy for head and neck cancers as a treatment covered by public health insurance system in Japan: Real-world experiences over a 2-year period. Cancer Med. 2024 Jun;13(11):e7250. doi: 10.1002/cam4.7250.
8. Sato M, Hirose K, Takeno S, Aihara T, Nihei K, Takai Y et al. Safety of Boron Neutron Capture Therapy with Borofalan($^{10}$B) and Its Efficacy on Recurrent Head and Neck Cancer: Real-World Outcomes from Nationwide Post-Marketing Surveillance. Cancers (Basel). 2024 Feb 21;16(5):869. doi: 10.3390/cancers16050869.
9. Kankaanranta L, Seppälä T, Koivunoro H, Saarilahti K, Atula T, Collan J et al. Boron neutron capture therapy in the treatment of locally recurred head-and-neck cancer: final analysis of a phase I/II trial . Int J Radiat Oncol Biol Phys. 2012 Jan 1;82(1):e67-75. doi: 10.1016/j.ijrobp.2010.09.057.

# Abstracts session 8: Biology and clinical applications

**The prognostic value of cell-free DNA kinetics during chemoradiotherapy in squamous cell carcinomas of the anus**

**Author information:**
Anne Vittrup Jakobsen, avj@oncology.au.dk
Department of Experimental Clinical Oncology, Aarhus University Hospital, Aarhus, Denmark
Department of Clinical Medicine, Aarhus University, Aarhus, Denmark

**Authors:**
Anne Vittrup Jakobsen[1,2], Camilla Kronborg[2,3], Anne Ramlov[4], Christian Andreas Hvid[4], Karen-Lise Garm Spindler[1,2]

1. Department of Experimental Clinical Oncology, Aarhus University Hospital, Aarhus, Denmark
2. Department of Clinical Medicine, Aarhus University, Aarhus, Denmark
3. The Danish centre for particle therapy, Aarhus University Hospital, Aarhus, Denmark
4. Department of Oncology, Aarhus University Hospital, Aarhus, Denmark

**Purpose:** In squamous cell carcinomas of the anus (SCCA), reliable biomarkers for prognosis and response monitoring during chemoradiotherapy (CRT) are lacking. Measuring cell-free DNA (cfDNA) using a simple direct fluorescent assay (DFA) holds promise as a minimally invasive approach. This study investigated the prognostic value of cfDNA kinetics during CRT.

**Materials and methods:** Clinical data and blood samples were prospectively collected from SCCA patients undergoing CRT. cfDNA levels (ng/µL) were measured in serum using a DFA at baseline, mid-therapy, and end of treatment (EOT). Baseline levels were correlated with patient characteristics using the Mann-Whitney U test, and longitudinal changes during CRT were analysed using the Wilcoxon signed-rank test. Kaplan-Meier curves were used to evaluate survival, and log-rank test was used for group comparison. A Cox proportional hazards model was applied to calculate hazard ratios (HR).

**Results**: A total of 126 patients were included. cfDNA measurements were available at baseline (n=126), mid-therapy (n=103) and EOT (n=108) with median cfDNA levels of 0.78ng/µL 95% CI(0.72-0.85), 0.62ng/µL 95%CI(0.56-0.72) and 0.66ng/µL 95%CI(0.58-0.74), respectively. Patients with high-risk disease (T3-T4, or N+, or M+) and performance status 1-2 had higher baseline cfDNA levels ($p<0.05$), but baseline levels did not seem to affect the outcome. From baseline to mid-therapy and EOT, cfDNA levels declined ($p<0.001$). The median follow-up time was 22 months. Compared to complete responders, a lower percentage decline was observed in non-responders with persistent or progressive disease within 6 months after CRT (-9% 95% CI(-24;33) and -37% 95%CI(-44;-29), $p<0.05$) and the treatment failure group including non-responders, locoregional and distant recurrences (-18% 95%CI(-36;9) and -36% 95%CI(-44;-28), $p<0.05$). Low cfDNA elimination, where cfDNA levels remained above the baseline 75th percentile, was associated with worse disease-free survival (HR=4.23, 95%CI (1.50-11.93), $p<0.05$)

**Conclusion:** cfDNA quantification with DFA proved feasible in SCCA. A low cfDNA decline during CRT correlated with inferior outcomes, highlighting its clinical potential as a prognostic biomarker to guide personalised treatment strategies in SCCA.

# Highlighting proton RBE Complexities: RBE changes with biological endpoint, dose fractionation, and SOBP position in a murine leg model

Cathrine Overgaard[1], Fardous Reaz[2], Mateusz Krzysztof Sitarz[2], Jacob Johansen[2], Harald Spejlborg[3], Cai Grau[2], Jens Overgaard[1], Per Poulsen[2,3], Niels Bassler[2,4.], Brita Singers Sørensen[1,2]

[1]Department of Experimental Clinical Oncology, Aarhus University Hospital, Denmark,
[2]Danish Centre for Particle Therapy, Aarhus University Hospital, Aarhus, Denmark,
[3]Department of Oncology, Aarhus University Hospital, Aarhus, Denmark,
[4]Department of Clinical Medicine, Aarhus University, Aarhus, Denmark

**Introduction:** Proton therapy commonly employs a constant relative biological effectiveness (RBE) of 1.1 to translate photon doses into isoeffective proton doses. However, increasing evidence indicates that the RBE is not fixed but varies with multiple parameters, including biological endpoint, dose per fraction, and linear energy transfer (LET). Here, we compare RBE findings for acute and late radiation damage following photon and proton irradiations in either the center or the distal edge of a spread-out Bragg peak (SOBP) and explore the impact of fractionation on the RBE (Overgaard et al. 2025; Overgaard et al. 2025).

**Materials and Methods:** Unanesthetized mice were restrained in jigs, where their right hind legs were irradiated with either one fraction or four fractions of protons at the center (LET, $_{all}$=5.3 keV/μm) and one fraction at the distal edge (LET, $_{all}$=7.6 keV/μm) of a spread-out Bragg peak (SOBP). 6 MV photons were used as the reference. Acute skin damage was assessed daily until day 30 after treatment, and the late damage response of radiation-induced fibrosis was evaluated biweekly using a joint contracture assay for one year following treatment.

**Results:** The RBE is calculated based on the dose of 50% responders and the RBE results are summarized in Figure 1. Using one fraction, an acute skin damage RBE of 1.06 (1.02-1.10) and fibrosis RBE of 1.16 (1.00-1.32) were found in the center of the SOBP, displaying an enhanced RBE for fibrosis. The RBE increased to 1.25 (1.13-1.36) for fibrosis using a hypofractionated dose schedule of 4 fractions. When irradiating at the distal edge using one fraction, the RBE was 1.15 (1.10-1.19) for acute skin damage and 1.26 (1.07-1.44) for fibrosis, demonstrating an increased RBE at the distal edge of the SOBP for both endpoints.

**Conclusion:** Collectively, these data highlight that a single, constant RBE value underestimates proton biological effectiveness, especially considering late side effects, fractionated protocols, or the elevated LET regions near the distal SOBP edge. These results underscore a more nuanced, site- and endpoint-specific RBE approach to optimize proton therapy treatment planning.

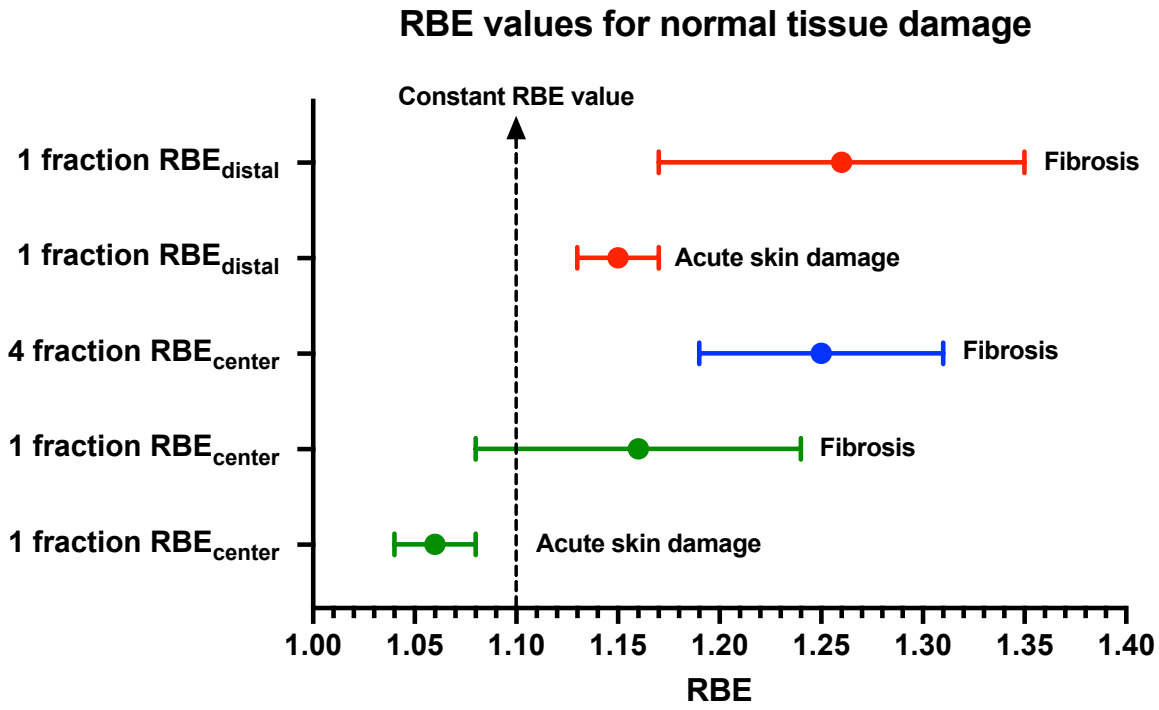


*Figure 1. Forest plot with RBE values. Horizontal bars indicate the standard deviation.*

**References:**

Overgaard, Cathrine Bang, Fardous Reaz, Christina Ankjærgaard, Claus E. Andersen, Mateusz Sitarz, Per Poulsen, Harald Spejlborg, et al. 2025. 'The Proton RBE and the Distal Edge Effect for Acute and Late Normal Tissue Damage in Vivo'. *Radiotherapy and Oncology* 203 (February). https://doi.org/10.1016/j.radonc.2024.110668.

Overgaard, Cathrine Bang, Fardous Reaz, Per Poulsen, Harald Spejlborg, Jens Overgaard, Cai Grau, Niels Bassler, and Brita Singers Sørensen. 2025. 'The Fractionation Effect on Proton RBE in a Late Normal Tissue Damage Model in Vivo'. *Radiotherapy and Oncology* 206 (May). https://doi.org/10.1016/j.radonc.2025.110792.

**Cellular responses in murine salivary glands to fractionated irradiation: Implications for fibrosis and hyposalivation**

Inga Solgård Juvkam[1,2], Olaf Joseph Franciscus Schreurs[2], Olga Zlygosteva[3], Nina Jeppesen Edin[3], Hilde Kanli Galtung[2], Eirik Malinen[1,3], Tine Merete Søland[2,4]

(1) Department of Radiation Biology, Institute of Cancer Research, Oslo University Hospital, Oslo, Norway
(2) Institute of Oral Biology, Faculty of Dentistry, University of Oslo, Oslo, Norway
(3) Department of Physics, Faculty of Mathematics and Natural Sciences, University of Oslo, Oslo, Norway
(4) Department of Pathology, Oslo University Hospital, Oslo, Norway

**Background:** Radiotherapy (RT) of head and neck cancer patients may cause detrimental late side effects such as fibrosis and hyposalivation, due to RT-induced damages to the salivary glands. Our aim was to investigate late RT-induced cellular and molecular changes of the salivary glands after fractionated irradiation to the head and neck in a murine model.

**Methods:** 12-week-old female C57BL/6J mice were irradiated with X-rays to a total dose of 66 Gy, given in 10 fractions over 5 days. The radiation field covered the oral cavity and major salivary glands. Salivary gland function was assessed by collecting saliva at baseline and at various time points after irradiation. The submandibular (SMG), sublingual (SLG), and parotid glands (PG) were dissected at day 105. Using different staining techniques, morphological, cellular, and molecular changes were investigated in RT and control SMG, SLG, and PG.

**Results:** Saliva production was significantly reduced in RT mice compared to control mice at day 35, 80, and 105. We observed a decrease in total gland area and an increase in fibrotic area in RT SMG compared to control SMG at day 105. Atrophy of acinar cells was observed in all RT SMG and SLG, but not in PG. Surprisingly, the acinar atrophy was only located in one region of each RT gland. Increased number of chronic inflammatory cells and proliferating cells ($Ki67^+$) were found in these atrophic regions compared to non-atrophic regions of RT glands and control glands (Figure 1). Moreover, increased expression of the excretory duct cell marker, keratin 19 (K19), was found in ductal cells of the atrophic regions of RT glands compared to control glands. Interestingly, some of these cells also co-expressed the acinar cell marker, sodium potassium chloride cotransporter 1 (Nkcc1). This may demonstrate a cellular plasticity where ductal cells adopt an acinar cell phenotype upon stress or injury.

**Conclusion:** This work is a thorough histological description of the cellular and molecular changes in the SMG and SLG of irradiated mice displaying fibrosis and hyposalivation as late RT-induced side effects. We observed signs of cellular plasticity which have previously been seen after duct ligation in mice and after RT in humans. This suggests a potential for regeneration of salivary glands after RT.

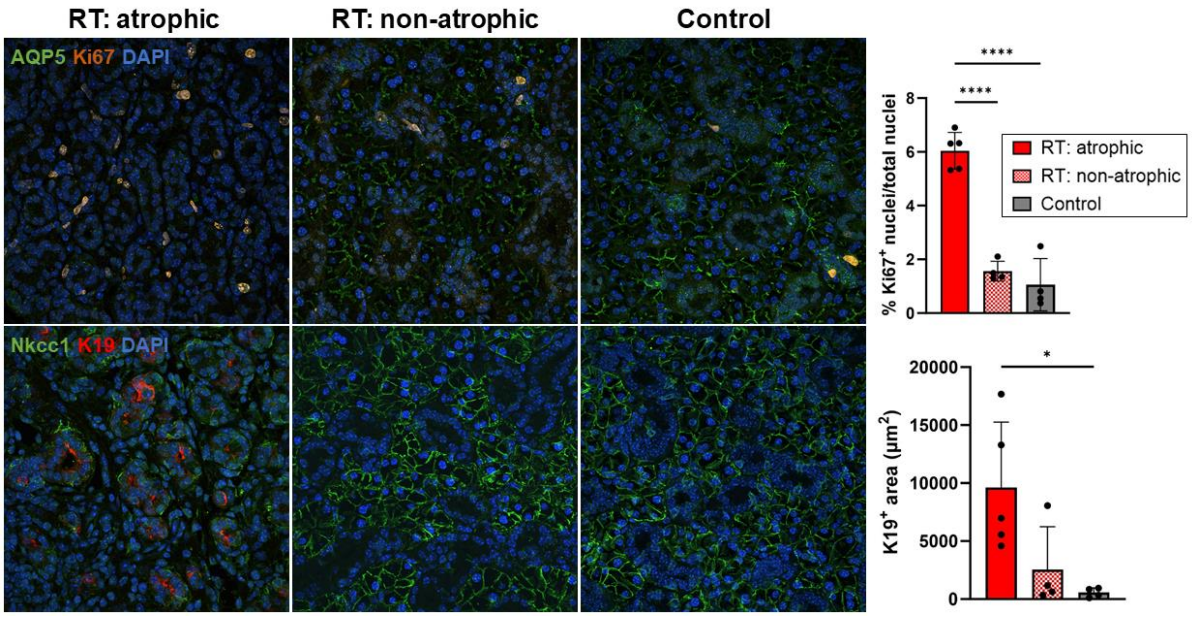


**Figure 1:** Atrophic and non-atrophic regions of irradiated (RT) and control submandibular glands labelled with immunofluorescent markers. (A) Acinar cells are labelled green with aquaporin 5 (AQP5), proliferating cells are labelled orange with Ki67, and DAPI labels all cell nuclei blue. Increased numbers of proliferating cells were found in the atrophic regions of RT glands compared to non-atrophic regions in RT glands and control glands.
(B) Acinar cells are labelled green with sodium potassium chloride cotransporter 1 (Nkcc1), Keratin 19 (K19) is labelled red, and DAPI labels all cell nuclei blue. Increased expression of K19 were found in the atrophic regions of RT glands compared to control glands. Some $K19^{+}$ cells also co-expressed Nkcc1.

# [$^{68}$Ga]Ga-PSMA-11 vs [$^{18}$F]F-PSMA-1007 PET/MRI of recurrent prostate cancer: detection rates at different PSA-levels and implications for salvage radiotherapy

[1]Knudtsen IS, [1]Abrahamsen BS, [2]Selnæs KM, [1,3]Elschot M, [4,5]Tulipan AJ, [5]Hernes E, [6,7]Bogsrud TV, [2]Keil TM, [2]Johansen H, [2]Langørgen S, [4]Ringheim A, [6]Castillejo MJG , [8]Honoré A, [9]Haugnes HS, [10,11]Tandstad T, [1,2]Bathen TF

180°N WP1 Prostate Cancer Consortium

[1]Department of Circulation and Medical Imaging, NTNU

[2]Department of Radiology and Nuclear Medicine, St. Olav's Hospital

[3]Research Department, St Olav's Hospital

[4]Department of Radiology, Haukeland University Hospital

[5]Division of Radiology and Nuclear Medicine, Oslo University Hospital

[6]PET Imaging Centre, University Hospital of North Norway

[7]PET-Centre, Aarhus University Hospital

[8]Department of Urology, Haukeland University Hospital

[9]Department of Oncology, University Hospital of Northern Norway

[10]Cancer Clinic, St. Olav's Hospital

[11]Department Clinical and Molecular Medicine, NTNU

## Introduction

After radical prostatectomy, salvage radiotherapy is recommended at biochemical recurrence (BCR), and PSMA-PET is the most sensitive imaging method for detection of metastases [1]. However, PSMA-PET has reduced sensitivity at low PSA levels and the sensitivity also depends on the PSMA tracer applied. We have compared the detection rates of the two most commonly used tracers, [$^{68}$Ga]Ga-PSMA-11 and [$^{18}$F]F-PSMA-1007, in a cohort of patients included in the prospective multi center 180°N PSMA PET/MRI recurrence study.

## Materials and methods

Patients were included from May 2020 to April 2023. Inclusion criteria were 1) had undergone primary radical treatment, 2) presented with biochemical relapse according to standard definitions, and 3) were candidates for loco-regional salvage treatment.

The imaging protocol consisted of PET/MRI (neck to proximal thigh), PSMA PET/CT (vertex to thighs), and mpMRI (pelvic region) performed sequentially. Imaging results and clinical data were reported according to a pre-specified study protocol. Individual patient

disease status was categorized as 1) no lesions detected, 2) uncertain or 3) lesions detected. Detected lesions were defined as findings suspicious of local recurrence and/or metastatic disease. This analysis is based on the reports by the nuclear medicine physicians of the PET images from the PET/MRI, for which matching anatomical MRI sequences were available. Detection rates were calculated and presented for four strata of PSA-levels: PSA1 ≤0.2 ng/ml, PSA2 >0.2 - ≤0.5 ng/ml, PSA3 >0.5 - ≤1.0 ng/ml and PSA4 >1.0 ng/ml. Fisher's exact test was used to test differences in detection rates between the two tracers. A $p<0.05$ was considered statistically significant.

**Results**

At the time of analysis, PET reports and clinical data were available for 262 patients, of which 220 (84%) had radical prostatectomy as primary treatment. In this group, median age was 68 (range 46-82) years, time to BCR 32 (1-188) months and median PSA at imaging 0.35 (0.10-21.8) ng/ml. 63% were imaged with [$^{18}$F]F-PSMA-1007 and 37 % with [$^{68}$Ga]Ga-PSMA-11. Detection rates for the different PSA ranges are presented in the table and are significantly higher for [$^{18}$F]F-PSMA-1007 than [$^{68}$Ga]Ga-PSMA-11 for all PSA ranges except PSA3.

**Conclusions**

[$^{18}$F]F-PSMA-1007 should be considered the tracer of choice for patients who are candidates for salvage radiotherapy, in particular at PSA levels below 0.5 ng/ml.

[1] EAU Guidelines. Edn. presented at the EAU Annual Congress Madrid 2025. ISBN 978-94-92671-29-5. https://uroweb.org/guideline/prostate-cancer/

**Table: Patient level detection rates. (2/3) includes patients where disease status, based on PET/MRI, is uncertain, (3) only certain disease status. F: [$^{18}$F]F-PSMA-1007, Ga: [$^{68}$Ga]Ga-PSMA-11. Numbers in parentheses are (patients with detected disease)/(all patients in PSA group). * indicates that the detection rate is significantly higher among the patients examined with [$^{18}$F]F-PSMA-1007 than the patients examined with [$^{68}$Ga]Ga-PSMA-11 in the corresponding PSA group.**

| | Status | PSA1<br>≤0.2 ng/ml | PSA2<br>>0.2 - ≤0.5 ng/ml | PSA3<br>>0.5 - ≤1.0 ng/ml | PSA4<br>>1.0 ng/ml |
|---|---|---|---|---|---|
| [$^{18}$F]F-PSMA-1007, Prior surgery (n=139) | 2/3 | 56%*<br>(15/27) | 76%*<br>(54/71) | 69%<br>(11/16) | 96%*<br>(24/25) |
| | 3 | 40%*<br>(11/27) | 62*<br>(45/71) | 56%<br>(9/16) | 88%*<br>(22/25) |
| [$^{68}$Ga]Ga-PSMA-11, Prior surgery (n=81) | 2/3 | 10%<br>(1/10) | 12%<br>(5/40) | 44%<br>(8/18) | 62%<br>(8/13) |
| | 3 | 0%<br>(0/10) | 10%<br>(4/40) | 39%<br>(7/18) | 54%<br>(7/13) |

# Abstracts session 9:
# Harnessing grand-scale data sets

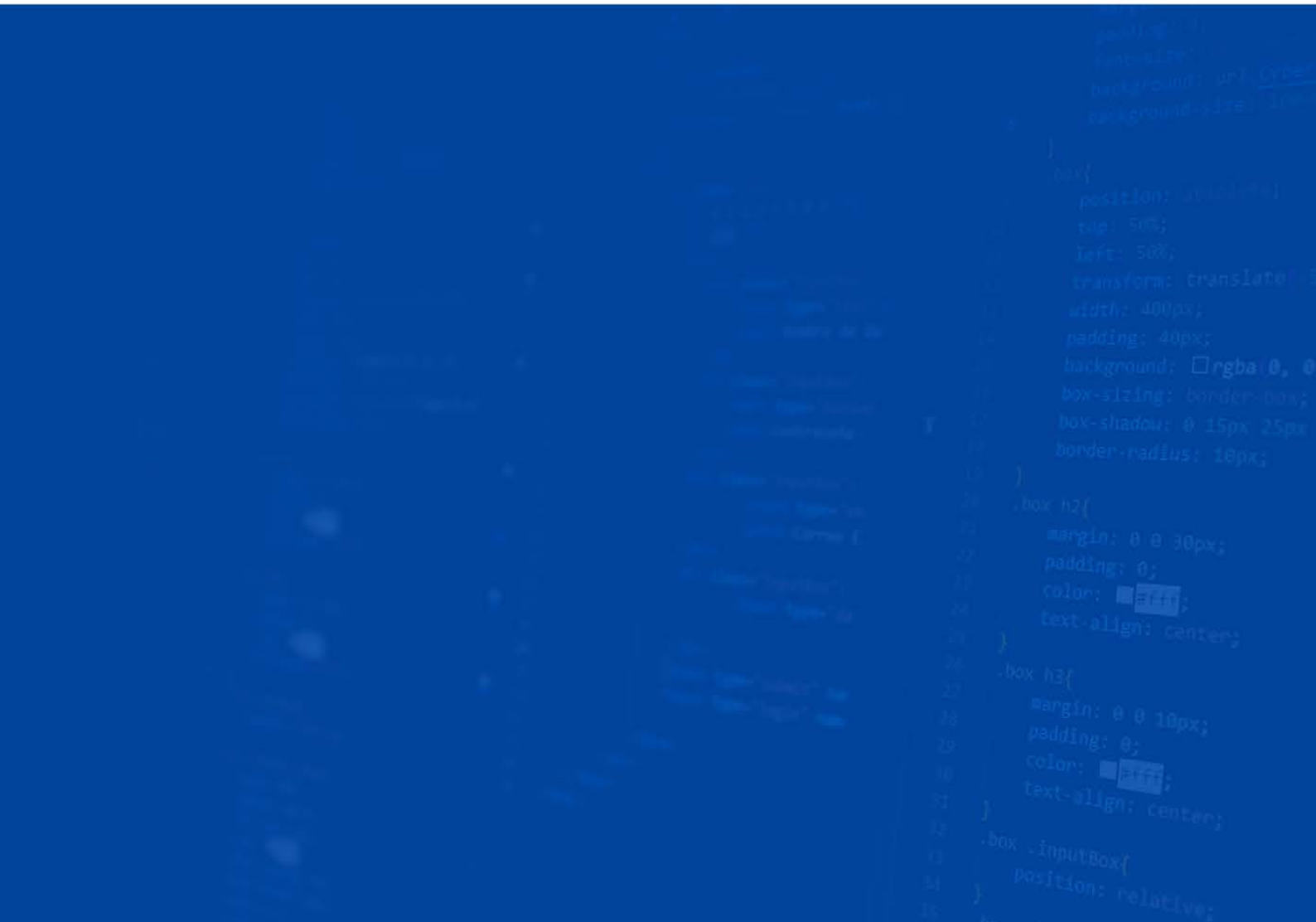

# Seasons, socioeconomics, comorbidities, and stages,: Unraveling the factors correlating with diagnostic intervals in cancer care

Azadeh Abravan, azadeh.abravan@manchester.ac.uk; Gareth Price, gareth.price@manchester.ac.uk

*Division of Cancer Sciences, The University of Manchester, Manchester, United Kingdom*

*The Christie NHS Foundation Trust*

**Purpose:** This study aims to explore the impact of socioeconomic factors, the stage of cancer at diagnosis, the level of comorbidity, and the season of symptom onset on the diagnostic interval (time between patients first reporting symptoms and their subsequent cancer diagnosis) among individuals with cancer.

**M&M:** Data from 6,857 patients diagnosed with head and neck (H&N:1,030), non-small cell lung (NSCLC:3,078), small cell lung (SCLC:756), and upper gastrointestinal (upper GI:1,993) cancers from 2010 to 2022 at The Christie NHS FT, UK were analyzed. Patient variables included age, sex, comorbidity score, cancer stage, and dates of symptom onset and diagnosis. To ensure accuracy, intervals outside 14-365 days were excluded due to potential errors in the dates of symptom onset. Seven domains of index of multiple deprivation (IMD) were categorized into high, medium, and low levels. These domains, tested individually due to their interrelations, along with other predefined factors, were analyzed using a general linear model to determine their associations with diagnostic intervals.

**Results:** The median diagnostic interval times for NSCLC, SCLC, H&N, and upper GI cancers were 63, 58, 80, and 63 days, respectively. In multivariable linear regression analyses, significant variations were observed (Figure 1). For upper GI cancer, older age and being male, as well as seasons such as spring, summer, and fall, markedly reduced the time to diagnosis. No significant IMD-related differences were observed. In NSCLC, advanced cancer stages were associated with delayed diagnoses, while seasonal reductions during spring and summer, as well as shorter intervals, were noted for those with a high level of health. For SCLC, spring, along with high employment levels significantly shortened the diagnostic interval, although moderate level of comorbidity delayed diagnoses. H&N cancer exhibited a significant decrease in diagnostic delays for loco-regional stages and across spring, summer, and fall, with reduced times also observed for those with a medium level of education.

**Conclusion:** This study reveals that diagnostic interval varied by cancer type and were associated with biological, temporal, and socioeconomic variables. Seasonal changes, which may affect both the level of healthcare business and the way symptoms present, significantly associated with diagnostic intervals for all four cancers examined. Advanced stages were associated with longer diagnostic times in NSCLC, highlighting the influence of disease severity. Socioeconomic disparities, including employment and education levels, also corelated with diagnostic intervals. These findings emphasize the complex factors associated with diagnosis times, suggesting areas for further investigation to optimize diagnostic processes and reduce delays.

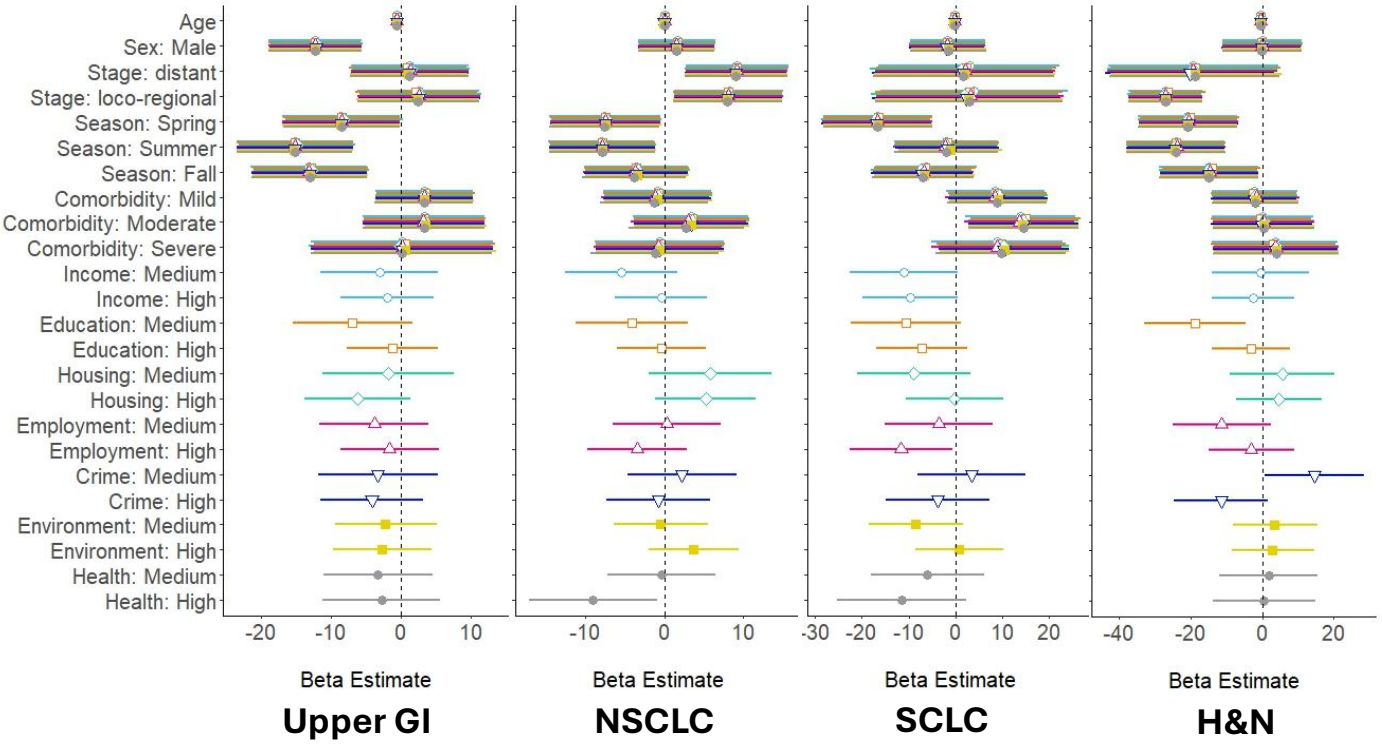


**Figure 1:** Forest plots for four cancers with adjusted estimates from multivariable linear regression analyses of diagnostic intervals. Seven analyses were conducted to test seven domains of the IMD. All models included age, sex, stage, season of symptom onset, and overall comorbidity level. Additionally, each model incorporated one of the IMD domains:

*The reference levels for the categorical variables were:* ***Sex*** *(female),* ***Stage*** *(local),* ***Season*** *(winter),* ***Comorbidity*** *(none), and* ***IMD domains*** *(low).*

*Model 1: Income*
*Model 2: Education*
*Model 3: Housing*
*Model 4: Employment*
*Model 5: Crime*
*Model 6: Environment*
*Model 7: Health*

# Impact of GTV-CTV Margin and Other Predictors on Radiation-Induced Dysphagia in Head and Neck Cancer Patients

Stougaard SW (1,2), Zukauskaite R (3), Röttger R (4), Lorenzen EB (1), Konrad ML (1,2), Nielsen CP (1,2), Krogh SL (1), Sommer JFA (1), Johansen J (3,5), Eriksen JG (6,7), Lonkvist CK (8), Friborg J (9), Brink C (1), Hansen CR (1,2,5)

1: Laboratory of Radiation Physics, Odense University Hospital, Odense, Denmark

2: Department of Clinical Research, University of Southern Denmark, Odense, Denmark

3: Department of Oncology, Odense University Hospital, Odense, Denmark

4: Department of Mathematics and Computer Science, University of Southern Denmark, Odense, Denmark

5: Danish Centre for Particle Therapy, Aarhus University Hospital, Aarhus, Denmark

6: Department of Oncology, Aarhus University Hospital, Aarhus, Denmark

7: Department of Experimental Clinical Oncology, Aarhus University Hospital, Aarhus, Denmark

8: Department of Oncology, Copenhagen University Hospital Herlev, Herlev, Denmark

9: Department of Clinical Oncology, Rigshospitalet, Copenhagen, Denmark

**Introduction**

In Denmark 2013, national radiotherapy guidelines in head and neck cancer standardised the margin of gross tumour volume to clinical target volume (GTV-CTV) from 0-10 mm to 5 mm (1). This study aimed to develop a predictive model for radiation-induced dysphagia in head and neck cancer patients, focusing specifically on the role of GTV-CTV margin size and dose-related factors.

**Materials and methods**

This retrospective study included 1,948 patients with pharyngeal or laryngeal squamous cell carcinomas treated with definitive IMRT at three Danish hospitals from 2010 to 2015 (2). Patient data, including physician-reported post-treatment dysphagia (grade 0–4), tumour characteristics, and treatment data were included. An artificial intelligence-based segmentation method, previously validated, was employed to delineate organs at risk consistently (3,4). The primary predictor of interest for dysphagia was GTV-CTV margin size, while secondary predictors included mean doses to oral cavity and pharyngeal constrictor muscles (PCM), (log-transformed) GTV volume, chemotherapy, tumour site, fractionation, nimorazole, sex, smoking status, and age. Ordinal mixed-effects models were used to analyse dysphagia severity over time, accounting for patient-specific differences and variability in the number of measurements. Data was randomly split into training (70%) and test (30%) sets. Model selection was done using backward and forward stepwise procedures with GTV-CTV margin forced into the model. Model performance was assessed using calibration plots, and significant predictors were visualised using a forest plot.

**Results**

After excluding cases with missing data, 1,421 patients (7,829 observations) were analysed over a 5-year follow-up. The GTV-CTV margin was not significantly associated with dysphagia risk (odds ratio (OR)=1.00 per cm, p=0.90). However, higher mean radiation doses to the lower PCM (OR=1.06 per 5 Gy, p<.001) and oral cavity (OR=1.04 per 5 Gy, p<.001) significantly increased dysphagia risk. Other significant predictors are detailed further in the forest plot (Figure 1).

The model showed good calibration overall, though slightly underestimating the probability of grade 3+ dysphagia.

**Conclusion**

The ordinal mixed-effects model identified radiation doses to the oral cavity and lower PCM as important modifiable predictors of radiation-induced dysphagia. The model's underestimation for grade 3+ dysphagia may be related to the low prevalence. While GTV-CTV margin reduction did not directly affect dysphagia outcomes, it may indirectly influence the risk by allowing dose sparing to relevant organs. Chemotherapy unexpectedly appeared protective against higher-grade dysphagia, possibly reflecting patient selection bias.

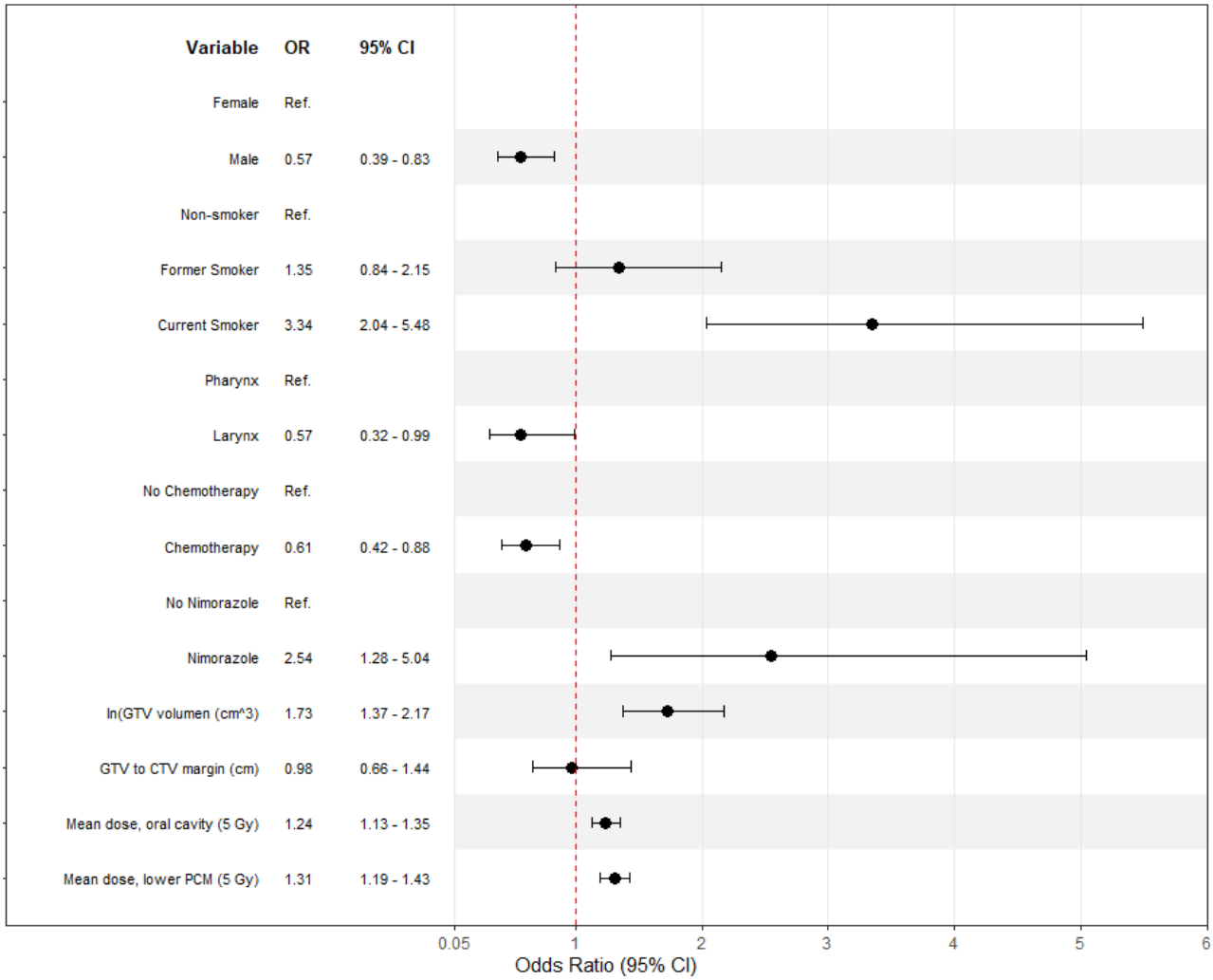


**Figure 1.** Forest plot of variables associated with the risk of dysphagia, displaying odds ratios (OR) with 95% confidence intervals (CI). The vertical dashed line at OR = 1 denotes no effect. An OR greater than 1 indicates an increased risk of higher-grade dysphagia, whereas an OR less than 1 indicates a decreased risk. The reference category for each variable is noted as "Ref.".

**References:**


1. Zukauskaite R, Hansen CR, Grau C, Samsøe E, Johansen J, Petersen JBB, et al. Local recurrences after curative IMRT for HNSCC: Effect of different GTV to high-dose CTV margins. Radiother Oncol J Eur Soc Ther Radiol Oncol. 2018 Jan;126(1):48–55.
2. Zukauskaite R, Kristensen MH, Eriksen JG, Johansen J, Samsøe E, Johnsen L, et al. Comparison of 3-year local control using DAHANCA radiotherapy guidelines before and after implementation of five millimetres geometrical GTV to high-dose CTV margin. Radiother Oncol J Eur Soc Ther Radiol Oncol. 2024 Jul;196:110284.

3. Nielsen CP, Lorenzen EL, Jensen K, Sarup N, Brink C, Smulders B, et al. Consistency in contouring of organs at risk by artificial intelligence vs oncologists in head and neck cancer patients. Acta Oncol Stockh Swed. 2023 Nov;62(11):1418–25.
4. Nielsen CP, Lorenzen EL, Jensen K, Eriksen JG, Johansen J, Gyldenkerne N, et al. Interobserver variation in organs at risk contouring in head and neck cancer according to the DAHANCA guidelines. Radiother Oncol J Eur Soc Ther Radiol Oncol. 2024 Aug;197:110337.

**Beyond the First Cut: A Comparison of Breast Induration in Breast Cancer Patients With and Without Repeat Surgery Based on DBCG Data**

**Authors**: Kristine W Høgsbjerg[1,2], Else Maae[3], Mette H Nielsen[4], Lars E Stenbygaard[5], Maja V Maraldo[6], Mette S Thomsen[7], Peer M Christiansen[8], Jens Overgaard[1], and Birgitte V Offersen[1,2]; on behalf of the Danish Breast Cancer Group Radiation Therapy Committee

*1: Department of Experimental Clinical Oncology, Department of Oncology, Palle Juul-Jensens Boulevard 99, 8200 Aarhus N, Aarhus University Hospital, Denmark. kwh@oncology.au.dk*
*2: Department of Oncology, Aarhus University Hospital, Aarhus, Denmark*
*3: Department of Oncology, Vejle Hospital, University of Southern Denmark, Denmark*
*4: Department of Oncology, Odense University Hospital, Denmark*
*5: Department of Oncology, Aalborg University Hospital, Denmark*
*6: Department of Oncology, Copenhagen University Hospital, Rigshospitalet, Denmark*
*7: Department of Medical Physics, Aarhus University Hospital, Aarhus, Denmark*
*8: Department of Plastic and Breast Surgery, Aarhus University Hospital, Aarhus, Denmark*

**Purpose/Objective:**

Breast-conserving surgery followed by whole breast irradiation (WBI) is standard for most breast cancer patients. For patients with node-negative breast cancer long-term survival, optimising treatment while minimising late effects is essential [1-3]. Repeat surgery (RS), often required due to incomplete margins, may increase late effects. This study aimed to evaluate late effects in contemporarily treated patients undergoing repeat surgery.

**Material/Methods:**

Patients receiving WBI were included from the two randomised phase III trials, DBCG HYPO (2009-2014) and PBI (2009-2016) [2, 3] and categorised based on RS yes/no performed within 60 days. The primary endpoint in the DBCG HYPO and PBI trials was the 3-year grade 2–3 breast induration rate. Evaluations were conducted annually from 1 to 5 years and at 10 years of follow-up. This study reports the cumulative incidence of grade 2–3 induration at 3 and 5 years, calculated using the Aalen-Johansen estimator with competing risk analysis. The cumulative incidence of induration was assessed starting from year two to disregard initial surgical healing.

**Results:**

A total of 1,919 patients were included, with 303 undergoing RS and 1,616 not (NoRS). The median age was 63.6 years, with 62.7 years in the RS group and 63.8 years in the NoRS group. Overall, 193 had ductal carcinoma in situ (DCIS) and 1,726 had invasive cancer. DCIS was more common in the RS group (19.1%) compared to the NoRS group (8.4%). Tumor bed boost was delivered in 220 patients of which 173 patients had 10 Gy/5 fx and 47 patients had 16 Gy/8 fx.

Induration rates were higher in the RS group compared to the NoRS group. At 3 years, rates were 15.6% vs. 11.7%, and at 5 years, 20.0% vs. 14.9%, HR 0.75 (95% CI, 0.56-1.00). For patients receiving a boost, rates at 3 years were 22.0% (RS) vs. 18.9% (NoRS), and at 5 years, 30.7% (RS) vs. 25.7% (NoRS). In patients without a boost, 3-year rates were 14.7% (RS) vs. 10.8% (NoRS), and 5-year rates were 18.1% (RS) vs. 13.5% (NoRS) (Figure 1).

**Conclusion**: Repeat surgery was associated with an increased cumulative incidence of grade 2–3 breast induration at 3 and 5 years, with further increases observed in patients receiving a tumor bed boost. Compared to using a boost, RS appears to induce less induration of the breast. Adjustments for age, smoking, and irradiated breast volume will be conducted in the final analysis [4, 5]

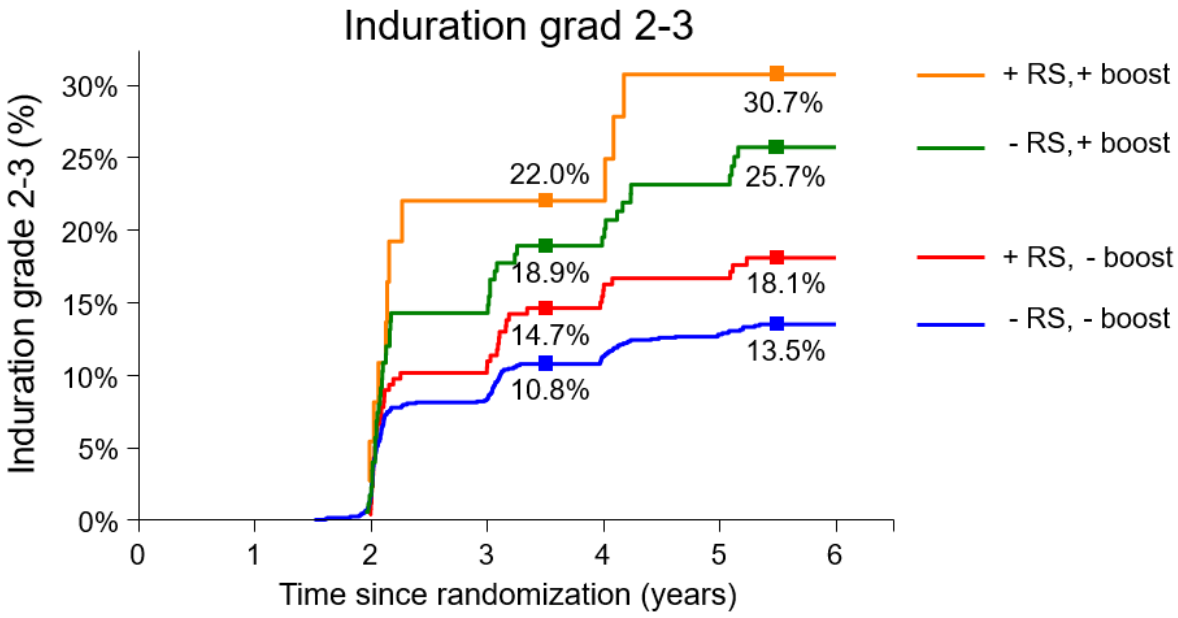


At risk

| | | | | | | | |
|---|---|---|---|---|---|---|---|
| - RS, + Boost | 264 | 259 | 248 | 208 | 188 | 164 | 118 |
| - RS, - Boost | 1435 | 1405 | 1310 | 1179 | 1081 | 957 | 728 |
| + RS, - Boost | 39 | 38 | 34 | 27 | 24 | 18 | 16 |
| + RS, + Boost | 181 | 177 | 169 | 143 | 130 | 114 | 95 |

*Figure 1: Cumulative incidence of grade 2-3 induration. The follow-up period is recorded in years post-radiotherapy. Rates at 3 and 5 years are evaluated at 3.5 and 5.5 years to ensure consistent annual follow-ups for all patients. RS, repeat surgery; NoRS, no repeat surgery; boost were delivered as 10Gy/5fx or 16Gy/8 fx.*

**References**


1. Society, A.C. *Understanding a Breast Cancer Diagnosis* 2021.
2. Offersen, B.V., J. Alsner, H.M. Nielsen, E.H. Jakobsen, M.H. Nielsen, L. Stenbygaard, et al. *Partial Breast Irradiation Versus Whole Breast Irradiation for Early Breast Cancer Patients in a Randomized Phase III Trial: The Danish Breast Cancer Group Partial Breast Irradiation Trial.* J Clin Oncol, 2022. **40**(36): p. 4189-4197 DOI: 10.1200/jco.22.00451.
3. Offersen, B.V., J. Alsner, H.M. Nielsen, E.H. Jakobsen, M.H. Nielsen, M. Krause, et al. *Hypofractionated Versus Standard Fractionated Radiotherapy in Patients With Early Breast Cancer or Ductal Carcinoma In Situ in a Randomized Phase III Trial: The DBCG HYPO Trial.* J Clin Oncol, 2020. **38**(31): p. 3615-3625 DOI: 10.1200/jco.20.01363.
4. Thomsen, M.S., J. Alsner, H.M. Nielsen, E.H. Jakobsen, M.H. Nielsen, M. Møller, et al. *Volume matters: Breast induration is associated with irradiated breast volume in the Danish Breast Cancer Group phase III randomized Partial Breast Irradiation trial.* Radiother Oncol, 2022. **177**: p. 231-235 DOI: 10.1016/j.radonc.2022.09.024.
5. Thomsen, M.S., J. Alsner, C.M. Lutz, M. Berg, I. Jensen, E.L. Lorenzen, et al. *Breast induration and irradiated volume in the DBCG HYPO trial: The impact of age, smoking, and boost.* Radiother Oncol, 2024. **201**: p. 110574 DOI: 10.1016/j.radonc.2024.110574.

# Local recurrence with and without a tumour-bed boost: a post-hoc analysis of the DBCG IMN2 study

Anders W. Mølby Nielsen(1,2,3) · Lise B. J. Thorsen(1,2,3) · Demet Özcan (1,4) · Louise W. Matthiessen(5) · Else Maae(6) · Marie L.H. Milo(7) · Mette H. Nielsen(8) · Trine Tramm(1,4) · Jens Overgaard(1,2) · Birgitte V. Offersen (1,2,3,9) on behalf of the DBCG RT Committee.

1: Department of Experimental Clinical Oncology, Aarhus University Hospital, Aarhus, Denmark
2: Department of Clinical Medicine, Aarhus University, Aarhus, Denmark
3: Department of Oncology, Aarhus University Hospital, Aarhus Denmark

4: Department of Pathology, Aarhus University Hospital, Aarhus, Denmark
5: Department of Oncology, Copenhagen University Hospital Herlev and Gentofte, Copenhagen, Denmark
6: Department of Oncology, Vejle Hospital, University Hospital of Southern Denmark, Vejle, Denmark
7: Department of Oncology, Aalborg University Hospital, Aalborg, Denmark
8: Department of Oncology, Odense University Hospital, Odense, Denmark
9: Danish Center for Particle Therapy, Aarhus University Hospital, Aarhus Denmark

## Introduction

In early-stage breast cancer, a tumour-bed boost (TBB) reduces the risk of local recurrence (LR) by around 50% but increases the risk of breast induration and does not improve survival. LR incidences of 3% at 5 years and 6% at 10 years have been proposed as thresholds where benefits outweigh the potentially detrimental effects of a TBB. Therefore, this post-hoc analysis of the Danish Breast Cancer Group (DBCG) IMN2 study aimed to investigate LR rates according to prognostic risk factors to identify indications for a TBB.

## Material and methods

From the DBCG IMN2 study, 2,430 node-positive patients operated with breast-conserving surgery were included for analysis. They received irradiation to the residual breast and regional nodes with or without internal mammary node irradiation according to laterality. Radiotherapy was 3D-conformal. TBB was delivered sequentially as 10Gy/5Fx (41-49 years) and 16Gy/8Fx (≤40 years or margin < 2mm). Systemic therapy was given postoperatively and included anthracyclines, taxanes, aromatase inhibitors, and trastuzumab. Patients with and without a TBB were analysed separately. Prespecified subgroups included known prognostic risk factors.

## Results

Median follow-up was 13.7 years, and the cumulative incidence of LR was 1.7% (95% CI, 1.2-2.2) at 5 years and 3.6% (95% CI, 2.9-4.3) at 10 years. The corresponding cumulative incidence of contralateral BC was 2.9% (95% CI, 2.2-3.6) at 10 years.
In patients ≥ 50 years, 1,871 patients were treated without a TBB. Among these, 145 patients with an ER-/HER2- tumour had a 10-year cumulative incidence of LR of 8.3% (95% CI, 4.6-13.6), Fig. 1. No other subgroups exceeded 6% at 10 years.

## Conclusion

Our results suggest that node-positive patients 50 years or older with an ER-/HER2- tumour may obtain a clinically relevant benefit from a TBB. Based on these data, the DBCG has updated the Danish guidelines to recommend a 16Gy/8 Fx TBB for all patients with ER-/HER2- tumours, regardless of age.

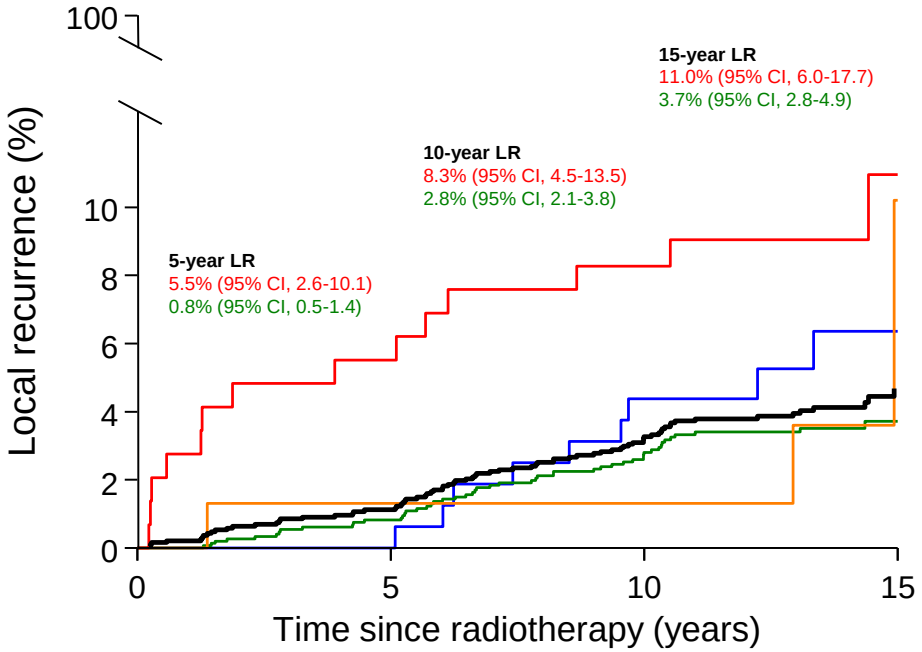


Number at risk

| | | | | |
|---|---|---|---|---|
| ER+/HER2- | 1465 | 1269 | 941 | 164 |
| ER+/HER2+ | 160 | 133 | 107 | 19 |
| ER-/HER2+ | 76 | 59 | 48 | 8 |
| ER-/HER2- | 145 | 106 | 78 | 18 |
| All patients | 1872 | 1585 | 1188 | 209 |

**Fig. 1**. The cumulative incidence of local recurrence according to IHC subtypes in node-positive breast cancer patients ≥ 50 yr treated without a TBB. ER+/HER2- (green), ER+/HER2+ (blue), ER-/HER2+ (orange), and ER-/HER2- (red). The black line depicts all patients ≥ 50 yr treated without a TBB. Abbreviations: LR, local recurrence; IHC subtype, immunohistochemical subtype; yr, years TBB, tumour-bed boost.

**Quality assessment of 2705 treatment plans in the randomised Danish Breast Cancer Group Skagen trial 1**

M.S. Thomsen[1], E.L. Lorenzen[2], J. Alsner[3], S.L. Krogh[2], E.S. Yates[1], M. Berg[4], K.I. Dybvik[5], K. Boye[6], C. Kirkove[7], I. Jensen[8], M.M.B. Nielsen[9], S. Makocki[10], V. Tømmerås[11], P. Schilling[12], M.P. Hasler[13], K. Andersen[14], L. Stick[15], M.-B. Jensen[16] and B.V. Offersen[3,17]

[1]Department of Medical Physics, Aarhus University Hospital, Aarhus, Denmark
[2]Laboratory of Radiation Physics, Odense University Hospital, Odense, Denmark
[3]Department of Experimental Clinical Oncology, Aarhus University Hospital, Denmark
[4]Department of Medical Physics, University Hospital of Southern Denmark, Vejle, Denmark
[5]Department of Medical Physics, Stavanger University Hospital, Stavanger, Norway
[6]Department of Oncology, Copenhagen University Hospital, Rigshospitalet, Copenhagen, Denmark
[7]Department of Radiotherapy, Université Catholique de Louvain, Cliniques Universitaires St-Luc, Bruxelles, Belgium
[8]Department of Medical Physics, Aalborg University Hospital, Aalborg, Denmark
[9]Department of Oncology, Zeeland University Hospital, Denmark
[10]Department of Clinical Medicine, UiT, The Arctic University of Norway, Tromsø, Norway
[11]Praxis for Radiotherapy, Academic Teaching Hospital Dresden-Friedrichstadt, Dresden, Germany
[10]Department of Radiation Oncology and Faculty of Medicine Carl Gustav Carus, Technische Universität Dresden, Dresden, Germany
[13]Department of Oncology, Sørlandet Hospital, Kristiansand, Norway
[14]Department of Oncology, Herlev and Gentofte University Hospital, Herlev, Denmark
[15]Danish Centre for Particle Therapy, Aarhus University Hospital, Aarhus, Denmark
[16]Danish Breast Cancer Group, Copenhagen University Hospital, Rigshospitalet, Copenhagen, Denmark
[17]Department of Oncology, Aarhus University Hospital, Denmark

**INTRODUCTION** Inter-center variation in radiotherapy practices can be substantial, encompassing differences in contouring guidelines, planning doses to targets and organs at risk (OAR) and delivery techniques. Understanding these variations is critical for interpreting the findings of large clinical trials and assessing their relevance to current and future clinical practice. This study investigates how radiotherapy (RT) was conducted in the multi-centre, randomised phase III SKAGEN 1 trial (NCT02384733).

**METHODS** From 2015 to 2021, 2963 breast cancer patients referred to adjuvant, locoregional breast radiotherapy after breast conserving surgery (BCS) or mastectomy were randomised to 50Gy/25fractions versus 40Gy/15fractions. Tumour-bed boost after BCS was delivered as a simultaneous integrated boost

(SIB). Delineated target volumes were per ESTRO guidelines. Each lymph node level was delineated as a separate volume. Treatment plans were prospectively uploaded to the Danish treatment plan data bank allowing detailed analysis of various dosimetric parameters from the individual treatment plans.

**RESULTS** RT plans from 2705 patients treated at 14 centres in 4 countries were available for analysis corresponding to treatment plans from 94% of the per-protocol patient cohort (n= 2869) in the trial. Overall, 1407 patients had BCS, 426 of these (30%) had a SIB and 1298 had mastectomy. The randomisation was balanced with 1329 (50Gy) and 1376 (40Gy) patients. All plans had target volume delineations and no significant difference was observed regarding the delineated volumes between the two arms. Furthermore, no difference in inter-centre dose variations was detected between 40Gy and 50Gy plans (figure 1). Centre specific differences in the prioritising between target coverage and OAR sparing were observed especially for internal mammary nodes versus heart and axillary level 1 lymph nodes versus humeral head. The compliance to protocol constraints was generally high, however, the compliance to ”hot spot” constraints was higher in 50Gy plans where 98% complied to the 50Gy constraint: V107%≤2% whereas only 80% of the 40Gy plans complied to the stricter 40Gy constraint: V105%≤2%. No significant difference (p=0.45) was found in the number of plans with V110%>0 (<1% in both arms). The minimum coverage of target volumes was similar in the two arms. Respiratory gated technique was used in 83% of the patients. Dividing into subgroups per laterality and gating technique, significantly higher lung and heart doses were detected in free-breathing plans compared to gated plans.

**CONCLUSIONS** No differences were found between the treatment plans in the two arms and compliance with the protocol constraints was high.

**Figure 1**: Box-plots showing the intra-centre and inter-centre variations in mean doses to target structures with 50Gy plans to the left and 40Gy plans to the right. The mean doses to the breast and chest wall in the treatment plans without boost are shown in the first row, whereas the mean tumour-bed doses in the simultaneously integrated boost plans are shown in the second row. The CTVn plots only include the treatment plans where the specific lymph node level was target.

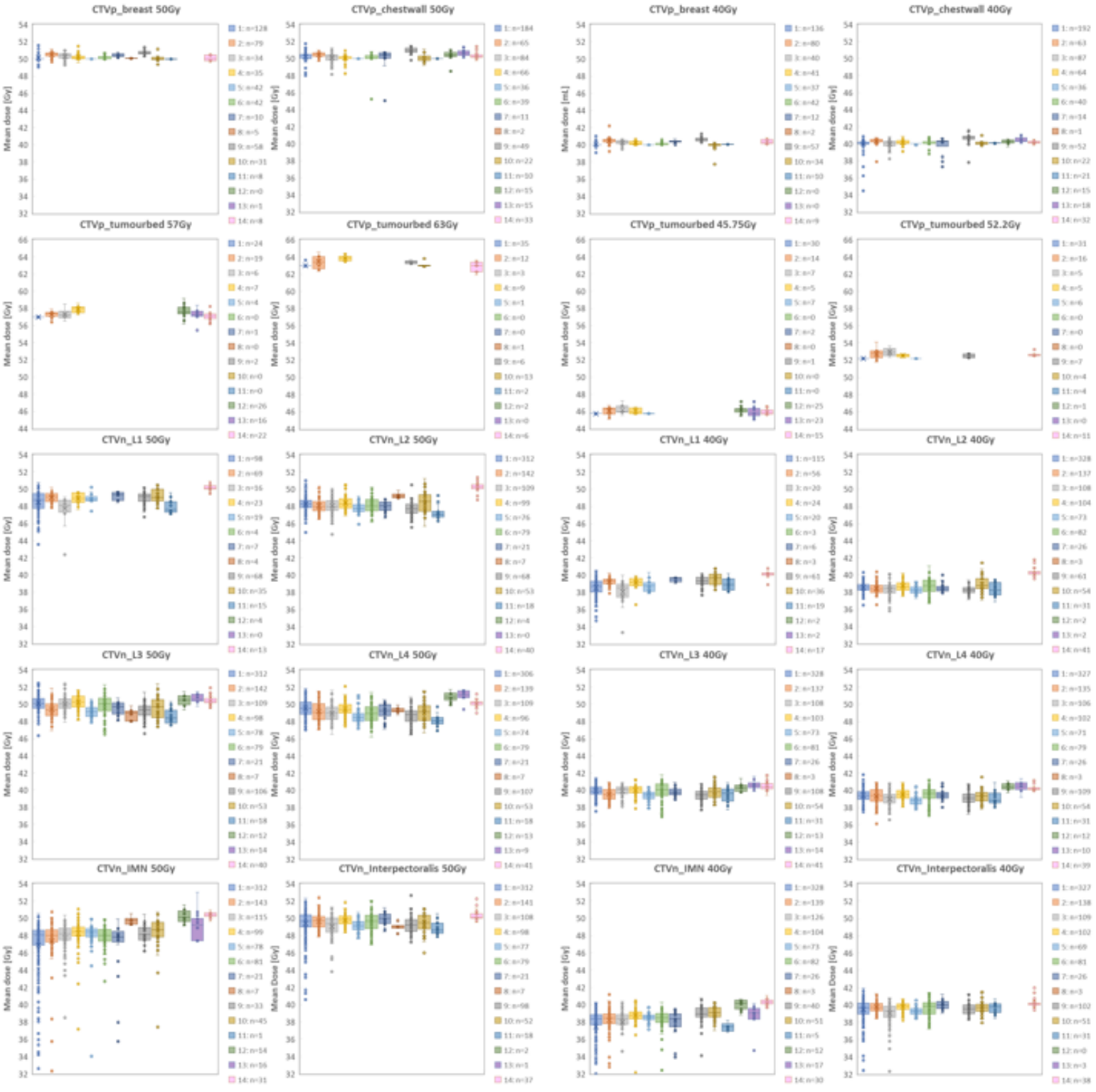

# POSTERS

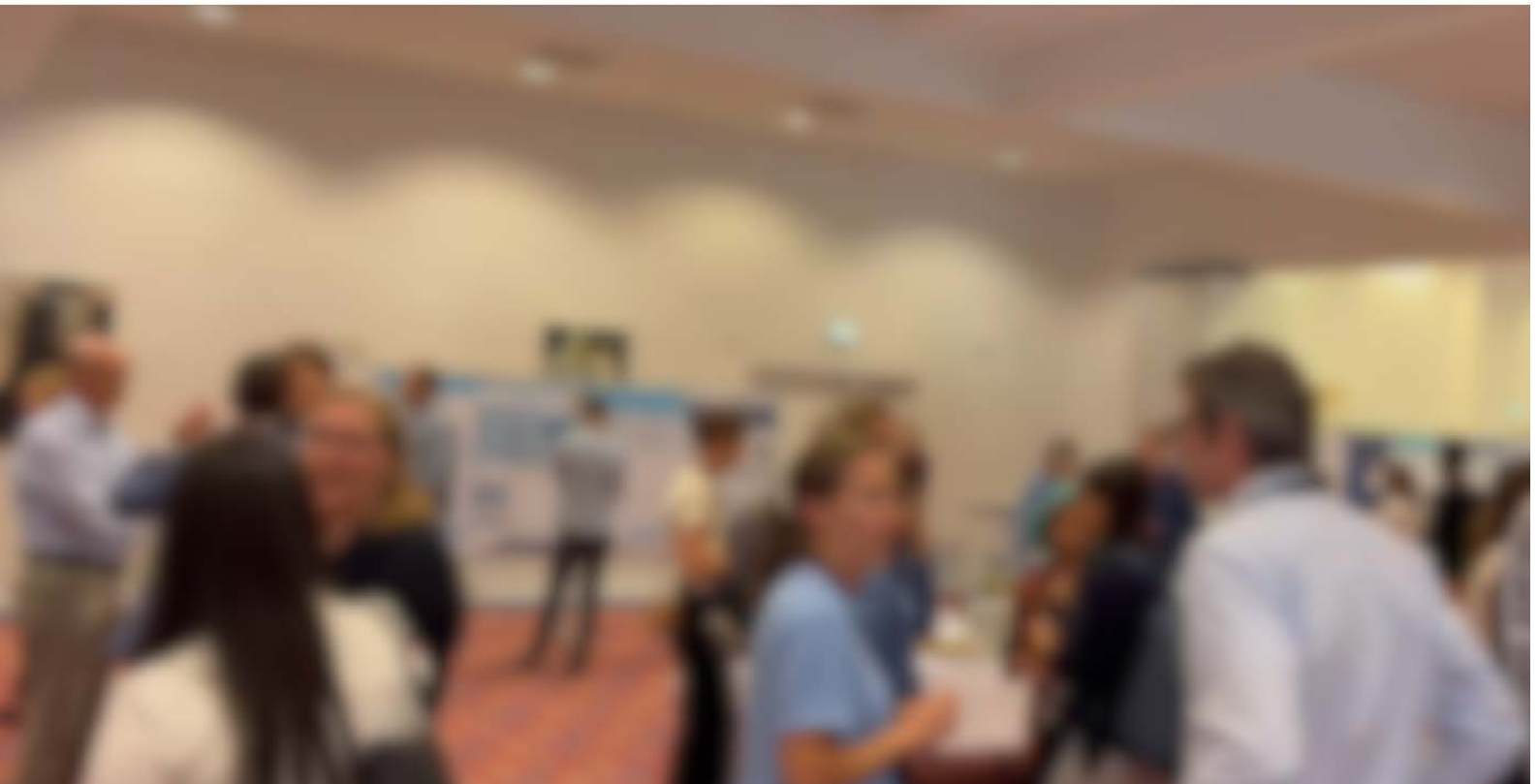

# Paraffin wax as a bolus material in accelerator-based boron neutron capture therapy

**Author information:** Jenna Tarvonen

jenna.tarvonen@hus.fi

Comprehensive Cancer Center, Helsinki University Hospital (HUS) and University of Helsinki, Haartmaninkatu 4, Helsinki, 00290, Finland

Jenna Tarvonen[1], Lauri Wendland[1], Liisa Porra[1], Tiina Seppälä[1], Mikko Tenhunen[1]

[1]Comprehensive Cancer Center, Helsinki University Hospital (HUS) and University of

Helsinki, Haartmaninkatu 4, Helsinki, 00290, Finland

## Introduction

Boron neutron capture therapy (BNCT) is a unique type of radiation therapy that enables biological targeting of cancer at the cellular level. With an epithermal neutron beam, the dose maximum typically occurs approximately 2 cm deep in tissue. Consequently, when treating superficially located tumors, such as head and neck cancers, a sufficient dose for effective tumor control may not reach the skin surface. As in external beam radiation therapy (EBRT), surface dose can be increased by using a bolus as a moderating material placed on the surface of the target. Contrary to EBRT, tissue equivalency is a complex question in BNCT, and depends strongly on elemental composition. The purpose of this study was to examine the impact of a paraffin wax bolus on the epithermal neutron beam in accelerator-based BNCT and to evaluate the agreement between treatment planning system calculations and measured results.

## Materials and methods

The neutron beam characterization was performed using the neutron activation method with diluted manganese and gold foils, as well as manganese wires. Manganese is particularly important for boron dose estimation due to its high cross section with thermal neutrons. The irradiations were conducted in a 3D water tank, and in an anthropomorphic head-shaped phantom simulating the geometry of a typical patient treatment. The tested boluses were 5 and 10 millimeters thick.

## Results

The results demonstrated that the calculated and measured activation values agree within 5% accuracy in the significant dose region (over 50% dose). Near the surface and at the deepest measurement points, the agreement was slightly weaker but remained still within 10%. The bolus shifted the neutron activation depth curve towards the surface by 4 mm - 13 mm depending on its thickness.

## Conclusions

Paraffin wax serves as an effective neutron energy modulator, making it an appropriate bolus material. Additionally, it is cost-effective and easily adaptable for individual patient needs. With

a carefully controlled and reproducible manufacturing process, paraffin wax is well-suited for use as a bolus material in BNCT treatments where an increased surface dose is needed.

**Dosimetric impact of esophageal inter-fraction motion in esophagus-sparing radiotherapy for meta-static spinal cord compression.**

**Corresponding author**

Anna Mann Nielsen

Department of Oncology, Copenhagen University Hospital - Herlev and Gentofte

Borgmester Ib Juuls Vej 7

2730 Herlev, Denmark

Telephone : 26718136

Email: anna.mann.nielsen@regionh.dk

**Authors**

Anna Mann Nielsen[1], Laura A. Rechner[1], Sebastian Moretto Krog[1], Vanja Gram[1], Morten H. Suppli[2], Patrik Sibolt[1], Ivan R. Vogelius[2,3], Claus P. Behrens[1,4], Gitte Persson[1,3]

**Affiliations**

[1]Department of Oncology, Copenhagen University Hospital - Herlev and Gentofte, Borgmester Ib Juuls Vej 7, 2730 Herlev, Denmark

[2]Department of Oncology, Copenhagen University Hospital, Rigshospitalet, Blegdamsvej 9, 2100 Copenha-gen, Denmark

[3]Department of Clinical Medicine, University of Copenhagen, Blegdamsvej 3B, 2200 Copenhagen, Denmark

[4]Department of Health Technology, Technical University of Denmark, Ørsteds Plads 349, 2800 Kongens Lyngby, Denmark.

**Introduction**

The phase III randomized trial ESO-SPARE (NCT05109819) investigates whether esophagus-sparing Volu-metric Modulated Arc Therapy (VMAT) or Intensity-Modulated Radiation-Therapy reduces dysphagia in patients with cervical or thoracic Metastatic Spinal Cord Compression (MSCC). We hypothesize that esoph-ageal inter-fraction motion may undermine the esophagus-sparing strategy. This study aims to quantify the dosimetric impact of esophageal inter-fraction motion using high-quality CBCTs.

**Methods**

Patients treated on high-quality CBCT-equipped units (HyperSight, Varian a Siemens Healthineers com-pany) between September 2023 and December 2024 were screened. Inclusion criteria were treatment in free-breathing, ≥ 5 consecutive CBCTs with T1-T10 vertebrae in the field of view, and visible esophagus. The esophagus was contoured on the planning CT ($_{pCT}$Esophagus) and five consecutive CBCTs ($_{CBCT}$Esophagus$_{1-5}$). Standard and esophagus-sparing 25 Gy in 5 fractions VMAT plans were created for simulated spinal tar-gets (T1-2, T3-4, T5-6, T7-8, T9-10). For the esophagus-sparing plans, the $_{pCT}$Esophagus near-max dose D0.027cc was constrained to 8.5 Gy. CBCTs were registered to the pCT using bony matching, and $_{CBCT}$Esophagus$_{1-5}$ were rigidly transferred to the pCT. Dose values from the original VMAT plan were ex-tracted for each $_{CBCT}$Esophagus, including esophagus mean dose, D0.027cc–D5cc and V8.5Gy. For each plan, the estimated delivered dose for each metric was calculated by averaging the dose values from $_{CBCT}$Esophagus1-5. Dose metrics were compared between standard and esophagus-sparing plans (Wilcoxon rank-sum test). Esophageal inter-fraction motion was assessed using 95% Hausdorff distance (95%HD). As a surrogate for CBCT image quality, the $_{CBCT}$Esophagus was delineated by two observers in two patients with six targets and compared using DICE. The 95%HD between the $_{CBCT}$Esophagus structures delineated by the two observers was analyzed to quantify interobserver variation.

**Results**

Twelve patients with 23 simulated targets were included. The estimated delivered D0.027cc violated the con-straint in 20 of 23 simulated plans. All dose metrics, including the volume of esophagus receiving > 8.5 Gy, were significantly lower in esophagus-sparing plans compared to standard plans ($p<0.001$), ***Figure 1.*** The mean 95%HD was 4 mm (range: [1.4,7.0] mm) the mean interobserver 95%HD was 2.5 mm (range:[1.4,5.4] mm). All DICE scores were > 0.80 indicating sufficient CBCT quality for accurate esophagus delineation.

**Conclusion**

Esophageal inter-fraction motion led to violation of esophagus-sparing constraints in 20/23 plans. However,

only a small portion of the esophagus moved into the high-dose area, and substantial esopahgus-sparing re-mained. The magnitude of inter-fraction motion, as measured by 95% HD, was similar to the variation caused by interobserver differences.

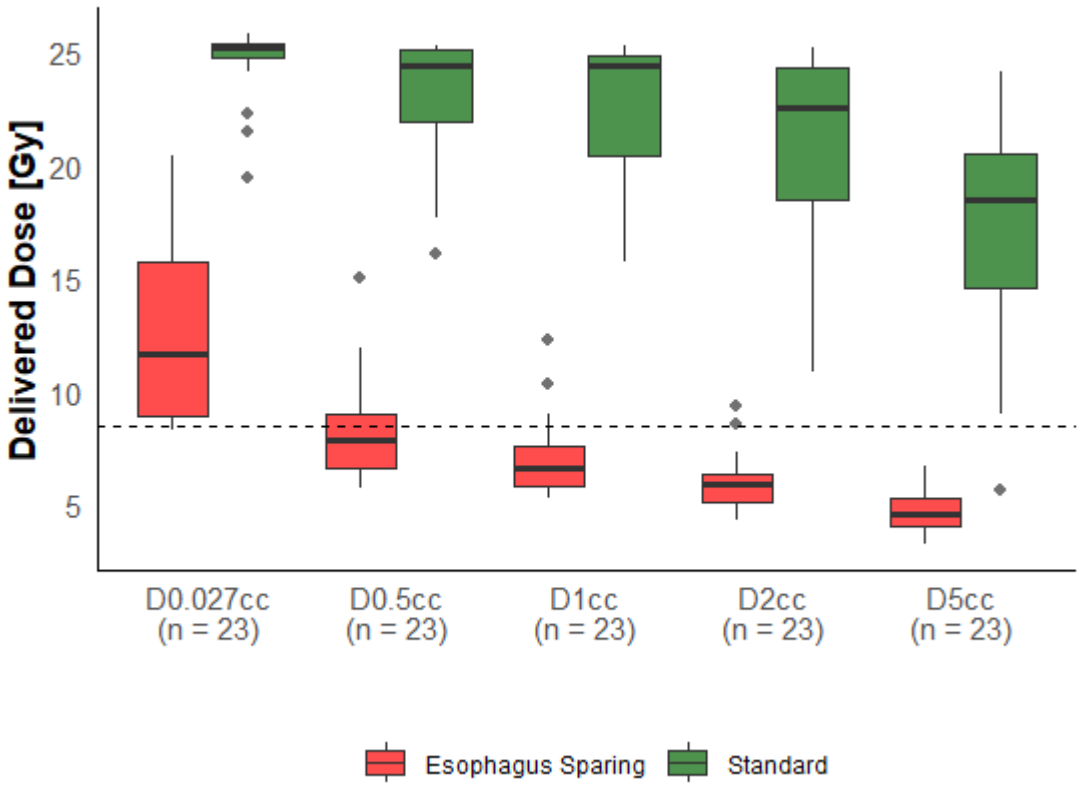


***Figure 1.*** *Estimated delivered dose to esophagus D0.027cc, D0.5cc, D1cc, D2cc, and D5cc in esoph-agus-sparing and standard plans. Each box represents data from 23 simulated plans. The thick horizontal line indicates the median, while the box represents the interquartile range (IQR). Whiskers extend to the smallest and largest values within 1.5 times the IQR from Q1 and Q3. Black dots represent outliers. The dashed horizontal line marks 8.5 Gy: the protocol-defined esophagus constraint for D0.027cc. For all dose metrics, the difference between treatment groups was statistically significant according to the Wilcoxon rank-sum test ($p < 0.001$).*

**Decision Support Model for referral of patients with glioma to proton therapy**

Siri Grøndahl[1], Jesper Folsted Kallehauge[2,3], Slavka Lukacova[1,3]

[1] Department of Oncology, Aarhus University Hospital, Aarhus, Denmark
[2] Danish Centre for Particle Therapy, Aarhus University Hospital, Aarhus, Denmark
[3] Institute for Clinical Medicine, Aarhus University, Aarhus, Denmark

**Introduction:**

The referral of patients with gliomas for proton treatment (PT) in Denmark is based on the comparison of individual photon and PT plans and demonstrating > 20% dose reduction to the healthy brain or critical structures. The aim of this retrospective study was to identify clinical parameters associated with referral to PT and build a prediction model.

**Method:**

The dataset consisted of adult patients with glioma and candidates for PT at Aarhus University Hospital between 2019 and 2023. Clinical (age, diagnosis, tumor grade, target volume) and dosimetric (prescribed dose and mean dose to healthy brain) parameters were collected. Univariate and multivariate logistic regression was used for the analysis of clinical parameters associated with PT. The dataset was split into training cohort (n=38, 2019-2022) and validation cohort (n=12, 2023). Prediction models were built using logistic regression and support vector machine (SVM) algorithms.

**Results:**

Age (p=0.02), mean dose to healthy brain (P=0.02) and target volume (P<0.001) were independently associated with PT. Age and target volume used for model prediction (Figure 1). The SVM model demonstrated superior predictive accuracy when applied to the validation cohort, with an area under the curve (AUC) for the receiver operating characteristic (ROC) = 1 (95% CI: 1-1) and precision/recall (PR) = 1, compared to AUC-ROC = 0.8 (95% CI: 0.38-1) and AUC-PR = 0.96 for the logistic regression model. Using probability threshold > 90% the SVM model predicted 10 true positives and 2 true negatives, and no false negatives referrals.

**Conclusion:**

SVM model using age and target volume demonstrated high predictive accuracy. Validation in larger dataset is needed.

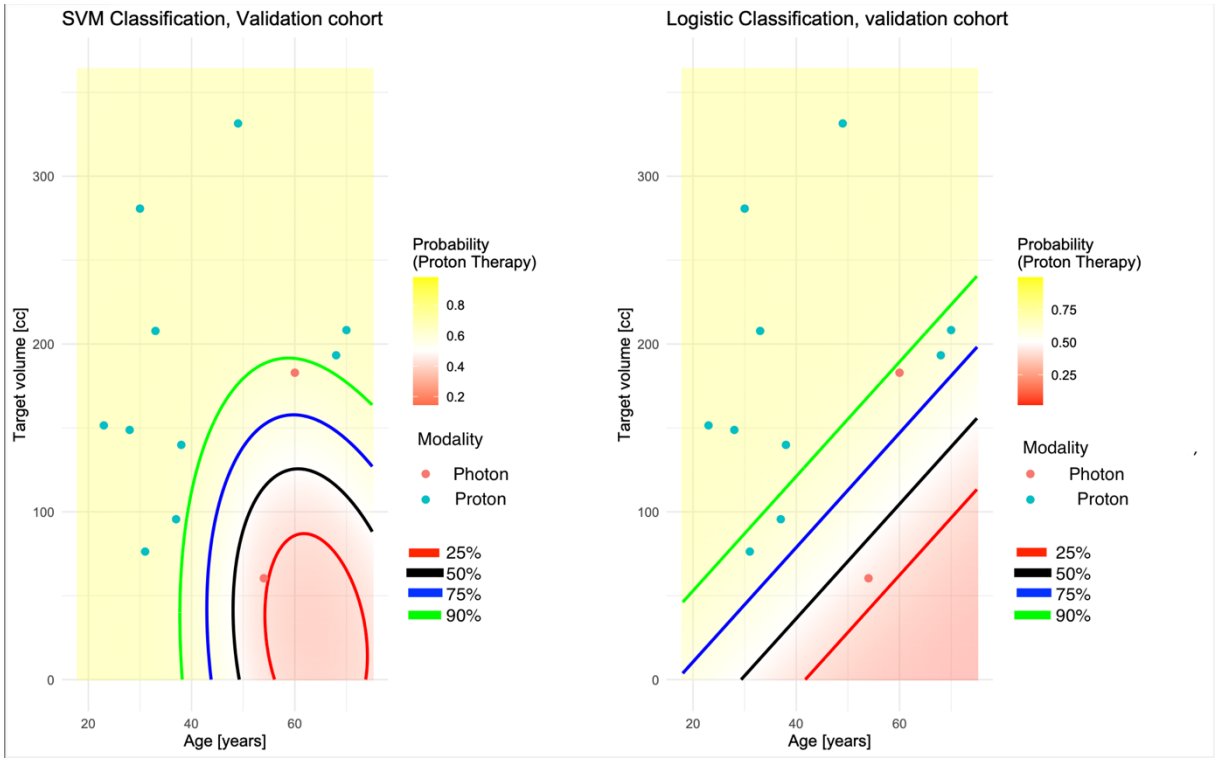


Figure 1: The SVM model (left) and the logistic regression model (right) with four different probability thresholds for patients in the validation cohort categorized based on the treatment modality. The color in the background indicates probability for proton treatment.

# Proton versus photon treatment planning in the Scandinavian CURE Lung trial for reirradiation of thoracic tumours

Maria Fuglsang Jensen, marfugje@rm.dk, Danish Centre for Particle Therapy, Aarhus University Hospital, Denmark

**Authors**

Maria Fuglsang Jensen[1], Marianne Marquard Knap[2], Mai-Britt Linaa[2], Hanna Rahbek Mortensen[1,3], Ane Appelt[4], Lone Hoffmann[2,3]

[1]Danish Centre for Particle Therapy, Aarhus University Hospital, Denmark

[2]Department of Oncology, Aarhus University Hospital, Aarhus, Denmark

[3] Department of Clinical Medicine, Aarhus University, Aarhus, Denmark

[4]Leeds Institute of Medical Research, University of Leeds, UK

## Introduction

The upcoming Scandinavian CURE Lung trial examines the safety of high-dose reirradiation of thoracic tumours. This study compares photon and proton reirradiation plans in a retrospective cohort to identify when protons could be beneficial.

## Materials and Methods

Fourteen patients with recurrent or new non-small cell lung cancer, treated with reirradiation (type I or II [1]) between 2013 and 2023, were included. Ten received stereotactic radiotherapy, and four long-course radiotherapy in the previous treatment. The previous treatment dose was transferred to the new CT using deformable image registration and EQD2 rescaling (spinal cord: $\alpha/\beta=2$, otherwise: $\alpha/\beta=3$). Two plans were created for each modality: 66Gy/33 fractions and 50Gy/24 fractions, with dose escalation up to mean doses of 66Gy for tumours and larger lymph nodes. Photon plans were IMRT with 5-7 fields and a 5mm CTV-PTV margin, while proton plans were robustly optimized IMPT with 1-5 fields, evaluated with 5mm setup error and 3.5% range uncertainty. Reirradiation plans were assessed using standard Danish dose constraints, followed by cumulative EQD2 evaluation using the CURE Lung constraints. If these constraints were not met, target coverage was iteratively compromised. OAR doses for all plans were compared using a two-sided paired sample Wilcoxon signed-rank test.

## Results

For both modalities, 9/14 66Gy-plans and 10/14 50Gy-plans met full target coverage constraints (V95% >98% and V95%>99.5%, respectively) while adhering to CURE Lung constraints. The target compromises for the remaining patients were similar between modalities and primarily due otherwise overdosage of connective tissue (D0.3cc>110Gy EQD2). For three 66Gy-plans the target coverage was V95%<80%, while for two V95%>95%. For two 50Gy-plans the target coverage was V95%<80%, while for three V95% >95%. Proton plans delivered 1.3Gy and 1.7Gy lower mean lung doses for 66Gy and 50Gy-plans, respectively. Mean heart doses were 1.3Gy and 1.2Gy lower, see Figure 1. These differences were significant ($p<0.001$).

## Conclusions

Reirradiation plans can be created with both modalities without a target compromise for most patients, but no target coverage benefit was observed for protons compared to photons. Proton plans, however, achieved better cumulative dose sparing of the heart and lungs. Proton treatment is therefore beneficial in patients where the dose to these OARs is the main concern.

[1] Andratschke N et al. European Society for Radiotherapy and Oncology and European Organisation for Research and Treatment of Cancer consensus on re-irradiation: definition, reporting, and clinical decision making. Lancet Oncol. 2022 Oct;23(10):e469-e478.

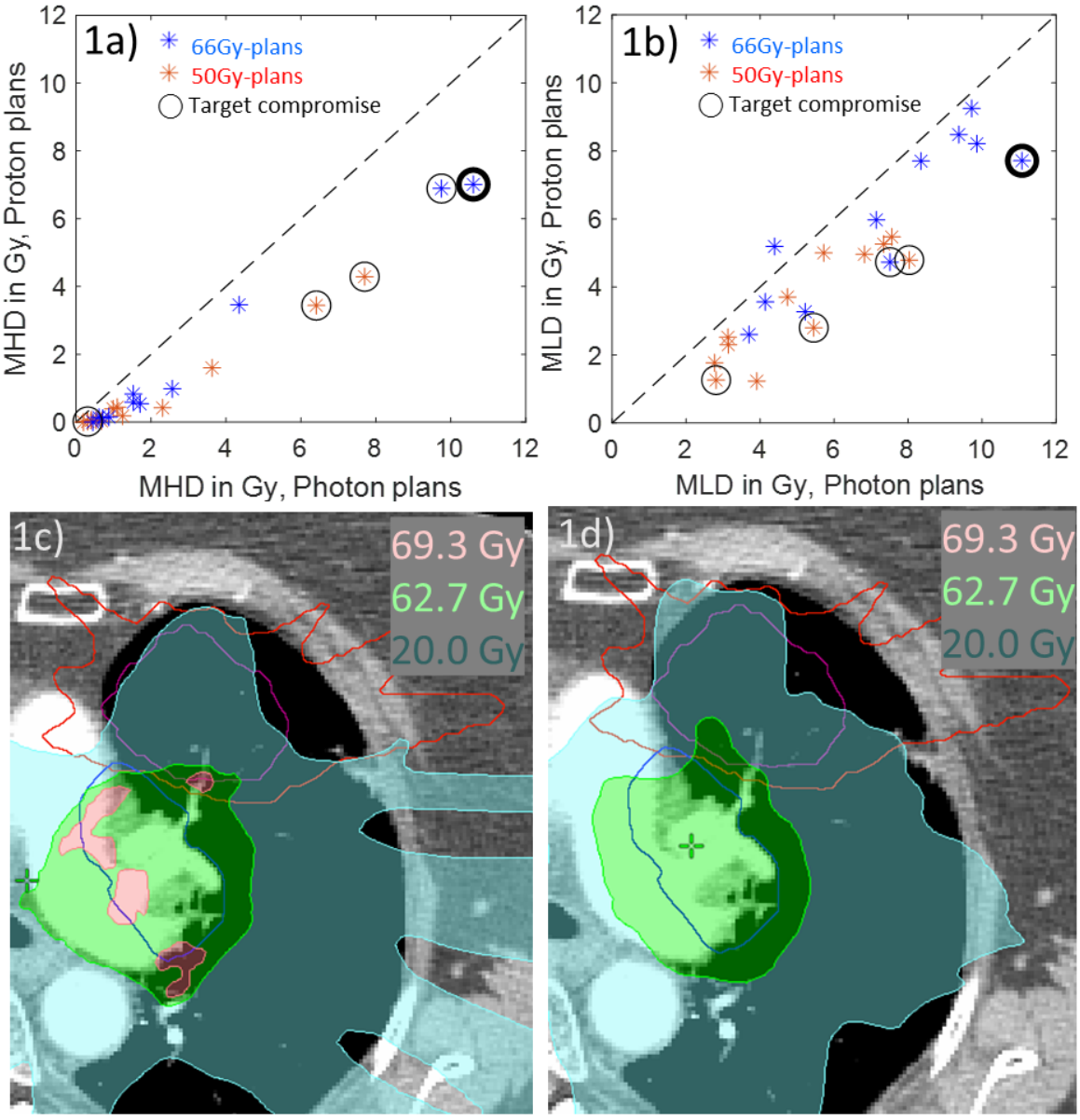


Figure 1a) Mean heart dose for photon vs. proton and figure 1b) mean lung dose for photon vs proton. Plans with target V95%>95% are included. Red markers are 50Gy-plans, blue markers are 66Gy-plans. Black circles indicate the plans where a smaller target compromise allowed the CURE Lung constraints to be achieved. The two 66Gy-plans indicated with a thick black circle are illustrated in 1c) for photons and in 1d) for protons. The blue contour within the dose colour wash is the CTV. The red contour is the 50Gy and the purple contour is the 90Gy EQD2 dose from the previous treatment.

**Intercentre reirradiation treatment planning consistency: Pre-trial QA in the CURE Lung trials for recurrent or new thoracic cancers**

Lone Hoffmann[1,2], Mai-Britt Linaa[1], Mai Ehmsen[3], Maria Fuglsang Jensen[3], Marianne Marquart Knap[1], Christina Larsen[4], Mikkel Drøgemüller Lund[5], Laura Patricia Kaplan[6], Morten Nielsen[7], Wiviann Ottosson[4], Cécile Peucelle[8], Arpit Saini[6], Hella Sand[9], Simon Nyberg Thomsen[1,2], Ane Appelt[10]

1) Department of Oncology, Aarhus University Hospital, Aarhus, Denmark
2) Department of Clinical Medicine, Aarhus University, Aarhus, Denmark
3) Danish Centre for Particle Therapy, Aarhus University Hospital, Denmark
4) Department of Oncology, Radiotherapy Research Unit, Copenhagen University Hospital - Herlev and Gentofte, Herlev, Denmark
5) Department of Oncology, Vejle Hospital, University Hospital of Southern Denmark, Vejle, Denmark
6) Department of Oncology and Palliative Units, Zealand University Hospital, Næstved, Denmark.
7) Department of Oncology, Odense University Hospital, Odense, Denmark
8) Department of Oncology, Centre for Cancer and Organ Diseases, Copenhagen University Hospital -Rigshospitalet, Copenhagen, Denmark.
9) Department of Oncology, Aalborg University Hospital, Aalborg, Denmark
10) Leeds Institute of Medical Research, University of Leeds, UK

Corresponding author: Lone Hoffmann; e-mail: Lone.Hoffmann@aarhus.rm.dk

## Introduction

The number of long-term lung cancer survivors is increasing, but many develop recurrent or new thoracic cancers following previous radiotherapy. High-dose reirradiation (reRT) is promising but associated with high toxicity risk, demanding careful treatment planning. This study investigates adherence to proposed national reRT guidelines and intercentre dose planning consistency before initiation of the Scandinavian CURE Lung trial.

## Materials and methods

Six lung cancer cases, treated with high-dose reRT, were distributed to seven Danish radiotherapy centres and one proton centre. Previous treatments were stereotactic (cases 1,3,4,5) or normo-fractionated (cases 2,6). ReRT treatments were stereotactic (cases 1,6) or normo-fractionated (cases 2,3,4,5). The physical 3D dose distribution of previous treatment was rescaled to EQD2Gy ($\alpha/\beta$=3Gy, except spinal cord: $\alpha/\beta$=2Gy) and transferred to reRT-CT. Planning target volumes (PTV) and organs at risk (OAR) were delineated on reRT-CT. For all cases, the 40Gy EQD2Gy isodose line of previous plan overlapped with PTV of current plan. Cumulative EQD2Gy OAR limits, based on Danish guidelines and international literature were (selected constraints): Airways $D_{0.3cc}$<90Gy, oesophagus and heart $D_{0.3cc}$<85Gy, great vessels and chest wall $D_{0.3cc}$<110Gy, spinal cord $D_{0.3cc}$< 50Gy, skin $D_{20cc}$<78Gy, and lungs $D_{mean}$<20Gy. For chest wall, if previous treatment was stereotactic, $D_{0.3cc}$<20Gy was applied to current plan in regions with D>95Gy from previous plan.

Each centre optimised reRT treatment plans using institutional systems. The prescribed PTV dose was 66Gy/33fractions or 45Gy/3fractions (GTV 67.5Gy); with $V_{95\%}$(PTV)≥98%. For protons, $V_{95\%}(CTV_{worst\text{-}case\text{-}scenario})$≥98% in robust evaluation.

After cases 1-4 were completed, prioritisation between OAR constraints and target coverage were discussed at a national workshop.

## Results

For the first three cases, all centres complied with dose constraints. For case 4, it was impossible to fully cover PTV while respecting OAR constraints. Two centres covered PTV, resulting in $D_{0.3cc}$(great vessels) of 139-142Gy, one centre reduced number of fractions, and five centres respected OAR constraints, resulting in $V_{95\%}$(PTV) of 83-95%. At the workshop, consensus was reached to respect OAR constraints over target coverage, and centres reoptimized case 4 accordingly.

For cases 5 and 6, $V_{95\%}$(PTV) ranged between 85-97% and 95-99%, respectively, to comply with OAR limits. Cumulative $D_{mean}$(lungs) and $D_{mean}$(heart) doses varied with up to 6Gy between centres (Figure 1).

## Conclusions

This pre-trial study generally found compliance with proposed CURE Lung trial dose constraints, but with considerable variation in cumulative OAR doses and sometime target under-dosage. To comply with OAR dose limits, reRT requires clear guidelines for clinical decision-making, now provided in the trial protocol.

Figure 1:

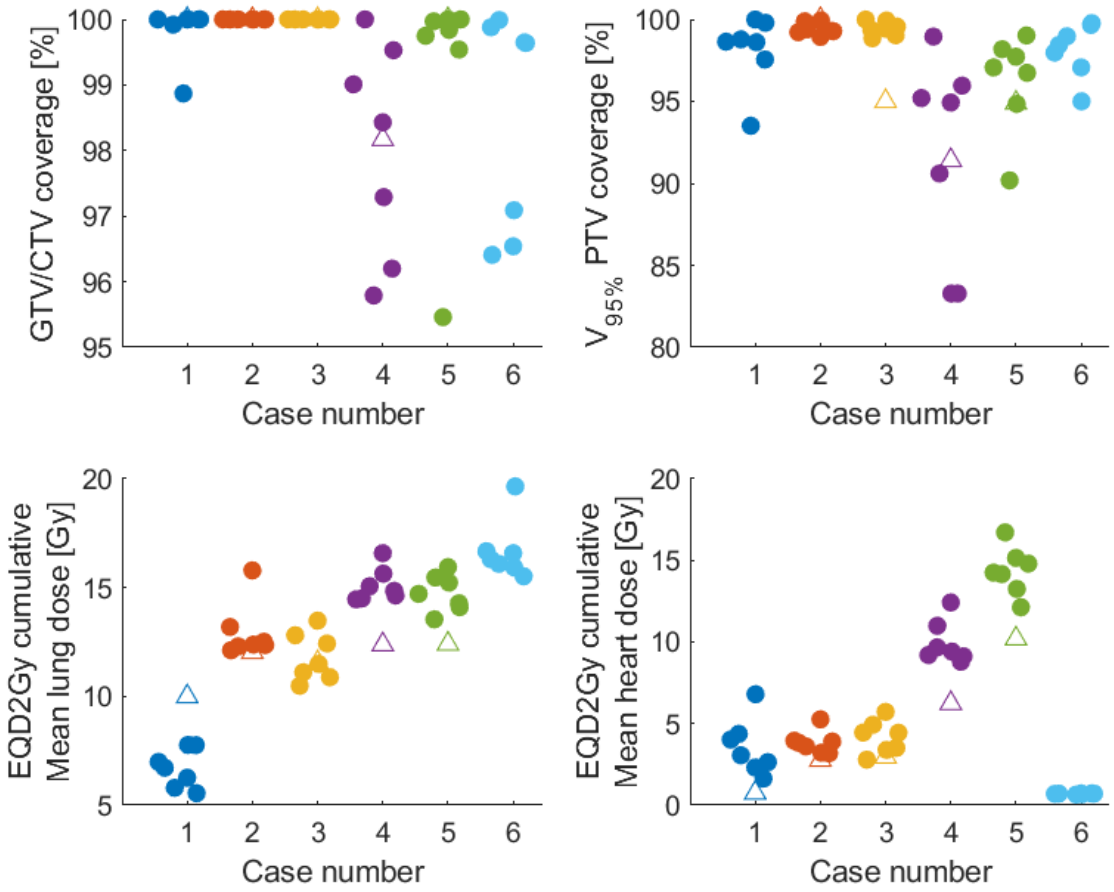


Figure1. Swarm chart illustrating dose coverage of gross tumour volume (GTV) for cases 1,6 and clinical target volume (CTV) for cases 2,3,4,5 (upper left), dose coverage of PTV for radiotherapy or worst case scenario for proton therapy (upper right), cumulative EQD2Gy mean lung dose (lower left), and mean heart dose (lower right) on current CT image for each of the six cases. For case 4, data for the reoptimized plans is shown. Each chart includes data from all seven radiotherapy centres (filled bullets) and one proton centre (open triangles). Case1 (blue): 45Gy/3fractions(previous) and 45Gy/3fractions(current), Case 2(orange): 45Gy/30fractions(previous) and 66Gy/33fractions(current), Case 3 (yellow): 45Gy/3fractions(previous) and 66Gy/33fractions(current), Case 4 (purple): 45Gy/3fractions(previous) and 66Gy/33fractions(current), Case 5 (green): 45Gy/3fractions(previous) and 66Gy/33fractions(current), Case 6 (light blue): breast 40Gy/15fractions(previous) and 66Gy/33fractions(previous) and 45Gy/3fractions(current).

# Dose accumulation for reirradiation: a national study of inter-center variation across eight treatment sites

Isak Wahlstedt[1], Ane Appelt[2], Rasmus L Christiansen[3], Ulrik V Elstrøm[4], Irene Hazell[3], Kenneth Jensen[4], Laura Patricia Kaplan[5], Marianne M Knap[6], Camilla Kronborg[4], Mikkel D Lund[7], Martin S Nielsen[8], Morten Nielsen[3], Tine B Nyeng[6], Lotte Nygård[1], Wiviann Ottosson[9], Raúl Argota-Pérez[9], Laura A Rechner[9], Signe L Risumlund[1], Heidi S Rønde[4], Hella Sand[8], Simon N Thomsen[6], Rebecca J Tobin[1], Steffen B Vestergaard[8], Esben S Worm[6], Lone Hoffmann[6]

[1]Department of Oncology, Centre for Cancer and Organ Diseases, Copenhagen University Hospital - Rigshospitalet, Copenhagen, Denmark.

[2]Leeds Institute of Medical Research, University of Leeds, Leeds, United Kingdom.

[3]Department of Oncology, Odense University Hospital, Odense, Denmark.

[4]Danish Centre for Particle Therapy, Aarhus University Hospital, Aarhus, Denmark.

[5]Department of Oncology and Palliative Units, Zealand University Hospital, Næstved, Denmark

[6]Department of Oncology, Aarhus University Hospital, Aarhus, Denmark.

[7]Department of Oncology, Vejle Hospital, University Hospital of Southern Denmark, Vejle, Denmark.

[8]Department of Oncology, Aalborg University Hospital, Aalborg, Denmark.

[9]Department of Oncology, Radiotherapy Research Unit, Copenhagen University Hospital - Herlev and Gentofte, Herlev, Denmark

**Introduction**

We investigated inter-center variations in dose accumulation for reirradiation due to (i) image registration variation, and (ii) local radiobiological dose considerations among eight Danish radiotherapy centers for patient cases covering different anatomical regions.

**Materials and methods**

Eight patient cases (Table 1) were evaluated. Organs at risk (OAR) delineations were validated by expert clinicians. Seven cases had direct overlap of irradiated volumes

(ESTRO-EORTC reirradiation Type 1), while the lung case had concern of toxicity from cumulative doses (Type 2) [1]. Each center mapped dose from the previous CT scan to the reirradiation CT scan using either rigid (RIR) or deformable (DIR) image registration based on local clinical practice. Subsequently, all centers accumulated the mapped dose from the previous treatment with the reirradiation dose in (i) physical dose, (ii) equieffective dose in 2 Gy fractions (EQD2), and (iii) EQD2 with dose scaling factors (DSFs) to account for tissue recovery (if used in clinical practice). We used institutional $\alpha/\beta$ values and DSFs to reflect variation in local clinical practice. We evaluated dose accumulations for one clinically relevant OAR in high dose overlap regions for each patient case.

**Table 1:** Patient cases and treatments included in this study.
CTV = clinical target volume, GTV = gross tumor volume, IMPT = intensity-modulated proton therapy, IMRT = intensity-modulated radiation therapy, MWA = microwave ablation, NA = not applicable, OAR = organ at risk, PTV = planning target volume, RT = radiotherapy, VMAT = volumetric-modulated arc therapy, 3D-CRT= three-dimensional conformal radiation therapy.

| | | | Previous radiotherapy | | | Reirradiation | | |
|---|---|---|---|---|---|---|---|---|
| **Treatment site (evaluated OAR)** | **Time between RT [months]** | **Surgery in irradiated anatomy?** | **Dose prescribed to PTV** | **Treatment technique** | **PTV Volume [cc][1]** | **Dose prescribed to PTV** | **Treatment technique** | **PTV Volume [cc][1]** |
| **Abdomen (Kidney_L)** | 4 | No | 2 Gy x 20 | VMAT | 258.8 | 5 Gy x 4 | VMAT | 1732.6 |
| **Anal (Bladder)** | 8 | No | 2.15-1.8 Gy x 28 | VMAT | 1707.0 | 1.25 Gy x 44 | IMPT | 21.2 |
| **Brain (Chiasm)** | 15 | No | 18 Gy x 1 | HyperArc | 1.23 | 13 Gy x 1 | HyperArc | 9.6 |
| **Breast (Heart)** | 57 | Yes | 2.67 Gy x 15 | 3D- CRT | 287.12 | 2.67 Gy x 15 | 3D- CRT | 969.5 |
| **Head and neck (Mandible)** | 96 | Yes | 2 Gy x 34 | VMAT | 101.0 | 1.2 Gy x 50 | IMPT | 22.6 |
| **Liver (ChestWall)** | 37 | Yes+MWA | 15 Gy x 3 | IMRT | 23.5 | 15 Gy x 3 | IMRT | 38.9 |
| **Lung (Aorta)** | 72 | no | 2 Gy x 33 | IMRT | 88.4 | 4.5-12.9 Gy x 8 | IMRT | 19.5 |
| **Rectum (BowelBag)** | 51 | Yes | 2 Gy x 30 | VMAT | 1050.8 | 1.25 Gy x 52 | IMPT | 267.5 |

[1]Proton and breast plans did not have PTVs. Thus, we reported CTVs instead.

## Results

RIR was used for dose mapping by three centers for anal and rectum cases, by two centers for brain and abdomen cases, and by one center for the breast case. DIR was performed using MIM (two centers, all registrations intensity-based), Velocity (five centers, two structure-based, remaining intensity-based), and RayStation (one center, intensity-based). The inter-center range (maximum-minimum) in near-maximum dose ($D_{1\%}$) to the selected OARs ranged from 0.7 Gy for aorta in the lung case (Lung: Aorta) to 16.7 Gy (Abdomen: Kidney_L) for physical dose accumulations and from

1.1 Gy (Lung: Aorta) to 24.3 Gy (Abdomen: Kidney_L) for EQD2-rescaled dose accumulations. For the eight selected OARs, $\alpha/\beta$ values ranged from 2 Gy to 5 Gy. One center applied DSFs to bowel bag in the rectum case (DSF=0.75), chiasm in the brain case (DSF=0.75), and bladder in the anal case (DSF=0.9). This changed the $D_{1\%}$ inter-center range compared to EQD2-scaled doses from 6.7 Gy to 13.5 Gy (Anal: Bladder), from 6.2 Gy to 6.1 Gy (Brain: Chiasm), and from 4.7 Gy to 19.2 Gy (Rectum: BowelBag).

## Conclusions

Inter-center variation in dose accumulation for reirradiation is more impacted by differences in radiobiological dose rescaling than by image registration variation, especially when doses are scaled to account for recovery. These findings stress the need for guidelines for reirradiation dose accumulation.

## References

[1] Andratschke N, Willmann J, Appelt AL, Alyamani N, Balermpas P, Baumert BG, et al. European Society for Radiotherapy and Oncology and European Organisation for Research and Treatment of Cancer consensus on re-irradiation: definition, reporting, and clinical decision making. Lancet Oncol 2022;23:e469–78. https://doi.org/10.1016/S1470-2045(22)00447-8.

**CURE Lung: CUratively intended thoracic REirradiation. An observational study of curative intended reirradiation of thoracic tumours including lung-cancer recurrences, solitary lung metastases, or new primary lung cancer in the thorax**


**Author information**

Stine Overvad Fredslund, stin.fred@auh.rm.dk, Department of Oncology, Aarhus University Hospital, Denmark

**Authors**

Stine Overvad Fredslund, Department of Oncology, Aarhus University Hospital, Denmark

Ane Appelt, University of Leeds, Leeds, West Yorkshire, United Kingdom

Mikkel Drøgemüller Lund, Department of Oncology, Vejle Hospital, Denmark

Mai Ehmsen, Danish Centre for Particle Therapy, Aarhus University Hospital, Denmark

Torben Schjødt Hansen, Department of Oncology, Vejle Hospital, Denmark

Vladimira Horvat, Department of Oncology, Næstved Hospital, Denmark

Maria Fuglsang Jensen, Danish Centre for Particle Therapy, Aarhus University Hospital, Denmark

Laura Patricia Kaplan, Department of Oncology, Næstved Hospital, Denmark

Marianne M. Knap, Department of Oncology, Aarhus University Hospital, Aarhus, Denmark.

Lotte Holm Land, Department of Oncology, Odense University Hospital, Denmark

Hanna Mortensen, Danish Centre for Particle Therapy, Aarhus University Hospital, Denmark

Morten Nielsen, Department of Oncology, Odense University Hospital, Denmark

Wiviann Ottosson, Department of Oncology, Herlev Hospital, Denmark

Gitte Persson, Department of Oncology, Herlev Hospital, Denmark

Cécile Peucelle, Department of Oncology, Rigshospitalet, Denmark

Mette Pøhl, Department of Oncology, Rigshospitalet, Denmark

Arpit Saini, Department of Oncology, Næstved Hospital, Denmark

Hella Sand, Department of Oncology, Aalborg University Hospital, Denmark

Tine Schytte, Department of Oncology, Odense University Hospital, Denmark
Filippa Sundbye, Department of Oncology, Herlev Hospital, Denmark
Weronika Szejniuk, Department of Oncology, Aalborg University Hospital, Denmark
Simon Nyberg Thomsen, Department of Oncology, Aarhus University Hospital,
Denmark Lone Hoffmann, Department of Oncology, Aarhus University Hospital,
Aarhus, Denmark.

## Introduction

The number of long-term lung cancer survivors increases; however, many patients are diagnosed with recurrent or new thoracic cancers. High-dose reirradiation is promising but associated with high severe toxicity rates. Existing studies are small, lacking high-quality data, with no clear correlation between toxicity risk and delivered radiotherapy dose.

## Materials and methods

The Danish Oncological Lung cancer Group for radiotherapy has created the national prospective CURE Lung trial offering curative type 1 and 2 reirradiation (Figure 1). Available digital 3D-dose plans from previous radiotherapy courses are mandatory. Image registration must be performed to transfer dose from previous CT-image to current CT-image. Cumulative equieffective trial dose constraints are based on national and international literature. First-priority constraints, mandatory to comply with, are set for all mediastinal tissues, mean lung dose, thoracic wall, and skin. Target under-dosage is accepted in order to respect OAR constraints. National guidelines must be used for OAR delineation. The patients must be treated using daily image guidance. All treatment plans must be uploaded to a national repository.

A pre-trial quality assurance (QA) programme consisting of image registration and dose accumulation, dose planning, and OAR delineation is mandatory to conduct.

Data on previous radiotherapy, systemic treatments, and surgery is collected at baseline. Grade 3-4 thoracic toxicity is scored. Clinical follow-up, including thoracic CT-imaging, is performed every three months until three years and bi-annually until five years. Early and late radiotherapy-related toxicity is scored. EORTC quality-of-life questionnaires C30 and LC13 evaluates patient-reported outcomes at three months and yearly. Potential patient decision regret regarding reirradiation is collected in a decision regret questionnaire from the Ottawa Hospital.

The trial aims for 500 patients in five years. The primary endpoint is grade 4-5 radiotherapy-related toxicity. Interim analyses will be performed after inclusion of 50, 100, 200, and 300 patients to evaluate the rate of radiotherapy-related toxicity grade 4-5.

## Results

All centres completed pre-trial QA. Two national workshops were conducted to discuss the trial, which has been submitted for ethical approval. Patient inclusion is expected to start summer 2025.

## Conclusion

The CURE Lung trial has been finalized and will be open for reirradiation of all Danish lung cancer patients. The trial is based on pre-trial QA, clinical follow-up, up and interim analyses, which will ensure safe reirradiation for the increasing number of long-term lung cancer survivors.

Figures/tables:

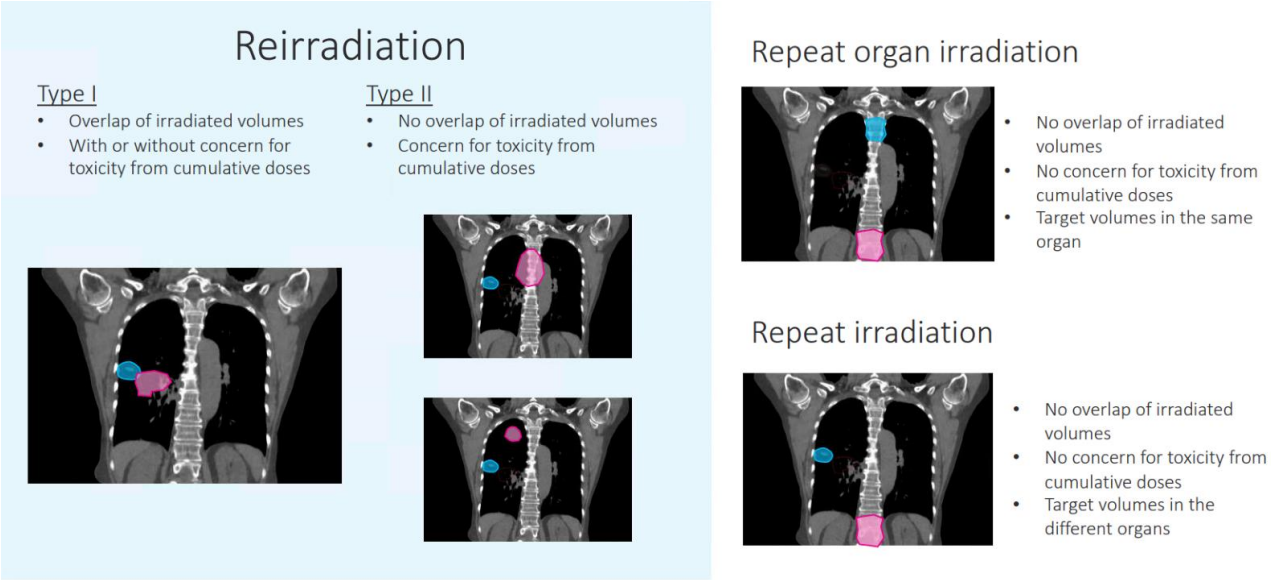


**Figure 1:** *Examples of scenarios of reirradiation and repeat irradiation as per the ESTRO-EORTC consensus guidelines (redrawn from Andratschke et al). Reirradiation type I and II are candidates for the CURE Lung trial.*

**Clinical workflow for reirradiation: National consensus recommendations on imaging, treatment planning, dose accumulation, and treatment delivery**

Laura P Kaplan[1*†], Rebecca J Tobin[2*$], Eliana Vasquez Osorio[3], Ane L Appelt[4], Isak Wahlstedt[2], Rasmus L Christiansen[5], Martin S Nielsen[6], Laura A Rechner[7], Simon N Thomsen[8,9], Mikkel D Lund[10], Kenneth Jensen[9,11], Camilla Kronborg[9,11], Lone Hoffmann[8,9]

1: Department of Oncology and Palliative Units, Zealand University Hospital, Næstved, Denmark

2: Department of Oncology, Centre for Cancer and Organ Diseases, Copenhagen University Hospital - Rigshospitalet, Copenhagen, Denmark

3: Division of cancer sciences, University of Manchester, Manchester, UK; The Christie NHS Foundation Trust, Manchester, UK

4: Leeds Institute of Medical Research, University of Leeds, Leeds. UK

5: Laboratory of Radiation Physics, Department of Oncology, Odense University Hospital, Odense, Denmark

6: Department of Oncology, Aalborg University Hospital, Denmark

7: Department of Oncology, Herlev and Gentofte Hospital, University of Copenhagen, Herlev, Denmark

8: Department of Oncology, Aarhus University Hospital, Denmark

9: Department of Clinical Medicine, Faculty of Health Sciences, Aarhus University, Denmark

10: Department of Oncology, Vejle Hospital, University Hospital of Southern Denmark, Vejle, Denmark

11: Danish Centre for Particle Therapy, Aarhus University Hospital, Department of Clinical Medicine, Aarhus University, Denmark

* Joint first authors
† lakap@regionsjaelland.dk
$ rebecca.jean.tobin@regionh.dk

## Introduction

Reirradiation is becoming increasingly frequent in clinical practice. However, workflows and practices vary widely between clinics, as general guidelines are scarce or lacking in practical detail. We present comprehensive national Danish consensus recommendations covering all steps of the reirradiation workflow. The aim is to standardise and improve reirradiation treatment quality and provide guidance for much-needed large-scale clinical trials.

## Methods

An expert panel consisting of physicians, clinical physicists, and researchers from all Danish radiotherapy centres was formed. An in-person two-day workshop was followed by multiple online meetings. Recommendations were based on expert consensus, supported by review of existing literature, and were reviewed by all radiotherapy-relevant Danish Multidisciplinary Cancer Groups before publication.

## Results

Patients receiving reirradiation should be identified and designated as such at each workflow step. Review of patient cases at multidisciplinary reirradiation conferences is encouraged. Patient selection depends on clinical factors such as time since previous treatment, previous (non-radiotherapy) treatments, side effects from previous treatment(s), comorbidity, other treatment options (surgery, systemic treatment), as detailed in the ESTRO-EORTC Reirradiation Consensus Statement. Treatment decisions should consider risk versus benefit, preferably as part of a shared decision-making process.

Immobilization, positioning, and motion management should, where feasible for current treatment delivery, mirror previous treatment(s). Contouring guidelines should be used, if available and appropriate; contours from previous treatments relevant for cumulative dose evaluation should be reviewed and edited where not aligned with current standards. Additional OAR contours may be necessary for reirradiation planning and dose evaluation compared to de novo treatments.

Information on previous dose should be used in planning and evaluation. The degree of complexity (e.g. summation of dose maxima, rigid/deformable image registration, 3D dose accumulation) should reflect the clinical situation and the extent/quality of available information (see table). Careful quality assurance of mapping prior dose(s) to current imaging is necessary. Dose should always be converted to equieffective dose (e.g. EQD2) before summation. Model parameters for radiobiological correction (e.g. $\alpha/\beta$) should be supported by relevant literature.

Daily image-guidance and regular evaluation of delivered dose are recommended if deemed relevant clinically. Clear instructions for structures to prioritize in treatment image matching should be provided to treatment staff. Relevant DVH metrics should be reported in patient charts, and information on clinical considerations, registration process, biological correction, and uncertainties should be documented.

## Conclusion

We present national consensus guidelines for reirradiation treatment workflows. The guidelines have been approved by all RT-relevant site-specific Danish Multidisciplinary Cancer Groups.

| Scenario | Information available | Recommendations |
|---|---|---|
| **No overlap with previously irradiated tissue** | Any information about prior treatment. | Confirm the previous treatment is not in the vicinity of the reirradiation target |
| **Low dose overlap between previous and current treatment area** | CT-scan + 3D dose distribution | Import the previous plan(s) and transfer isodose curves rigidly. |
| | Any images 2D or 3D, information about fields | Add a conservative margin around the previously irradiated area and perform some simple calculations. |
| | Patient records: Prescribed dose, treatment area, and treatment technique | Confirm the previous treatment area and prescription dose. Any other assessment of overlap will depend on the exact information available. |
| **High dose overlap within a critical OAR** | CT-scan + 3D dose distribution | Perform DIR + 3D equieffective dose correction for dose accumulation, provided this is technically feasible. |
| | Any images 2D or 3D, information about fields | Attempt reconstruction of fields and dose on current imaging. If deemed reliable, perform biological rescaling and 3D dose accumulation. |
| | Patient records: Prescribed dose, treatment area, and treatment technique | Estimate max point dose with equieffective dose correction (based on prescribed dose). |
| | Limited information on prior treatment | As essential information is missing, any treatment decisions will require shared decision-making between the physician and the patient about the potential risks of reirradiation. |
| **Severe risk of fatal/debilitating toxicity** | CT-scan + 3D dose distribution | Perform DIR + 3D equieffective dose correction for dose accumulation. |

Table: Recommendations for evaluation of dose from multiple radiotherapy courses, based on the clinical need and the extent of available information. DIR: deformable image registration, OAR: organ at risk.

**Time efficiency, geometric accuracy, and clinical impact of AI-assisted contouring in head and neck cancer radiotherapy**

johan.martin.sobstad@helse-bergen.no

JOHAN MARTIN SØBSTAD, TURID HUSEVÅG SULEN, GRETE MAY ENGESETH, LUKAS HIRSCHI, HELGE EGIL SEIME PETTERSEN, CAMILLA HANQUIST STOKKEVÅG [1]

[1]: THE CANCER CLINIC, HAUKELAND UNIVERSITY HOSPITAL, BERGEN, NORWAY

**Introduction**:

Accurate delineation is a critical step in radiotherapy treatment planning, especially for head and neck cancer patients, where the complex anatomy poses challenges. Advances in artificial intelligence (AI) have made AI-assisted contouring promising to reduce the workload. In this study, we conducted a comprehensive analysis of the integration of AI-assisted contouring into the clinical workflow for patients with head and neck cancers. Our evaluation focused on time saved, consistency and quality the AI-generated contours and the dosimetric impact of using manual or AI-generated segmentation.

**Materials and methods:**

Twenty head and neck cancer patients were included in this study. For each patient, twelve organs at risk (OAR) were AI-segmented using ART-plan™ (TheraPanacea) version 2.1. The structures were also independently contoured by twelve dosimetrists, with contouring time recorded. A peer-reviewed manual contour set was selected as ground truth (GT) for each patient. To evaluate the resources required for assessing the AI-segmented structures, modifications were made to the AI-generated contours by the observers (mod-AI). The geometric accuracy of the contour groups (manual, AI and modified-AI) was evaluated against the GT using the Dice Similarity Coefficient (DICE), Hausdorff Distance (HD), Mean Surface Distance (MSD), Volume Difference (VD) and Centre of Mass Difference (CMD). Time efficiency was measured by time spent on manual contouring and modifying AI-generated contours. Dose-volume metrics for the OARs were assessed to evaluate the clinical impact.

**Results**:

Average manual contouring time of the OARs was 61(range:48-73) minutes per patient, while the modified AI-based structures required 16(14-21), resulting in 74% time saved. Compared to the GT, the mandible resulted in the most consistent contouring (Figure 1): For manual and modified-AI, the mean DICE was 0.93±0.04 and 0.94±0.01, respectively. Conversely, the pharyngeal constrictor muscles (PCM) produced a DICE of 0.67± 0.07(manual) and 0.68±0.05(mod-AI). The larynx produced the largest deviation across all geometric measures. The HD, MSD, VD and CMD analysis aligned with these results. The average mean dose difference from the GT were lowest for the mandible, with an absolute difference of 0.08±0.61Gy(manual) and 0.50±0.77Gy(mod-AI), and highest for the larynx with -0.39±3.10Gy(manual) and -0.88±2.43Gy(mod-AI).

**Conclusions**:

Our results show that the use of AI-assisted contouring in head and neck radiotherapy, offers comparable geometric accuracy to manual contouring while significantly reducing the time required for delineation. With minimal dosimetric impact, the clinical implications are limited, indicating that AI tools can be safely implemented with little to no adjustment for head and neck cancer patients.

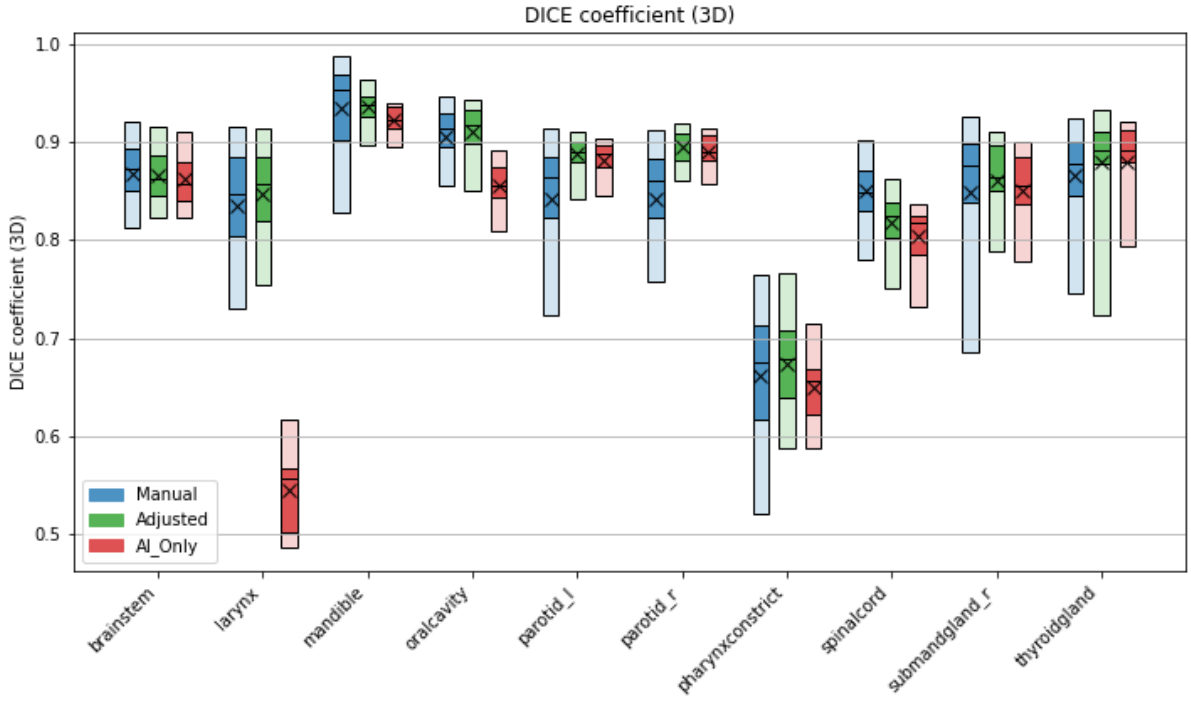


*Figure 1: Geometrical analysis of manually contoured OAR (Blue), corrected contours from AI (Green) and original contours from AI (Red). The DICE score describes how well the structures overlap, where 1 is 100% overlap and 0 is no overlap. The Y-axis is limited to 0.5-1.0. The figure shows 5-25-50-75-95th percentiles, as well as the average (X) of the results for each structure group. The last two structures (Cochlea_L and R) that were part of the study were omitted. The Cochlea's were not corrected in this study as per our clinical practise. This is because such corrections would not save time vs. manual contouring.*

**The Influence of AI-Assisted Delineation on Final Delineations of Targets and Organs at Risk Over Time**

Henrik Dahl Nissen[1], Lars Ulrik Fokdal[2,3], Birgitte Mayland Havelund[2], Christine Vestergaard Madsen[2]
[1]Dept. of Medical Physics, Vejle Hospital, University Hospital of Southern Denmark, Vejle, Denmark
[2]Dept. of Oncology, Vejle Hospital, University Hospital of Southern Denmark, Vejle, Denmark
[3]Dept. of Regional Health Research, University of Southern Denmark, Odense, Denmark

**Email:** henrik.dahl.nissen@rsyd.dk

## Introduction

The use of artificial intelligence (AI) to assist in the delineation of targets and organs-at-risk (OARs) for radiotherapy is rapidly increasing. AI aims to reduce the time required for manual delineation and minimize inter-observer variability. However, concerns remain that AI may compromise the individualization of delineations by biasing clinicians toward AI-generated segmentations, potentially leading to fewer and smaller corrections over time. This study investigates whether clinicians gradually adapt their delineation practices toward AI-generated contours when using AI-assisted segmentation.

## Materials and Methods

AI segmentations were generated using an in-house model for prostate cancer, including elective lymph nodes. Data were collected from two time periods: December 2023–June 2024 and October 2024–February 2025. During these periods, three experienced oncologists delineated 19 and 20 patients, respectively, using AI assistance as part of routine clinical practice. The AI model remained unchanged throughout the study.

The raw AI segmentations and the final clinician-adjusted delineations were collected. To quantify the modifications made by clinicians, we used the added path length (APL) as an evaluation metric. APL measures the total length of clinician-made adjustments to the AI-generated segmentation. We normalized the APL by the total contour length for each structure to account for inter-patient organ size differences. The evaluated volumes included the prostate (CTVp), seminal vesicles (CTVp_SV), elective lymph nodes
(CTVn_E), bladder, rectum, anal canal, bowel cavity, and penile bulb. To mitigate pixelation effects, a minimum change threshold of 1 mm (corresponding to voxel size) was applied to distinguish real modifications from noise. To assess the scale of corrections, APL was recalculated across a range of minimum change thresholds (2–15 mm).

## Results

The figure illustrates the proportion of the final clinical contour that deviated from the AI segmentation by at least 1 mm (left) and 8 mm (right). Blue and orange represent the first and second delineation rounds, respectively. Overall, less than 10% of the contour differed from the AI-generated segmentation. In the second round, the extent of corrections at 1 mm remained stable or increased, with this trend persisting across all evaluated scales except for the bowel cavity, where the number of corrections decreased for differences greater than 5 mm.

## Conclusion

For experienced oncologists, no general trend toward making fewer modifications to AI-generated segmentations over time was observed. This finding alleviates concerns that clinicians progressively adapt their delineations to match AI model predictions, suggesting that expert oversight remains robust even with AI-assisted segmentation.

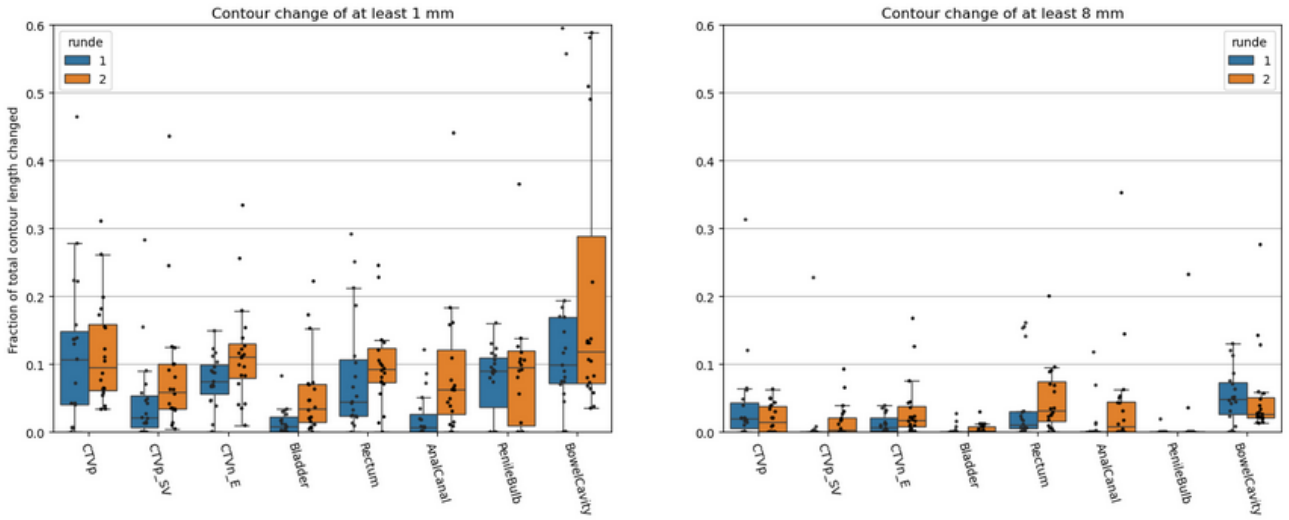

# Application of a Neural Network for Predicting Stereotactic Radiotherapy Field Orientations.

Anders Traberg Hansen, Aarhus University Hospital, Aarhus, Denmark.

E-mail: andehans@rm.dk

## Introduction

This study investigates the ability of a neural network to predict the arrangement of stereotactic radiotherapy treatment fields.

## Materials and methods

Treatment planning data from 171 patients having 205 tumors were used to create two types of images. The first set of images represent projection of the tumor, brainstem, optical apparatus and the hippocampi. The second set shows the corresponding field arrangement in polar projection. A neural network was trained to correlate these two image types, allowing it to predict the expected field arrangement for an unknown patient case.

For model evaluation, a separate set of patients, not included in the training sets, was used. The predicted field arrangements from the neural network were compared to those generated by human planners. For each pixel in the image, a weighted mean of surrounding pixel values was calculated, with the weight inversely proportional to the square of the distance from the given pixel. This set of mean values was then compared to a corresponding set, calculated in the same way, but only for the pixels representing fields placed by a human planner. The Wilcoxon rank-sum test was applied to assess differences in the mean values between these two sets.

## Results

The neural network's predictions for unknown patient cases showed statistically significant ($P<0.002$) similarities to the original human-designed field arrangements. An example is shown in figure 1.

## Conclusion

This study demonstrates that neural networks have the potential to assist in automatic stereotactic radiotherapy plan design, providing a promising tool for enhancing the efficiency and consistency of treatment planning.

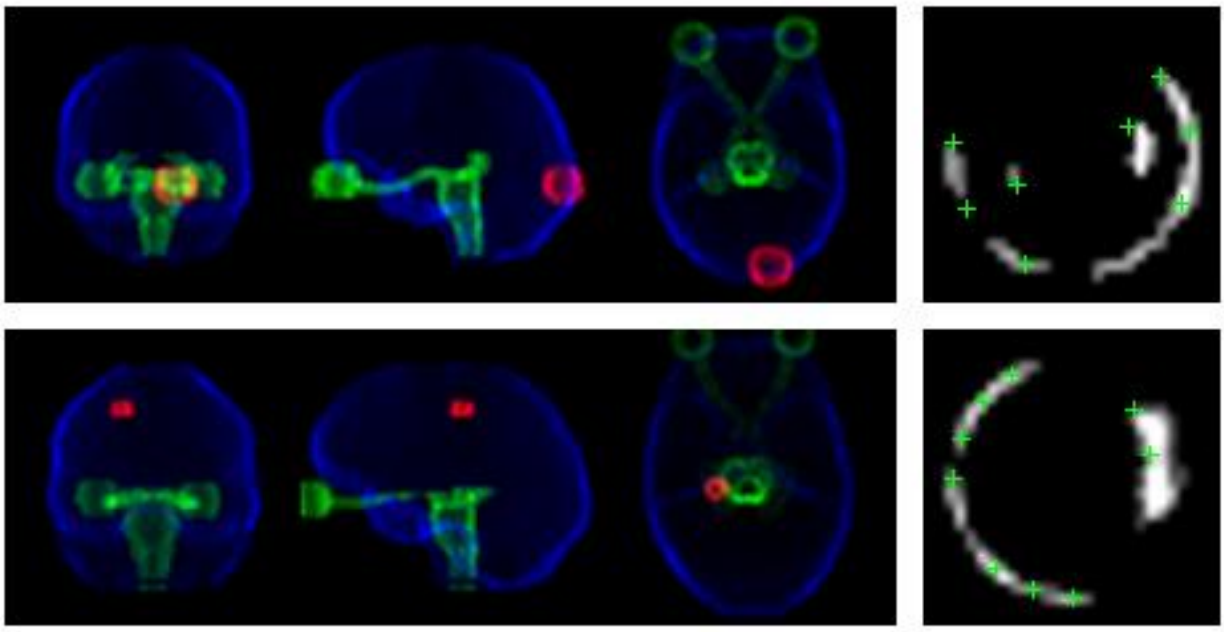

Figure 1. On the left, projection images of two patients are shown. On the right, the corresponding output images from the neural network are displayed, with the human planner's field placements indicated by green crosses.

**Uncertainty-Aware Deep Learning-Based Auto-Segmentation of Glioblastoma Using Conformal Prediction**

Jintao Ren[1,2,], Kim Hochreuter[1,2], Slávka Lukacova[1,3], Charlotte Aaquist Haslund[4], Aida Muhic[5], Morten Høyer[2], Rikke Dahlrot[2,6,7], Anders Schwartz Vittrup[3], Camilla Skinnerup Byskov[3], Thomas Overgaard Kristensen[4], Mikkel Skaarup[5], Bob Smulders[2,5], Christian Rønn Hansen[2,6,7], Søren Nielsen Agergaaard[6], Stine Korreman[1,2,3], Jesper Folsted Kallehauge[1,2]

[1] Department of Clinical Medicine, Aarhus University, Aarhus, Denmark

[2] Danish Centre for Particle Therapy, Aarhus University Hospital, Aarhus, Denmark

[3] Department of Oncology, Aarhus University Hospital, Aarhus, Denmark

[4] Department of Oncology, Aalborg University Hospital, Aalborg, Denmark

[5] Department of Oncology, Rigshospitalet, Copenhagen, Denmark

[6] Department of Oncology, Odense University Hospital, Odense, Denmark

[7] Institute of Clinical Research, University of Southern Denmark, Odense, Denmark

**Background**
Accurate segmentation of gross tumor volume in Glioblastoma (GBM) is essential for radiation therapy planning, but inter-observer variability (IOV) introduces uncertainty in delineation. Conformal Prediction (CP) provides statistical guarantees for generating uncertainty-aware segmentations. This study evaluates CP-based segmentation across multiple coverage levels and assesses its effectiveness in capturing expert variability compared to traditional threshold-based segmentation and clinical reference delineations.

**Materials and Methods**
We developed a deep learning-based segmentation model trained on contrast-enhanced T1-weighted MRI data, using a retrospective dataset of 85 GBM patients acquired under a national prospective Danish Neuro Oncology Group (DNOG) imaging protocol. A separate calibration set of 19 patients was employed to determine the CP quantiles, while an independent test set of 10 patients was reserved for evaluation. The test set included one clinical and six expert delineations per patient, gathered during a DNOG workshop across four centers in Denmark.

Predictions were generated using nnUNetv2 Resenc(M) with an ensemble of five-fold 3D full-resolution models. The CP calibration step involved computing nonconformity scores on the calibration set to derive multiple valid empirical confidence levels (CLs). These CL quantiles were subsequently used to adjust segmentation thresholds, ensuring that each coverage level aligned with its corresponding uncertainty bounds.

CP-based segmentations were compared to a baseline threshold-based approach (t = 0.5), workshop expert annotations - IOV, and the clinical reference. Performance was evaluated using

the surface Dice similarity coefficient with a 2 mm tolerance (sDSC) and the 95th percentile Hausdorff distance (HD95).

**Results**

We obtained valid empirical CLs (0.45-0.90) from calibration, with optimal coverage at 0.80. Across all CLs, CP-based segmentation achieved an average sDSC/HD95 of 0.69/6.04 mm to IOV and 0.72/3.95 mm to the clinical reference. The optimal segmentation at 0.80 showed the highest agreement with experts (0.82/5.5 mm to IOV; 0.91/2.7 mm to clinical). The baseline achieved 0.80/5.7 mm to IOV and 0.92/2.9 mm to clinical, while the clinical reference had 0.80/5.3 mm to IOV, indicating that CP-based segmentation at 0.80 closely approximates expert consensus while quantifying uncertainty. Figure 1 provides a qualitative visualization of CP-based segmentations.

**Conclusion**

CP-based segmentation effectively quantifies uncertainty while maintaining segmentation accuracy. At a coverage level of 0.80, it outperforms the baseline in agreement with IOV delineations. The results highlight CP's potential for uncertainty-aware radiation therapy planning in GBM, offering a robust approach for quantifying delineation variability.

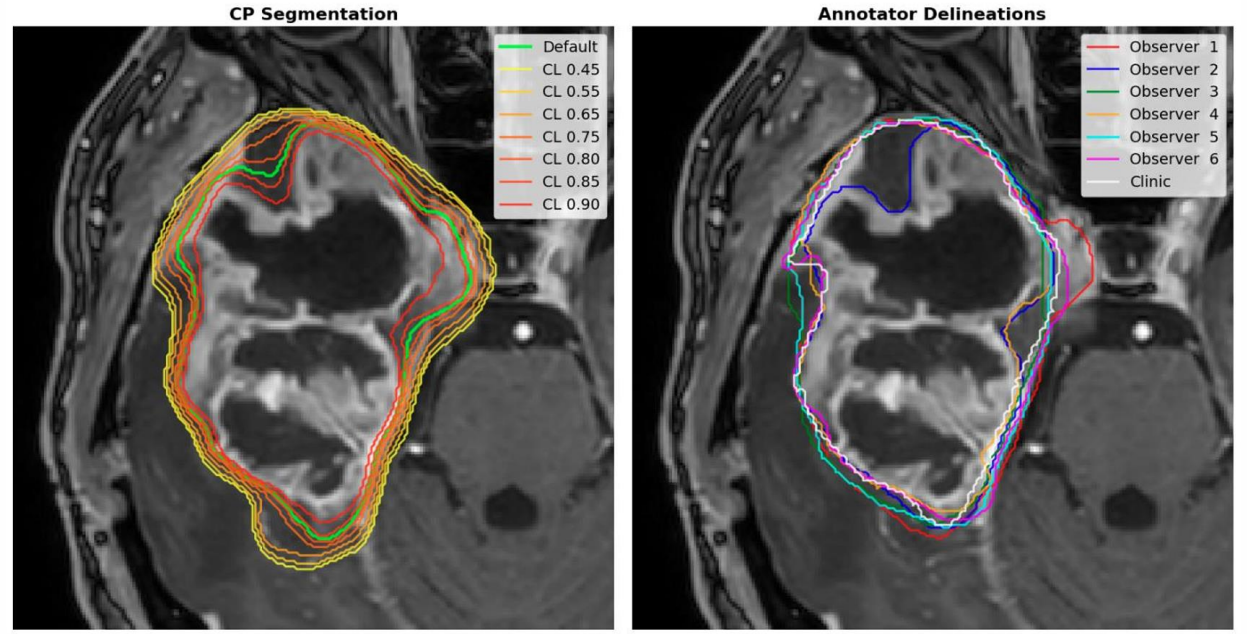


Figure 1: Visualization of deep learning-based segmentation results and expert annotations for a selected slice. **(Left)** Confidence-based segmentation using conformal prediction (CP), with contours representing different confidence levels (CLs). The default threshold-based segmentation is shown in lime. **(Right)** Manual delineations from multiple expert centers. Retrospective clinic contours are labeled as 'Clinic,' while other contours correspond to anonymized centers ('Observer 1' to Observer 6').

# Towards objective cosmetic outcome self-evaluation: machine-learning on photographic data from breast-conserving treatment

[1,2]Morten Sahlertz, [2,3,4]Birgitte Vrou Offersen, [5,6]Tine Engberg Damsgaard, [7]Mette Eline Brunbjerg, [1,2]Jasper Nijkamp

[1]Department of Clinical Medicine, Aarhus university, Aarhus, Denmark
[2]Danish Center for Particle Therapy, Aarhus University Hospital, Aarhus, Denmark
[3]Department of Oncology, Aarhus University Hospital, Aarhus, Denmark
[4]Experimental Clinical Oncology, Aarhus University Hospital, Aarhus, Denmark
[5]Department of Plastic Surgery, Odense University Hospital and University Hospital of Southern Denmark, Odense, Denmark
[6]Department of Regional Health Research, University of Southern Denmark, Odense, Denmark
[7]Departments of Breast and Plastic Surgery, Aalborg University Hospital, Aalborg, Denmark

**Introduction:**
Cosmetic outcome (CO) following breast-conserving treatment influences long-term patient satisfaction and quality of life. However, systematic CO follow-up is no longer routine clinical practice. Our long-term goal is to develop selfie-based imaging via a mobile app for automated CO assessment, enabling remote monitoring.
To build machine learning (ML) models for this task, we leveraged CO data from clinical trials, where clinician-assessed CO includes both physical examination and photographic assessment. This study investigates whether CO can be assessed from photographs alone by testing different ML training strategies, feature sets, and an outlier detection method to improve model robustness.

**Materials and Methods:**
We used clinical trial data from two Danish Breast Cancer Group (DBCG) trials (HYPO and PBI), comprising 11,114 images from 2,359 patients across five institutions. Standardized photographs were collected at baseline (pre-radiotherapy) and follow-up visits (years 1–10). Clinicians assigned four-point CO scores (Excellent, Good, Fair, Poor) based on physical examination and scores for dyspigmentation, telangiectasia, induration, scar visibility, and oedema. Patient-reported outcomes (satisfaction, pain, analgesic use) were also collected. ML models were trained to predict CO scores using 237 image-based features (comparing treated with non-treated on asymmetry and colour dissimilarity). Performance was evaluated using binary accuracy (Excellent/Good vs. Fair/Poor) and macro F1-score. We compared:

- Institution-based vs. multi-institutional training: Assessing the effect of training on individual institution datasets vs. a combined dataset.
- Filtering to cases where clinician and patient scores aligned: Testing whether restricting training data to agreed-upon assessments improved model performance.
- Incorporating additional features: Since physical examinations provide more information than images, we tested including factors like induration, scar visibility, and patient-reported outcomes as additional inputs.
- Outlier detection and removal: Cases consistently misclassified across 5-fold cross-validation were excluded before final model training.

[1] https://www.sciencedirect.com/science/article/abs/pii/S0960977607000951

**Results:**
Institution-based training outperformed multi-institution models, highlighting scoring inconsistencies across sites. Filtering data to include only clinician-patient aligned assessments improved binary accuracy, but had mixed effects on the F1-score. Adding additional features enhanced both accuracy and F1-score, suggesting CO perception extends beyond visual appearance.
Outlier removal (13.5% data was removed) provided the largest improvement, increasing binary classification accuracy to 94.2% (F1-score=0.889), outperforming all other approaches, including BCCT.core [1], currently most used objective scoring method.

**Conclusions:**
Photograph-only CO assessment seems possible, but we need to deal with the fact that clinician-assessed CO scores integrate physical examination findings, and subjectivity in scoring. Outlier detection provided the most performance enhancement, and therefore, data quality needs to be addressed first.

## Classification Accuracy Across Institutions

Classification binary accuracy and macro F1-score across institutions, collectively, with outlier detection performed and for BCCT.core. The table compares performance for feature-based models, cases where clinician and patient assessments align, and models incorporating additional features.

| Institution | Image Features | | Agreement Subset | | | Image + Additional Features | |
|---|---|---|---|---|---|---|---|
| | Binary Acc (%) | Macro F1 | Binary Acc (%) | | Macro F1 | Binary Acc (%) | Macro F1 |
| Aarhus N=6081 | 83.30 | 0.701 | (N=2730) | 89.50 | 0.685 | 86.80 | 0.781 |
| Aalborg N=1041 | 90.20 | 0.629 | (N=467) | 96.80 | 0.748 | 94.30 | 0.840 |
| Odense N=1749 | 82.60 | 0.711 | (N=692) | 91.70 | 0.761 | 88.30 | 0.819 |
| Vejle N=1346 | 89.00 | 0.717 | (N=680) | 92.90 | 0.668 | 91.80 | 0.799 |
| Dresden N=714 | 83.20 | 0.741 | (N=292) | 91.50 | 0.747 | 88.10 | 0.821 |
| Combined Dataset | 84.80 | 0.685 | (N=4861) | 90.70 | 0.676 | 87.70 | 0.777 |
| No outlier subset (N=9446) | 94.21 | **0.889** | | N/A | N/A | N/A | N/A |
| BCCTcore | 75.85 | 0.665 | | N/A | N/A | N/A | N/A |

**Rethinking the Elective Target Volume in Patients with Oropharyngeal Cancer.**

Kristoffer Moos[1,2], Julie K. Kaae[4], Anne I. Holm[4], Jesper G. Eriksen[3], Stine S. Korreman[1,2]

Affiliations: [1]Danish Centre for Particle Therapy, Aarhus University Hospital, Aarhus, [2]Department of Clinical Medicine, Aarhus University, Aarhus, [3]Department of Experimental Clinical Oncology, Aarhus University Hospital, Aarhus, [4]Department of Oncology, Aarhus University Hospital, Aarhus

**Introduction**:

The aim of this study was to investigate the potential for volume de-escalated radiotherapy in oropharyngeal cancer patients by omitting lymph node levels (LNLs) with low risk of harbouring nodal involvement. The risk of spread was modelled statistically and were correlated with analysis of nodal recurrence patterns.

**Materials and Methods:**

We developed a Bayesian Network (BN) to estimate probability of nodal involvement within the LNLs for central oropharyngeal cancer (situated ≤ 1 cm of the midsagittal line). Each LNL is represented by a binary variable (yes/no) indicating whether it harbours nodal involvement and is linked to an observed variable, indicating whether that LNL is visibly involved in diagnostic imaging. The BN-model structure imitates the drainage of the lymphatic system, guided by the nodal spread patterns in the cohort.

A retrospective cohort of 428 patients previously treated with radiotherapy at our department was divided into 275 early-stage (T1–T2) and 153 advanced-stage (T3–T4) tumours, and separate BN-models were developed for each group. Volume de-escalation was realized through omission of LNLs with <5% risk of harbouring nodal involvement from the elective target volume.

For the same cohort, recurrence patterns were mapped by reviewing patient records and diagnostic imaging for LNLI–IV. These data were then compared with the risk obtained from the BN-models.

**Results**

The risk of nodal involvement and incidence of recurrences are shown in figure 1. Figure 1a demonstrates that, in early-stage tumours, elective coverage can often be confined to the ipsilateral side when only ipsilateral LNLs are involved, as contralateral LNLs typically remain below 5%. However, in the case of contralateral LNLs involvement, coverage can generally be limited to that specific level.

By contrast, as seen in figure 1b, for advanced-stage tumours, multiple LNLs exceed 5%, both ipsilaterally and contralaterally, thereby requiring more extensive elective coverage. These findings correlate with the recurrence patterns shown in figures 1c and 1d. LNLs estimated to have risk of harbouring nodal involvement <5% consistently exhibit low (<5%) recurrence rates. Conversely, the higher-risk LNLs show increased recurrence rates in line with their higher estimated risks.

**Conclusion**

In this study, we presented a statistical model for assessing risk of nodal involvement within the LNLs for early-stage and advanced-stage central oropharyngeal tumours. The results correlated well with actual nodal recurrence patterns, opening the possibility of rethinking current treatment guidelines to consider volume de-escalated radiotherapy by selectively omitting LNLs with low risk of harbouring nodal involvement.

| Observed Involved LNLs On diagnostic imaging | At-Risk LNLs for Nodal Involvement | | | | |
|---|---|---|---|---|---|
| | | *Ipsi. I* | *Ipsi. II* | *Ipsi. III* | *Ipsi. IV* |
| | *Ipsi. I* | 28.6 | 19.2 | 1.2 | 0.1 |
| | *Ipsi. II* | 0.3 | 97.1 | 4.2 | 0.2 |
| | *Ipsi. II+III* | 0.3 | 99.3 | 86.9 | 1.9 |
| | *Ipsi. III* | 0.3 | 49.1 | 64.1 | 1.4 |
| | *Ipsi. IV* | 0.3 | 19.6 | 4.4 | 13.1 |
| | $N_0$ | 0.3 | 18.0 | 1.2 | 0.1 |
| | | *Cont. I* | *Cont. II* | *Cont. III* | *Cont. IV* |
| | *Cont. I* | 5.3 | 1.3 | 0.1 | <0.1 |
| | *Cont. II* | 0.1 | 64.1 | 1.2 | < 0.1 |
| | *Cont. II+III* | 0.1 | 85.7 | 64.7 | 1.6 |
| | *Cont. III* | <0.1 | 3.8 | 12.6 | 0.3 |
| | *Cont. IV* | <0.1 | 1.2 | 0.4 | 3.3 |
| | $N_0$ | <0.1 | 1.2 | 0.1 | <0.1 |

**(a) Risk Assessment for Early-stage Tumours (%)**

| Observed Involved LNLs On diagnostic imaging | At-Risk LNLs for Nodal Involvement | | | | |
|---|---|---|---|---|---|
| | | *Ipsi. I* | *Ipsi. II* | *Ipsi. III* | *Ipsi. IV* |
| | *Ipsi. I* | 61.2 | 26.3 | 2.0 | 0.3 |
| | *Ipsi. II* | 1.2 | 97.9 | 5.9 | 0.4 |
| | *Ipsi. II+III* | 1.2 | 99.6 | 90.6 | 2.0 |
| | *Ipsi. III* | 1.1 | 62.8 | 74.5 | 1.7 |
| | *Ipsi. IV* | 1.0 | 25.8 | 5.6 | 30.9 |
| | $N_0$ | 1.0 | 23.7 | 1.9 | 0.3 |
| | | *Cont. I* | *Cont. II* | *Cont. III* | *Cont. IV* |
| | *Cont. I* | 9.2 | 5.6 | 0.4 | 0.1 |
| | *Cont. II* | 0.1 | 89.5 | 1.9 | 0.2 |
| | *Cont. II+III* | 0.1 | 96.2 | 74.7 | 3.2 |
| | *Cont. III* | 0.1 | 14.2 | 35.7 | 1.6 |
| | *Cont. IV* | 0.1 | 5.8 | 2.3 | 15.3 |
| | $N_0$ | 0.1 | 5.3 | 0.4 | 0.1 |

**(b) Risk Assessment for Advanced-stage Tumours (%)**

| Observed Involved LNLs On diagnostic imaging | Recurrent LNL | | | | |
|---|---|---|---|---|---|
| | | *LNL I* | *LNL II* | *LNL III* | *LNL IV* |
| | *LNL I* | 0.0 | 0.0 | 0.0 | 0.0 |
| | *LNL II* | 1.4 | 12.4 | 1.4 | 1.8 |
| | *LNL III* | 0.0 | 9.1 | 1.1 | 2.3 |
| | *LNL IV* | 0.0 | 15.0 | 0.0 | 10.0 |
| | $N_0$ | 0.0 | 2.0 | 0.0 | 2.0 |

**(c) Incidence of Recurrence for Early-stage (%)**

| Observed Involved LNLs On diagnostic imaging | Recurrent LNL | | | | |
|---|---|---|---|---|---|
| | | *LNL I* | *LNL II* | *LNL III* | *LNL IV* |
| | *LNL I* | 0.0 | 10.5 | 0.0 | 0.0 |
| | *LNL II* | 0.0 | 14.2 | 5.2 | 3.7 |
| | *LNL III* | 0.0 | 10.8 | 1.5 | 3.1 |
| | *LNL IV* | 0.0 | 17.7 | 0.0 | 0.0 |
| | $N_0$ | 0.0 | 12.5 | 0.0 | 0.0 |

**(d) Incidence of Recurrence for Advanced-stage (%)**

**Figure 1:** This figure summarizes both the estimated risk of nodal involvement within the LNLs and the observed recurrence patterns. **(a)** Risk estimates for early-stage tumours. Here '*Ipsi.*' is short for ipsilateral and '*Cont.*' for contralateral, **(b)** Risk estimates for advanced-stage tumours. Here '*Ipsi.*' is short for ipsilateral and '*Cont.*', **(c)** Incidence of recurrence patterns for different observed involved LNLs on diagnostic imaging for early-stage tumours, **(d)** Incidence of recurrence patterns for different observed involved LNLs on diagnostic imaging for advanced-stage tumours. One should note that, the reported recurrence patterns for early- and advanced-stage tumours are grouped to encompass both ipsilateral and contralateral recurrences for each LNL.

**Attitudes towards AI-generated risk prediction in patients with early breast cancer: an international multi-center survey.**

**Author information:**
1 – Frederik Voigt Carstensen
frederik.voigt.carstensen@regionh.dk
Dept. of Oncology, Copenhagen University Hospital Rigshospitalet, Denmark

2 – Sofie A.M. Gernaat
Division of Imaging and Oncology, University Medical Center Utrecht, Utrecht University, Utrecht, the Netherlands

3 – Friederike Banning
Breast Center, Dept. of OB&GYN, LMU University Hospital, Germany

4 – Eva Batista
Breast Unit, Champalimaud Foundation, Lisbon, Portugal.

5 – Desiree van den Bongard
Dept. of Radiation Oncology, Amsterdam UMC, Cancer Center Amsterdam, Cancer Treatment and Quality of Life / Cancer Biology and Immunology, Amsterdam, the Netherlands

6 – Merle Hattink
Division of Imaging and Oncology, University Medical Center Utrecht, Utrecht University, Utrecht, the Netherlands

7 – Icro Meattini
Radiation Oncology & Breast Unit, Azienda Ospedaliero-Universitaria Careggi, Florence, Italy
Department of Experimental and Clinical Biomedical Sciences "M. Serio", University of Florence, Florence, Italy

8 – Jens Petersen
Dept. of Oncology, Copenhagen University Hospital Rigshospitalet, Denmark
Department of Computer Science, University of Copenhagen, Copenhagen, Denmark

9 – Ivica Ratosa
Division of Radiotherapy, Institute of Oncology Ljubljana, Zaloska cesta 2, Ljubljana, Slovenia and Faculty of Medicine, University of Ljubljana, Vrazov trg 2, Ljubljana, Slovenia.

10 – Helena Verkooijen
Division of Imaging and Oncology, University Medical Center Utrecht, Utrecht University, Utrecht, the Netherlands.

11 – Ivan Vogelius
Dept. of Oncology, Copenhagen University Hospital Rigshospitalet, Denmark

12 – Maja Vestmø Maraldo
Dept. of Oncology, Copenhagen University Hospital Rigshospitalet, Denmark.

On behalf of the ARTILLERY consortium
Institution: Rigshospitalet

**Affiliations**

(1) Dept. of Oncology, Copenhagen University Hospital Rigshospitalet, Denmark.
(2) Dept. of Oncology, Copenhagen University Hospital Herlev and Gentofte, Denmark.
(3) Dept. of Oncology, Zealand University Hospital Næstved, Denmark.
(4) Division of Imaging and Oncology, University Medical Center Utrecht, Utrecht University, Utrecht, the Netherlands.
(5) Dept. of Radiation Oncology, Amsterdam UMC, Cancer Center Amsterdam, Cancer Treatment and Quality of Life / Cancer Biology and Immunology, Amsterdam, the Netherlands
(6) Breast Center, Dept. of OB&GYN, LMU University Hospital, Germany
(7) Radiation Oncology & Breast Unit, Azienda Ospedaliero-Universitaria Careggi, Florence & Department of Experimental and Clinical Biomedical Sciences "M. Serio", University of Florence, Florence, Italy.
(8) Division of Radiotherapy, Institute of Oncology Ljubljana, Zaloska cesta 2, Ljubljana, Slovenia and Faculty of Medicine, University of Ljubljana, Vrazov trg 2, Ljubljana, Slovenia.
(9) Breast Unit, Champalimaud Foundation, Lisbon, Portugal.

**Purpose:**
Globally, breast cancer is the most common type of cancer in women and patients with early breast cancer generally have a good prognosis. With a long life-expectancy and with 80% of patients being diagnosed after age 50, there is a substantial risk of developing chronic conditions such as cardiovascular disease (CVD), osteoporosis, interstitial lung disease, and weight gain, with treatment induced toxicity being a contributing factor. 60-70% of patients with early breast cancer receive radiation therapy (RT) as a component in their adjuvant treatments. ARTILLERY (funded by Horizon Europe, grant no. 101080983) aims to develop reliable AI-models to predict the risk of developing CVD, osteoporosis, chronic obstructive pulmonary disease (COPD), and unfavorable body composition based on RT planning CT-scan (www.artillery-project.eu). The objective of this survey was to clarify patients' attitude towards such risk prediction in clinical practice.

**Materials and Methods:**
The survey was developed by the investigators. The survey consisted of patient characteristics (age and smoking status) and four hypothetical questions on the patient's interest of knowing their AI-generated risk prediction of developing CVD, osteoporosis, COPD, and unfavorable body composition based on the planning CT-scan. Patients were recruited either prior to or immediately after the planning CT-scan. The aim was to recruit 360 patients: 40 consecutive patients from nine institutions in six European countries (Denmark, Germany, Italy, the Netherlands, Portugal, and Slovenia). Data collection was ongoing at time of abstract submission.

**Results**:
From February 2024 to March 2025 a total of 289 patients had answered the survey. For all respondents the median age was 60 years (range: 28-94) and 14.8% (CI95% 10.9-19.3) were active smokers. Amongst all respondents, the majority had positive attitudes towards a risk prediction, 87.6% (CI95% 83.3-91.1), 88.9% (CI95% 84.8-92.3), 86.9% (CI95% 82.5-90.5), and 85.6% (CI95% 81.1-89.4) for CVD, osteoporosis, COPD, and unfavorable body composition, respectively (Figure 1). Notably, a less positive attitude was observed in Italy (n=40) and the Netherlands (n=20), with 70.0% (CI95% 53.5-83.4) and 75.0 (CI95% 50.9-91.3) answering positively for CVD, 70.0% (CI95% 53.5-83.4) and 65.0% (CI95% 40.8-84.6) for osteoporosis, 70.0% (CI95% 53.5-83.4) and 70.0% (CI95% 45.7-88.1) for COPD, and 65.0% (CI95% 48.3-79.4) and 60.0% (CI95% 36.1-80.9) for unfavorable body composition.

**Conclusions:**
In an unselected cohort of early breast cancer referred for postoperative RT, we found a highly positive attitude towards the use of an AI-generated risk prediction of developing common chronic diseases. Preliminary data suggests some differences in the attitude across European countries.

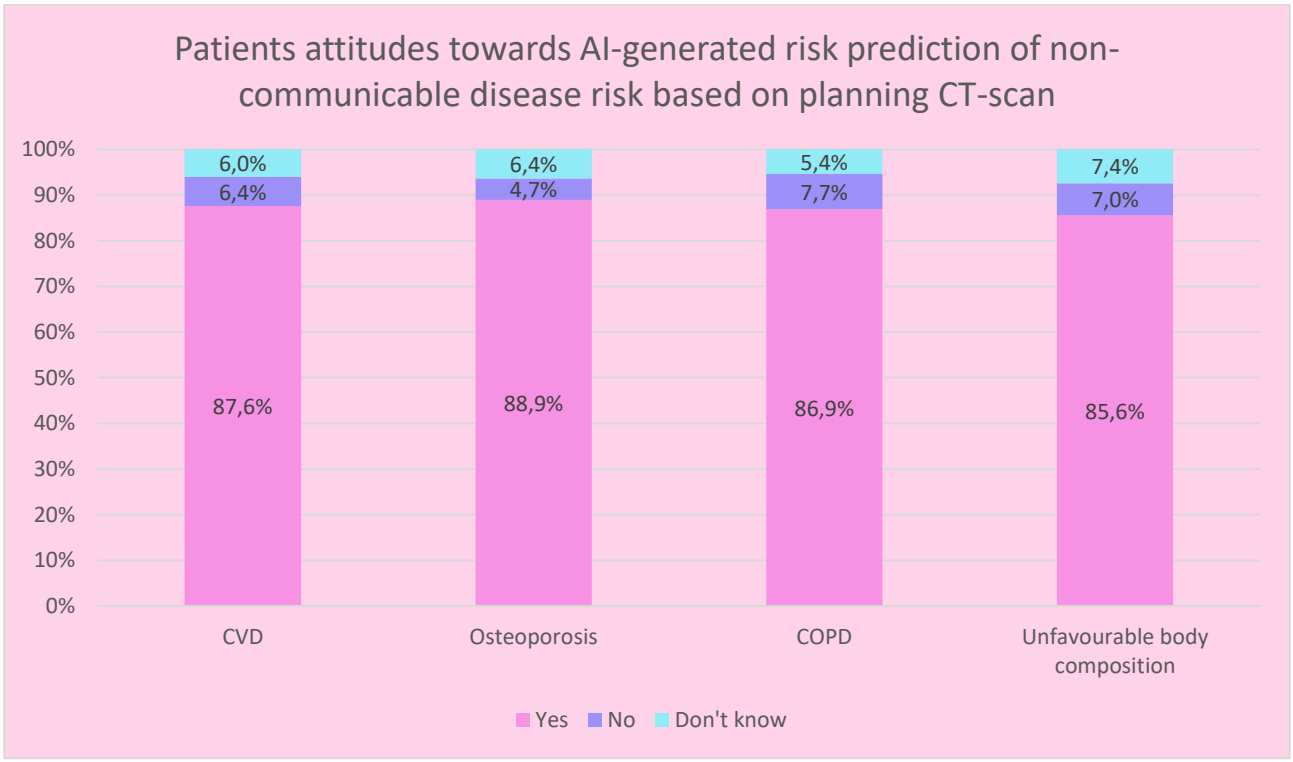


Figure 1: Reponses (n=298) from all sites, given in percentage, on the questions about '*if an AI-system could determine your risk of developing CVD/osteoporosis/COPD/fat and muscle distribution, would you be interested in that information?*'.

# Monitoring the performance of AI segmentation of organ at risk in clinical practice at the Department of Oncology at Aarhus University Hospital

Lise Bech Jellesmark Thorsen[a, c], Christina Maria Lutz[a], Tine Bisballe Nyeng[a], Ditte Sloth Møller[a, c], Jesper Folsted Kallehauge[b, c], Jesper Grau Eriksen[a, c], Marianne Marquard Knap[a], Anne Ivalu Sander Holm[a]

Presenting Author: Lise Bech Jellesmark Thorsen, Department of Oncology, Aarhus University Hospital. E-mail: liseb@oncology.au.dk

Author affiliations:

[a] Department of Oncology, Aarhus University Hospital, Aarhus, Denmark

[b] Danish Center for Particle Therapy, Aarhus University Hospital, Aarhus, Denmark

[c] Department of Clinical Medicine, Aarhus University, Aarhus, Denmark

## Introduction

The use of Artificial Intelligence (AI) for segmenting organs-at-risk (OARs) in radiation therapy (RT) has increased during the last decade, mainly because traditional OAR delineation is labor-intensive and prone to variability. While AI improves accuracy and efficiency of OAR segmentation, it can introduce biases. Continuous evaluation and monitoring of AI-models across diverse clinical cases is essential to identify and address biases in real-world applications and prevent impact on clinical outcomes.

## Materials and Methods

AI-assisted OAR segmentation was implemented for all patients receiving RT for head-and-neck (HN), esophageal, or lung cancer (NSCLC, SCLC, and SBRT) at Aarhus University Hospital in June 2023. The OARs are segmented with a combination of CE-approved and in-house developed AI-models. The in-house developed models were specifically generated for HN/thoracic CT-scans with contrast. In clinical practice, AI-generated structures were reviewed, corrected when needed, and approved by expert oncologists. The initial AI and the corrected segmentations were stored and compared using Surface Dice Similarity Coefficient (SDSC) with 1mm (small structures) and 2mm (others), along with mean Hausdorff distance
(mHD). Acceptance thresholds (SDSC=0.7-0.9, mHD=2mm/3mm) for outlier detection were set, and all metrics were monitored over time.

## Results

The performance of AI segmented OARs was monitored over 10 (HN – 140 patients) and 20 months (thorax – 474 patients). During this period, no significant drift was observed in either the SDSC or mHD values for all OARs, indicating stable OAR corrections, even if the corrections were few mm. The percentage of outliers was below 5% for 18 of 27 OARs, below 15% for 5 OARs and above 15% for the remaining four OARs (fig1). These includde the three pharyngeal constrictor muscles (PCMs), with outlier levels of 27%-32% for SDSC, while mHD remained low (1-3 mm). For the thin structure of the PCMs, this is likely due to limitations in the brush size used to correct the AI suggestions. The fourth OAR was the esophagus segmentation for SBRT in the thoracic region, with an outlier level of 20%, likely because the model was developed using contrast CT-scans but was applied to non-contrast CT scans.

## Conclusions

In the continuous systematic evaluation of our AI OAR segmentation in clinical practice, no drift in frequency or magnitude of corrections was observed. The outlier level was below 5% for most OARs.  Continuous monitoring allows us to improve the used AI-models where needed and raise awareness of areas where care should be taken by the correcting oncologists.

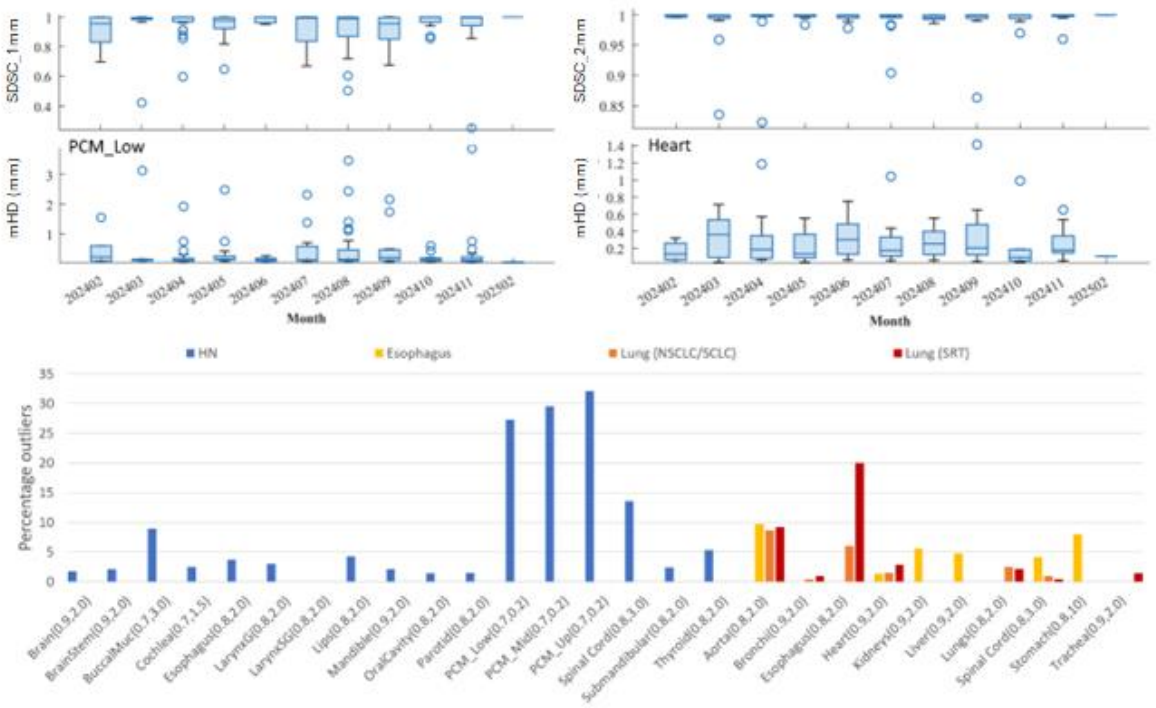


*Figure 1. Top: Surface Dice Similarity Coefficient (SDSC) and mean Hausdorff distance for lower pharyngeal constrictor muscle (PCM, left) and the heart (right) for the last 11 months. Bottom: Percentage of outlier patients for patients receiving RT for head and neck, esophageal, or lung cancers (NSCLC, SCLC, and SBRT). The acceptance limits for the two metrics SDSC 1mm/2mm and mean Hausdorff distance are given in the parentheses.*

**Study pitch: Diffusion MRI for Enhanced Tumour Delineation and Outcome Prediction in Pancreatic Cancer Using Artificial Intelligence.**

**Authors**

Emilie H. Karlsson[1] Emilie.helgesen.karlsson@rsyd.dk
Smith K. Khare[2]
Uffe Bernchou[1,3]
Per Pfeiffer[3,4]
Faisal Mahmood[1,3]

**Affiliations**

[1]Laboratory of Radiation Physics, Department of Oncology, Odense University Hospital, Odense, Denmark [2]The Maersk Mc-Kinney Moller Institute, Applied AI and Data Science, University of Southern Denmark [3]Department of Clinical Research, University of Southern Denmark, Odense, Denmark
[4]Department of Oncology, Odense University Hospital, Odense, Denmark

**Introduction**

Pancreatic cancer (PC) remains one of the deadliest cancers, with a 5-year survival rate of 3-8% [1]. The introduction of MRI-linac improves soft-tissue visualization and enables adaptive radiotherapy (RT) [2], but biological imprecision remains a challenge. Diffusion-weighted imaging (DWI) shows promise for assessing tumour microstructure and could play a pivotal role in improving RT outcomes [3]. However, its realization is hampered due to target and organs-at-risk inter-fraction motion. Strategies to address this motion and investigate the spatial correlation between DWI and local control are necessary in order to explore DWI's potential in dose modulation. This study aims to explore the potential of artificial intelligence (AI) in leveraging DWI for enhanced tumour delineation and treatment outcome prediction for patients with PC. By addressing motion-related challenges in DWI, this research seeks to enhance the precision of adaptive RT, as successful individualization can improve local control, survival, and toxicity reduction.

**Materials and methods**

This retrospective study will develop two AI models to support personalized RT for patients with PC. Using MRI, DWI and DWI-derived maps (such as ADC), machine and deep-learning models will be tested and compared for automated tumour segmentation and prediction of voxel-by-voxel local tumour control. To overcome the challenge of deformation in the tumour and surrounding structures both analytical and AI-based methods will be explored to account for inter-fraction motion and align longitudinal imaging data. The AI models will learn from DWI and MRI data to improve initial tumour delineation by predicting regions at risk of local recurrence, aiming to refine dose escalation strategies. Follow-up scans will serve as reference for regions with lack of control, and the first model will learn these as regions that should be included/prioritized in the initial delineation.

The study includes >140 patient with locally advanced PC, treated with RT (5 fractions of 5 Gy) on a 1.5 T MRI-Linac. The dataset consists of pre-treatment and longitudinal MRI and DWI scans acquired before and at each fraction along with a follow-up scan.

## Results

Current status: Data from 124 patients, who have completed treatment and received five fractions, have been collected and cleaned. An Example is shown in figure 1. Dataset has equal gender representation, with age reflecting real-world patterns.

**a. MRI-Linac scans**

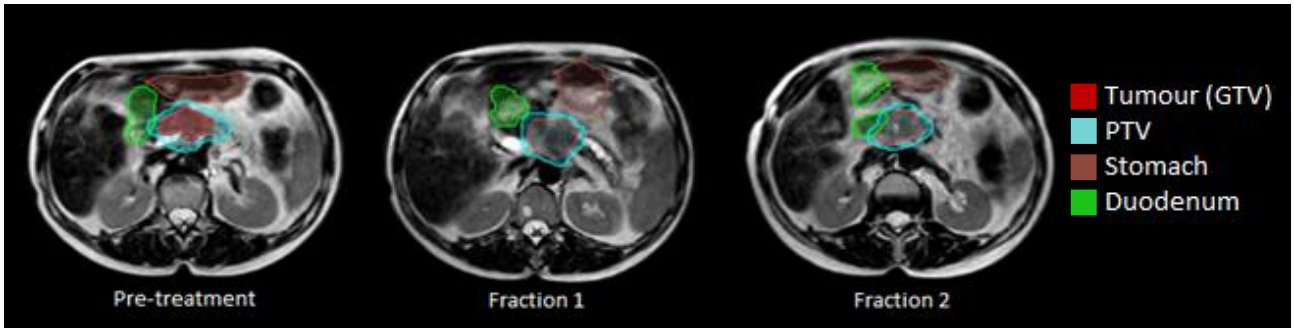


**b. Anatomical MRI vs. DWI**

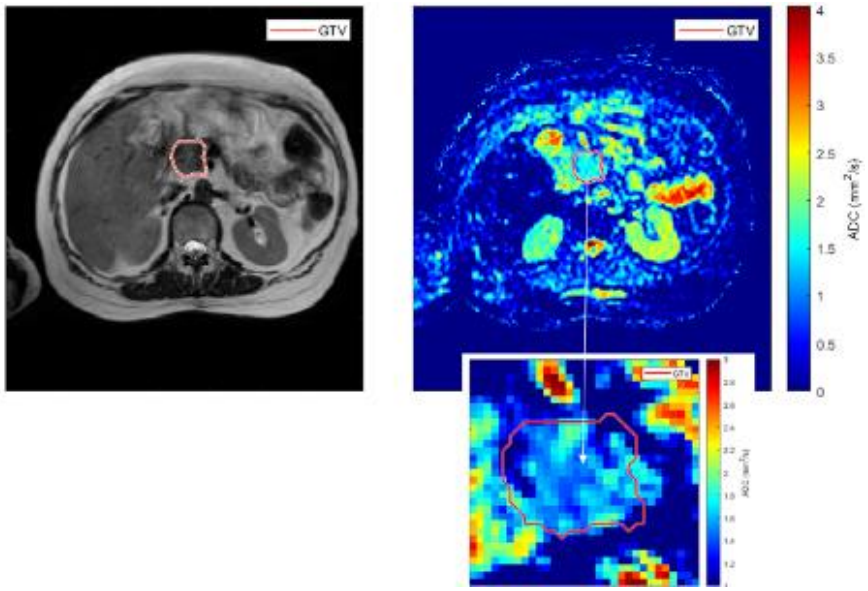


*Figure 1: Example of a patient's pre-treatment scan along with scan from fraction 1 and 2 demonstrating the challenge of motion (a) and a comparison between a T2-weighted scan and a DWI scan (b).*

## Conclusions

Expected outcomes include improved accuracy in tumour delineation and early prediction of treatment responses, with the aim of enabling a more tailored RT strategies, leading to potentially better outcomes for patients with PC.

## References

[1] Sung H, Ferlay J, Siegel RL, et al. Global Cancer Statistics 2020: GLOBOCAN Estimates of Incidence and Mortality Worldwide for 36 Cancers in 185 Countries. CA Cancer J Clin. 2021;71:209–249.
[2] Raaymakers BW, Jürgenliemk-Schulz IM, Bol GH, et al. First patients treated with a 1.5 T MRI-Linac: Clinical proof of concept of a high-precision, high-field MRI guided radiotherapy treatment. Phys Med Biol. 2017;62:L41–L50.
[3] Koh DM, Collins DJ. Diffusion-weighted MRI in the body: Applications and challenges in oncology. Am J Roentgenol 2007;188:1622–35.

**Mechanisms of Radiation-Induced Bone Damage: In Vitro Studies**

Hild Milde Bekkevoll[1], Pernille Dalen Ekvall[1], Diamante Boscaro[1], Pawel Sikorski[1], and Kathrine Røe Redalen[1]

[1]Department of Physics, NTNU, Trondheim, Norway.

Contact Email: hild.m.bekkevoll@ntnu.no

**Background and aims:** Osteoradionecrosis (ORN) of the jaw is a devastating toxicity which may occur after radiotherapy to the head- and neck region. It is characterized by exposed necrotic bone within the radiation field, and the mechanisms behind the condition remains poorly understood. The aim of this study was to estab-lish an experimental bone model allowing investigation and comparison of photon and proton radiation. This could contribute to new knowledge on the mechanisms behind radiation-induced bone damage, which could be important for improving future radiotherapy and the quality of life for cancer survivors.

**Materials and Methods:** MC3T3-E1 cells, a pre-osteoblast cell line with osteoblast differentiation potential, were exposed to photon doses between 0 and 20 Gy. The viability of the cells after radiation exposure was quan-tified by the Cell Counting Kit-8 assay and the impact on cell cycle progression was analyzed by flow cytometry with propidium iodide staining. Quantification of DNA double-strand breaks was performed using fluorescence microscopy by detecting γ-H2AX foci at various time points following radiation exposure. The mineralization capacity of the osteoblasts following irradiation was evaluated by cultivating the cells in osteogenic media for 21 days post-irradiation and staining the mineralized matrix with Alizarin Red.

**Results:** A method for growth and differentiation of the MC3T3-E1 cells has been established. The viability assay showed a dose-dependent decrease in cell survival following radiation exposure (Figure 1a). At 20 Gy, the viability was reduced to 20% compared to the control at day 7 post-irradiation. At day 1 following irradiation, a higher G2/M peak was observed for the higher doses in the flow cytometric analysis. The mineralization assay revealed a small reduction in mineralization for lower dose (< 6 Gy), and a larger reduction for the cells irradi-ated with 10 and 20 Gy (Figure 1b). Cells receiving 10 Gy had a 22% reduction in mineralization nodule area compared to the control, while at 20 Gy the reduction was 98%. The formation of γ-H2AX foci demonstrated, as expected, an increase in DNA double-strand breaks following irradiation (Figure 1c-d).

**Conclusion:** We have established an experimental bone model and found a dose-dependent decrease in cell viability, increase in DNA damage and decrease in mineralization for photon doses above 6 Gy. Further studies will include a comparison between photon and proton radiation, and an expansion to a more clinically relevant bone model for further mechanistic studies.

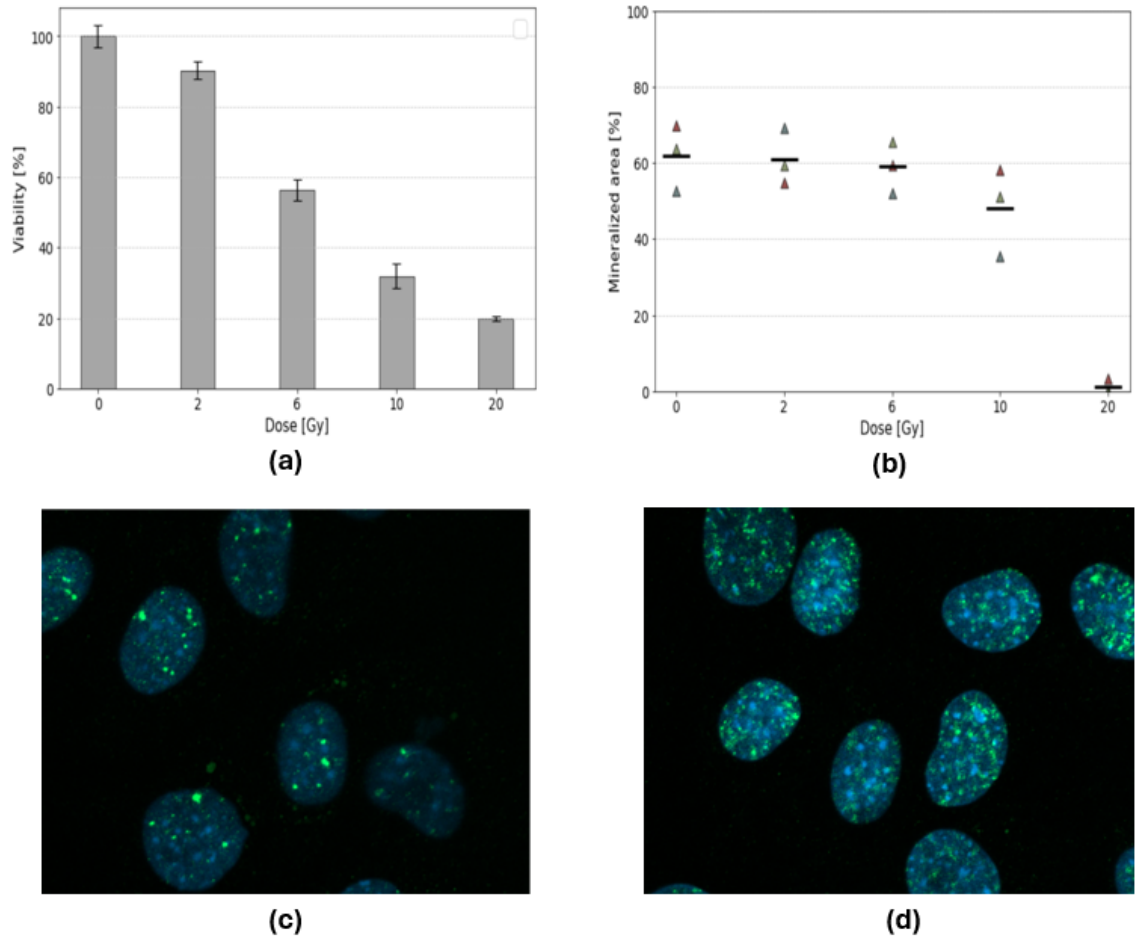


**Figure 1:** Radiation response of MC3T3-cells to photon doses ranging from 0 to 20 Gy. **(a)** Cell viability compared to the control measured at 7 days post-irradiation. The viability was assessed by the Cell Counting Kit-8 assay. The data is shown as mean ± SEM. **(b)** Mineralized area measured 21 days after irradiation. Mineralized nodules were stained with Alizarin Red and imaged with phase contrast microscopy. The images was analyzed in ImageJ. The data is shown for n = 3 replicates with mean value. **(c)** and **(d)** Immunofluorescent images of control cells and cells irradiated with 6 Gy, respectively. The cells were fixed 1h after irradiation. The nuclei were stained with DAPI (blue), and $\gamma$-H2AX was stained using a primary antibody against $\gamma$-H2AX, followed by the secondary antibody AF-488 (green).

# Natural killer cell activity in patients treated with curatively intended radiotherapy for prostate cancer: An observational study

**Corresponding author:**
Stine Vestergaard Eriksen, MD
stine.vestergaard.eriksen@rsyd.dk
Department of Oncology, Vejle Hospital, University Hospital of Southern Denmark, Vejle, Denmark
Department of Regional Health Research, University of Southern Denmark, Odense, Denmark

SV Eriksen[1,3*], CV Madsen[1*], S Timm[1,3], AH Zedan[1,3], L Raunkilde[1], TF Hansen[1,3], L Nederby[2]

1 Department of Oncology, Vejle Hospital, University Hospital of Southern Denmark, Vejle, Denmark
2 Department of Biochemistry and Immunology, Vejle Hospital, University Hospital of Southern Denmark, Vejle, Denmark
3 Department of Regional Health Research, University of Southern Denmark, Odense, Denmark
* Joint first authorship

**Introduction:** Natural killer (NK) cells are key components of the innate immune system and play an important role in the biological cancer defence. Some studies indicate a correlation between low NK activity (NKA) and the risk of detecting prostate cancer (PCa). Lower NKA has been reported pre- than postoperatively in PCa patients undergoing radical prostatectomy. Additionally, high NKA may be associated with better prognosis in metastatic PCa.

While radiotherapy (RT) can influence immune responses, data on NKA dynamics in patients receiving RT with or without androgen deprivation therapy (ADT) remains limited. This study examines NKA fluctuations in PCa patients treated with RT ± ADT for PCa.

**Materials/Methods:** Between 2019 and 2023, 150 patients treated with curatively intended RT for PCa were included consecutively in a biomarker study, with blood samples collected into NK Vue® tubes before the start of RT, after end of RT (EOT), and during follow-up (3, 6, 9, 12, 18, and 24 months). Based on EAU risk group classification, patients received either no ADT (n=15), 6 months of ADT (n=23), or 36 months of ADT (n=112), starting 3 months before RT. The dose to the prostate was either 78Gy/39 fractions (n=128) or 60Gy/20 fractions (n=22). The majority of patients (n=126) received elective lymph node irradiation.

NK Vue® tubes were incubated for 24 hours after which IFN-γ, serving as surrogate marker for NKA, was measured in the plasma using the NK Vue® ELISA. A cut-off of 250 pg/mL was used to distinguish between low (<250 pg/mL) and high (≥250 pg/mL) NKA.

Data were analyzed using descriptive statistics.

**Results:** Baseline characteristics were similar between high (n=46) and low NKA (n=104) groups, though smoking was more prevalent in the low NKA group (28% vs. 11%). IFN-γ levels fluctuated throughout follow-up, with some patients showing extreme elevations (>20,000 pg/mL). IFN-γ levels did not mirror PSA dynamics. NKA distributions varied over time and among ADT groups, with a marked decrease in interquartile range at EOT (BL median 832 pg/mL, IQR 2901; EOT median 312 pg/mL, IQR 708)

**Conclusion:** This study revealed unexpectedly high and fluctuating NKA levels, distinct from patterns observed in other cancer types, raising questions about NKA reliability as a biomarker in localized PCa treated with RT ± ADT. Considerable variations were seen in NKA both within and between the ADT groups over time. Further research evaluating NKA before ADT initiation may enhance understanding of its role in PCa.

**Figure 1.** Boxplot displaying IFN-γ release in the three ADT groups at BL, EOT, and at each follow-up.
Outliers are not depicted but are included in the statistical analyses. N for each group and time point is indicated below the figure.

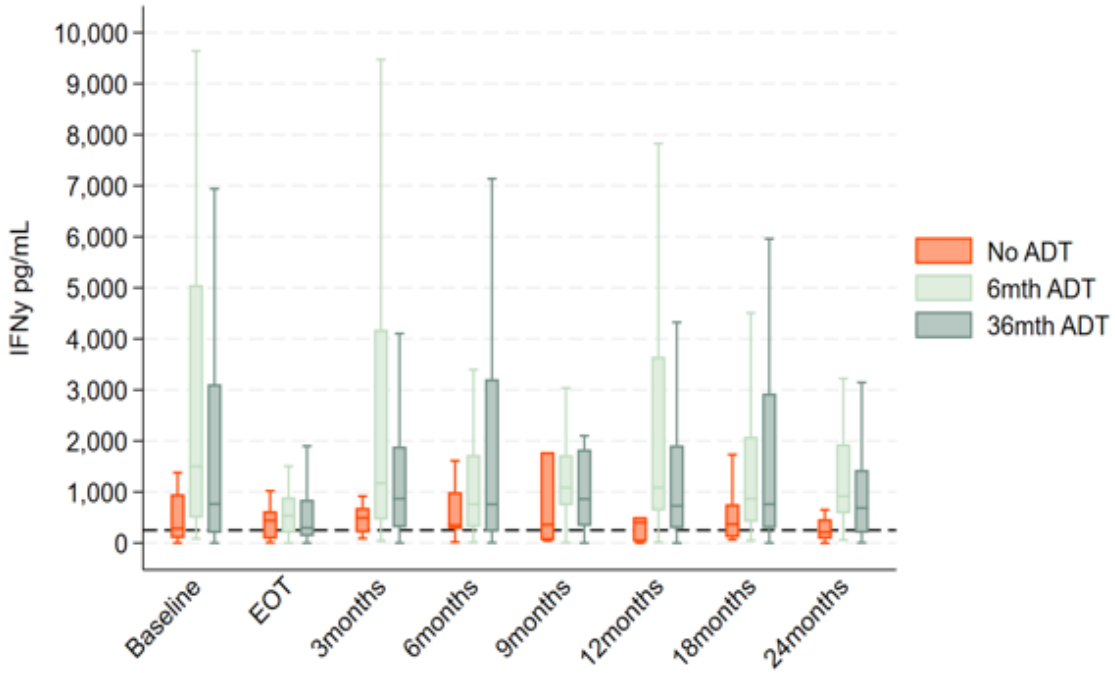


| | Baseline | EOT | 3months | 6months | 9months | 12months | 18months | 24months |
|---|---|---|---|---|---|---|---|---|
| No ADT | 15 | 15 | 11 | 9 | 7 | 10 | 8 | 8 |
| 6 months ADT | 23 | 20 | 18 | 19 | 16 | 15 | 15 | 14 |
| 36 months ADT | 112 | 105 | 85 | 82 | 67 | 71 | 63 | 53 |
| **Total** | **150** | **140** | **114** | **110** | **90** | **96** | **86** | **75** |

**Spatial correlation of FAZA PET and FDG PET for head and neck cancer: a search for a more accessible way to image hypoxia**

Laura A Rechner, Christian Maare[a], Henriette Klitgaard Mortensen[a], Kristin Skougaard[b], Camilla Kjaer Lonkvist[a] and Jens Edmund[a]*
a Department of Oncology, Herlev & Gentofte Hospital, Herlev, Denmark.
b Department of Oncology, University Hospital Roskilde, SUH, Denmark.
* Presenting author

**Purpose**

Hypoxia is a known negative prognostic factor for patients with head and neck cancer (HNC) [1]. The hypoxic volume (HV) could be targeted with dose escalated radiotherapy (RT), but hypoxia PET tracers such as F-MISO and FAZA have not reached widespread clinical use due to feasibility and cost. There is some evidence of a moderate correlation between FDG PET and hypoxia PET tracers [2], but the overlap of FDG PET-positive volumes and hypoxia PET HVs is not well understood. The purpose of this study was to explore the spatial correlation of FDG volumes and FAZA HVs for patients with HNC.

**Materials and Methods**

Six patients with HNC were scanned with FDG PET/CT for their RT planning and with FAZA PET/CT to image hypoxia in the beginning, middle, and end of their RT course (approval H-19083440). All scans were acquired in treatment position with immobilization. The clinical FDG PET-positive volume was delineated by a nuclear medicine specialist, and additional percentage-based contours of the FDG standard uptake volumes (SUV in g/ml) were created as 30%, 40%, and 50% of the maximum SUV within the GTV (FDG SUV30, 40 and 50, respectively). The HV within the GTV was defined as a FAZA signal above 1.4 times that of a reference oxic muscle (ref). FAZA HVs were rigidly transferred to the FDG PET/CT and compared using a Bland-Altman plot, Dice similarity coefficients (DSCs), and Boolean subtractions (Eclipse, Varian, a Siemens Healthineers Company).

**Results**

FAZA HVs were stable in location and reduced in volume (or eliminated) midway, and eliminated by the end of RT. FDG volumes were generally larger than FAZA HVs, and DSCs were consequently low (Figure 1). False negative volumes, i.e. assumed hypoxic by FDG, but non-hypoxic by FAZA, were very small (range: 0.0-2.7 $cm^3$) and false positive volumes, i.e. non-hypoxic regions by FAZA, but within the FDG volume, were larger (range: 1.2-21.4 $cm^3$).

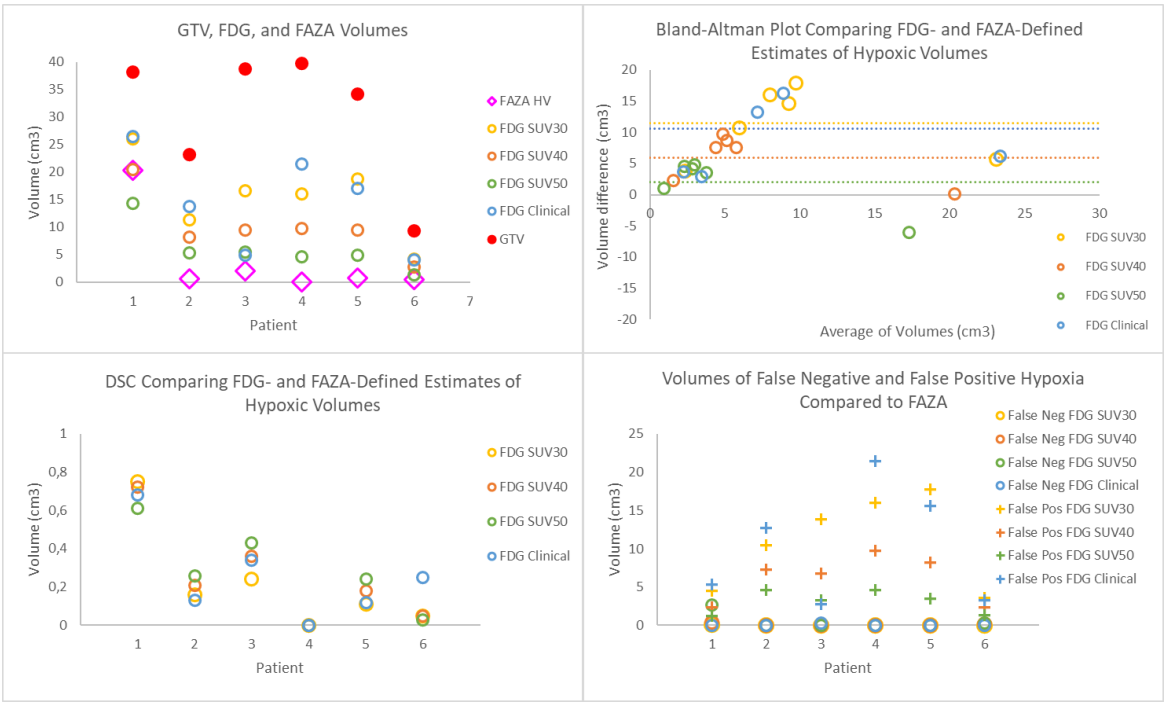


**Figure 1.** GTV, FDG SUV, and FAZA hypoxic volume (HV) PET-defined volumes (top left). Bland-Altman plot comparing FDG-defined volumes to the FAZA based HVs (top right). Dice similarity coefficients (DSCs) (bottom left). False negative and false positive volumes were defined as the FAZA-FDG volumes and the FDG-FAZA volumes, respectively (bottom right).

## Conclusion

In this small study for patients with HNC, FDG was able to roughly localize HVs as defined by FAZA, and FDG volumes were generally larger than FAZA HVs. FDG clinical, SUV30, and SUV40 volumes provided conservative estimates of the HVs resulting in almost no false negative volume. This study demonstrates that the spatial correlation of FDG PET and hypoxia PET warrants further investigation, and the clinical significance of false positive errors should be weighed against the challenge of implementing FAZA clinically.

References

[1] Nordsmark M, Overgaard J. A confirmatory prognostic study on oxygenation status and loco-regional control in advanced head and neck squamous cell carcinoma treated by radiation therapy. Radiotherapy and Oncology 2000;57:39–43.
[2] Thorwarth D, Eschmann S-M, Holzner F, Paulsen F, Alber M. Combined uptake of [18F]FDG and [18F]FMISO correlates with radiation therapy outcome in head-and-neck cancer patients. Radiotherapy and Oncology 2006;80:151–6. https://doi.org/10.1016/j.radonc.2006.07.033.

# PRECLINICAL STUDY OF REIRRADIATION WITH HYPERTHERMIA IN RECURRENT MURINE TUMORS

Charlemagne A. Folefac* [1], Priyanshu M. Sinha[1], Niels Basler[2], Brita S. Sørensen[12], Michael R. Horsman[1]

[1]Experimental Clinical Oncology-Department of Oncology, Aarhus University Hospital, DK-8200, Aarhus, Denmark
[2]Danish Center for Particle Therapy, Aarhus University Hospital, DK-8200, Aarhus, Denmark·

Corresponding Authors: charlemagne@oncology.au.dk bsin@oncology.au.dk

**BACKGROUND:** Recurrent tumors are resistant to conventional therapies, and while reirradiation (Re-Rt) is a potential strategy for such treatment, high doses can damage healthy tissues. Combining Re-Rt with hyperthermia may improve tumor control, reduce the required tumor control Re-Rt dose, and lower toxicity.

**MATERIAL AND METHODS:** The study began with a pilot study to determine the minimum irradiation dose (10 or 40 Gy) to shrink a 200 mm³ tumor in the animal's leg to an undetectable size before regrowth, identifying 40 Gy as optimal. For reirradiation, tumors regrown to 200 mm³ within 30–35 days post-40 Gy treatment retreated with doses (Re-Rt: 25–60 Gy, Re-Rt: 5–45 Gy + heat at 42.5°C for 30 minutes post Re-Rt) to create dose-response curves, with tumor control (TC) evaluated at 90 days. Similarly, a pilot study on non-tumor-bearing animals (26–36 Gy single dose treatment) found that 30 Gy caused very mild acute skin toxicity after 30 days. In the main study, animals received 30 Gy, followed by varying reirradiation doses (Re-Rt: 25–35 Gy, Re-Rt15–25 Gy + heat:42.5°C for 30 minutes) to establish dose-response relationships for acceptable moderate acute skin score after 30 days post reirradiation. The tumor and skin data are fitted to non-linear regression curves to determine the tumor control Re-Rt dose 50(TCD50) and moist desquamation Re-Rt dose 50(MDD50) for each group. The thermal enhancement ratio (TER) and therapeutic gain factor (TGF) are also calculated.

**RESULTS AND DISCUSSION:**

For tumor control, reirradiation alone (Re-Rt) required 49.37 Gy (95% CI: 41.33–58.97), while reirradiation with hyperthermia (Re-Rt + heat) needed only 26.04 Gy (95% CI: 13–49), with a thermal enhancement ratio (TER) of 1.90. In skin toxicity studies, reirradiation alone (Re-Rt) at 24.63 Gy (95% CI: 23.22–26.12) caused moderate moist desquamation, compared to 17.55 Gy (95% CI: 15.34–20.07) with Re-Rt + heat, yielding a TER of 1.4. The therapeutic gain factor (TGF = 1.4) highlights the potential of Re-Rt + hyperthermia in recurrent cancer treatment, though this study also underscores challenges especially relating to animal toxicity in conducting such investigations.

**CONCLUSION:** In conclusion, combining reirradiation with hyperthermia enhances tumor control, reduces the required Re-Rt dose, and lowers toxicity, offering a promising strategy for recurrent cancer treatment.

# The CAM Model: A Novel Preclinical Platform for Proton Radiotherapy and Nuclear Imaging in Oncology

Emil Leth Villumsen[1,2] (emvi@clin.au.dk), Morten Busk[2] (morten@oncology.au.dk), Signe Bauenmand[1,3] (au635002@forens.au.dk), Mikkel H Vendelboe[5,6] (mhve@biomed.au.dk), Lars Thrane[1] (lath@clin.au.dk), Jörg Männer[7] (jmaenne@gwdg.de), Niels Bassler[4] (bassler@clin.au.dk), Michael R Horsman[2] (mike@oncology.au.dk) and Michael Pedersen[1] (michael@clin.au.dk)

## Author affiliation

1: Comparative Medicine Lab, Department of Clinical Medicine, Aarhus University, Aarhus, Denmark.

2: Department of Experimental Clinical Oncology, Aarhus University Hospital, Aarhus, Denmark.

3: Molecular Bone Histology Team, Department of Forensic Medicine, Aarhus University Hospital, Aarhus, Denmark.

4: Danish Center for Particle Therapy, Department of Clinical Medicine, Aarhus University Hospital, Aarhus, Denmark.

5: Department of Nuclear Medicine & PET Centre, Aarhus University Hospital, Aarhus, Denmark.

6: Department of Biomedicine, Aarhus University, Aarhus, Denmark.

7: Institute for Anatomy & Embryology, Center of Anatomy, University of Göttingen, Göttingen, Germany

## Introduction

Preclinical alternatives to murine models are attractive due to the high cost, logistical challenges and ethical issues of using mice. The chorioallantoic membrane (CAM) model of birds has long been an underutilized alternative model in various oncological areas. We demonstrate new applications of the CAM model by using advanced dual tracer autoradiography for the first time. Furthermore, our work improves upon the workflow in the use of already established methods such as optical coherence tomography (OCT), MRI, proton irradiation and PET scans. We are poised to make significant contributions to preclinical

radiation research using this effective alternative model, combining proton irradiation, nuclear medicine techniques and *in vivo* optical imaging.

## Materials and Methods

Dekalb White chicken eggs were opened with a handheld multitool creating a window in the shell on embryonic development day (EDD) 3. Tumor grafts from a murine host were transplanted to the model on EDD 8. Grafts grew until EDD 17-18 when the model was sacrificed to avoid hatching. Techniques used include 1) dynamic PET scans using the glucose analogue [18F]-fluorodeoxyglucose (FDG) or the hypoxia-selective tracer [18F]-Fluoroacomycin Arabinoside (FAZA), 2) dual-tracer autoradiography combining FDG with $^{14}$C-acetate or FAZA with the FDG analogue $^{14}$C-2DG, 3) proton irradiation, 4) MRI scans and 5) OCT angiography.

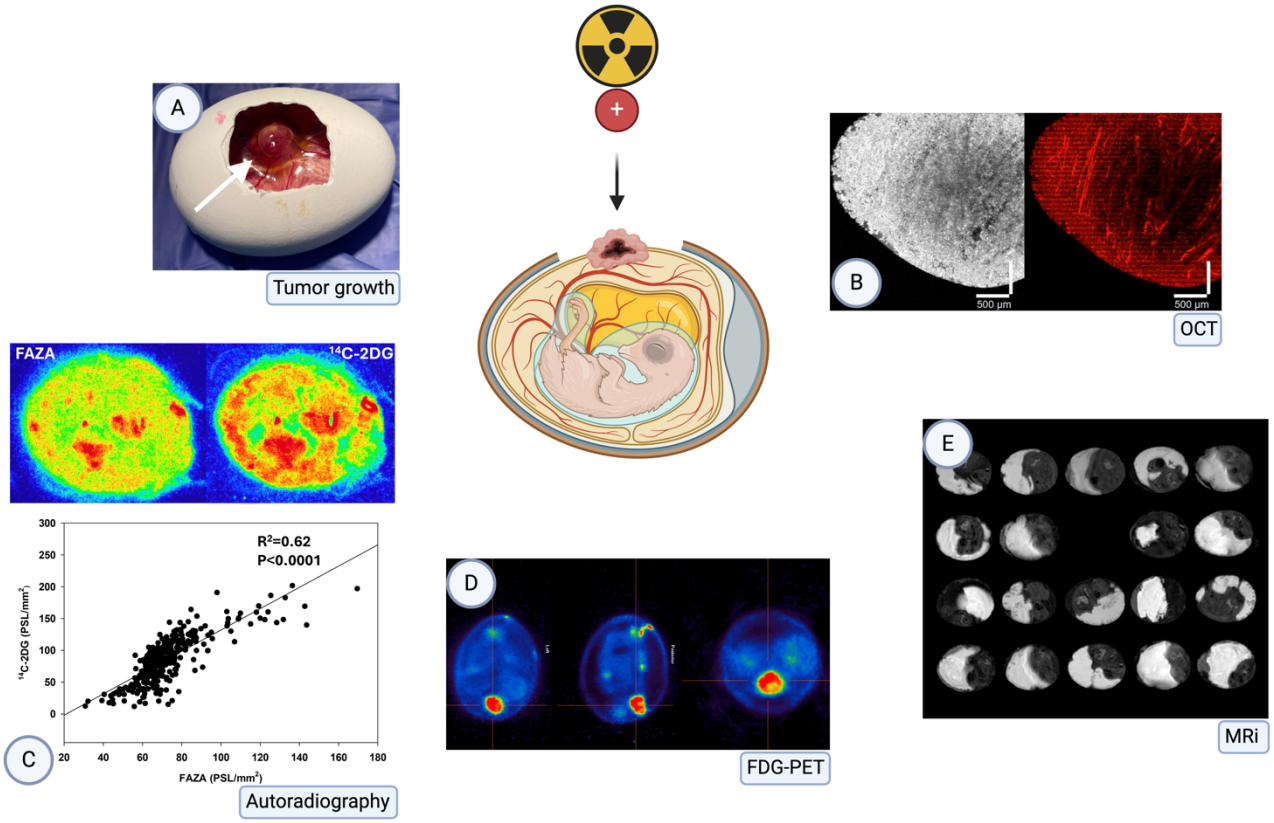


**Figure 1. Our capabilities with a CAM model proton irradiation platform.**
**A)** White arrow: C3H tumor in the CAM; **B)** Side-by-side of structural OCT (left) and OCT angiography (right); **C)** Dual-tracer autoradiography results of a single tumor slice from a C3H tumor harvested 3h after dual administration of FAZA and $^{14}$C-2DG administration. Comparing distributions reveals a considerable spatial overlap of the two tracers with an $R^2$-value of 0.62; **D)** FDG-PET of FDG uptake in a C3H-CAM model 3h post-injection; **E)** MRI of CAM models.

**Results**

We observed robust tumor growth with a mean weight for 68 C3H tumors of 0.32 g 95% CI [0.28–0.37 g] and 0.19 g [0.09–0.38 g] for 4 MOC2 tumors. Importantly, tumors established directly from solid tumors derived from mice were considerably larger than in literature studies using cell lines as seeding material, making these ideal for imaging studies with low resolution (e.g., PET). Via PET and autoradiography, we demonstrated that a yolk sac injection of tracers is distributed to the fetal circulation, replacing the technically challenging intravenous administration. With autoradiography experiments of 53 CAM-tumors we have investigated the intra-tumoral distribution of FDG, FAZA, $^{14}$C-acetate and $^{14}$C-2DG, as well as the hypoxia marker pimonidazole.

**Conclusions**

Our findings demonstrate the CAM model as a feasible and simpler alternative for radiation experiments, potentially applicable with novel preclinical radiation modalities including spatially fractionated radiation therapy (SFRT), FLASH radiotherapy, and hyperthermia experiments. In conjunction with autoradiography, PET and OCT as a non-invasive *in vivo* technique to evaluate vessel morphology, we present a simple, robust platform for advanced oncological research.

**Mutational profile of oropharyngeal cancer in relation to HPV, tobacco smoking and prognosis with validation in the DAHANCA 19 randomized trial.**

**Author information**
Jacob Kinggaard Lilja-Fischer. Department of Experimental Clinical Oncology, Aarhus University Hospital, Denmark. jaclil@rm.dk

**Authors and affiliations**
Jacob Kinggaard Lilja-Fischer (1,2), Morten Horsholt Kristensen (1), Pernille Lassen (1,5), Torben Steiniche (3,4), Trine Tramm (3,4), Magnus Stougaard (5), Anders Frederiksen (1), Benedicte Ulhøi (4), Jan Alsner (1), Kasper Toustrup (1,6), Christian Maare (7), Jørgen Johansen (8), Hanne Primdahl (6), Claus Andrup Kristensen (9), Maria Andersen (10), Jesper Grau Eriksen (1,6), Jens Overgaard (1,6).

1) Department of Experimental Clinical Oncology, Aarhus University Hospital, Denmark.
2) Department of Otolaryngology – Head & Neck surgery, Aarhus University Hospital, Denmark.
3) Department of Clinical Medicine, Aarhus University, Denmark.
4) Department of Pathology, Aarhus University Hospital, Denmark.
5) Department of Clinical Genetics, Aarhus University Hospital, Denmark.
6) Department of Oncology, Aarhus University Hospital, Denmark.
7) Department of Oncology, Herlev Hospital, Denmark.
8) Department of Oncology, Odense University Hospital, Denmark.
9) Department of Oncology, Copenhagen University Hospital - Rigshospitalet, Denmark.
10) Department of Oncology, Aalborg University Hospital, Denmark.

**Introduction**
This study aimed to identify prognostic biomarkers in oropharyngeal squamous cell carcinoma (OPSCC). Additionally, we investigated potential molecular markers of tobacco exposure, as smoking has been hypothesized to induce specific genetic alterations and contribute to the poorer prognosis observed in smokers.
First, we characterized the molecular profiles of OPSCC patients, focusing on HPV-induced tumors and their correlation with smoking history. Subsequently, we sought to independently validate our findings and assess the prognostic significance of molecular alterations in patients treated with curative (chemo-)radiotherapy in a randomized controlled trial (RCT).

**Materials and methods**
The exploration cohort included 56 patients with previously untreated OPSCC. We analyzed HPV status and the expression of genes related to hypoxia, tumor subtype, and radiosensitivity, alongside next-generation sequencing (NGS) of a broad panel of cancer-related genes. Based on these findings, we designed a custom NGS panel, to validate our findings and explore effect on prognosis in 162 OPSCC patients from the DAHANCA 19 RCT.

**Results**
In the exploration cohort of 56 patients (40 HPV+, 79%), the most frequent molecular alterations in HPV+ tumors were mutations or alterations in the *PIK3CA* and *ATR* genes, along with amplification of chromosome 3q. Mutations in *ATR* and *CREBBP* were more frequent in patients with more than 10 pack-years. However, these findings could not be reproduced in the DAHANCA 19 cohort. No distinct mutational signature of tobacco exposure was identified, and no association with *TP53* mutations was observed.
In the DAHANCA 19 cohort there were 17 locoregional failures (LRF) in 128 patients with p16+ tumors, corresponding to a cumulative incidence at five years of 11% (95% CI: 6 - 16%). Overall survival at five years was 88% (95% CI: 81-93).
No common defining features were identified among these patients, although mutations in *NFE2L2* and *CASP8* as well as amplifications in genes located at 3q (*BCL6*, *SOX2*) were associated with LRF.

**Conclusions**
In HPV+ OPSCC, no mutations or molecular alterations that were prognostic in a high-quality cohort, and very few seem to be molecular drivers, or suitable as prognostic biomarkers. We identified no molecular features of tobacco exposure, contrary to previously proposed mechanisms.
On this basis, we propose to refute the hypothesis of molecular alterations driving the worse prognosis in smokers with HPV+ OPSCC.

# DUAL-TRACER AUTORADIGRAPHY IN ORTHOTOPIC TUMOR MODELS: TOWARDS PERSONALIZED PET-GUIDED THERAPY

MORTEN BUSK[1, 2], MARTIN K THOMSEN[3], JENS OVERGAARD[1], MARTIN F BERTHELSEN[4], HENRIK HAGER[5], JOHAN BUSSINK[6], KIM V HANSEN[7], EBBE BØDTKJER[3], MIKKEL H VENDELBO[3,7]

*[1]Department of Experimental Clinical Oncology, Aarhus University Hospital (AUH), Denmark; [2]Danish Centre for Particle Therapy, AUH; [3]Department of Biomedicine, Aarhus University (AU), Aarhus, Denmark; [4]Department of Clinical Medicine, AU; [5]Department of Pathology, AUH; [6]Department of Radiation Oncology, Radboud University, Nijmegen Medical Centre, Nijmegen, The Netherlands; [7]Department of Nuclear Medicine and PET Centre, AUH.*

**Background.** Tumor hypoxia is a driver of treatment resistance and metastatic potential. Pre-treatment characterization of tumor hypoxia may guide treatment decision-making, including choice of modality and intensity. Hypoxia-selective PET tracers, like FAZA, allows imaging-based assessment of tumor hypoxia, but since hypoxia stimulates glucose use (anaerobic glycolysis), FDG- and hypoxia-PET may provide similar information. Clinical dual-tracer PET studies have been inconclusive, even in comparable patient groups, possibly due to the complexity of such trials where decisive conclusions essentially rely on accurate co-registrations and the unfounded assumption that metabolism and microenvironment are unaltered between time-separated scans. Ultimately, such limitations may weaken or fully eliminate a true spatial association between elevated FDG uptake and poor oxygenation. Accordingly, we developed high-resolution dual-tracer autoradiography techniques ($^{14}$C-2DG+FAZA), to allow detailed assessment of intratumoral tracer heterogeneity and their spatial coupling, without time-separation and co-registration related inaccuracies. Since traditional subcutaneous tumors may not faithfully recapitulate human disease, including the carcinogenic process, microenvironment, necrosis and inherent energy metabolism, we focused on orthotopic tumor models

**Methods.** Lung adenocarcinomas were induced in CRISPR/*Cas9* knock-in mice by inhalation of an adeno-associated virus-vector to generate loss of function mutations in p53, KRAS and LKB1. Mammary adenocarcinomas were established in transgenic mice that overexpress ErbB2 specifically in breast epithelium. Tumor growth was monitored by MRI (lung) or caliper (mammary) examination. When ready for experiments, mice were administered the hypoxia marker pimonidazole (60 mg/kg), FAZA (~40 MBq) and $^{14}$C-2DG (37 kBq) and sacrificed. Breast tumors or lungs, with embedded tumors, were cryosectioned and analyzed for $^{18}$F and $^{14}$C using dual-tracer autoradiography, and pimonidazole adduct formation, supplemented with HE staining (lung) for accurate tumor delineation of small lesions embedded in healthy lung tissue. Reference tissue sections used for normalization of $^{14}$C-2DG (mid-sagittal brain section) and FAZA (thigh muscle) were included.

**Results/discussion.** Tumors suitable for experiments developed over a course of several months. Typically, mice presented with several lesions of variable sizes. FAZA and pimonidazole displayed near-identical distribution. Autoradiographic analysis

revealed FAZA-positive sub-volumes in most larger tumors, with a more intense uptake in the breast tumor model. A clear spatial overlap of FAZA and $^{14}$C-2DG were observed in many tumors of both models, but in some breast tumors, especially those without large intense foci of FAZA retention, the linkage was weak/absent. Further analysis is ongoing. Some examples of dual-tracer autoradiography and spatial correlation analysis are shown in the figure below.

**DUAL-TRACER AUTORADIOGRAPHY OF FAZA AND $^{14}$C-2DG REVEALS A PARTLY, BUT VARIABLE, HYPOXIA-DRIVEN GLUCOSE RETENTION PATTERN IN ORTHOTOPIC TUMORS**

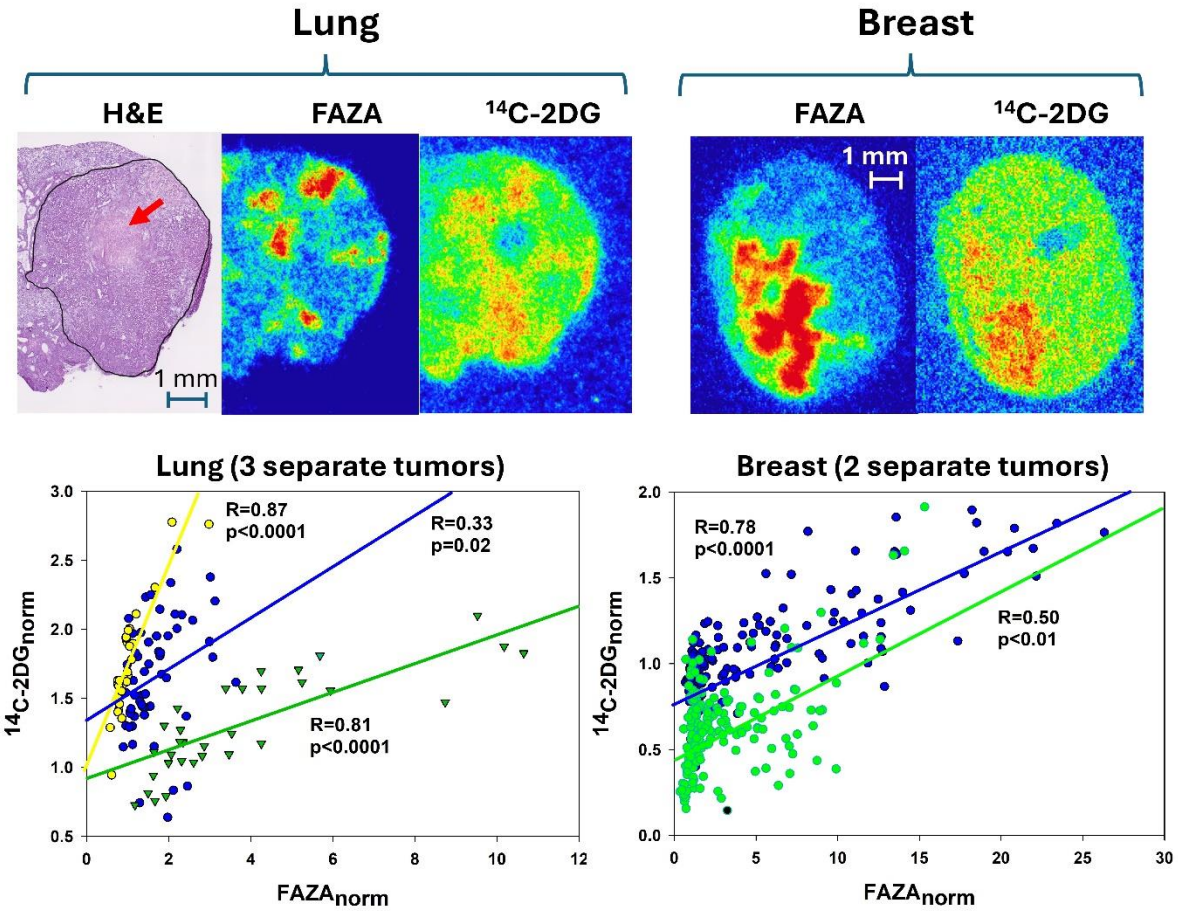


The drawn ROI in the H&E stained section depicts the lung tumor periphery, and the red arrow shows a necrotic area. Tumor autoradiograms were normalized to reference tissue uptake and covered by a grid (0.5 mm x 0.5 mm) and compared pixel-by-pixel. Blue points/regression lines are the analyses based on the portrayed tumors.

**Vision transformers may enable early detection of radiation-induced toxicity in submandibular glands from a murine model**

Manish Kakar[1], Inga Solgård Juvkam[1,3], Olga Zlygosteva[2], Nina Edin[2], Eirik Malinen[1,2]

[1] Department of Radiation Biology, Institute for Cancer Research, The Norwegian Radium Hospital, Oslo University Hospital, Oslo, Norway

[2] Department of Physics, University of Oslo, Oslo, Norway

[3] Institute for Oral Biology, Faculty of Dentistry, University of Oslo, Norway

**Introduction:** Radiotherapy of head and neck cancer can damage the salivary glands, leading to impaired saliva production. Stem cells, primarily located around the excretory ducts, can restore homeostasis, but this depends on the degree of stem-cell depletion. Therefore, it is highly desired to have an explainable AI-based approach that can, preferably early in the treatment course, provide information about damage to the glands in general and the stem cells in particular. Our aim was to test if attention-based vision transformer could detect changes in MR images of irradiated mouse salivary glands.

**Material and Methods:** C57BL/6J mice (n=29) were given 66 Gy of fractionated radiotherapy covering the oral cavity, swallowing muscles and salivary glands over five or ten days in one or two fractions per day, respectively. This treatment schedule is known to cause substantial early and late toxicity. Fifteen unirradiated control mice and 14 irradiated mice were included. We acquired T2-weighted MR images 3-5 days after irradiation, and a foundation model SAM was used to segment the submandibular glands. Vision transformers (ViT Base 16) were trained and used to classify the glands into control and irradiated groups. As the dataset was small, we employed a transfer learning strategy.

**Results**: Using the raw MRI data, the ViT base model achieved an average accuracy of about 72% in classifying images of control and irradiated glands. The 11 attention heads, each highlighting different aspects of the images in the ViT model, were systematically compared between control and irradiated animals. One of these attention heads, averaged over all glands in each group, was significantly higher for the irradiated mice (figure 1). No other differences were found between irradiated and control mice,

**Conclusion:** Vision transformers may be used to detect radiation-induced changes in MR images of a murine model. This preclinical strategy shows promise, but extending it with explainability techniques and clinical validation are required before it can be used in routine clinical practice.

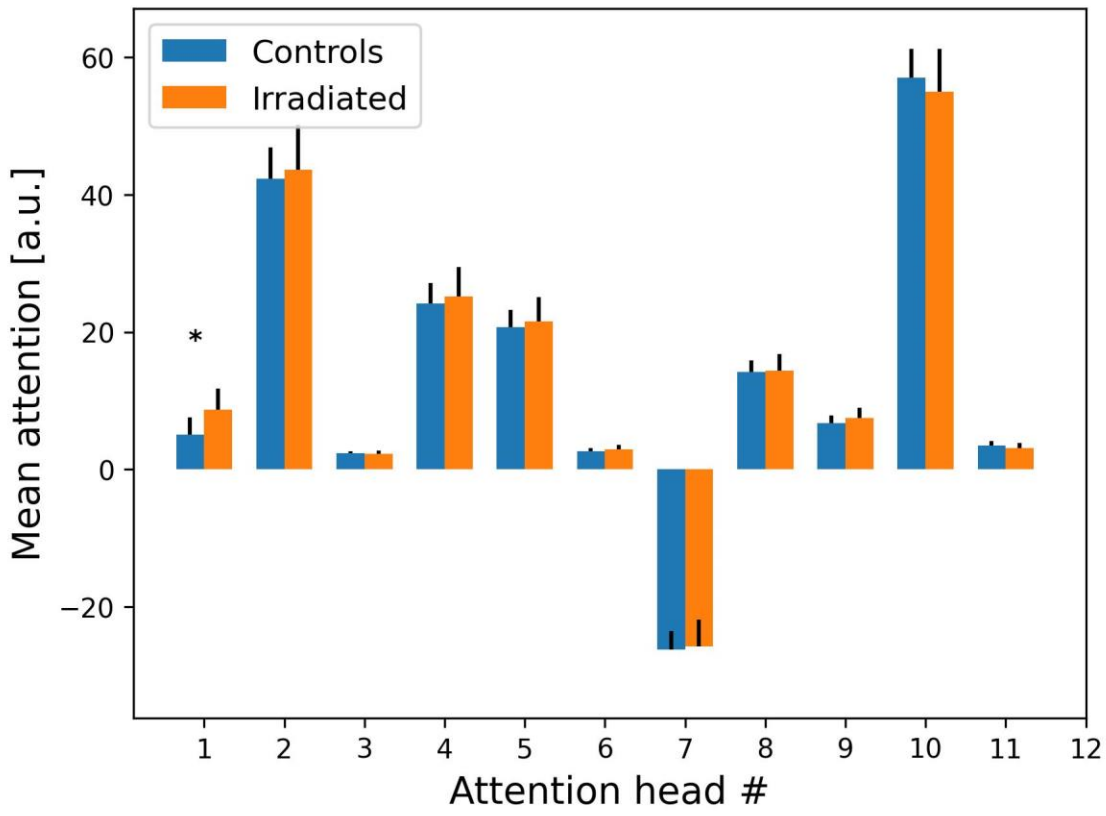


Figure 1: Mean attention scores in each treatment group for each of the 11 attention heads. (*p<0.05).

# Detecting Early Toxicity in a Murine Head and Neck Model Using Explainable CNNs

Bao Ngoc Huynh[1], Manish Kakar[2], Olga Zlygosteva[3], Inga Solgård Juvkam[2,4], Nina Edin[3], Oliver Tomic[5], Cecilia Marie Futsaether[5], Eirik Malinen[2,3]

[1] Department of Medical Physics, Oslo University Hospital, Oslo, Norway

[2] Department of Radiation Biology, Institute for Cancer Research, The Norwegian Radium Hospital, Oslo University Hospital, Oslo, Norway

[3] Department of Physics, University of Oslo, Oslo, Norway

[4] Institute for Oral Biology, Faculty of Dentistry, University of Oslo, Norway

[5] Faculty of Science and Technology, Norwegian University of Life Sciences, Ås, Norway

## Introduction

Head and neck cancer patients who undergo radiotherapy (RT) may experience serious side effects. Therefore, early identification of patients at risk for radiation toxicity is essential for developing personalized treatment and follow-up plans. This study investigates the potential of using convolutional neural networks (CNNs) for early toxicity risk identification by (1) developing a CNN model capable of detecting differences in Magnetic Resonance (MR) images of irradiated and non-irradiated mice and (2) analyzing model explainability heatmaps highlighting areas in the MR images that contribute to model decisions.

## Materials and Methods

Twenty-nine C57BL/6J mice were included. Mice in the irradiated group (n=14) received 66 Gy of fractionated RT under anesthesia targeting the oral cavity, swallowing muscles, and salivary glands, while control mice (n=15) were treated identically but not irradiated. T2-weighted (T2w) MR images were obtained from all mice 3-5 days after irradiation. CNN models based on different architectures (VGG, MobileNet, ResNet, EfficientNet) were developed for classifying sagittal slices of the MR images into control (class 0, 304 slices) or irradiated (class 1, 282 slices) groups. Nested 5-fold cross-validation was used to fine-tune and train these CNNs, ensuring that each fold was used as a training, validation, or test set at least once. Note that all MR image slices of the same mouse were always included in the same fold. The metrics accuracy, Matthew's correlation coefficient, the area under the curve (AUC), and F1 score on both classes were used for model evaluation. The explainability method VarGrad was used to identify regions in the MR images that contributed to the predictions made by the highest-performing CNN model.

## Results

The EfficientNet B3 CNN model achieved the highest performance, with an average accuracy of 83% across all slices. Based on the average predicted class probability calculated across all MR image slices of the same mouse, this CNN model correctly classified 28 out of 29 mice, with one control mouse incorrectly classified into the irradiated group. Explainability heatmaps from the EfficientNet model (Figure 1A) showed that the irradiated areas containing the mouth and throat contributed more to the model's prediction than areas covering the brain and nape (Figure 1B & C).

## Conclusions

The high classification accuracy of the CNN model as well as the regions highlighted by the explainability approach suggest that CNNs, together with MRI, can potentially identify individuals at risk of developing early toxicity.

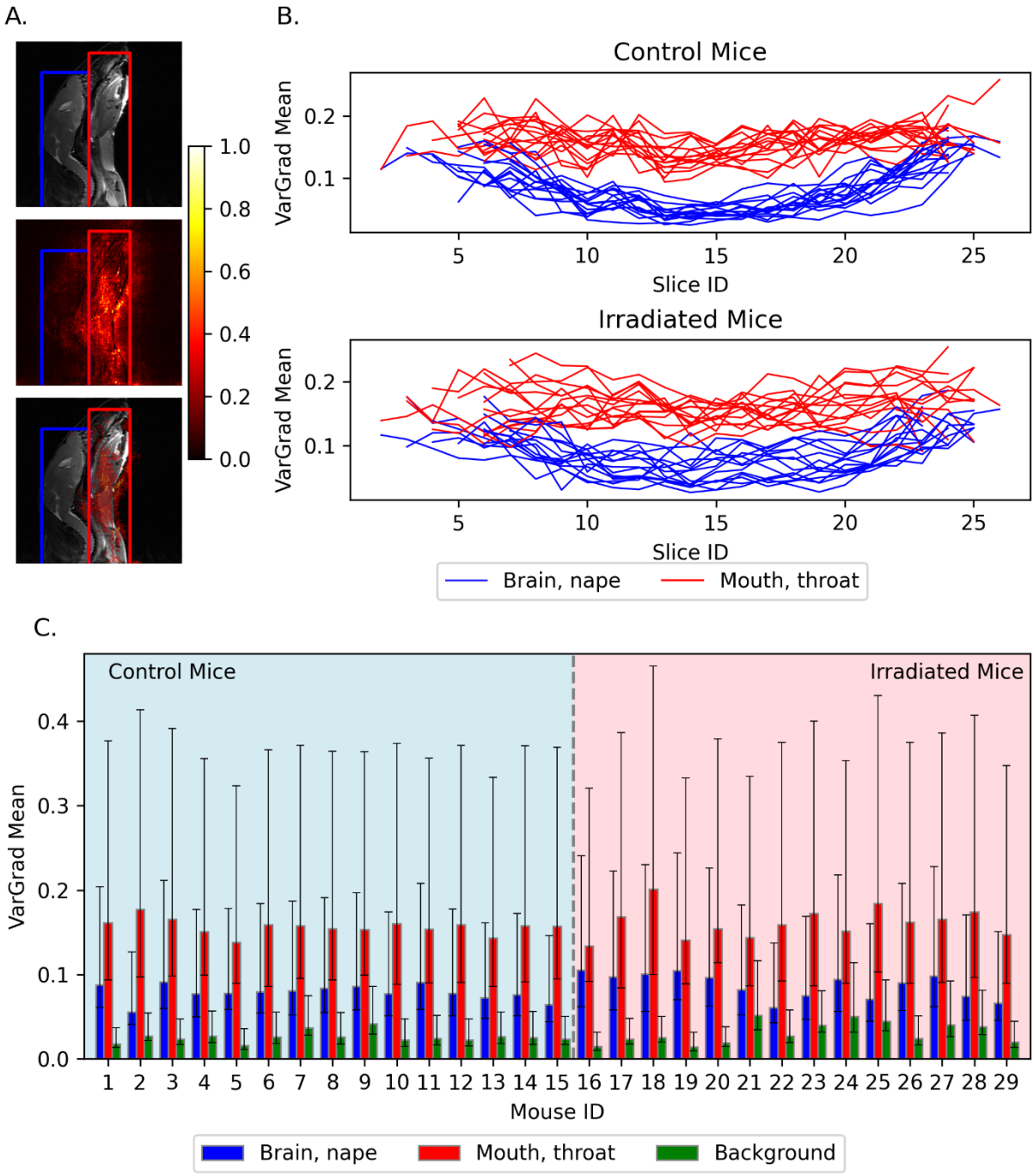


Figure 1: (A) Example of a T2w image slice (top row) of an irradiated mouse. The corresponding explainability heatmap based on the normalized VarGrad values is shown, both standalone (middle) and overlaid on the corresponding T2w image slice (bottom). Pixels with higher VarGrad values indicate higher contributions to the model's prediction. Two regions of interest (ROIs) are marked: non-irradiated areas (brain and nape) in blue and irradiated areas (mouth and throat) in red. (B) Each line shows changes in the mean VarGrad value within the brain & nape ROIs (blue) and mouth & throat ROIs (red) across all image slices for each mouse in the control group (top row) and irradiated group (bottom row). (C) Mean VarGrad of each mouse in the corresponding regions: brain & nape (blue), mouth & throat (red), and the background (green). The error bars indicate the 25th and 75th percentile.

**Squamous cell carcinoma in the oral cavity – need for risk stratification of the neck?**

Josef Ali Khalid, (josefali2000@hotmail.com) Experimental Clinical Oncology, Aarhus University Hospital, Aarhus, Denmark

Thomas Kjærgaard, Dept of Otorhinolaryngology, Head and Neck Surgery, Aarhus University Hospital, Aarhus,

Denmark

Jesper Grau Eriksen, Experimental Clinical Oncology, Dept. of Oncology, Aarhus University Hospital, Aarhus, Denmark

**Introduction:**

In squamous cell carcinomas of the oral cavity, it is well known that the lymph node metastases primarily occur in levels I, II and III. Traditionally, these lymph node levels are treated irrespective of the location of the tumor in the oral cavity, only taking laterality into consideration. The aim of the present study is to analyze the influence of the size, lateralization and site of the tumor in the oral cavity on pattern of lymphatic spread.

**Material and methods:**

From 2019 to 2023, 351 consecutive patients at Aarhus University Hospital, Denmark with oral cavity cancer were included in the study. Patient, tumor and treatment characteristics were collected from the local DAHANCA database and enriched with tumor characteristics from the pathology rapports. Tumor location and measure, preferably in three dimensions, were estimated by using available CT, MR and PET-CT imaging. Data was analysed using descriptive statistics.

**Results:**

For the lateralized tumors, lymph node involvement was almost exclusively ipsilateral (98%). In particular, the lateralized tumors located on the 2/3 anterior part of the tongue only spread to ipsilateral lymph nodes (100%). Ipsilateral metastases were most frequently seen in tumors located in the lower gingiva (42%) as well as the retromolar trigone (46%), predominantly involving levels I, II and III, whereas tumors located in the floor of mouth and centralized tumors of the 2/3 anterior part of the tongue had frequent involvement of both unilateral (48%) and bilateral (14%) lymph nodes, also including distal levels IV and V.

Furthermore, an advanced T-category showed a significantly higher lymph node involvement compared to an early T-category ($p \leq 0.001$) and higher tumor volume showed a significantly higher lymph node involvement compared to a lower tumor volume ($p \leq 0.001$).

**Conclusion:**

Treatment of the neck with either primary surgery, primary radiotherapy or both can probably be further stratified according to upfront risk parameters like tumor location, lateralization, T-category and tumor volume. This has to be further explored by a pattern of recurrence analysis and validated in an external cohort.

Figure 1: Distribution of lymph node metastases according to tumour localisation

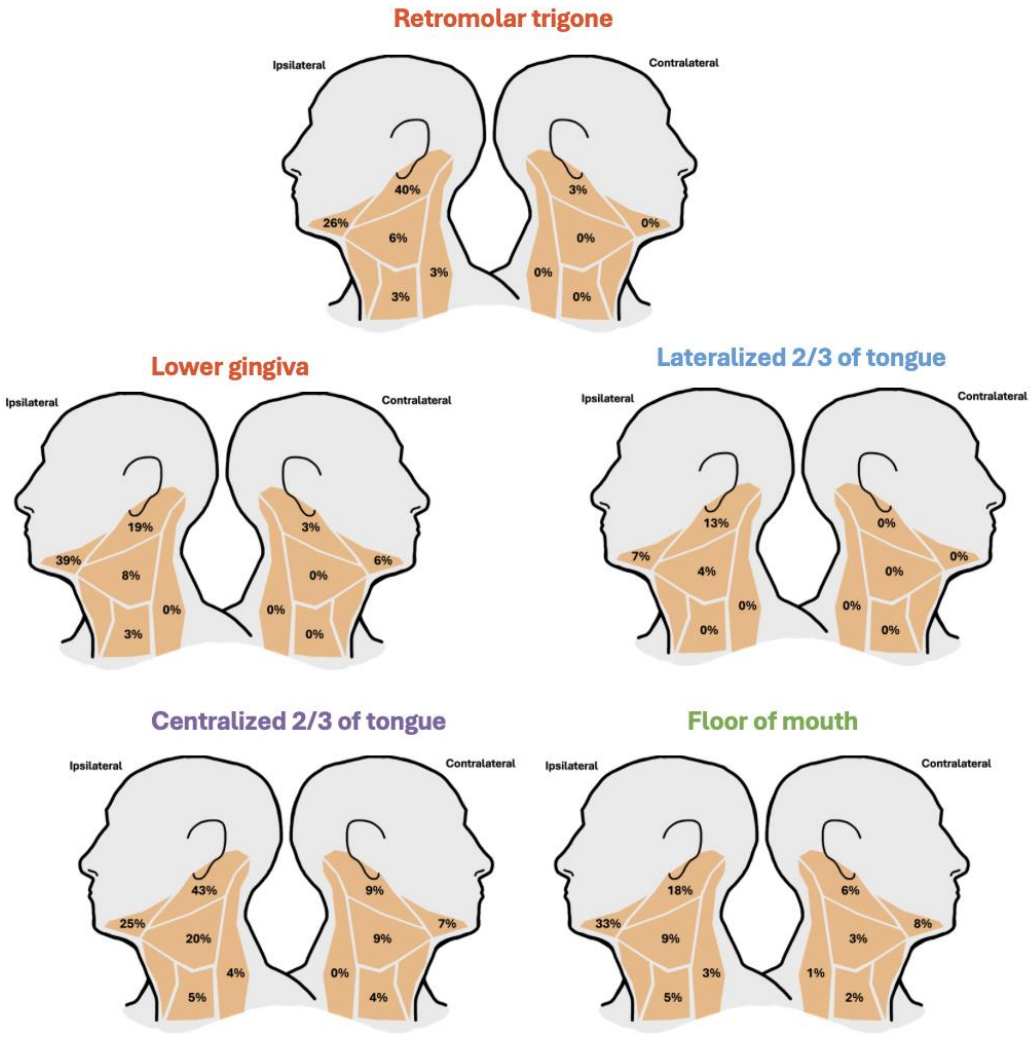

**Trends in feeding tube insertion and weight loss over time in patients with Head and Neck Cancer undergoing curative (chemo)radiotherapy**

Maiken M. Hjelt[1] email: mamojs@rm.dk

M.M. Hjelt[1], H. Primdahl[2], A.I.S. Holm[2], J.G. Eriksen[1]
[1] Experimental Clinical Oncology, Dept of Oncology, Aarhus University Hospital, Denmark
[2] Dept of Oncology, Aarhus University Hospital, Denmark

**Background**
Malnutrition and weight loss are common concerns in patients with head and neck cancer (HNC) undergoing curative (chemo)radiotherapy. The use of enteral nutrition via feeding tubes is an essential strategy to maintain nutritional status. The aim was to investigate trends in feeding tube dependency and weight loss among patients with HNC treated with curative (chemo)radiotherapy from 2014 to 2023.

**Methods**
This retrospective study included 1618 patients diagnosed with HNC and treated with curative (chemo)radiotherapy at Aarhus University Hospital between 2014 and 2023. Data were extracted from the local DAHANCA database. The prevalence of feeding tube use at the end of treatment was analyzed across diagnosis groups, and trends in weight loss were assessed using median weight difference between pre-radiotherapy weight and weight at radiotherapy completion, with 95% confidence intervals (CI). Diagnosis groups were categorized as oropharynx, other pharynx, larynx, and other (which includes sino-nasal, salivary gland, and CUP cases). All analyses were done in SPSS.

**Results**
From 2014 to 2023, 45% (721 patients) completed treatment with a feeding tube (95% CI: 42%–47%). Despite an increase in median weight loss over time, the proportion of patients receiving a feeding tube at treatment completion declined throughout the study period (see figure 1).

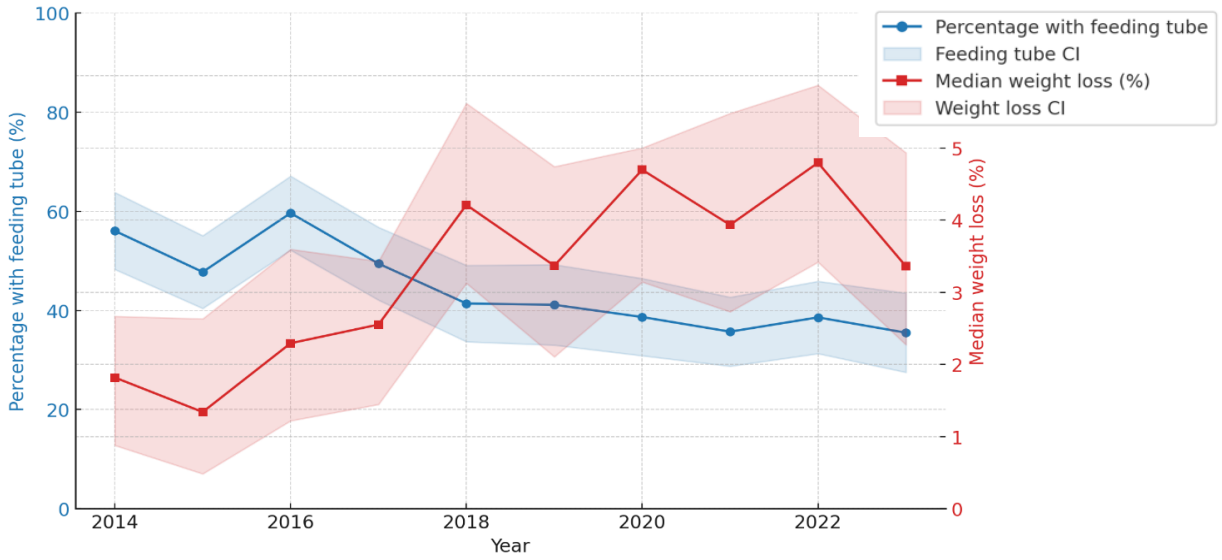


Figure 1: Percentage with feeding tube at treatment completion and median percentage weight loss over time (2014-2023)

Feeding tube insertion varied across diagnosis groups, with the highest prevalence in oropharyngeal cancer patients with 52% (95% CI 48-55%). The lowest prevalence of 7% (95% CI 5-9%) was observed in the 'other' category. Despite these between-group differences, the overall trend showed a decreasing feeding tube prevalence across all diagnosis groups.

The median weight loss from start to end of treatment was 3.3% of body weight (95% CI: 3.0–3.5%), corresponding to 2.8 kg (95% CI: 2.6–3.1 kg). Over time, median weight loss increased from 1.8% (95% CI: 0.9-2.8) in 2014 to 3.7% (95% CI: 2.6-4.8%) in 2023, with the highest recorded median weight loss in 2022 (5.1%, 95% CI: 4.2-6%).

**Conclusion**
This study found an inverse correlation over time between the declining use of feeding tubes and increasing weight loss trends, raises concerns about potential undernutrition and its clinical consequences. These preliminary findings highlight the need for further investigations regarding the trends in weight development and feeding tube insertion throughout the treatment trajectory.

# Oral Hygiene Habits and Fluoride Levels after Head and Neck Radiotherapy: An Exploatory Clinical Study

Sara Volf Jensen, Sara.volf@dent.au.dk

S. Volf Jensen[1], L.M.A. Tenuta[2], T. B. Bondesen[3], S. E. Nørholt[1,3], J.G. Eriksen[4,5], L. Staun Larsen[1]

**[1] Department of Dentistry and Oral Health, Aarhus University, Aarhus, Denmark.**

**[2] Department of Cariology, Restorative Sciences & Endodontics, School of Dentistry, University of Michigan, Michigan, USA.**

**[3] Department of Oral and Maxillofacial Surgery, Aarhus University Hospital, Aarhus, Denmark.**

**[4] Department of Experimental Clinical Oncology, Aarhus University, Aarhus, Denmark.**

**[5] Department of Oncology, Aarhus University Hospital, Aarhus, Denmark.**

**Introduction**: Reduced salivary flow is a frequent side effect after curative-intended head and neck cancer radiotherapy. These individuals are at high risk of developing rampant dental caries. Yet, we know little about their oral fluoride levels and oral hygiene habits.

The aim of this study is to contribute to future best-practice recommendations for the oral hygiene regimen in patients following radiotherapy. This study aims specifically to explore important physiological oral parameters and oral hygiene habits in head and neck cancer patients at Aarhus University Hospital.

**Materials and methods**: The study is a descriptive exploratory clinical study collecting data from individuals following curative-intended head and neck radiotherapy. Individuals are enrolled at their 6-months follow-up, sialometries are conducted and dental biofilm is sampled. All samples are analysed for fluoride using a modified fluoride ion-selective electrode. Further, an oral examination and a questionnaire-based interview regarding oral hygiene habits are conducted and the Groningen Radiotherapy-Induced Xerostomia questionnaire (GRIX) completed.

**Results**: Thus far, 40 participants have been recruited, of which 21 have been examined. The diagnoses included larynx, salivary gland, oropharyngeal and thyroid cancer. All patients were treated with 66-68Gy, 33-34 fx, 6fx/w; receiving <19G-68Gy as peak doses to the oral cavity.

The unstimulated salivary flow was 0-0.41 ml/min, with 16/21 subjects within the definition of hyposalivation (<0.16 ml/min). The stimulated salivary flow was 0.04-2.82 ml/min with 8 subjects having hyposalivation (<0.7 ml/min). The fluoride results yielded great variation; fluoride concentrations in saliva, biofilm fluid and biofilm solids were <0.02-3.92, 0.08-3.18 and 3-2,620 ppm F, respectively. The individuals had 4-29 teeth present and active caries in 0-62 surfaces. 17/21 had inadequate oral hygiene and 4/21 used prescribed high-dosage fluoride toothpaste (5,000 ppm). Most patients had not visited the dentist since before they started treatment.

8/16 individuals with unstimulated hyposalivation reported moderate-to-severe xerostomia-during-daytime complaints (scores above 50 in the GRIX questionnaire). 3/8 of these individuals had a stimulated saliva flow rate within normal range.

**Conclusion**: Many participants had hyposalivation, suffered from xerostomia and had trouble maintaining a sufficient oral hygiene level. In general, absence of dental visits after the beginning of treatment were reported. The oral fluoride levels showed great variation and only 4/21 individuals used high-dosage fluoride toothpaste. The results suggest a great need for optimizing the oral health following radiotherapy, and establishing future best-practice recommendations for the oral hygiene regimen could help individuals to maintain their teeth and uphold their quality of life.

**Acknowledgement:** Funded by The Danish Dental Association's Research Committee (FORSKU) and Research Fund.

**The effect of evolving clinical practice in head and neck radiotherapy**

Eva Onjukka[1,2], Jeehong Lee[3], Emmy Dalqvist[1,2], Erik Lampa[4], Ingmar Lax[5], Claes Mercke[2,5], Signe Friesland[2,5], Anna Embring[2,6]

[1]Department of Nuclear Medicine and Medical Physics, Karolinska University Hospital, Stockholm, Sweden
[2]Department of Oncology Pathology, Karolinska Institutet, Stockholm, Sweden
[3]Department of Physics, Stockholm University, Stockholm, Sweden
[4]Epistat AB, Uppsala, Sweden
[5]Department of Head, Neck, Lung and Skin, Karolinska University Hospital, Stockholm, Sweden
[6]Department of Radiotherapy, Karolinska University Hospital, Stockholm, Sweden

**Purpose/Objective**

Technology is central to the development of radiotherapy. When evaluating the clinical benefit of incremental improvements, randomised controlled trials are not the obvious method of choice [1], while real-world data from quality registries can be expected to capture the impact of evolving clinical practice. We used a local quality registry for radiotherapy of head and neck cancer (HNC) to evaluate how the risk of late side effects has changed over time, specifically after the introduction of knowledge-based auto-planning and after the implementation of international guidelines for CTV definition [2]. We analysed the recorded outcome and planned dose for ten organs-at-risk (OAR).

**Materials and Methods**

At follow-up, side effects of patients treated for HNC are recorded in a local quality registry. Late side effects are evaluated using the RTOG/EORTC radiation morbidity scoring scheme. Patients with oropharyngeal- and oral cavity cancers were considered for this study. This period was chosen to capture the introduction of knowledge-based planning around June 2019, and the implementation of the new CTV definition around May 2020. The mean dose (Dmean) and near maximum dose (D2%) were extracted for each OAR.

**Results**

In total, 503 patients were included in the analysis, distributed over: 1) January 2017 – May 2019, 2) June 2019 – April 2020 and 3) May 2020 – Dec 2022. Figure 1A shows the difference in Dmean comparing each of the time periods: 2-1 (introduction of auto-planning), 3-1 (the new CTV definition and auto-planning compared to before either change), and 3-2 (the implementation of the new CTV, exclusively).

The dose was significantly reduced in 2-1 and 3-1 for the ipsilateral parotid gland. The brainstem had a reduced D2%, but this may be a result of missing delineations in cases with low dose in period 1. While mean values did not change significantly for the oral cavity, a scatter plot of D2% revealed a benefit for some patients from the new CTV definition.

No statistically significant effect on the risk of toxicity was observed in this analysis (Figure 1B).

**Conclusions**

The reductions in dose and the risk of side effects resulting from the studied changes in clinical practice were modest, indicating effective manual planning protocols pre auto-planning. On a population level, the new CTV definition did not offer a reduction in Dmean to major OAR. Ideally, changes to clinical practice should be introduced strategically with prospective follow-up.

## References

1. Lievens et al. Towards an evidence-informed value scale for surgical and radiation oncology: a multi-stakeholder perspective. Lancet Oncol. 2019;20(2):e112-e123

2. Grégoire et al. Delineation of the primary tumour Clinical Target Volumes (CTV-P) in laryngeal, hypopharyngeal, oropharyngeal and oral cavity squamous cell carcinoma: AIRO, CACA, DAHANCA, EORTC, GEORCC, GORTEC, HKNPCSG, HNCIG, IAG-KHT, LPRHHT, NCIC CTG, NCRI, NRG Oncology, PHNS, SBRT, SOMERA, SRO, SSHNO, TROG consensus guidelines. Radiother Oncol., 2018, 126:3–24

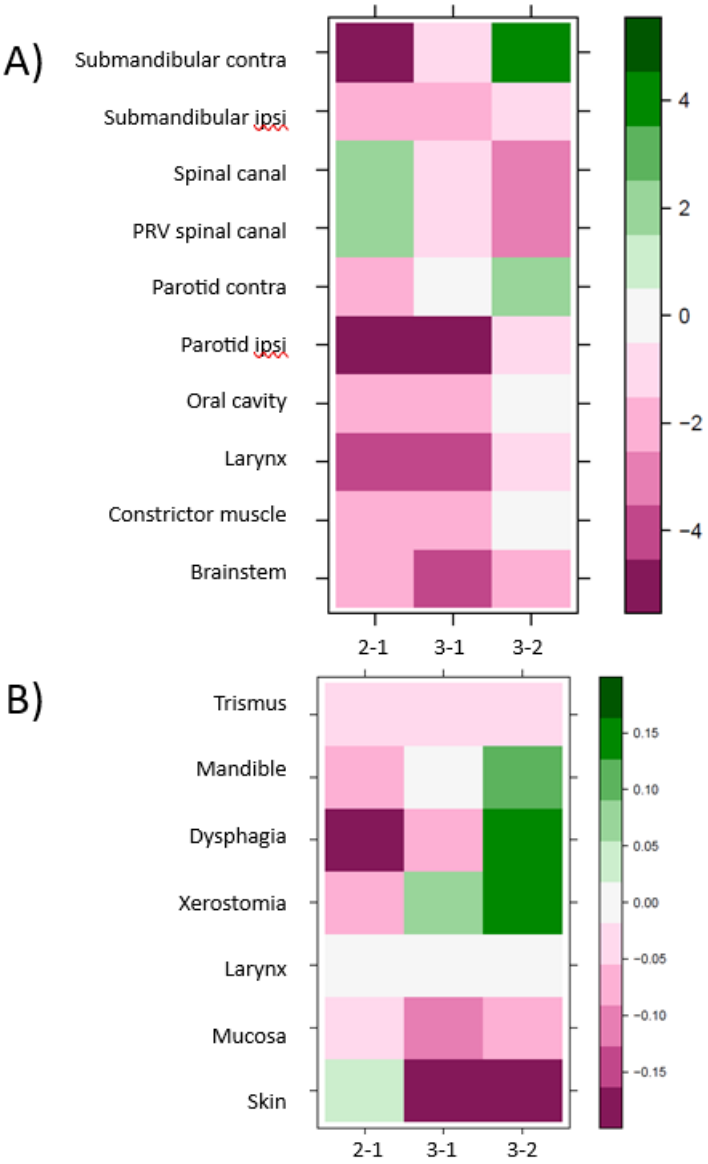


Figure 1. A) Change in Dmean (Gy) between compared time periods, and B) Change in grade of complication between compared time periods.

# Radiotherapy in children treated for neuroblastoma: comparative photon/proton treatment plans and side effects

Corresponding author: Anna Embring, anna.embring@ki.se

Anna Embring[1,2], Ingrid Kristensen[3,4], Martin P. Nilsson[3], Jacob Engellau[3], Malin Blomstrand[5,6], Charlotta Fröjd[5], Måns Agrup[7], Anna Flejmer[8], Anna-Maja Svärd[9], and Anna Asklid[1,2]

[1] Department of Oncology, Karolinska University Hospital, Stockholm, Sweden

[2] Department of Oncology-Pathology, Karolinska Institute, Stockholm, Sweden

[3] Department of Hematology, Oncology and Radiation Physics, Skåne University Hospital, Lund, Sweden

[4] Department of Oncology, Clinical Sciences, Lund University, Lund, Sweden

[5] Department of Oncology, Sahlgrenska University Hospital, Gothenburg, Sweden

[6] Department of Oncology, Institute of Clinical Sciences, University of Gothenburg, Sweden

[7] Department of Oncology, and Department of Biomedical and Clinical Sciences, Linköping University, Linköping, Sweden

[8] Department of Immunology, Genetics and Pathology, Uppsala University, Uppsala, Sweden

[9] Department of Radiation Sciences, Oncology, Umeå University, Sweden

## Introduction

Neuroblastoma is the most common type of extracranial solid tumour in children with about 20 new cases in Sweden each year. All radiotherapy centres in Sweden have access to proton radiotherapy and for patients considered for proton radiotherapy comparative photon/proton treatment plans are calculated. The aim of this study is to analyse doses to organs at risk in comparative photon/proton treatment plans for children treated for neuroblastoma and report side effects.

## Materials and methods

All children in Sweden treated with curative intent radiotherapy for neuroblastoma in the abdomen during 2017-2024 with comparative photon/proton treatment plans were included. Patients were identified through a national registry (RADTOX), where data on side effects were collected. Doses to relevant structures were extracted from clinical

treatment plans. Doses to organs at risk were compared in each individual patient's clinical photon/proton treatment plans and differences were tested through Wilcoxon signed-rank test. Integral dose was defined as the percentage of the scanned body that received ≥5 Gy (Body $V_{5Gy}$) and ≥10 Gy (Body $V_{10Gy}$).

## Results

Thirty children with a median age of 45 months (range 11-150) were included. Fifteen (50%) females and 15 (50%) males. The majority (90%) were treated with 21 Gy and the remainder (10%) with 36 Gy. The integral dose was significantly lower in the proton treatment plans compared to the photon treatment plans measured as both Body $V_{5Gy}$, $p$ = <0.001 and Body $V_{10Gy}$, $p$ = <0.001 (Figure 1). Mean doses to the kidneys, liver, pancreas and spleen were significantly lower in the proton treatment plans compared to the photon treatment plans (Figure 1).

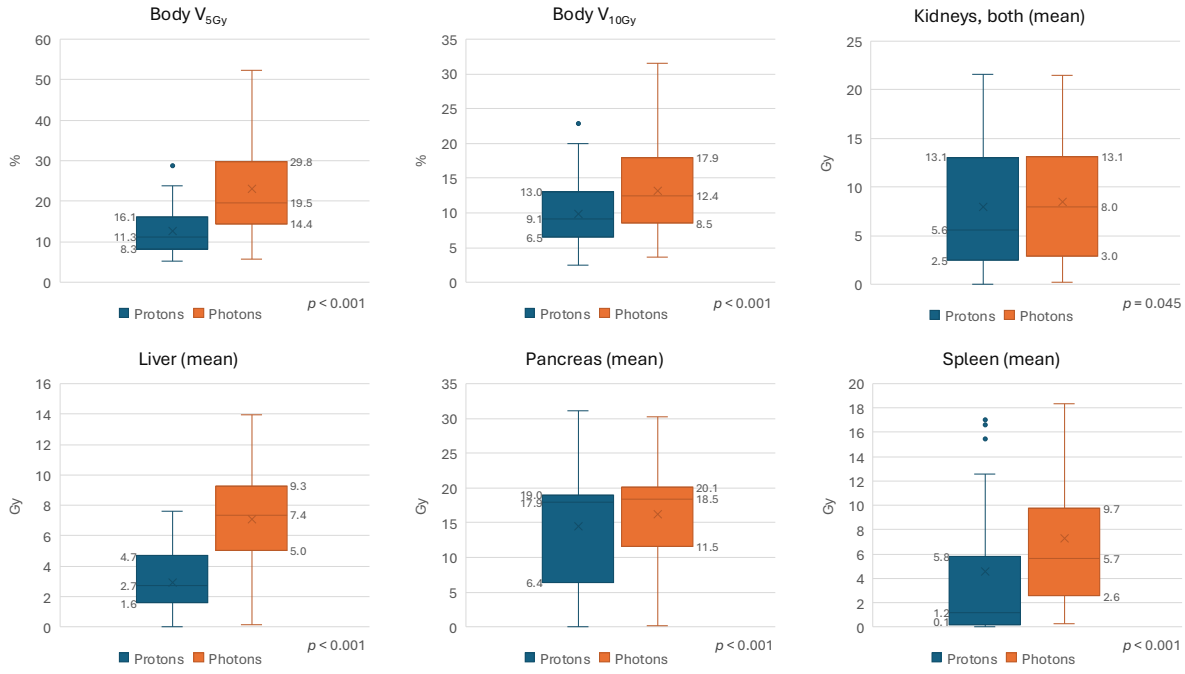


**Figure 1.** Integral dose and doses to organs at risk in comparative proton and photon treatment plans.

The median follow-up was 14 months (range 1-61 months), and the 2-year OS was 75.3%. Twelve patients (40%) experienced radiotherapy related grade ≥2 acute side effects and 7 patients (13%) experienced radiotherapy related grade ≥2 late side effects. The most common types of both acute and late side effects were upper gastrointestinal tract side effects and decrease in complete blood count. There was no significant correlation between side effects and treatment modality.

## Conclusions

In selected cases proton treatment can offer both lower doses to organs at risk and less low dose spread compared to photon treatment in children treated for neuroblastoma in the abdomen. The most common side effects were haematological and upper gastrointestinal tract side effects.

# How to account for temporal patterns of dysphagia scores in a real-world dataset

Eva Onjukka[1,2], Emmy Dalqvist[1,2], Erik Lampa[3], Anna Embring[2,4]

eva.onjukka@regionstockholm.se

[1]Department of Nuclear Medicine and Medical Physics, Karolinska University Hospital, Stockholm, Sweden

[2]Department of Oncology-Pathology, Karolinska Institutet, Stockholm, Sweden

[3]Epistat AB, Uppsala, Sweden

[4]Department of Radiotherapy, Karolinska University Hospital, Stockholm, Sweden

## Introduction

Normal-tissue complication probability (NTCP) models typically use endpoints defined at a single time-point. Quality registries and similar real-world data sources often contain multiple scores per patient, revealing the development of symptoms over time (however, at non-standardised intervals between scores). Endpoints reflecting the temporal pattern of symptoms would make NTCP models more clinically useful.

It has been shown that patients can experience different temporal patterns of dysphagia, suggesting that single time-point scores are not sufficient to indicate the severity of a patient's symptoms. In the current study, the aim is to evaluate several methods of representing temporal patterns of dysphagia scores, in a local quality-registry cohort.

## Matrials and Methods

Since 2014, side effects after radiotherapy are systematically recorded in a local quality registry for head and neck cancer at our institution. Late effects are recorded at the follow up visits at a frequency of 6 months, for the first two years, and thereafter yearly for the next three years. Grading is according to the RTOG/EORTC radiation morbidity scoring scheme.

The study cohort was extracted from our quality registry, including patients with at least three separate dysphagia scores, at more than five months after radiotherapy.

Three methods of categorization with regard to temporal patterns were tested: 1) a k-means algorithm for longitudinal data, 2) Gaussian processes and 3) Trajectory analyses. The evaluation focused on the clinical usefulness of identified categories, and the stability of the output.

## Results

The extracted cohort consisted of 735 patients, with 3-8 recorded scores (90% had ≤5 scores). The figure shows a heatmap of the 97 cases with at least one score of grade ≥2 dysphagia.

None of the tested methods produced stable categories for our cohort. The k-means method does not optimise the number of categories, and the output was very sensitive to the chosen number. The Gaussian processes indicated that a single category was optimal in our dataset. While more categories can be enforced, the resulting predicted temporal patterns were neither stable, nor clinically relevant due to their synthetic character. The trajectory analysis showed a more stable output. However, it failed to effectively identify the small groups of patients with high scores.

**Conclusions**

Statistical methods of categorising data based on the temporal patterns of side effects seem ineffective. On the other hand, investigators with clinical expertise can use visual representations, like heat maps, to detect general patterns.

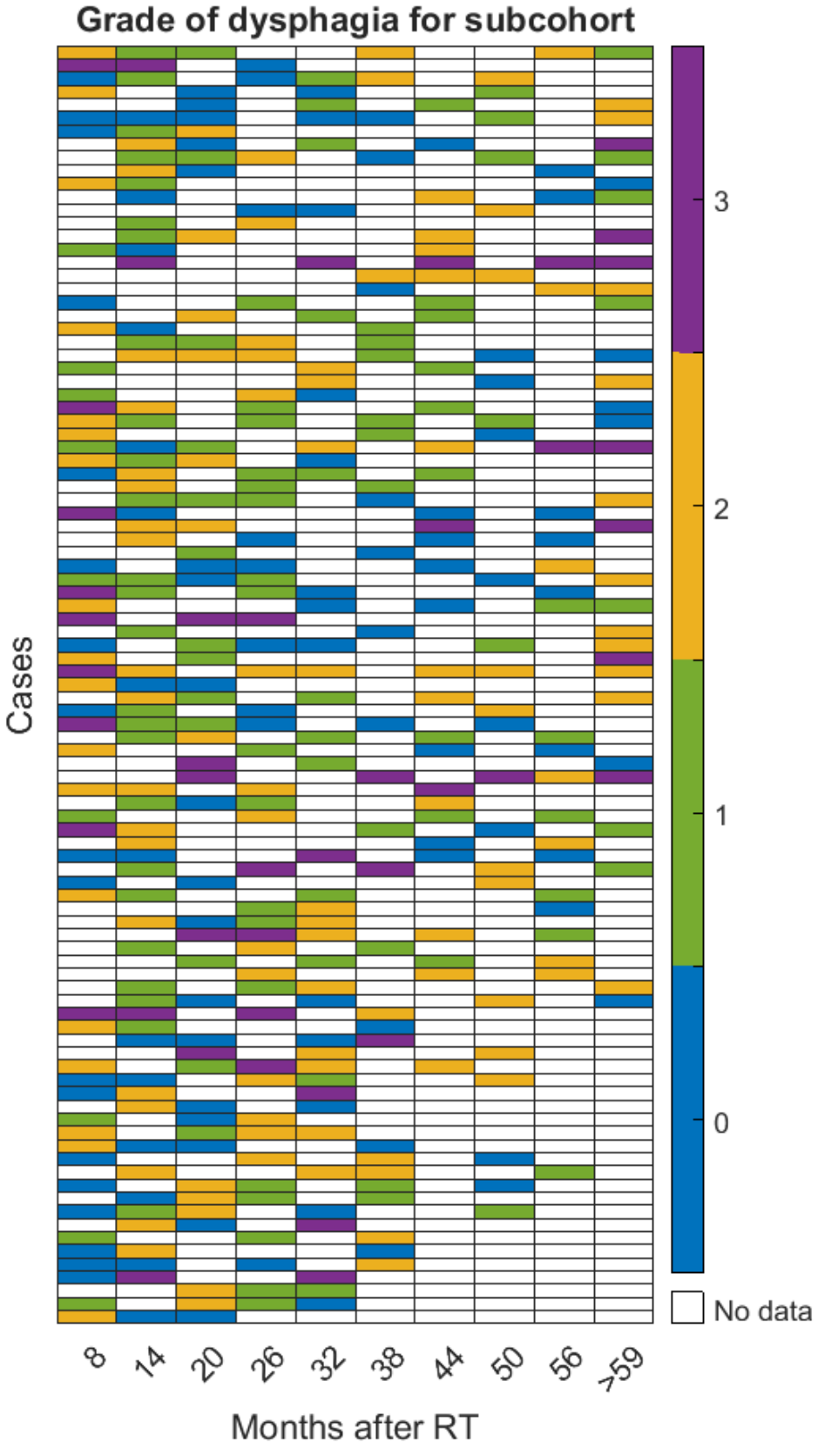

# Real-world experience of pediatric radiotherapy over two decades (to guide future treatments)

Daniella Elisabet Østergaard[1+2], Yasmin Lassen-Ramshad[3], Lisa Lyngsie Hjalgrim[4], Maja Vestmø Maraldo[1+2]

[1] Department of Oncology, Copenhagen University Hospital – Rigshospitalet, Copenhagen, Denmark

[2] Dept of Clinical Medicine, University of Copenhagen, Copenhagen, Denmark

[3] Department of Clinical Medicine - DCPT - Danish Center for Particle Therapy, Aarhus, Denmark

[4] Department of Paediatric and Adolescent, Copenhagen University Hospital – Rigshospitalet, Copenhagen, Denmark

## Introduction

Advancements in pediatric cancer treatment have significantly improved survival rates, with Denmark reporting an overall 5-year survival of ~85%. Radiotherapy remains an important treatment modality, but systematic registration and quality monitoring have not been standard practice. To ensure state-of-the-art treatment with equal access and to monitor acute and late toxicity, we established a national radiotherapy registry within the Danish Child Cancer Registry (DCCR) Register —the first quality database to record historical treatment data from 2008 onward. Here, we present preliminary findings on patient population and treatment patterns.

## Method/material

Data: Data collection was based on data for all pediatric cancer patients receiving radiotherapy between January 2008 and June 2021. Electronic patient records and archives and treatment planning systems was the information source. Verification was sometimes limited for proton therapy conducted abroad.

DCCR was expanded to include dedicated radiotherapy information, capturing comprehensive data. This includes patient status before treatment (height, weight, functional impairments, prior surgery, chemotherapy, fertility preservation, neurocognitive and endocrine screenings) and detailed radiotherapy parameters:

- Treatment specifics: Target areas, boost, anatomy involved, and therapy modality (Photons: 2D, 3D-CRT, IMRT, VMAT, gating, DIBH; Protons: active scanning, pas-sive scattering, gating, DIBH for protons).
- Image guidance: CBCT, kV, other techniques, and frequency of imaging.

- Dose and fractionation: Total dose (Gy), number of fractions (F), Gy/F, and fractions/ week.
- Course: Start/end dates, treatment interruptions, and toxicity (only prospectively recorded).

**Results**

Preliminary data is presented here, with a comprehensive dataset from 2008–2024 expected in June 2025. Between January 2008 and June 2021, 434 pediatric cancer patients under-went radiotherapy in Denmark. Treatments were administered at Rigshospitalet, Aarhus Uni-versity Hospital, the Danish Center for Particle Therapy, Odense University Hospital, or abroad (USA, Germany, France, Sweden). Modalities included photons (274 patients, 63,1%), protons (143 patients, 32,9%), brachytherapy (8 patients, 1,8%) and unknown (17 patients, 2,1%). Brain tumors were the most frequent diagnosis (34,9 % of all photons, 62,1% of all proton plans) and sarcomas the second most frequent diagnosis, more details available in figure 1A-B. Radiotherapy doses varied widely. Figure 1C categorizes dose by diagnosis with a schematic overview of treatment modality trends over time.

**Conclusion**

From 2008 to 2021, 434 Danish pediatric cancer patients received radiotherapy. Photon ther-apy was most used, while proton therapy was the preferred for brain tumors and tumors near the brain (e.g., head/neck carcinomas and sarcomas). This registry enables long-term quality monitoring including secondary cancers and ensures equitable treatment access across Denmark.

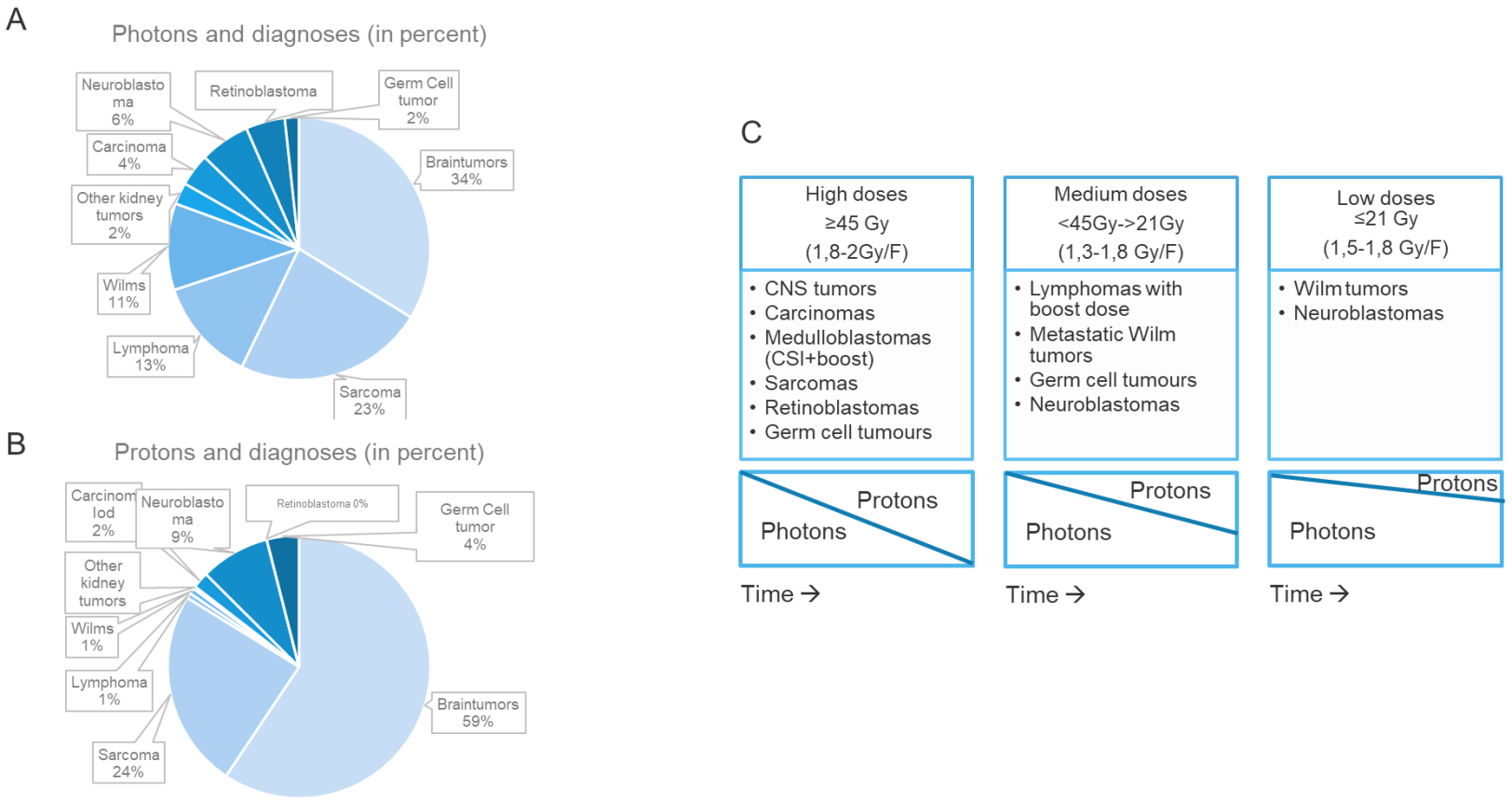


**Figure 1 A: Distribution of diagnoses irradiated with photons from 2008-2021 B Distribution of diagnoses irradiated with protons from 2008-2021 C Doses (high, intermediate and low) and diagnoses. Below is seen a time trend of modalities for the dose categories.**

**Survival prediction in cancer patients receiving whole brain radiotherapy for brain metastases**

Authors: Fokdal L (1,3), Stougaard J (1), Timm S (1,3), Thing RS (2), Nissen HD (2), Berg M (2), Madsen CV (1), Kristiansen C (1)

1. Department of Oncology Vejle Hospital, University Hospital of Southern Denmark, Denmark

2. Department of Medical Physics Vejle Hospital, University Hospital of Southern Denmark, Denmark.

3. Department of Regional Health Research, University of Southern Denmark, Odense, Denmark

**Introduction:** Brain metastases (BM) have significant impact on morbidity and mortality in cancer patients. Treatment for BM includes surgery or stereotactic radiotherapy in selected patients. The remaining patients may be treated with whole brain radiotherapy (WBRT) or best supportive care. The life expectancy after WBRT is generally short and patient selection for treatment is crucial. This study investigates the outcome and identifies prognostic factors for survival after WBRT. Furthermore, a prognostic model with three prognostic groups was designed.

**Material and methods:** Consecutive patients treated with WBRT in the Department of Oncology, Vejle Hospital, Denmark from 2018-2023 were included. WBRT was delivered with 3D-technique without hippocampus sparing. Patient demographics (gender, age, ECOG performance status (PS)), disease variables (diagnosis, number of brain metastases, meningeal carcinomatosis, extent of systemic disease) and treatment variables (systemic treatments, dose, fractionation) were analyzed with survival statistics and Cox regression analysis. A prognostic model for survival after WBRT was designed with inclusion of all significant prognostic factors. Scores were calculated for each prognostic factor based on 3-month survival probability, which was considered a clinical meaningful survival gain to justify WBRT. In each patient a total score was calculated and three prognostic groups were defined.

**Results:** A total of 392 patients (lung cancer n=240, breast cancer n=103, other cancers n=49) were evaluated. Radiotherapy schedule was 30 Gy/10 fractions in 266 (67.9%) patients and 20 Gy/4-5 fractions in 126 patients (32.1%).
Median follow-up was 3 (0-65) months. During the study period 364 (92.9%) of all patients died. One month, 3 months and 6 months survival were, 85.5%, 52.8%, and 30.7%, respectively.
In the multivariate analysis, diagnosis, PS, and systemic disease remained significant factors for survival. These prognostic factors were given a score from 1 to 10 according to the 3-month survival probability, and a total cumulative score ranging from 9-23 was calculated. Based on the total scores three prognostic groups were defined with a median survival of 30 days (group 1 (score 9-12): 59 patients), 78 days (group 2 (score 13-16): 179 patients), and 228 days (group 3 (score 17-23): 154 patients), respectively (figure 1).

**Conclusion**: Careful patient selection for WBRT is essential. Based on diagnosis, PS and extent of systemic disease, a prognostic score was developed with categorization of patients into three prognostic groups. This score can assist clinicians in identifying patients who are likely to benefit from WBRT, thereby helping to minimize unnecessary overtreatment.

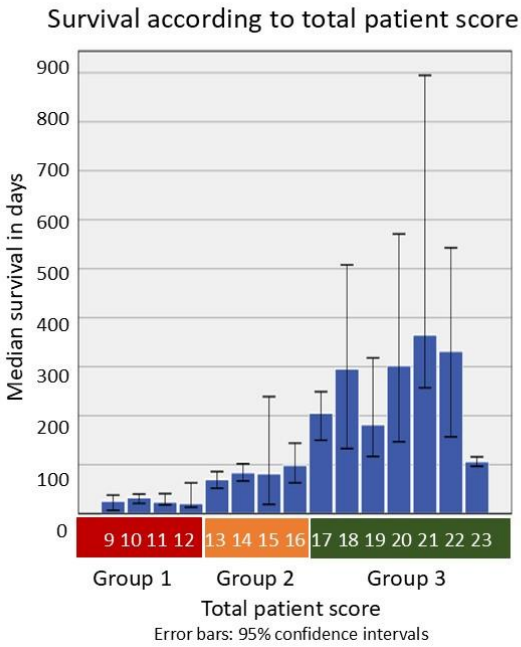
Survival according to total patient score
Median survival in days
900
800
700
600
500
400
300
200
100
0
9 10 11 12
13 14 15 16
17 18 19 20 21 22 23
Group 1
Group 2
Group 3
Total patient score
Error bars: 95% confidence intervals

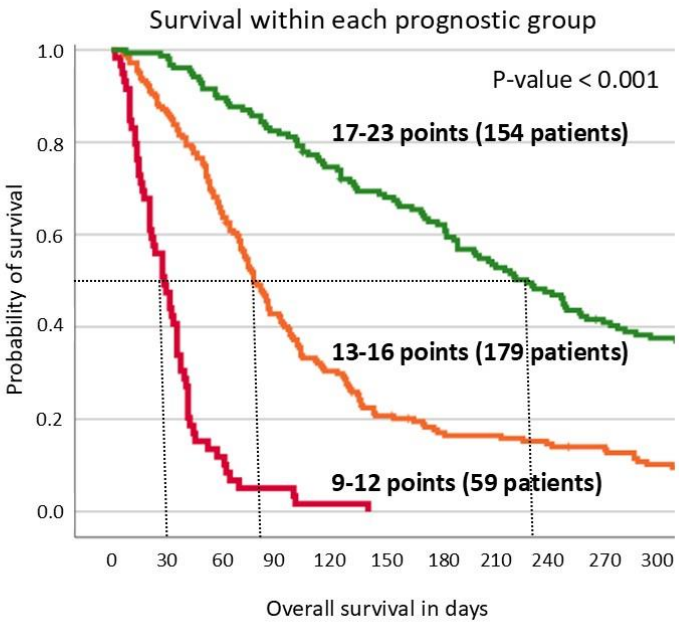
Survival within each prognostic group
Probability of survival
1.0
0.8
0.6
0.4
0.2
0.0
P-value < 0.001
17-23 points (154 patients)
13-16 points (179 patients)
9-12 points (59 patients)
0
30
60
90
120
150
180
210
240
270
300
Overall survival in days

**Sexual Function-Related Organs at Risk in Rectal Cancer: Opportunities for Sparing in Radiotherapy Planning**

**Kronborg C[1,2], Arp DT[3], Bahij R[4], Biancardo SBN[5], Diness LV[5], Engstrøm KH[4], Fokdal LU[8], Pedersen BG[9], Havelund B[6], Hvid CA[8], Jakobsen KL[9], Lutz CM[8], Nyvang L[8], Pedersen SE[1], Poulsen LØ[3], Rønde H[1], Schou LK[1], Serup-Hansen E[5], Steffensen JH[8], Søndergaard J[3], Szpejewska JE[9], Nissen HD[6]**

[1]Danish Centre for Particle Therapy, Aarhus University Hospital, Aarhus, Denmark
[2]Department of Clinical Medicine, Aarhus University, Aarhus, Denmark
[3]Department of Oncology, Aalborg University Hospital, Aalborg, Denmark
[4]Department of Oncology, Odense University Hospital, Odense, Denmark
[5]Department of Oncology, Copenhagen University Hospital - Herlev and Gentofte, Herlev, Denmark
[6]Department of Oncology, University Hospital of Southern Denmark, Lillebaelt Hospital, Vejle, Denmark
[7]Department of Radiology, Aarhus University Hospital, Aarhus, Denmark
[8]Department of Oncology, Aarhus University Hospital, Aarhus, Denmark
[9]Department of Oncology, Zealand University Hospital, Næstved, Denmark

**Introduction**

Sexual dysfunction is a significant consequence of pelvic radiotherapy (RT), driven by a complex interplay of psychological, physical, social, and relational factors. Research on radiotherapy dose effects to sexual function-related organs at risk (SF-OAR) has primarily focused on vaginal dose and stenosis in females (F) and penile bulb dose and erectile dysfunction in males (M), with less emphasis on arousal, desire, and satisfaction.

In the Danish Colorectal Cancer Radiotherapy Group (DCCG-RT), we aimed to: 1. Develop an atlas of SF-OARs relevant to sexual dysfunction. 2. Evaluate which SF-OARs could be spared without compromising target coverage in rectal cancer radiotherapy planning.

**Methods and materials**

The DCCG-RT adopted a multidisciplinary approach, involving oncologists and physicists from seven treatment centers, along with a psychologist specializing in sexology, a surgeon with expertise in late effects, and a radiologist with pelvic MRI expertise.

In the first meeting, MRI-based anatomical analysis of structures relevant to sexual function was conducted. A draft atlas for both males and females, including identified SF-OARs, was then distributed including plexus hypogastricus inferius, Pudendal vessels nerve/Alcock´s canal, neurovascular bundle (M), penile bulb (M), Vagina (F), paracolpium (F), and bulboclitoris (F). During the second, two-day meeting, all structures were delineated through a consensus process, followed by a radiological review. In a subsequent online meeting, delineation of additional cases was discussed, leading to the finalization of the atlas.

All patients fulfilled standard indication for neoadjuvant rectal RT and plans aligned with national dose planning guidelines (IMRT-based). Standard elective volumes included presacral, mesorectal and lateral pelvic volumes. All targets received a uniform dose of 50.4 Gy in 28 fractions**.** Wilcoxon Signed-rank test with exact p-value calculation was used for comparison

**Results**

A national consensus atlas for SF-OAR (both genders) was developed.

Standard plans (n=15) and SF-OAR sparing plans (n=15) for 7 males and 8 females were compared (table 1). Sparing of especially pudendal vessels and bulboclitoris was possible without compromising target coverage and dose to standard OAR. For SF-OARs in or close to the target D2% could often be improved.

**Conclusion**

Our consensus-based delineation and planning demonstrate that radiation dose to many SF-OAR can be spared or optimized without compromising target coverage or standard OARs. The next steps include implementing a sexual health and function questionnaire, analyzing the relationship between radiotherapy dose to SF-OARs and sexual function, and ultimately integrating SF-OARs into standard radiotherapy optimization for rectal cancer and potentially other pelvic cancers.

| | Standard plan n=15 Median (IQR) | SF-OAR-sparing n=15 Median (IQR) | p-value |
|---|---|---|---|
| **Standard parameters - target and OAR** | | | |
| CTV-T V95% (%) | 100 (100-100) | 100 (100-100) | 1 |
| PTV-T V95% (%) | 99.98 (99.7-100) | 99.9 (99.8-100) | 0.94 |
| PTV-T 105% (%) | 0.0 (0.0-0.0) | 0.0 (0.0-0.1) | 0.063 |
| PTV-E V95% (%) | 99.4 (98.6-99.9) | 99.3 (98.9-99.9) | 0.98 |
| PTV-E 105% (%) | 0.0 (0.0-0.08) | 0.07 (0-0.37) | 0.08 |
| Bowel Bag V45Gy(cc) | 239 (120-468) | 249 (122-443) | 0.99 |
| Bowel Bag V30Gy(cc) | 439 (228-700) | 445 (210-660) | 0.07 |
| Bladder V50Gy(%) | 5.1 (0.5-9.4) | 4.4 (1-8.5) | 0.94 |
| Bladder V35Gy(%) | 33.7 (22-42.8) | 32.6 (22.4-40.8) | 0.038 |
| Sacral bone V50Gy(%) | 5.6 (2.9-8.7) | 4.4 (3.9-7.1) | 0.92 |
| Femoral heads V50Gy(%) | 0.0 (0.0-0.0) | 0.0 (0.0-0.0) | 1 |
| **Sexual function - OAR common** | | | |
| Plexus hypogastricus inferius V30Gy(%) | 100 (100-100) | 100 (100-100) | 1 |
| Plexus hypogastricus inferius V40Gy(%) | 100 (100-100) | 100 (100-100) | 1 |
| Plexus hypogastricus inferius D2%(Gy) | 52 (51.8-52.3) | 50.9 (50.1-51.7) | 0.0029 |
| Pudendal artery and nerve + Alcocks canal V30Gy(%) | 90.6 (60.2-98.6) | 67.4 (41.4-93.3) | 0.0001 |
| Pudendal artery and nerve + Alcocks canal V40Gy(%) | 45.4 (38.2-72.5) | 38.5 (26.3-56.0) | 0.0001 |
| Pudendal artery and nerve + Alcocks canal D2%(Gy) | 51.3 (50.8-51.5) | 50.1 (49.8-51.0) | 0.021 |
| **Sexual function - OAR male, n=7** | | | |
| Neurovascular bundle V30Gy(%) | 100 (100-100) | 100 (99.8-100) | 0.5 |
| Neurovascular bundle V40Gy(%) | 100 (98-100) | 100 (97.7-100) | 0.5 |
| Neurovascular bundle D2%(Gy) | 51.8 (51.3-52.1) | 50.8 (50.1-51.3) | 0.03 |
| Penile bulb V30Gy(%) | 0.0 (0.0-20.4) | 0.0 (0.0-8.7) | 0.25 |
| Penile bulb V40Gy(%) | 0.0 (0.0-10.8) | 0.0 (0.0-3.8) | 0.5 |
| Penile bulb D2%(Gy) | 26.1 (4.2-50) | 10.14 (4.3-45.8) | 0.063 |
| **Sexual function - OAR female, n=8** | | | |
| Vagina V30Gy(%) | 100 (100-100) | 100 (97.9-100) | 0.25 |
| Vagina V40Gy(%) | 100 (999.5-100) | 100 (92.8-100) | 0.25 |
| Vagina D2%(Gy) | 51.0 (50.8-51.5) | 50.9 (50.0-51.4) | 0.46 |
| Paracolpium V30Gy(%) | 100 (100-100) | 100 (96.3-100) | 0.25 |
| Paracolpium V40Gy(%) | 100 (96.6-100) | 99.7 (90.5-100) | 0.13 |
| Paracolpium D2%(Gy) | 51.8 (51.1-52.0) | 50.8 (50.5-51.6) | 0.15 |
| Bulboclitoris V30Gy(%) | 63.6 (20.3-71.0) | 25.2 (3.1-54.2) | 0.015 |
| Bulboclitoris V40Gy(%) | 13.7 (0.86-37.0) | 5.1 (0.1-23.6) | 0.031 |
| Bulboclitoris D2%(Gy) | 46.0 (35.4-50.5) | 41.6 (28.0-50.7) | 0.13 |

**Dosimetry audits as part of the radiotherapy quality assurance (RTQA) program in the PROTECT-trial**

**Author information:**
Mai Lykkegaard Ehmsen, mai.ehmsen@rm.dk, Danish Centre for Particle Therapy, Aarhus University Hospital, Aarhus, Denmark.

**Authors:**
Mai L Ehmsen[1], Camilla S Byskov[2], Hanna R Mortensen[1,3], Rebecca Bütof[4], Richard Canters[5], Gilles Defraene[6], Karin Haustermans[6,7], Maria F Jensen[1], Arturs Meijers[8], Christina T Muijs[9], Ditte S Møller[2], Marianne Nordsmark[2], Pieter Populaire[6,7], Gloria Vilches-Freixas[5], Lars Nyvang[2], Liliana Stolarczyk[1], Sebastian Makocki[4], Sara Broggi[10], Francesco Fracchiolla[11], Andrea Martignano[11], Kenneth Poels[6], Séverine Rossomme[12], Stefan Vasiliniuc[13], Lone Hoffmann[2]

[1]Danish Centre for Particle Therapy, Aarhus University Hospital, Aarhus, Denmark. [2]Department of Oncology, Aarhus University Hospital, Aarhus, Denmark.
[3]Department of Clinical medicine, Aarhus University, Aarhus, Denmark.
[4]Department of Radiotherapy and Radiation Oncology, Faculty of Medicine and University Hospital Carl Gustav Carus, Technische Universität Dresden, Dresden, Germany.
[5]Department of Radiation Oncology (Maastro), GROW School for Oncology and Reproduction, Maastricht University Medical Centre, Maastricht, Netherlands.
[6]KU Leuven, Department of Oncology, Laboratory of Experimental Radiotherapy, Leuven, Belgium.
[7]Department of Radiation Oncology, University Hospitals Leuven, Leuven, Belgium.
[8]Center for Proton Therapy, Paul Scherrer Institut, Villigen, Switzerland.
[9]Department of Radiation Oncology, University Medical Center Groningen, Groningen, Netherlands.
[10]IRCCS Ospedale, San Raffaele, Milano, Italy.
[11]UO Fisica Sanitaria, APSS, Trento, Italy.
[12]Ion Beam Applications (IBA), Dosimetry Business Unit, Louvain-la-Neuve, Belgium.
[13]IBA Dosimetry, SSDL Laboratory, Schwarzenbruck, Germany

**Introduction:**
Beam output audit is a mandatory part of the comprehensive RTQA program in the PROTECT-trial. It must follow EORTC guidelines for photon radiotherapy (XT) and local dosimetry audits for proton radiotherapy (PT). This study reports on an on-site reference dosimetry audit conducted by the IBA Secondary Standard Dosimetry Laboratory (SSDL, Germany), aimed at ensuring dose consistency for QA across four PT and five XT centres.

**Materials and methods:**
The dosimetry audits employed IAEA TRS-398 (Rev. 1) protocols to determine absorbed dose to water under reference conditions.
For PT six beams were evaluated: three monoenergetic fields (100, 170, and 220 MeV) measured at 2 cm depth, and three modulated spread-out Bragg peak (SOBP) beams measured at the midpoint of the SOBP. IBA measurements utilized a gantry positioned at 90° (or 270°) with an IBA Blue Phantom PT and PPC05 ionization chamber in combination with a calibrated IBA Dose-1 or IBA Dose-X electrometer.
XT centres selected their beam energy with reference fields set to 10 x 10 $cm^2$ at the phantom surface and a 100 cm source-to-surface distance. IBA employed a vertical beam setup with an IBA WP1D water phantom and FC65-G Farmer chamber connected to either an IBA Dose-1 or IBA Dose-X electrometer. Local physicists replicated these experimental conditions using their own dosimetry equipment. All measurements were repeated at least three times to account for beam instabilities, with results reported as average dose per monitor unit.

**Results:**
The study demonstrates agreement in absorbed dose-to-water measurements between each center and IBA for both PT and XT, with discrepancies generally within 2 % (Figure 1).
Some measurements had to be adjusted subsequently; One proton center (C2) used a different setup (measurement depth of 2.3 cm instead of the recommended 2cm) and other beam quality correction factor values (using values from TRS-398 instead of TRS-398, Rev. 1). One photon center (C4) deviated from the IAEA recommendations by using a local dosimetry protocol. A closer agreement was achieved after accounting for these protocol variations (Figure 1). Combined uncertainty was 3.2 % for PT and 2.3 % for XT measurements.

**Conclusions:**
For all centres, agreement was well within 3% given as criteria for a valid Beam Output Audit by EORTC. The dosimetry audit results underscore the importance of consistent reference measurements in ensuring quality assurance for both proton and photon radiotherapy across multiple centres, thereby enhancing confidence in treatment accuracy within the PROTECT-trial.

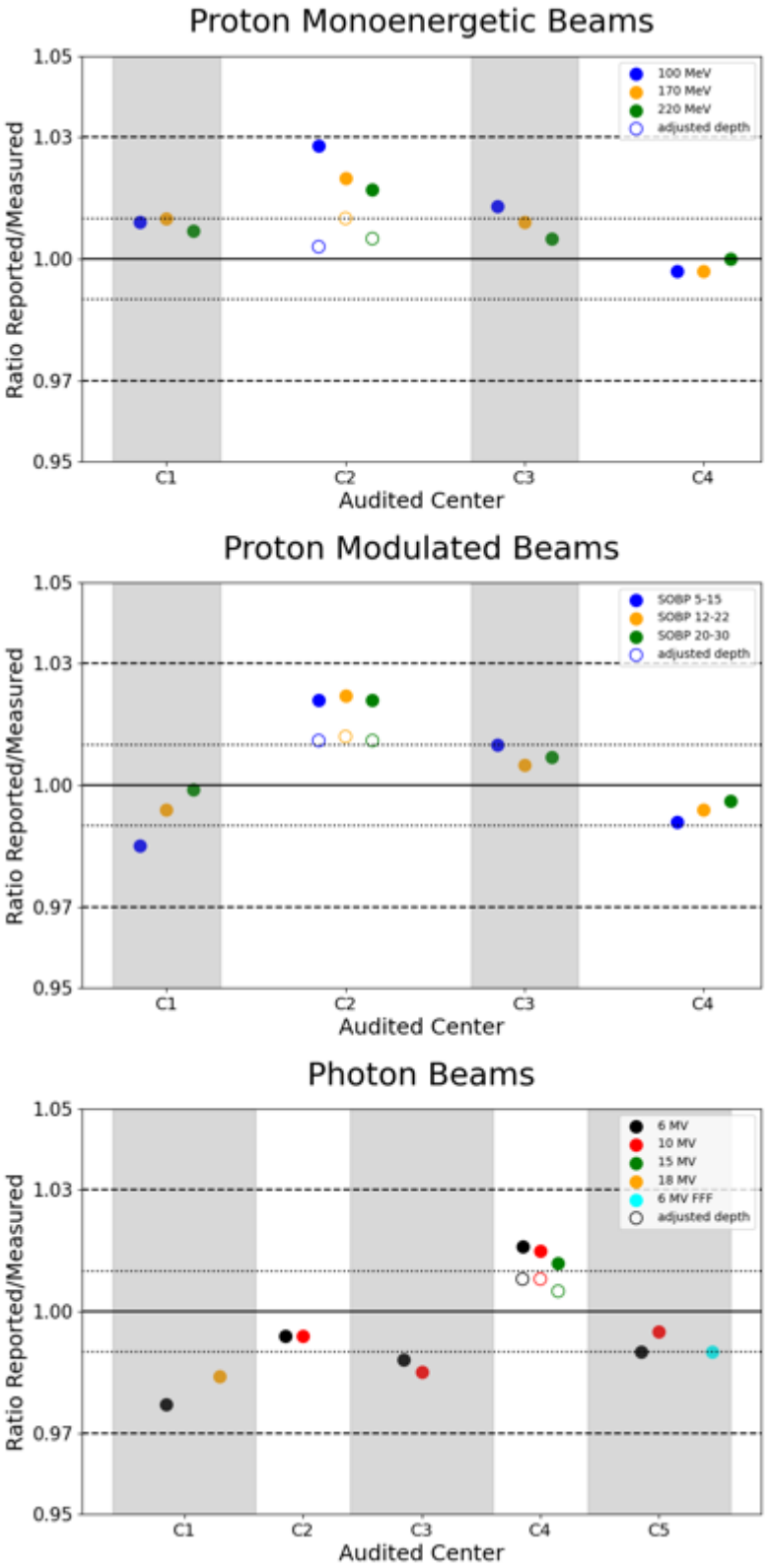


**Figure 1:** Ratio between the absorbed dose-to-water reported by the local medical physicist and that measured by IBA SSDL in monoenergetic proton beams (top), modulated proton beams (middle) and photon beams (bottom).

**The value of magnetic resonance imaging in the response evaluation of primary radiotherapy for squamous cell carcinomas of the oral cavity, pharynx and larynx.**

**Authors**

Malthe Fiil Bønløkke, Maltla@rm.dk, Department of Otorhinolaryngology, Head and Neck Surgery, Aarhus University Hospital, Aarhus, Denmark

Sandy Mohamed Ismail Mohamed, Department of Oncology, Aarhus University Hospital, Aarhus, Denmark

Morten Horsholt Kristensen, Department of Oncology, Aarhus University Hospital, Aarhus, Denmark

Mette Hjørringgaard Madsen, Department of Radiology, Scanning, and Nuclear Medicine, Esbjerg and Grindsted Hospital

Jacob Kinggaard Lilja-Fischer, Department of Otorhinolaryngology, Head and Neck Surgery, Aarhus University Hospital, Aarhus, Denmark

Jesper Grau Eriksen, Department of Oncology, Aarhus University Hospital, Aarhus, Denmark

**Introduction**

Residual disease after primary curative radiotherapy (RT) in head and neck squamous cell carcinoma (HNSCC) is associated with increased morbidity and mortality. Accurate post-treatment response evaluation is crucial for guiding further management, yet no consensus exists on the optimal follow-up schedule or imaging modality, if any. Since 2015, Aarhus University Hospital has incorporated routine clinical examination at 2 months post-RT and magnetic resonance imaging (MRI) at 3 months, as part of the follow-up protocol. This study aims to assess the value of routine MRI in response evaluation following primary curative RT.

**Materials and Methods**

This retrospective cohort study included consecutive patients treated with curative-intent RT for squamous cell carcinoma of the oral cavity, pharynx, or larynx at Aarhus University Hospital, with at least one year of follow-up. Patient and tumor data were retrieved from the DAHANCA quality database. Medical records, imaging reports, and multidisciplinary team (MDT) board notes were reviewed. The diagnostic performance of MRI was assessed using positive predictive value (PPV), negative predictive value (NPV), sensitivity, and specificity.

**Results**

A total of 394 patients treated over four years were included. Treatment failure within 1 year was histologically confirmed in 33 patients (8.4%). MRI demonstrated a PPV of 30.5% (95% CI: 22.8%–39.2%) and an NPV of 91% (95% CI: 86.2%–94.3%). Sensitivity and specificity

were 66.7% and 68.6%, respectively. Notably, MRI detected 5% of treatment failures in patients initially classified as in complete remission based on clinical examination.

**Conclusions**

These results suggest that MRI is a valuable modality to evaluate treatment response following primary curative RT in HNSCC. Given its high NPV, MRI can help exclude residual disease with confidence, potentially reducing unnecessary interventions.

# Real-world survival and morbidity after concurrent chemotherapy and radiotherapy in patients with gastroesophageal cancer

Mortensen HR[1,4], Hoffmann L[2,4], Nordsmark M[3,4], Thorsen LBJ[3,4] and Møller DS[2,4].
(1) Danish Center for Particle Therapy, Aarhus University Hospital, Aarhus, Denmark
(2) Department of Medical Physics, Aarhus University Hospital, Aarhus, Denmark
(3) Department of Oncology, Aarhus University Hospital, Aarhus, Denmark
(4) Department of Clinical Medicine, Faculty of Health Sciences, Aarhus University, Aarhus, Denmark.

Corresponding author: Hanna R Mortensen, hanna.mortensen@auh.rm.dk, Danish Center for Particle Therapy, Aarhus University Hospital, Aarhus, Denmark

**Introduction**
Standard curative treatment for patients with esophageal (EC) and gastroesophageal junction (GEJ) cancer is neo-adjuvant chemo-radiotherapy (nCRT) followed by surgery or definitive chemo-radiotherapy (dCRT) in patients not candidates for surgery. The aim of this study was to examine real-world survival and morbidity in EC patients treated with radiotherapy (RT).

**Material and Methods**
This retrospective study included patients with EC and GEJ treated with nCRT or dCRT at a single institution between January 2012 and March 2021. The primary endpoint was overall survival (OS), and secondary endpoints were loco-regional control, progression-free survival, pattern of failure, and toxicity.
Data were obtained from the Danish Esophago-Gastric Cancer database, patient records, and the Eclipse treatment planning system. RT treatment planning and target delineations were performed according to national guidelines. All patients received IMRT and had daily cone-beam CT for setup. The prescribed RT dose ranged from 41.4-50.4 Gy and 50-66 Gy in 23-33 fractions, 5 fractions per week for nCRT and dCRT, respectively.

**Results**
In total, 250 patients received nCRT and 167 patients received dCRT. Median age was 67 years, 78% were male, 86% had T3-T4 tumors, and 65% had node-positive disease. Histology was adenocarcinoma (50%) and squamous cell carcinoma (45%).
All but 49 patients (89,3%) completed prescribed RT dose, and 92.4% proceeded to surgery after nCRT. The median follow-up was 24 months. For nCRT and dCRT, the median OS was 31 vs 24 months and the 3-year OS was 46,4% vs 38,2%. Recurrent disease was 46% , and 10% had oligometastatic disease. The frequency of patients with combined loco-regional and metastatic recurrence was similar between nCRT and dCRT as well as between adenocarcinoma and squamous cell carcinoma patients.
Acute toxicity was recorded in 96% of patients, pain, dysphagia/esophagitis or fatigue being most common. Side effects were mild and manageable; 1/3 required hospitalization;12% required dilatation. Late side effects were not systematically recorded; the most common were

pain, fatigue and dysphagia. In multivariate analysis, performance status (PS), histology, GTV N size, and mean dose to the lungs were significantly associated with OS among patients receiving nCRT. For dCRT, PS and GTV T and GTV N size were significant (Figure 1).

**Conclusions**

In conclusion, OS among EC patients treated with nCRT or dCRT in clinical practice is acceptable and in line with published literature. The majority of patients treated with nCRT had surgery. Treatment side effects to nCRT and dCRT are frequent but largely manageable.

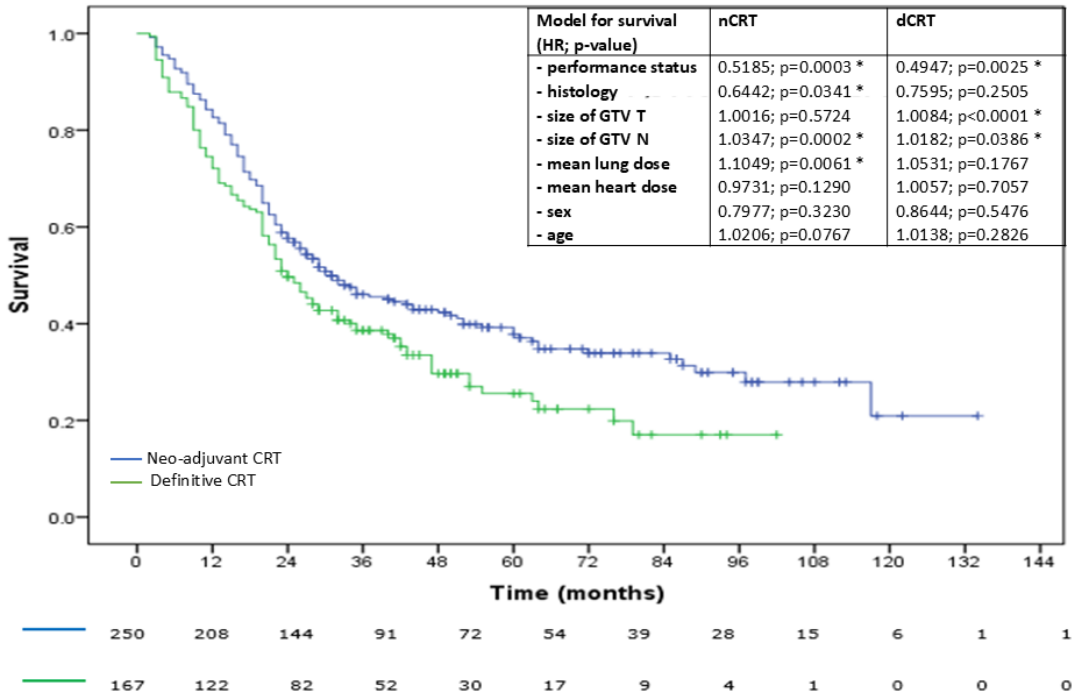


Figure 1: Overall survival for neo-adjuvant (nCRT) and definitive (dCRT) chemo-radiotherapy including multivariate analysis of factors associated with survival in patients with EC and GEJ cancer.

**Patient Perspectives on Participation in the DBCG Proton Trial: A Qualitative Research Study**

**Authors:** Kristine W. Høgsbjerg[1], Anne W. Kristensen[2], Mette Møller[3], Else Maae[4], Maja V. Maraldo[5], Louise W. Matthiessen[6], Sami Al-Rawi[7], Mette H. Nielsen[8], Cai Grau[2], Birgitte V. Offersen[1,2]

1: Department of Experimental Clinical Oncology, Department of Oncology, Palle Juul-Jensens Boulevard 99, 8200 Aarhus N, Aarhus University Hospital, Denmark. kwh@oncology.au.dk
2: Danish Centre for Particle Therapy, Aarhus University Hospital, Denmark
3: Department of Oncology, Aalborg University Hospital, Denmark
4: Department of Oncology, Vejle Hospital, University of Southern Denmark, Denmark
5: Department of Oncology, Copenhagen University Hospital, Rigshospitalet, Denmark
6: Department of Oncology, Copenhagen University Hospital - Herlev and Gentofte, Denmark
7: Department of Clinical Oncology and Palliative Care, Zealand University Hospital, Denmark
8: Department of Oncology, Odense University Hospital, Denmark

**Introduction:** Participation in clinical trials is critical to advancing oncological treatments, yet equitable trial access remains challenging. Ensuring diverse patient inclusion strengthens external validity and enhances the generalisability of trial outcomes. However, barriers to trial participation persist, and the factors influencing patient enrolment are not fully understood. This study investigates the patient perspective on participation in the Danish Breast Cancer Group (DBCG) Proton Trial (NCT04291378). By clarifying these factors, we aim to provide actionable insights to encourage broader recruitment in trials and promote equitable treatment opportunities for all eligible patients.

**Materials and Methods:** Patients eligible for the DBCG Proton Trial were selected for qualitative interviews. Candidates included those undergoing surgery for early-stage breast cancer or ductal carcinoma in situ (DCIS) with an indication for radiotherapy (RT) who, based on standard 3D conformal RT (3D CRT) planning, had a high cardiac (mean heart dose ≥ 4 Gy) or pulmonary (V17 lung ≥ 37%) dose. This randomised controlled trial compares proton and photon therapy in these patients. To ensure diverse representation, one randomised and one non-randomised patient were purposefully sampled from each of Denmark's eight radiotherapy clinics. Telephone interviews were conducted, transcribed, and systematically analysed using an inductive approach to identify key motivators and barriers to trial participation.

**Results:** A total of fifteen patients were interviewed, including seven randomised and eight non-randomised participants. The median age was 59 years (range: 35–78 years), and the median distance to the proton facility was 132 km (range: 3-310 km). Twelve patients underwent chemotherapy for 4–6 months prior to radiotherapy. The median interview duration was 31 minutes (range: 18–42 minutes).

The key factors influencing decision-making were frequently consistent between randomised and non-randomised patients. These factors included 1) distance to the treatment facility, 2) timing of trial communication, 3) availability of deliberation and decisional support, 4) perceptions of clinical equipoise and experimental treatment, and 5) individual patient needs, particularly mental and physical capacity to undergo additional treatment.

**Conclusion:** Distance to the proton treatment facility appeared as the most important barrier to participation in the DBCG Proton Trial, reflecting a common challenge in clinical trial enrolment. Conversely, the prospect of reduced late effects was the primary motivator for those considering participation. The decision was challenging for most patients, with often one individual, dominant factor ultimately guiding their final choice.

# Role of prophylactic cranial irradiation in patients with limited disease small cell lung cancer: a Danish single institution cohort

**Author information:** Sara Linde[1,2], sarlin@rm.dk

**Authors:** Sara Linde[1,2], Marianne M. Knap[1], Lone Hoffmann[1,2], Azza A. Khalil[1], Christina M. Lutz[1], Maria Kandi[3], Lise S. Mortensen[1], Ditte S. Møller[1,2], Hjørdis H. Schmidt[1]

[1]Department of Oncology, Aarhus University Hospital, Aarhus, Denmark
[2]Department of Clinical Medicine, Aarhus University, Aarhus, Denmark
[3]Department of Oncology, Gødstrup Regional Hospital, Gødstrup, Denmark

## Introduction

Prophylactic cranial irradiation (PCI) is part of standard treatment for patients with limited disease small cell lung cancer (LD-SCLC), treated with curative intent.
In the late 1990s, PCI was found to increase overall survival (OS) and reduce the risk of symptomatic brain metastases. However, doubt has been raised about whether the benefits outweigh the potential side effects since modern diagnostic workup has developed, including brain-MRI. Existing data remains sparse and conflicting. Therefore, we examined factors impacting PCI referral, the time to symptomatic brain metastases, and OS with and without PCI in a real-world setting.

## Materials and Methods

The records of 190 consecutively treated patients for LD-SCLC between 2012 and 2021 at Aarhus University Hospital were reviewed. All patients received thoracic radiotherapy, 45Gy in 30 fractions (fx), 10 fx per week. 184 of the patients also received platinum/etoposide. Patients were stratified based on whether they received PCI (PCI*yes*, n=119) or not (PCI*no*, n=71). Baseline characteristics, Kaplan-Meier estimates of OS, and time to symptomatic brain metastases were compared for the two groups.

## Results

PCI*no* patients were significantly older, had poorer performance status, were more likely to have been treated in the later period, and had more frequently undergone an MRI of the brain at the time of diagnosis. The median follow-up time was 74 months. PCI*no* had a median OS of 19 months (95% CI 14.1-24.0) compared to 24 months (95% CI 19.5-28.5) for PCI*yes*. However, there was no statistical difference in OS (P = 0.4), Figure 1a. 54 patients (23 in PCI*no* and 31 in PCI*yes*) developed symptomatic brain metastases in the follow-up time. In 15 patients, this was a first-time recurrence with no evidence of extracranial disease (8 in PCI*no* and 7 in PCI*yes*). The numbers of patients with, and time to, symptomatic brain metastases were not significantly different between the two groups (P= 0.3 and P = 0.1 respectively), with

a 2-year risk of symptomatic brain metastases of 36.7% (95%CI 23.8-49.6) for PCI*no* and 24.5% (95%CI 15.7-33.3) for PCI*yes*, Figure 1b.

## Conclusion

Despite being older and in worse health, PCI*no* patients did not have a statistically significant difference in OS compared to PCI*yes* patients. Similarly, time to symptomatic brain metastases did not differ significantly between the two groups.

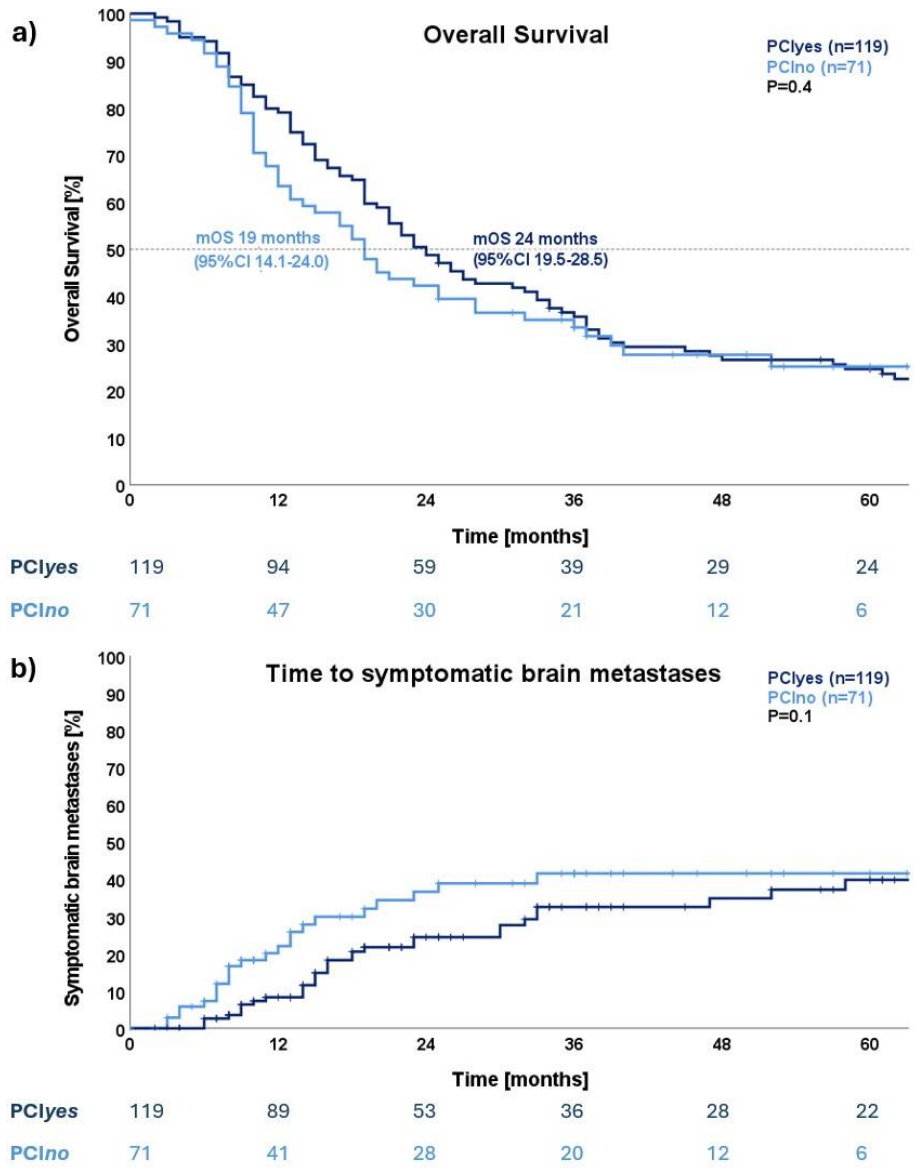


**Figure 1.** Overall survival (a) and time to symptomatic brain metastases (b) in 190 patients treated for limited disease small cell lung cancer, divided into patients that received prophylactic cranial irradiation (PCI) (PCI*yes*, n=119) and patients that did not (PCI*no*, n=71). Overall survival is from the start of thoracic irradiation to death or last seen. Time to symptomatic brain metastases is from the start of thoracic irradiation to the event of symptomatic brain metastases verified on a scan or censored (death or last seen).

**Patient reported respiratory symptoms 10 years after loco-regional breast cancer radiotherapy: Look for other causes than radiotherapy**

Maja Bendtsen Sharma*[1], Lasse Hindhede Refsgaard*[2,3], Elisabeth Bendstrup[3,4], Emma Skarsø Buhl[2,3], Robert Zachariae[1,3,5], Rasmus Blechingberg Friis[1], Stine Korreman[2,3], Birgitte Vrou Offersen[1,3,6]

*Shared 1st authors

1. Department of Oncology, Aarhus University Hospital, Aarhus, Denmark
2. Danish Centre for Particle Therapy, Aarhus University Hospital, Denmark
3. Department of Clinical Medicine, Aarhus University, Aarhus, Denmark
4. Department of Respiratory diseases and Allergy, Aarhus University Hospital, Denmark
5. Department of Psychology and Behavioural Sciences, Aarhus University, Denmark
6. Department of Experimental Clinical Oncology, Aarhus University Hospital, Denmark

**Purpose:**

Breast cancer survivors with respiratory symptoms frequently contact The Danish Patient-Association of Late-effects, suspecting the reason is adjuvant radiotherapy. This study investigated patient-reported respiratory symptoms in patients treated with locoregional adjuvant radiotherapy for node-positive breast cancer and evaluated the associations of the responses with the individual radiation doses to the ipsilateral lung.

**Materials/Methods:**

Patient-reported outcomes and radiotherapy plans were collected from patients treated in a single institution 2008-2016 and included in the DBCG RT Nation Study. The patients answered questions on the presence and severity of dyspnoea (4-point scale, EORTC QLQ-C30) and cough (5-point scale, PRO.CTCAE), smoking, and pulmonary and cardiac comorbidities. Dyspnoea and cough scores were converted to a scale ranging from 0 to 100. Radiotherapy plans were evaluated, and the dose volume parameters to the ipsilateral lung were registered, including mean lung dose (MLD) and the volume receiving 5Gy (V5) and 20Gy (V20). Responders were separated into tertiles based on MLD (‘low’/’intermediate’/’high’). Patient-reported outcomes and comorbidities were reported per group and compared using One-way ANOVA and Chi-squared test. Secondly, responders were dichotomised based on dyspnoea (‘no/little’ vs. ‘quite a bit/very much’) and coughing ('none/mild' vs. 'moderate/severe/very severe'). MLD, 5V and V20 were compared between groups using the two-sample t-test.

**Results:**

A total of 1011 questionnaires were sent out, of which 537(53%) were completed. The mean age of responders was 65.7years (SD 9.9); mean time from radiotherapy to questionnaire response was 11years (SD 2.3). Mean overall dyspnoea and cough scores were 17.9(SD 23.6) and 15.7(SD 24.2), respectively. Differences in dyspnoea and coughing scores between dose groups were small and statically insignificant with a tendency towards higher scores for lower MLD. There was no indication of increasing respiratory symptoms with increasing lung dose (*Figure 1*). For responders reporting 'no/little' dyspnoea MLD was 13.0Gy (SD 2.7) vs. MLD 12.0Gy(SD 3.0) for responders reporting 'quite a bit/very much' dyspnoea, (p=0.43). For coughing, MLD was 13.0 Gy(SD 2.7) for responders reporting 'none/mild' coughing vs.12.5Gy (SD 3.1) for responders reporting 'moderate/severe/very severe' cough (p=0.23). The same trends were found for V5 and V20.

**Conclusion:**

We found no associations between patient-reported respiratory symptoms and lung dose for node-positive breast cancer receiving radiotherapy with a median follow-up period of 11 years. New respiratory symptoms should be investigated irrespective of previous irradiation.

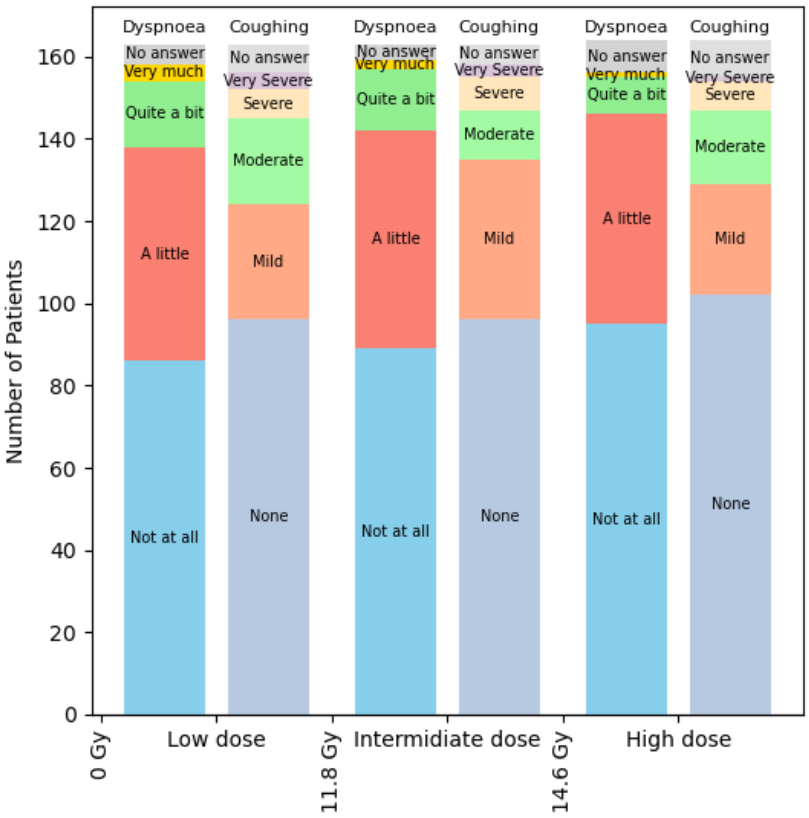


*Figure 1. Diagram showing the distribution of responses for the severity of dyspnoea and cough in responders who previously received 'little', 'intermediate' and 'high' dose to the ipsilateral lung during RT for breast cancer.*

# Factors Influencing Participation in a Proton Therapy Clinical Trial Among Patients with Pharyngeal and Laryngeal Cancer: A Cross-Sectional Study

Anne Wilhøft Kristensen[1] annkrs@rm.dk *(presenting and corresponding author)*

Kenneth Jensen[1] Kenneth.Jensen@auh.rm.dk

Jeppe Friborg[2] Jeppe.friborg@regionh.dk

Jesper Grau Eriksen[3] jesper@oncology.au.dk

Susanne Oksbjerg Dalton [4,5,6] sanne@cancer.dk

Annesofie Lunde Jensen[7] annesjen@rm.dk

Cai Grau[1] cai.grau@rm.dk

1. Danish Centre for Particle Therapy, Aarhus University Hospital, Denmark
2. Department of Clinical Oncology, Rigshospitalet, Denmark
3. Experimental Clinical Oncology, Aarhus University Hospital, Denmark
4. Department of Clinical Oncology & Palliative Care, Zealand University Hospital, Denmark
5. Institute for Clinical Medicine, Faculty of Health, Copenhagen University, Denmark
6. Danish Cancer Institute, Copenhagen, Denmark
7. Steno Diabetes Centre, Aarhus University Hospital, Denmark

## Introduction

Denmark has one proton therapy (PT) facility. For patients with pharyngeal and laryngeal cancer, PT is currently available through participation in an RCT.

Socioeconomically disadvantaged patients have lower enrollment rates in trials and may miss out on potential research benefits.

Geographical barriers also impact enrollment, as patients living farther from specialised treatment facilities, are more likely to decline participation.

This population-based study aimed to identify the potential influence of factors on disparities in PT clinical trial participation among Danish patients with pharyngeal and laryngeal cancer.

## Methods

DAHANCA 35, is a nationwide RCT comparing long-term treatment-induced toxicities following photon versus PT in individuals with pharyngeal and laryngeal cancer.

The present study compares DAHANCA 35 trial participants and non-participants across multiple factors, including self-reported educational level, income level, cohabitation status, place of residence, co-morbidities, health literacy, anxiety levels, and quality of life.

Questionnaires were provided to patients in seven radiotherapy clinics during their first two weeks of radiotherapy.

Data were collected using a 38-item questionnaire incorporating validated scales and measures. Clinical data were obtained from the DAHANCA database.

REDCap and Stata was used for data storage, management, and analysis.

**Results**

Between 2022 and 2025, a total of 330 patients completed the questionnaire, including 127 (38%) participants and 203 (62%) non-participants.

The final analysis is currently ongoing, but a description of participant selection and attrition in this study will be ready for presentation at BIGART 2025.

14 % percent of the respondents were not informed about the RCT. Among those informed, 54% were not enrolled: 10% were ineligible, 5% declined participation in general, 58% declined due to the geographical distance to PT, 12% declined because radiotherapy would be delayed by approximately one week if allocated to protons, and 16% declined for other reasons.

There were no significant differences in diagnosis, disease stage or HPV status between participants and non-participants.

Logistic regression revealed significant associations between participation in the trial and younger age (OR=0.95, $p<0.001$), being retired (OR=0.44, $p=0.025$), EQ-5D overall health status (OR=1.02, $p=0.02$), EQ-5D better mobility (OR=0.37, $p=0.006$), and shorter distance to study treatment (OR=0.99, $p=0.002$).

The association between hospital site and participation was significant but may have reflected the distance to proton therapy (PT) rather than site-specific differences in recruitment procedures.

Low health literacy, comorbidity or anxiety were not associated to participation.

**Conclusion**

Participation was associated with younger age, employment, better mobility, higher overall health, and shorter distance to PT.

# Cosmetic outcome after kilovoltage therapy of facial basal cell carcinoma: A Danish national prospective study of 932 patients

ON Brændstrup[1] (osnb@oncology.au.dk) P Lassen[2], AB Gothelf[3], SR De Blanck[3], J Friborg[3], CK Lonkvist[2], AL Nielsen[2], H Primdal[4], G Hanan[5], M Toure[5], M Andersen[6], K Nowicka-Matus[6], R Kjeldsen[6], JG Eriksen[1,4]

[1]Aarhus University Hospital, Dept. of Experimental Clinical Oncology, [2]Herlev and Gentofte University Hospital, Dept. of Oncology, [3]Copenhagen University Hospital, Dept. of Oncology, [4]Aarhus University Hospital, Dept. of Oncology, [5]Vejle Hospital, Dept. of Oncology, [6]Aalborg University Hospital, Dept. of Oncology

**Introduction**
Kilovoltage therapy is a viable treatment for basal cell carcinoma (BCC), offering tumor control rates and cosmetic outcomes comparable to surgery. Although BCC is the most common cancer in humans, evidence for kilovoltage therapy is largely retrospective, with heterogeneity in dose, fractionation, disease stage, and patient factors. As of January 2020, a nationwide prospective registry collecting patient/tumor characteristics, treatment factors, and outcomes including patient-reported satisfaction was initiated in Denmark. This study reports on patient-reported cosmetic outcomes six months post-kilovoltage therapy for BCC, including investigating any impact of fractionation and field size.

**Materials and methods**
Patients with facial BCC referred for kilovoltage therapy between January 2020 and December 2022 in five Danish centers were identified from the database. Therapy (70–100kV) was delivered as either 40.5–45Gy/9–10fx or 51Gy/17fx, with margins of 5–10mm depending on histological subtype. Follow-up visits occurred six months post-treatment. Patients rated cosmetic outcomes as very satisfied, satisfied, indifferent, or unsatisfied. Professional evaluations followed LENTSOMA criteria, i.e. dyspigmentation, fibrosis, teleangiectasia and any chronic wounds, resulting in an overall evaluation as no, minor, major, or disfiguring skin changes in the radiation field compared to surrounding skin.

**Results**
Of 1547 registered patients, 932 (60%) with follow-up data were included in the study. Overall, 97% (900) of patients reported being very satisfied or satisfied with cosmetic outcomes, aligning with independent professional evaluations ($p<0.001$), where 97% had no or minor skin changes.

Satisfaction was not related to age (p=0.7), sex (p=0.2), or smoking (p=0.2). Again, in alignment with overall professional evaluation.

For nasal located tumors, 69% of patients reported being very satisfied compared to 49% for other facial sites (p<0.001). Field size did not significantly affect satisfaction (p=0.6), but field sizes ≥2.5 cm were associated with higher dyspigmentation rates (69% vs. 60%, p=0.01). Fraction size (3 Gy/fx vs. 4.5 Gy/fx) showed no significant impact on patient-reported (p=0.9) or professional (p=0.5) evaluations.

**Conclusion**

Overall, 97% of patients were satisfied with cosmetic outcomes six months post-kilovoltage therapy for BCC. Field sizes ≥2.5 cm was associated with higher dyspigmentation rates, but didn't impact patient satisfaction or overall evaluation. No impact of fractionation schedule could be detected.

# Bowel delineation methods and predictors of acute and late diarrhea in radiotherapy for anal cancer

**Corresponding author:** Katrine Smedegaard Storm, Katrine.smedegaard.storm@regionh.dk (1)

**Authors:** KS Storm (1), S Homburg (1), GF Persson (1,2), CP Behrens (1,3), P Sibolt (1), S Spampinato (8), KLG Spindler (4,5), C Kronborg (6,7), E Serup-Hansen (1)

1) Department of Oncology, Copenhagen University Hospital – Herlev and Gentofte, Copenhagen, Denmark
2) Department of Clinical Medicine, Faculty of Health Sciences, University of Copenhagen, Copenhagen, Denmark
3) Department of Health Technology, Technical University of Denmark, Roskilde, Denmark
4) Department of Oncology, Aarhus University Hospital, Aarhus, Denmark
5) Department of Experimental Clinical Oncology, Aarhus University Hospital, Aarhus, Denmark
6) Danish Centre for Particle Therapy, Aarhus, Denmark
7) Department of Clinical Medicine, Aarhus University, Aarhus, Denmark
8) Erasmus MC Cancer Institute, University Medical Center Rotterdam, Department of Radiotherapy, Rotterdam, The Netherlands.

## Introduction

Acute and late treatment-related diarrhea is a significant challenge for patients treated with chemo-radiotherapy for anal cancer in a curative setting. This study aims to investigate dosimetric and clinical predictors of acute and late treatment-related diarrhea for patients treated with concurrent chemo-radiotherapy (CRT) or radiotherapy (RT) alone for anal cancer. Additionally, to determine the optimal bowel contouring model for prediction of treatment-related diarrhea.

## Materials and methods

Patients treated with CRT or RT alone in the DACG-I Plan-A study from 2015-2021 were included in this prospective post-hoc analysis.

Toxicity endpoints were Common Terminology Criteria of Adverse Events (CTCAE, v4.0) acute grade≥2 diarrhea, defined as the peak toxicity score during radiotherapy and up to four weeks after treatment and late grade≥1 diarrhea recorded at the one-year follow-up visit.

Bowel volumes were contoured post-hoc on the planning CT as 1) bowel cavity: the peritoneal cavity from the lower limit of the L4 vertebra to last visible bowel loop, 2), bowel bag: the part of the peri-toneal cavity including bowel loops, 3) individual bowel loops, and 4) terminal ileum. $V_{15Gy}$, $V_{30Gy}$, and $V_{45Gy}$ for the different bowel volumes were included as dosimetric variables in analysis. Clinical varia-bles included tumor size, N-stage, and chemotherapy regimen. Univariate- and multivariate logistic regression was used for evaluating association of clinical and dosimetric variables and toxicity end-points.

## Results

Of the 290 patients included for analysis, 116 (40 %) experienced acute grade≥2, and 56 of 256 (22 %) had late grade≥1 diarrhea. A trend indicating an increased risk of acute grade ≥2 diarrhea for pa-tients with larger bowel volumes receiving radiation was observed. This was most pronounced for bowel bag $V_{30Gy}$ (p=0.09) (Figure 1). A more detailed bowel contour did not increase the predictive value of the multivariable model. The risk of acute diarrhea was three times higher for patients treated with chemotherapy including 5-FU or Capecitabine compared to patients treated with weekly Cisplatin or radiotherapy only (p<0.001) (Figure 1). None of the explored dosimetric parameters or the presence of acute diarrhea were predictive of late diarrhea.

**Conclusion**

Treatment with 5-FU/Capecitabine showed a notable association with acute diarrhea which over-shadowed the radiation dose-response relationship. However, a trend suggesting an association be-tween Bowel Bag $V_{30Gy}$ and the risk of acute diarrhea was observed.

Figure 1.

**NTCP model for acute diarrhea and bowel bag V30 Gy**

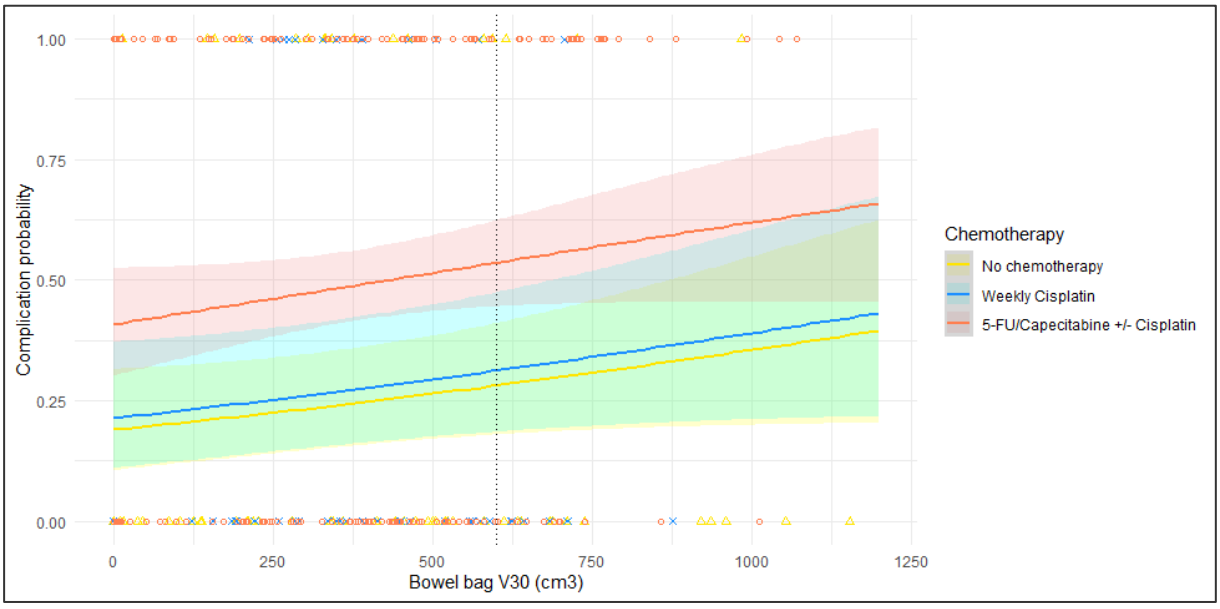

**Reducing preposition variations and monitor intrafraction movement with surface-guided radiation therapy for breast cancer patients**

*Corresponding author*

Trine O Kirkegaard
Medical Physicist
E-mail: trine.kirkegaard@rn.dk
Department of Medical Physics, Clinical Cancer Research Center
Aalborg University Hospital, Aalborg, Denmark

*Authors*

Trine O Kirkegaard[1], Ingelise Jensen[1], Thomas O Kristensen[1], Marie Louise Holm Milo[2,3], Martin S Nielsen[1,3]

[1]Department of Medical Physics, Clinical Cancer Research Center, Aalborg University Hospital, Aalborg, Denmark.
[2]Department of Oncology, Clinical Cancer Research Center, Aalborg University Hospital, Aalborg, Denmark. [3]Department of Clinical Medicine, Aalborg University, Aalborg, Denmark.

**Introduction***:* Surface guided radiation therapy (SGRT) presents the possibility to set up patients based on the 3D surface instead of skin marks. The primary aim of this study was to investigate the feasibility of SGRT using Exactrac Dynamic (ETD) for prepositioning of breast cancer patients treated in free breathing compared to conventional skin-marker setup. A secondary aim was to assess intrafraction movement using surface data captured during treatment.

**Materials and methods:** Twenty-one breast cancer patients were included. They were treated with whole- or partial-breast irradiation in free breathing using 3D conformal planning technique. In a crossover study design, each patient was setup with both the skin-marker- and SGRT procedure but for different fractions in random order. For the skin-marker setup, isocenter skin marks were aligned to the in-room lasers. For SGRT, reflections of an optical structured light identified the patient surface and compared it to the corresponding external structure from the CT-scan. The setup offset was evaluated using 3D couch shifts from subsequent image guidance, acquired as orthogonal MV-kV for whole-breast and kV-kV for partial-breast and boost plans.
Intrafraction movement, excluding periodic respiration, was evaluated using the log-files from ETD, where surface data was recorded per monitor unit delivered. For each main field a mean surface displacement from baseline was found, and the difference between the two main fields for each fraction represented the intrafraction movement.

**Results:** No significant difference was found in mean population setup offset between SGRT and skin-marker setup. SGRT demonstrated reduced random population errors in vertical (VRT) and longitudinal (LNG) direction and reduced systematic population errors in lateral (LAT) direction (table 1). A systematic vertical offset was observed for both SGRT and skin-marker setup.

Analysis of the intrafraction movement showed no mean population shift in LNG and LAT, but a small, significant shift of -0.3 mm in VRT. Random and systematic population errors where below 1 mm in all directions.

**Conclusions:** Surface guided setup using ETD showed no significant difference in mean population setup offset compared to conventional skin-marker setup. SGRT was, however, superior to skin-marker setup as the systematic- and random errors were reduced indicating improved consistency. Subsequent IGRT is still advisable for final patient positioning, due to individual patient shifts and patient relaxation resulting in systematic vertical shifts.
We demonstrated that ETD SGRT were able to track the individual patient movement and found a small mean population shift in VRT.

| | VRT (mm) | | | LNG (mm) | | | LAT (mm) | | |
|---|---|---|---|---|---|---|---|---|---|
| | **M (95%ci)** | **∑** | **σ** | **M (95%ci)** | **∑** | **σ** | **M (95%ci)** | **∑** | **σ** |
| **Skin-marker (n = 127 fx)** | -2.6 (-4.1, -1.1) | 3.4 | 3.5 | -0.8 (-2.0, 0.3) | 2.6 | 3.6 | -0.2 (-1.4, 0.9) | 2.5 | 2.6 |
| **SGRT (n = 201 fx)** | -2.5 (-3.6, -1.5) | 2.3 | 2.5 | -0.6 (-1.5, 0.3) | 2.0 | 2.4 | -0.9 (-1.6, -0.2) | 1.6 | 2.1 |
| **p-value** | 0.94* | 0.09** | 0.03* | 0.76* | 0.28** | 0.01* | 0.22* | 0.04** | 0.06* |

*Table 1: IGRT match after prepositioning showing the setup offset using the skin-marker- vs SGRT procedure in VRT, LNG and LAT direction in terms of mean population offset (M) with 95% confidence interval (95%ci), systematic population error (Σ) and random population error (σ). *Paired t-test. ** F-test. All tests are with 5% significance level.*

# The necessity of managing intra-fractional motion in stereotactic radiotherapy for central lung lesions

Simon Nyberg Thomsen[1,2], Ditte Sloth Møller[1,2], Marianne Knap[2], Hjørdis Hjalting Schmidt[2], Mette Pøhl[3], Lone Hoffmann[1,2]

[1]Dept. of Clinical Medicine, Faculty of Health Sciences, Aarhus University, Denmark.

[2]Department of Oncology, Aarhus University Hospital, Aarhus, Denmark.

[3]Department of Oncology, Copenhagen University Hospital, Rigshospitalet, Copenhagen, Denmark.

## Purpose

Stereotactic radiotherapy (SRT) for small peripheral lung tumors achieves high local control rates. However, previous SRT trials for centrally located tumors have reported high toxicity levels, including grade 5 events. The STRICT-lung trial (NCT05354596) investigates SRT for central lung tumors using an inhomogeneous dose distribution, delivering up to 85 Gy in GTV mean dose. To protect organs at risk (OAR), target coverage and GTV mean dose are compromised, resulting in a steep dose gradient that is highly sensitive to intra-fractional shifts. This study evaluates the dosimetric impact of intra-fractional motion in STRICT-lung patients.

## Material and Methods

Seventy-four patients were treated at Aarhus University Hospital according to the STRICT-lung protocol. The PTV margin was 4 mm. Patients were set up based on daily cone-beam CT (CBCT) soft tissue tumor matching to the planning CT (pCT). Following treatment delivery, a second CBCT was acquired to assess intra-fractional target shifts.

Retrospectively, both CBCTs were aligned to the pCT based on the target, and intra-fractional 3D target shifts were calculated. Contours delineated on the pCT were deformably transferred to both CBCTs, and dose was recalculated using stoichiometric calibration curves. The differences in $D_{GTVmean}$ and dose ($D_{0.5cc}$) to the OAR closest to the tumor were calculated for all eight fractions and presented as box plots.

These preliminary results include data from the first 18 patients. The results for the remaining 56 patients, along with an analysis of local control and toxicity, will be presented at the conference.

## Results

The median [range] tumor shift was 2.9 mm [0.1, 14.2]. A box plot of shifts per patient is shown in Fig. 1a, along with the PTV margin. Tumor shifts occurred primarily in the cranial and dorsal directions. The median

change in $D_{GTVmean}$ was 0.44 Gy [-14.11, 5.61], indicating that some patients received significantly lower tumor doses than planned due to intra-fractional motion (Fig. 1b). For most patients, the OAR closest to the tumor moved toward the high-dose region, resulting in increased dose (Fig. 1c). Both target shifts and their dosimetric impact were highly patient-specific, depending on tumor location and planned dose distribution.

## Conclusion

Intra-fractional movements of the target and OAR can compromise treatment by increasing the toxicity risk and, in some cases, tumor under-dosage. To ensure the safe delivery of SRT for centrally located lung tumors, monitoring and correction of target shifts are essential.

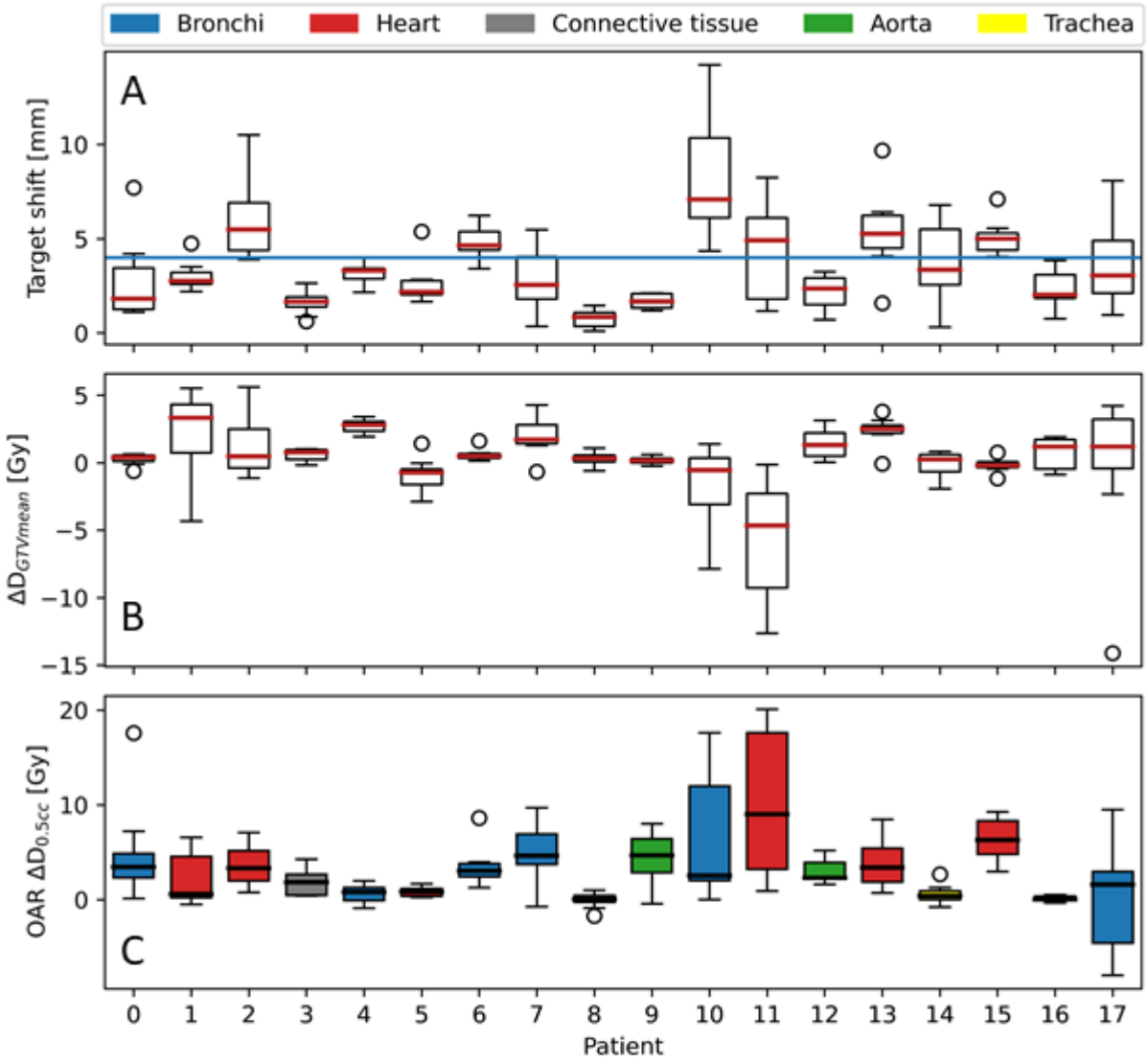


Figure 1: (A) Intra-fractional shifts of the target in the 8 fractions for each patient, the blue line indicates the PTV margin. (B) Change in mean dose to the target due to the intra-fractional shift for all patients. (C) Change in dose ($D_{0.5cc}$) for the OAR nearest the tumor for each patient.

**Increasing stability of chest wall position during deep-inspiration breath-hold under breast cancer radiotherapy**

Kristine Wiborg Høgsbjerg*[1,2], Anders W. Mølby Nielsen*[1,2], Harald Spejlborg[3], Esben Yates[3], Christina Maria Lutz[3], Per Rugaard Poulsen[3], Birgitte Vrou Offersen[1,2, 3] *Shared first authors*

*1: Department of Experimental Clinical Oncology, Department of Oncology, Aarhus University Hospital, Denmark*
*2: Department of Oncology, Aarhus University Hospital, Aarhus, Denmark*
*2: Department of Medical Physics, Aarhus University Hospital, Aarhus, Denmark*
*3: The Danish Centre for Particle Therapy and Department of Oncology, Aarhus University Hospital, Denmark*

**Background and purpose:** Internal mammary node (IMN) radiotherapy (RT) improves survival in node-positive breast cancer patients [1]. In 2021, at our institution, intrafractional chest wall instability was demonstrated to reduce the IMN RT dose considerably in left-sided breast cancer patients treated with deep-inspiration breath-hold (DIBH) [2]. To improve stability, several modifications were introduced at our institute. First, the DIBH marker block was repositioned to the sternal bone. Second, daily image-guided RT (IGRT) matching was prioritised in the IMN region. Third, IGRT imaging was delayed at least 5 seconds after stabilising the chest wall position in the DIBH. Finally, systematic evaluation of continuous portal (Cine MV) images was implemented after the second fraction.
This study assessed the geometric impact of these changes on intrafractional chest wall stability.

**Material and methods**: Cine MV images were analysed for 39 consecutive node-positive left-sided breast cancer patients treated in DIBH with tangential fields and IGRT between January and May 2024. DIBH was controlled using the Varian RGSC gating system. Cine images were recorded for all fractions at both tangential fields. Geometrical chest wall errors were measured by matching the final Cine MV image frame of each field with the Digitally Reconstructed Radiograph (DRR). Geometrical errors were quantified using van Herk's formula and compared with a similar 2021 cohort. Geometrical errors above 3 mm were regarded as clinically significant and above 5 mm as major errors.

**Results**: In total, 39 patients were included; 18 underwent mastectomy and 21 breast-conserving surgery. Median V90_CTV_IMN dose coverage was 99.6% (IQR 95.5-100%). Thirty-eight patients (97.5%) received the planned Cine MV evaluation, resulting in interventions in six patients (15.4%). Geometric accuracies were improved in the 2024 cohort, with errors of M = 0.1 mm, $\sum$ = 0.7 mm, and $\sigma$ = 3.6 mm compared to M = 0.7 mm, $\sum$ = 1.4 mm, and $\sigma$ = 1.7 mm in the 2021 cohort. Consequently, tangential fields delivered with a geometrical error exceeding 3 mm were reduced from 21.2% (95% CI, 19.1–23.4) to 4.7% (95% CI, 3.5–6.0), and field errors exceeding 5 mm declined from 3.0% (95% CI, 2.2–4.1) to 0.6% (95% CI, 0.2–1.2), resulting in an absolute risk reduction of 16.5% (95% CI, 14.0-19.0;$p<0.0001$) and 2.4% (95% CI, 1.5-3.4;$p<0.0001$) respectively.

**Conclusion**: Sternal positioning of the DIBH marker block and improved IGRT practices resulted in a statistically and clinically significant improvement in intrafractional chest wall stability in left-sided breast cancer patients.

| | 2021 | 2024 |
|---|---|---|
| No. of patients | 39 | 39 |
| Cine MV image observations | 1416 | 1176 |
| Geometric error > 3 mm* | 21.2% (300/1416) | 4.7% (55/1176) |
| Geometric error > 5 mm* | 3.0% (43/1416) | 0.6% (7/1176) |
| Geometric error, Van Herk | M = 0.7 mm<br>∑ = 1.4 mm<br>σ = 1.7 mm | M = 0.1 mm<br>∑ = 0.7 mm<br>σ = 3.6 mm |

*M, margin; ∑, systematic error; σ, random error*

*Geometrical errors relative to the total number of CINE MV image observations.

**Reference list**


1. Nielsen, A.W.M., L.B.J. Thorsen, D. Özcan, L.W. Matthiessen, E. Maae, M.L.H. Milo, et al. *Internal mammary node irradiation in 4541 node-positive breast cancer patients treated with newer systemic therapies and 3D-based radiotherapy (DBCG IMN2): a prospective, nationwide, population-based cohort study.* Lancet Reg Health Eur, 2025. **49**: p. 101160 DOI: 10.1016/j.lanepe.2024.101160.

2. Nielsen, A.W.M., H. Spejlborg, C.M. Lutz, P. Rugaard Poulsen, and B.V. Offersen. *Difference between planned and delivered radiotherapy dose to the internal mammary nodes in high-risk breast cancer patients.* Phys Imaging Radiat Oncol, 2023. **27**: p. 100470 DOI: 10.1016/j.phro.2023.100470.

**Post-treatment analysis of delivered dose in interstitial pulsed dose rate brachytherapy boosts of gynaecological cancers**

*Marjolein L.E. Heidotting[a*)], Soren Kynde Nielsen[b)], Anders Traberg Hansen[b)], Harald Spejlborg[b)], Jacob Lindegaard[b)], Simon Buus[b)], Kari Tanderup[ac)], Jacob Graversen Johansen[ac)]*
*)marjolein.heidotting@rm.dk

*a) Department of Clinical Medicine, Aarhus University, Aarhus, Denmark*
*b) Department of Oncology, Aarhus University, Aarhus, Denmark*
*c) Danish Centre for Particle Therapy, Aarhus University Hospital, Aarhus, Denmark*

**Introduction**
Due to the steep dose gradient in brachytherapy (BT), small offsets in the source position can lead to large deviations from the planned dose delivery. The validation of the actual delivered dose is thus important. However, in vivo dosimetry (IVD) is not a standard part of treatment at most facilities, due to lack of commercially available equipment. This work presents a clinical study of IVD using an in-house developed dosimeter.

**Materials and methods**
At Aarhus University Hospital (AUH), some gynaecological cancers are treated with external beam radiotherapy followed by one fraction of pulsed dose rate (PDR) BT with a prescribed dose of 30Gy. The treatment consists of 50 hourly irradiations (pulses) using interstitial catheters (8-18 per treatment). During the treatment, information on the delivered dose is collected using an in-house developed point detector, based on a scintillating ZnSe(O) crystal (0.5 x 0.5 x 1 $mm^3$), which is placed in an unused BT catheter. The scintillator is connected to a photodiode by an optical fibre. The measured voltage can be converted to dose rate (Gy/s) through a calibration factor and a correction for the non-water equivalence of the scintillator. The measured dose rate at each dwell position is used to reconstruct the most likely dosimeter location by fitting to the theoretical dose rate based on the planned source positions. The positional stability of the dosimeter is quantified as the deviation from the reconstructed dosimeter position in the first pulse. The difference between the planned and the measured dose at the point of the dosimeter was determined for the first pulse. Furthermore, the consistency of the delivered dose was explored through the change in dose per pulse between two successive pulses.

**Results**
IVD has been performed for 30 treatments. Data from 16 treatments has been analysed so far. The mean deviation of the reconstructed dosimeter position from the one in the first pulse was 0.6±0.4 mm (mean±1SD). The mean deviation of the planned dose from the measured dose in the first pulse was 7.2±4.7 % (mean±1SD) at the point of the dosimeter. The largest deviation between two successive pulses was 16.3%, fig. 1. The large deviations are expected to stem from dosimeter movements in steep dose gradients.

**Conclusions**
IVD was successfully used to investigate the stability of dose delivery during PDR BT with interstitial needles.

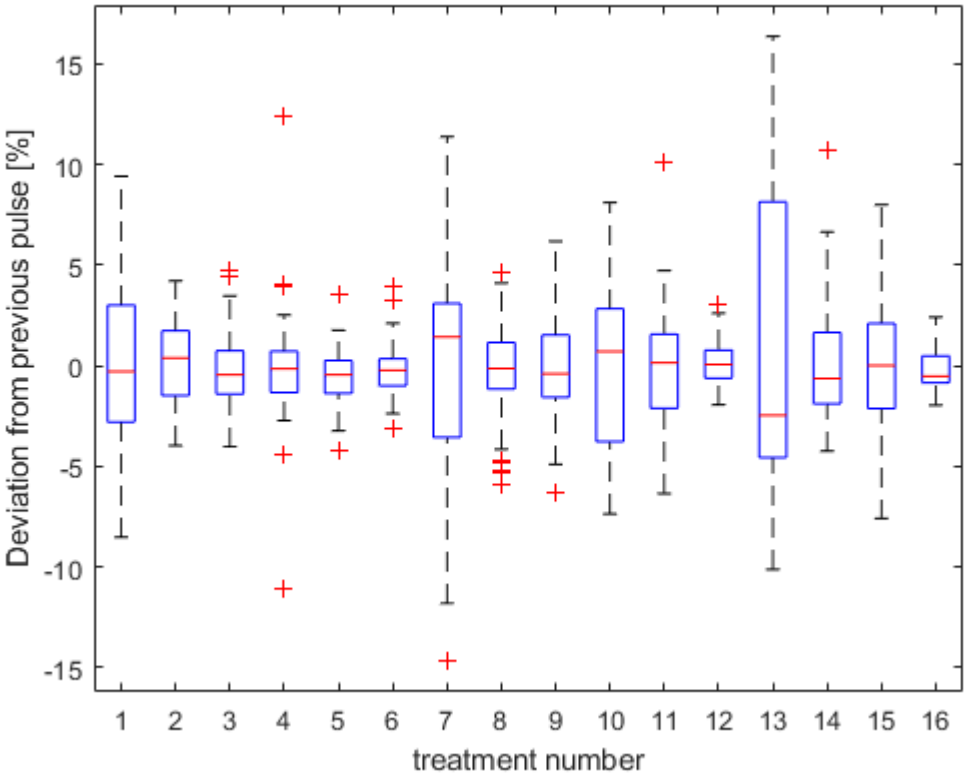


**Fig1. A box plot of the relative change in measured dose from one pulse to the next one for each of the 16 analysed treatments.**

**Position errors and drift motion of mediastinal lymph nodes during DIBH lung cancer radiotherapy**

Sara Shahzadeh[1], Lone Hoffmann[2], Mai Lykkegaard Ehmsen[1], Marianne Knap[2], Esben Worm[2], Ditte Sloth Møller[2], Per Rugaard Poulsen[1,2]

[1]Danish Centre for Particle Therapy, Aarhus University Hospital, Aarhus, Denmark

[2]Department of Oncology, Aarhus University Hospital, Aarhus, Denmark

**Purpose:** Deep-inspiration breath-hold (DIBH) during radiotherapy can potentially reduce dose to the lungs and heart compared to treatment in free breathing. However, breath-hold variations during treatment may impact the treatment accuracy. We investigated the 3D drift motion and geometrical position errors of mediastinal lymph node (LN) targets during DIBH lung cancer treatments.

**Methods:** This study includes seventeen locally-advanced lung cancer patients treated with 5-8 field intensity modulated radiotherapy for primary tumors and involved mediastinal LNs. The LN targets were marked with implanted fiducial markers. The patients were set up using daily DIBH cone-beam CTs with soft tissue match on the primary tumor. Each field was delivered during DIBH guided by an external gating block with 2mm external gating window. For 7-11 fractions per patient, 5Hz fluoroscopic kV images were acquired during treatment delivery perpendicular to the treatment beam. Post-treatment, the marker positions in each kV image were used to determine the 3D marker motion in patient coordinates during treatment by a probability-based method. For all monitored fields, the mean LN positional error relative to the planned position was determined. During intra-breath-holds of at least 10 seconds duration, intra-breath-hold drift motion was calculated as the difference between the mean position in the last 3 seconds and the first 3 seconds of the breath-hold. Inter-field drift motion was determined as the difference in mean position between two consecutive fields.

**Results:** The positional error, intra-breath-hold and inter-field drift motion for each patient in each direction are shown as box plots in Figure 1. The mean (standard deviation) LN positional error during field delivery was 0.0±1.1 mm (LR), 0.9±2.0 mm (CC), and -0.2±1.5 mm (AP) and exceeded 3 mm in 7.3% (LR), 24.0% (CC) and 13.5% (AP) of the field deliveries. Averaged over all patients the intra-breath-hold LN drift motion was 0.4 ±0.6 mm (LR), 1.9±1.6 mm (CC), and -0.1±1.3 mm (AP), and it exceeded 3mm in 2.0% (LR), 23.7% (CC) and 1.3% (AP) of the field deliveries.

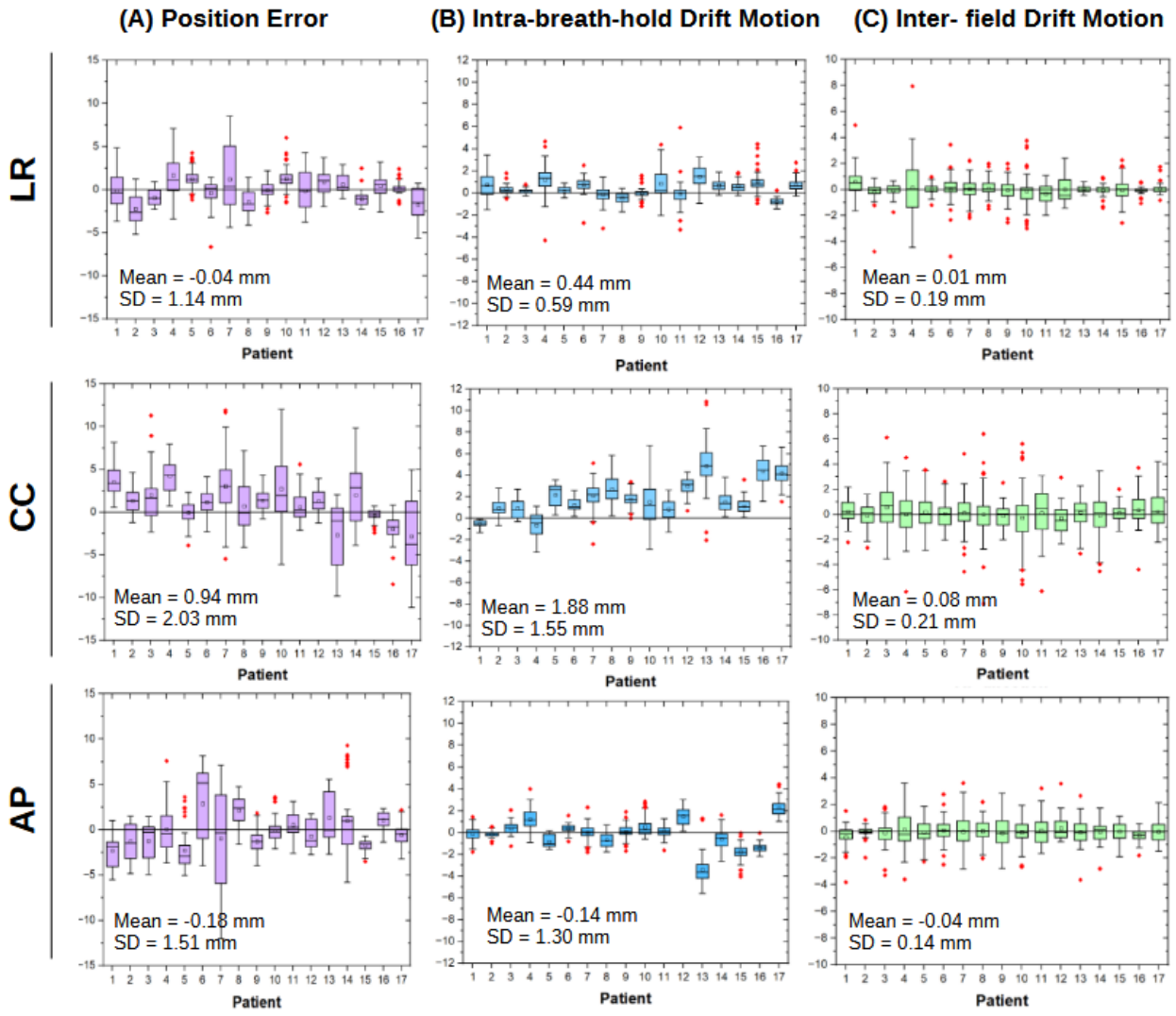


**Figure 1.** Box-plots of the (A) position error, (B) intra-field drift motion and (C) inter-field drift motion for the mediastinal lymph node targets in left-right (LR), cranio-caudal (CC) and anterior-posterior (AP) direction for all patients

**Conclusion:** Relatively large LN position errors were frequently observed, most likely caused by the setup on the primary tumor. Systemic cranial LN drift of up to 10.8 mm occurred during single breath-holds despite a small external gating window of 2mm. The intra-breath-hold drift motion was larger than the inter-field drift motion. The results highlight the importance of internal motion monitoring to ensure precise DIBH delivery for lung cancer radiotherapy.

**Preliminary studies of VMAT vs. RAD dose planning for high-risk breast cancer.**

*Jolanta Hansen[1], Anne Ivalu Sander Holm[1], Lars Nyvang[1], Esben Svitzer Yates[1], Harald Spejlborg[1]*

*[1:] Department of Medical Physics, Aarhus University Hospital, Aarhus, Denmark*

**Introduction:** Internal mammary node (IMN) radiotherapy (RT) improves survival in node-positive breast cancer patients [1]. Irradiating the internal mammary nodes increases the delivered dose to the heart and lungs, prompting the use of advanced dose planning techniques like Volumetric Modulated Arc Therapy (VMAT) or RapidArc Dynamic (RAD).

Most treatment planning systems are unable to optimize for dose robustness outside the patient's body. To address this, VMAT plans were developed, incorporating an artificial tissue rim during optimization to ensure a relevant skin flash; this rim is removed during final plan evaluation. This dual-phase process optimization and evaluation on separate CT scans can be cumbersome and time-consuming.

In this study, we evaluated the performance of Siemens Varian's new optimization and delivery method, RAD with VMAT. With RAD, the artificial tissue rim is integrated during the optimization phase, thereby streamlining the process and eliminating the need for the time-consuming iterative steps, reducing the optimization procedure to a single phase.

**Materials and Methods:** VMAT and RAD plans were calculated for 10 left-sided high-risk patients. The VMAT plans were set up using three arcs, with angles ranging from 179° to 310°. The RAD plans employed two arcs with the same angular spacing, accompanied by four static fields. The medial and lateral static fields were set up with angles between [315°;330°] and [130°;150°], respectively.

**Results:** For both VMAT and RAD dose plans, the target coverage was acceptable. Generally, RAD plans had a better coverage of CTVp_breast/CTVp_chestwall than VMAT plans and the Dmean to the OAR was equivalent or lower.

For the heart, the contralateral breast and the contralateral lung the Dmean was 16.6%, 22.1%, and 12.7% lower, respectively, compared to the VMAT plans.

The Dmean calculated for ipsilateral lung was 3.3% higher. This slight increase in dose is correlated to an increase in target coverage and is consistent with the RAD plans having a more tangentially opposing dose profile.

The RAD plans demonstrated better coverage of the CTVp_breast/CTVp_chestwall compared to the VMAT plans, as illustrated in Figure 1.

**Conclusion:** RAD is a relatively new program and the full potential of the new optimizer is yet to be seen. However, even at this stage, we can already observe significant dose reduction for OARs. This study will be expanded with an investigation of the robustness of both the VMAT and the RAD plans.

Reference list

1. Nielsen, A.W.M., L.B.J. Thorsen, D. Özcan, L.W. Matthiessen, E. Maae, M.L.H. Milo, et al. Internal mammary node irradiation in 4541 node-positive breast cancer patients treated with newer systemic therapies and 3D-based radiotherapy (DBCG IMN2): a prospective, nationwide, population-based cohort study. Lancet Reg Health Eur, 2025. 49: p. 101160 DOI: 10.1016/j.lanepe.2024.101160.

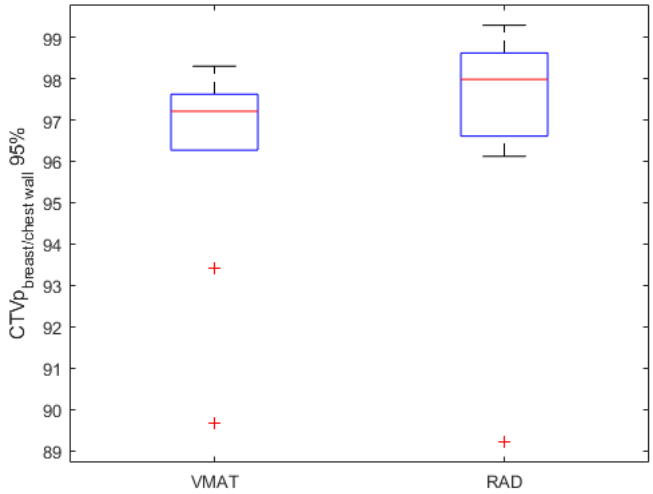


Figure 1. V95% for $CTVp_{breast/chestwall}$ in VMAT and RAD plans.

# First clinical motion-including prostate and bladder dose reconstruction in real-time during prostate SBRT delivery

*Karolina A Klucznik(1), Thomas Ravkilde(2), Simon Skouboe(1), Paul Keall(3) , Laura Happersett(4), Hai Pham(4), Brian Leong(4), Pengpeng Zhang(4), Grace Tang(4), Per R Poulsen(1,2)*

*(1)Danish Centre for Particle Therapy, Aarhus University Hospital, Aarhus, Denmark*
*(2)Department of Oncology, Aarhus University Hospital, Aarhus, Denmark*
*(3)Image X Institute, Sydney Medical School, University of Sydney, Australia*
*(4)Department of Medical Physics, Memorial Sloan Kettering Cancer Center, New York, US*

*Corresponding author: Karolina A Klucznik*
*E-mail: Karo.klucznik@rm.dk*

## Introduction

Radiotherapy doses can be distorted due to organ motion, resulting in compromised target coverage and variable normal tissue doses. Real-time prostate motion monitoring, being now available on conventional linear accelerators using research software, can be used for patient position corrections during treatment. However, treatment outcomes are more directly linked to the actual delivered dose - currently unavailable in real-time. In this study the first real-time, online motion-including dose reconstruction was performed during prostate stereotactic body radiotherapy (SBRT).

## Methods

Twenty patients received prostate SBRT of 40 or 35Gy in five fractions delivered using volumetric modulated arc therapy (VMAT). The planning criteria were: $D_{95\%}$ between 93.8% and 100% and $D_{min}$>93.8% for the prostate PTV, $D_{95\%}$=100% for the prostate CTV, and $V_{36Gy}$<10% for the bladder.

During prostate SBRT at the Memorial Sloan Kettering Cancer Center, the prostate motion is routinely monitored using MV-kV image pairs acquired every 20deg of gantry rotation, and the patient position is adjusted if the prostate position error exceeds 1.5mm (MV-kV guidance [1]). The in-house developed software DoseTracker [2] was integrated into this prostate SBRT workflow and utilized the prostate positions online for real-time motion-including prostate and bladder dose reconstruction during treatment.

For each fraction the motion-induced dose distortions were quantified as differences between delivered and planned prostate CTV $D_{95\%}$ ($\Delta D_{95\%}$) and bladder $V_{36Gy}$ ($\Delta V_{36Gy}$). Treatments without intrafractional patient repositioning were simulated retrospectively to assess the effectiveness of MV-kV guidance in mitigating motion. Real-time dose reconstruction was validated against treatment planning system (TPS) calculations by emulating motion with multiple isocenter shifts [3].

## Results

The mean (standard deviation, range) motion-induced CTV $\Delta D_{95\%}$ was -0.5% (1.0%, [-4.3, +1.6]%) under MV-kV guidance and the lowest CTV $D_{95\%}$ was 95.8% (Figure 1a, blue boxplots). Motion reduced the CTV

$D_{95\%}$ by 2% or more at five fractions. The bladder dose constraint $V_{36Gy}$<10% was fulfilled for all fractions (Figure 1b, blue boxplots).

Without MV-kV guidance the motion-induced prostate CTV $\Delta D_{95\%}$ increased in magnitude to -1.3% (5.0%, [-42.5,+1.8]%) and the bladder $\Delta V_{36G}$ to +0.5% (1.5%, [-5.8,+4.6]%). The CTV $\Delta D_{95\%}$ exceeded 2% for 13 fractions and for one fraction the bladder $V_{36Gy}$<10% dose constraint was violated.

The root-mean-square error between real-time calculated doses and TPS doses was 0.9% for prostate CTV $D_{95\%}$ and 0.3% for bladder $V_{36Gy}$.

**Conclusion**

This study presents the world's first online, real-time, motion-including dose reconstruction for prostate and bladder during prostate SBRT. MV-kV guidance effectively mitigated severe motion-induced dose distortions.

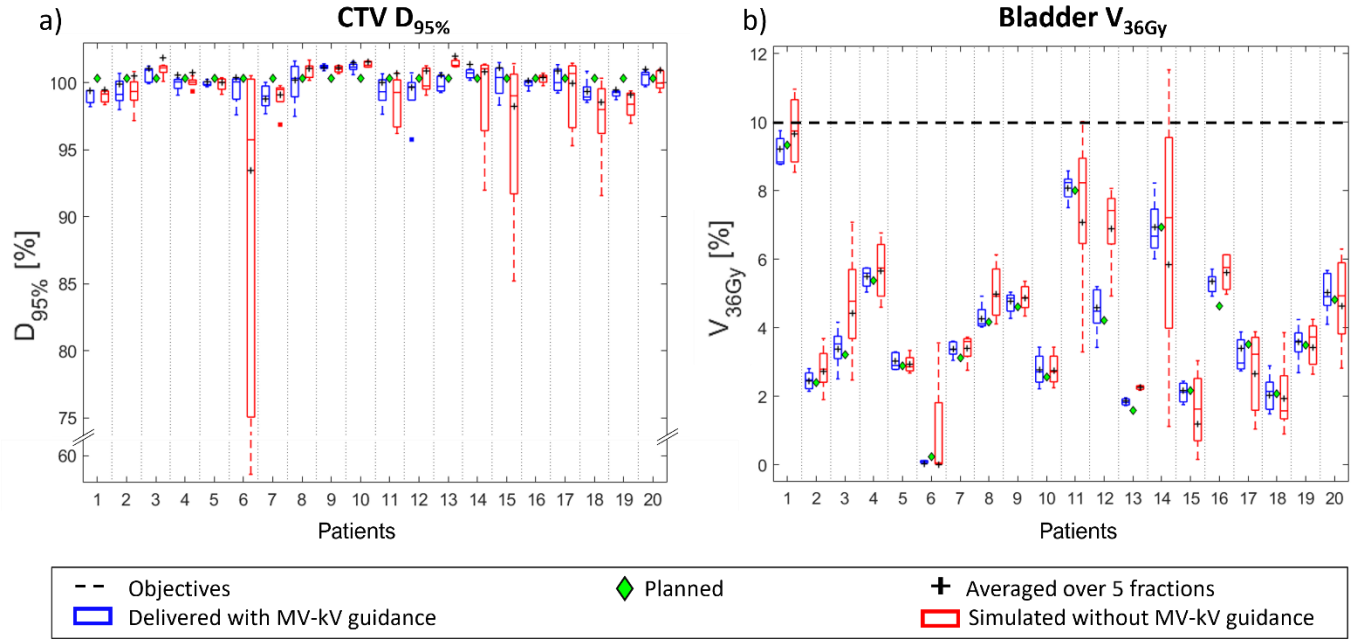


*Figure 1: Prostate CTV $D_{95\%}$ (left) and bladder $V_{36Gy}$ (right). The blue boxes correspond to the delivered dose distributions with MV-kV guidance and the red boxes represent the simulated treatments without intratreatment image guidance. The green diamonds show the planned (without motion) values and the black crosses the values averaged over all 5 fractions.*

References

[1] Hunt MA, Sonnick M Fau - Pham H, Pham H Fau - Regmi R, Regmi R Fau - Xiong J-p, Xiong Jp Fau - Morf D, Morf D Fau - Mageras GS, et al. Simultaneous MV-kV imaging for intrafractional motion management during volumetric-modulated arc therapy delivery. J Appl Clin Med Phys. 2016.
[2] Ravkilde T, Skouboe S, Hansen R, Worm E, Poulsen PR. First online real-time evaluation of motion-induced 4D dose errors during radiotherapy delivery. Medical Physics. 2018;45:3893-903
[3] Poulsen PR, Cho B, Keall PJ. Real-time prostate trajectory estimation with a single imager in arc radiotherapy: a simulation study. Physics in Medicine and Biology. 2009;54:4019-35

# An Assessment of the SIRMIO Beamline's Feasibility for pMBRT Experiments with Heterogeneous and Homogeneous Target Doses

Fardous Reaz[1,2] [fardous@clin.au.dk],
Ze Huang[3]
Marco Pinto[3]
Katia Parodi[3]
Niels Bassler[1,2]

1. Department of Clinical Medicine, Aarhus University, Aarhus, Denmark.
2. Danish Centre for Particle Therapy, Aarhus University Hospital, Aarhus, Denmark.
3. Department of Medical Physics, Ludwig-Maximilians-Universität München (LMU Munich), Munich, Germany.

**Introduction:** Spatially Fractionated Radiotherapy (SFRT) has shown potential in sparing healthy tissue. Proton minibeam radiation therapy (pMBRT), a form of SFRT, enhances this benefit by simultaneously exploiting the reduced integral dose of proton therapy and delivering a highly heterogeneous dose in normal tissue with a uniform target dose. This promising approach can enhance the therapeutic window in cancer treatment, potentially reducing normal tissue toxicity while maintaining or improving tumor control compared to conventional wide-field irradiation. However, successful clinical integration of pMBRT requires comprehensive investigations to establish the relationship between various pMBRT parameters and their associated biological effects. Such experiments are primarily dependent on small animal models. Therefore, a state-of-the-art small animal irradiation platform like SIRMIO developed at LMU Munich (lmu.de/sirmio), capable of delivering precisely controlled spatially fractionated dose, is highly desirable for advancing preclinical pMBRT research and facilitating its eventual clinical translation.

**Methods:** This study examined the characteristics of the SIRMIO beamline to determine its ability to provide sufficient dose contrast for pMBRT. We used the Geant4 Monte Carlo tool to investigate the generation of spatially fractionated dose profiles. The dose fractionation relies on the precise positioning of the irradiated subject. The proton beams are simulated using experimentally validated phase-space data from SIRMIO. We studied two configurations: one without a multislit collimator (MSC), and one using a 30-mm thick brass collimator. For both configurations, we examined center-to-center (CTC) of 3~mm, 4~mm, and 5~mm, with a constant 1~mm slit width for the MSC. In addition, we investigated the possibilities of delivering a homogeneous target dose with interlacing beams.

**Results:** Our results demonstrate that the SIRMIO beamline can effectively generate spatially fractionated dose profiles with varying CTC. Without MSC, sufficient dose contrast for pMBRT can be achieved with CTC of 4 mm and above, as evidenced by peak-to-valley dose ratios (PVDR) of 3.4 and 6.6 for 4 mm and 5 mm CTC, respectively. The incorporation of an MSC further enhances dose contrast, achieving PVDR of 11.3, 20.7, and 28.7 for 3 mm, 4~mm, and 5 mm CTC, respectively. Furthermore, our exploration of interlacing beams demonstrated

SIRMIO's capability to achieve a uniform target dose while maintaining dose contrast in normal tissue, aligning with the requirements for pMBRT experiments.

**Conclusions:** The findings of this study support the potential of the SIRMIO beamline for pMBRT studies, warranting subsequent experimental validation.

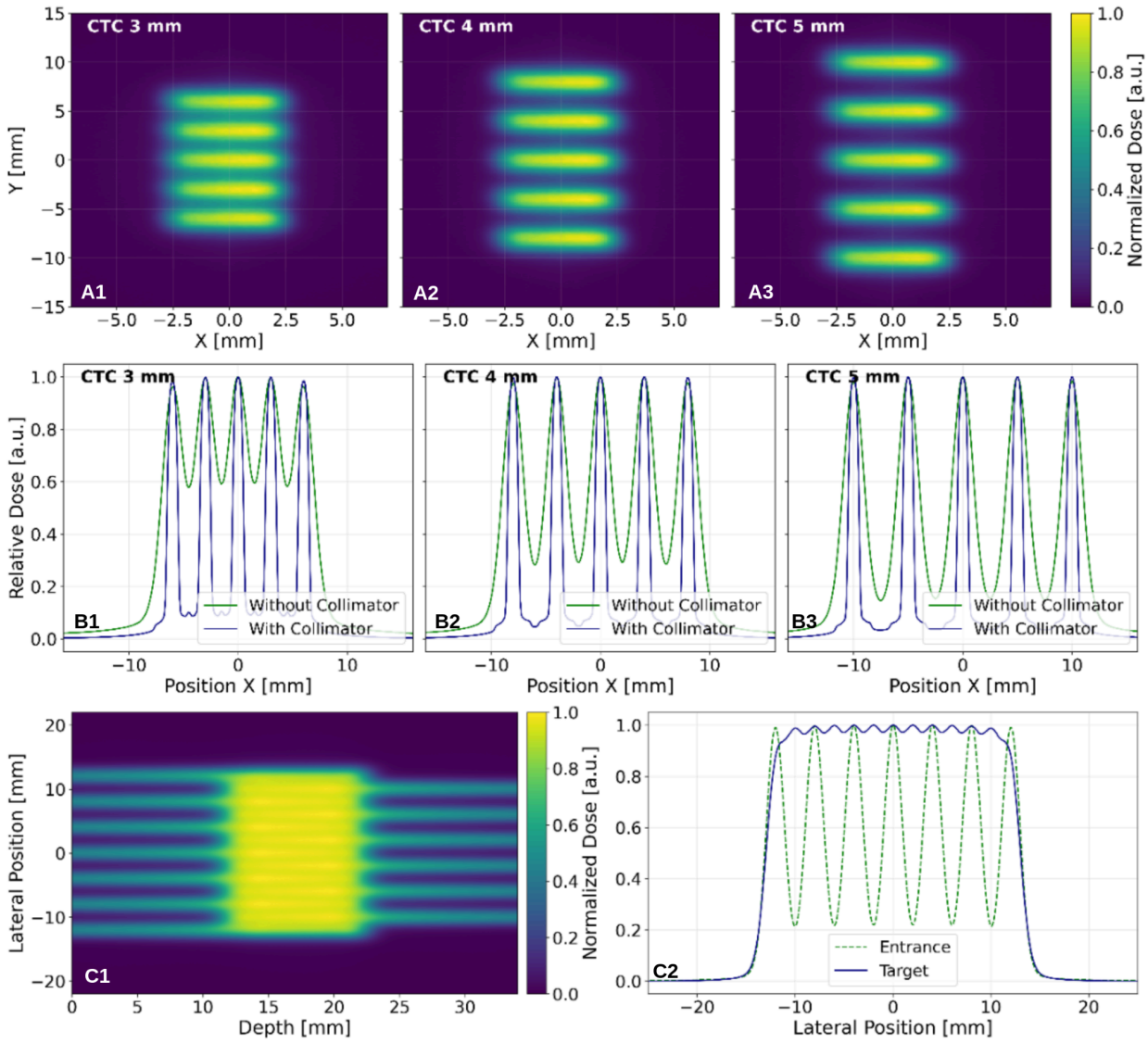


**Figure 1:** The top row (A1-A3) shows 2D simulated dose profiles without an MSC for CTC of 3 mm, 4 mm, and 5 mm. The middle row (B1-B3) compares 1D dose profiles with and without an MSC for the corresponding CTC. The bottom row (C1-C2) illustrates the concept of interlacing beams. C1 shows the resulting 2D dose distribution, while C2 presents the 1D dose profiles at the beam entrance and target depth, demonstrating a quasi-homogeneous dose at the target while maintaining sharp dose contrast at the entrance.

# First in-vivo application of the SIRMIO platform for precision, image-guided small animal IMPT proton irradiation

Jonathan Bortfeldt[1], Julie Lascaud[1], Munetaka Nitta[1], Marco Pinto[1], Peter G. Thirolf[1], Ze Huang[1], Eero Lönnqvist[1], Babak Sharifi[1], Guyue Hu[1], Margarita Kozak[1], Davide Boscaini, Francesco Evangelista[1], Giulio Lovatti[1], Prasannakumar Palaniappan[1], Marco Riboldi[1], Niels Bassler[2], Per Poulsen[2], Jasper Nijkamp[2], Brita Sørensen[2], Katia Parodi[1,*]

[1] Ludwig-Maximilians-Universität München (LMU), Department of Medical Physics, Munich, Germany

[2] Danish Centre for Particle Therapy (DCPT), Aarhus, Denmark

*Presenting author, Email: Katia.Parodi@physik.uni-muenchen.de

**Introduction** Despite the wide adoption of intensity modulation and image-guidance in clinical proton therapy, small animal experiments are still primarily performed with passively shaped proton fields and limited on-board imaging. To this end, we have developed the innovative SIRMIO platform (www.lmu.de/sirmio) at LMU. It performs proton spot scanning by delivering a horizontal, actively focused beam of ~1 mm size (sigma in air at focal point) at an adjustable energy of 20 – 50 MeV (degraded from the lowest energy beam of a clinical facility, typically 70 MeV) to an upright target, shifted to different positions with remote-controlled stages. On-board imaging solutions feature proton radiography with two Timepix3 detectors for target alignment and water-equivalent-thickness (WET) measurements, along with in-beam positron emission tomography (PET) with a spherical scanner for in-vivo verification. This contribution presents the first in-vivo application of SIRMIO for a pilot lung toxicity study in a cohort of 9 mice, performed at DCPT in fall 2024.

**Material and Methods** Few days before treatment, animals were imaged at a research spectral cone-beam computed tomography (CBCT) system in the treatment upright position. Treatments were planned with a research version of μRayStation using as input experimentally validated phase space data of the SIRMIO beamline. CT numbers were converted to density and stopping power based on a calibration phantom and previously evaluated mouse data, considering different lung densities. The actual lung WET was then evaluated with 12 equally spaced (over 360°) on-board proton radiographies just before treatment to decide on the plan for delivery. These radiographies were also used for setup corrections based on 2D-3D co-registration to the planning CBCT. Plans with median doses (D50%) of 30-50 Gy(RBE) were finally delivered to different lung volumes. In-beam PET provided 3D images continuously updated every 60s for comparison with predictions extracted from the research version of μRayStation. Post-radiation toxicity assessment is still ongoing with periodic follow-up spectral CBCT images.

**Results** On-board imaging, position correction and spot scanning irradiation could be done for each anesthetized mouse within ~ 60 min. Representative examples will be shown.

**Conclusion** We have demonstrated the first in-vivo application of a novel image-guided IMPT proton irradiation platform which can open new avenues in precision preclinical research.

**Acknowledgement** ERC/DFG grants 725539/455550444, past LMU SIRMIO project members, external collaborators (E. Traneus, R. Nilsson, K. Lauber, H. Palmans, T. Yamaya, J. Gordon, C. Oancea, C. Granja, F. Becker) and teams from PSI/HZB/TPTC/CNAO/HIT/PSI for early SIRMIO component tests.

**Treatment plan** **Post-treatment**

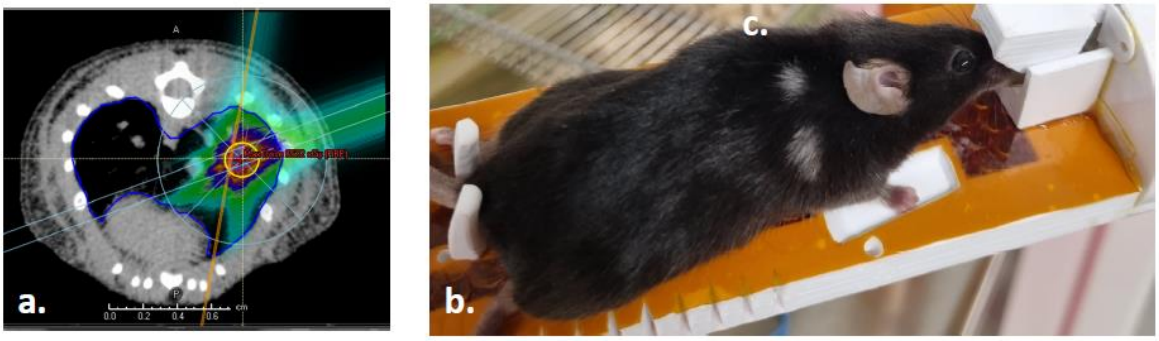


Figure: Illustrative example for one of the mice included in the pilot study: (a) planned IMPT treatment and (b) picture of the mouse on the mouse holder prior to the follow-up CBCT scan, 5 months post-treatment, showing two depigmented spots in the irradiated areas.

**Burden of dysphagia after changes in high-dose CTV margins for head and neck cancer patients**

Ruta Zukauskaite[1], Jesper Grau Eriksen[2], Jørgen Johansen[1], Eva Samsøe[3], Morten Horsholt Kristensen[2] , Lars Johnsen[4], Camilla Kjaer Lonkvist[5], Cai Grau[6], Jens Overgaard [2], Christian Rønn Hansen[4,6,7]

**Affiliations**

1) Department of Oncology, Odense University Hospital, Odense, Denmark;
2) Department of Experimental Clinical Oncology, Aarhus University Hospital, Aarhus, Denmark;
3) Zealand University Hospital, Department of Oncology, Næstved, Denmark;
4) Odense University Hospital, Laboratory of Radiation Physics, Odense, Denmark;
5) Department of Oncology, Herlev and Gentofte Hospital, University of Copenhagen, Herlev, Denmark
6) Danish Centre for Particle Therapy, Aarhus University Hospital, Aarhus, Denmark
7) Odense University Hospital, Laboratory of Radiation Physics, Odense, Denmark;
8) University of Southern Denmark, Department of Clinical Research, Odense, Denmark

**Purpose**: Radiotherapy for head and neck cancer aims to maximise cure rates while minimising late toxicities such as dysphagia. One key factor influencing local disease control and dysphagia risk is the selection of margins for microscopic disease spread. This study evaluates how different GTV to high-dose CTV (CTV1) margins impact on dysphagia in a large cohort of consecutively treated patients.

**Material/Methods:** Data of patients treated with primary IMRT-based radiotherapy for oro-/hypopharyngeal and laryngeal squamous cell carcinoma at three national treatment centres between 2010-2015 were retrospectively collected. Treatment planning followed two DAHANCA guideline periods: pre-2013, where GTV-CTV1 margins varied (0-10mm, or above), and post-2013, where a normalised isotropic 5mm margin was used nationally. Complete DICOM treatment plans were collected for 1913 patients. GTV-CTV1 margins were quantitatively assessed by calculating the median surface distance from GTV to CTV1. Clinical parameters were prospectively collected. Dysphagia was graded using a modified LENT-SOMA scale: 0) no dysphagia; 1) symptomatic, able to eat regular diet; 2) symptomatic and altered eating/swallowing, soft food; 3) symptomatic and altered eating/swallowing, only fluid food; 4) severely altered eating/swallowing; tube feeding or hospitalisation; urgent intervention indicated. The highest dysphagia score was chosen for analysis of individual patients during a 5-year follow-up. Dysphagia scores were dicotomized into grade 0-1 or ≥2 dysphagia for logistic regression to identify predictors influencing pronounced dysphagia after curative radiotherapy. They included: sex, smoking status, tumour site, radiotherapy dose, GTV volume (log-transformed), GTV-CTV1 margin, and use of radiosensitiser and chemotherapy.

**Results:** Dysphagia data were available for 1706 patients (89%). The median GTV-CTV1 margin was 9.0 mm (IQR 0.0-9.7) in 2010-2012 and 4.7 mm (IQR 4.0-5.5) in 2013-2015. The severity of dysphagia was more pronounced in patients treated during 2010-2012, i.e. grade 0-1 dysphagia 44% and 56%, grade 2-4 dysphagia 52% and 48 % during the two treatment periods, respectively (p=0.003). Predictors of pronounced dysphagia included tumour localisation other than oropharyngeal p16+ carcinomas (p=0.001), larger GTV (OR 1.7; p<0.001), and larger GTV-CTV1 margin (OR of 1.026 per mm; p=0.048). Male sex, non/previous smoking status, application of chemotherapy were associated with less severe dysphagia (Figure 1).

**Conclusion**: This real-world data analysis underscores that tumour volume and GTV-CTV1 margin are dominant geometric factors influencing dysphagia risk following curative

radiotherapy. A randomised trial testing further reduced margins compared to the standard may create the evidence.

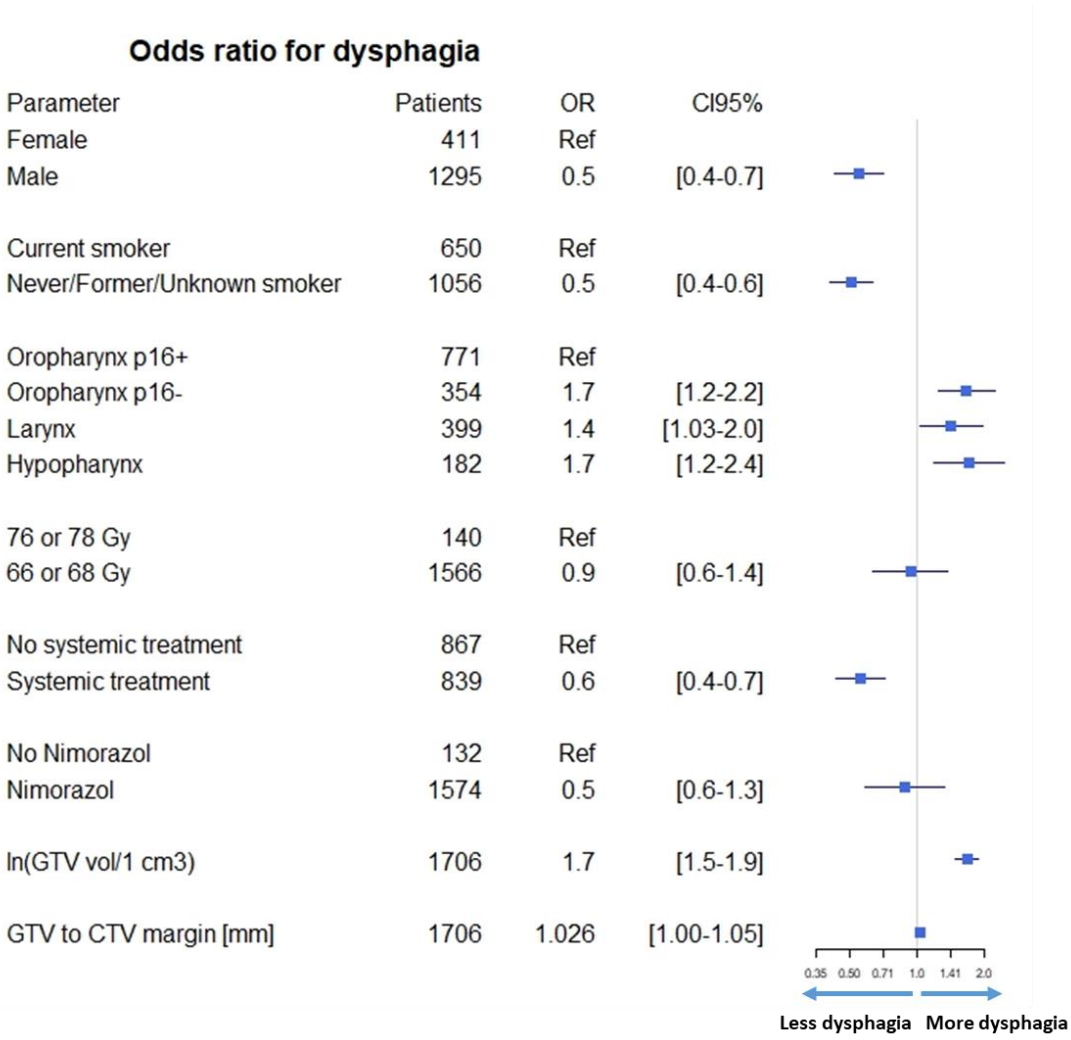

**Impact of GTV-to-CTV margin reduction on late toxicity in bilateral oropharyngeal radiotherapy: A treatment planning study**

Christian Rønn Hansen[1,2,3], Anders Bertelsen[1], Irene Hazell[1], Jørgen Johansen[3,4], Jens Overgaard[5], Jesper Grau Eriksen[5,6], Ruta Zukauskaite[1,3]

**Affiliations**

1) Laboratory of Radiation Physics, Odense University Hospital, Odense, Denmark;
2) Danish Centre for Particle Therapy, Aarhus University Hospital, Aarhus, Denmark
3) University of Southern Denmark, Department of Clinical Research, Odense, Denmark
4) Department of Oncology, Odense University Hospital, Odense, Denmark;
5) Department of Experimental Clinical Oncology, Aarhus University Hospital, Aarhus, Denmark;
6) Department of Oncology, Aarhus University Hospital, Aarhus, Denmark;

**Purpose**: Radiotherapy for head and neck cancer aims to irradicate the tumour while minimising damage to the organs at risk responsible for late toxicities such as dysphagia and xerostomia. Recent retrospective studies suggest that larger GTV to CTV1 margins have limited impact on local control [1, 2], while expanded treatment volumes increase the risk of late toxicity. Therefore, this study aimed to quantify the potential toxicity reduction achieved by omitting the standard 5 mm GTV-CTV1 margin in oropharyngeal cancer patients.

**Material/Methods**: Thirty consecutively treated oropharyngeal cancer patients receiving bilateral curative radiotherapy in 2023 were retrospectively analysed. All were planned and treated per DAHANCA 2020 guidelines with a 5 mm GTV-CTV1 margin [3]. Alternative treatment plans were generated with reduced margins; CTV1 being equal to GTV, and CTV2 was reduced from 10 to 5 mm. CTV to PTV margin remained at 3 mm in all plans. All treatment plans were generated using Pinnacle Autoplan [4], ensuring that margin reduction was the only variable altered [5].

Normal tissue complication probability (NTCP) for late grade 2+ dysphagia and grade 3+ xerostomia was estimated using the same models as for the DAHANCA35 proton trial [6, 7]. DVHs were analysed in MATLAB. Baseline toxicity was assumed to be zero, providing a conservative estimate of potential reductions.

**Results**: The median NTCP reduction for dysphagia in the reduced-margin plans was 6.0 percentage points (IQR: 3.4–8.5). For xerostomia, reductions were 0.1 percentage points (0.0–0.3).

Significant dose reductions (4–5 Gy) were observed in organs adjacent to the primary target, including the oral cavity, supraglottic larynx, and superior/mid-pharyngeal constrictor muscles (PCM). The parotid and submandibular glands showed mean dose reductions of 2.2 Gy and 5.1 Gy, respectively. No dose reductions were observed for PCM low, thyroid, or esophagus, all located far from the GTV. The mean DVH for the oral cavity demonstrated a 5.4 Gy reduction, statistically significant between 25–65 Gy, as shown in the figure.

The size of the NTCP reduction for dysphagia was comparable to the DAHANCA35 proton pilot trial (5.3 percentage points) [6].

**Conclusion**: This planning study quantifies the potential NTCP reduction from margin reduction in bilaterally treated oropharyngeal cancer. Substantial dose reductions were observed in structures close to the primary tumour, demonstrating a clinically meaningful reduction in late dysphagia risk.

Figure

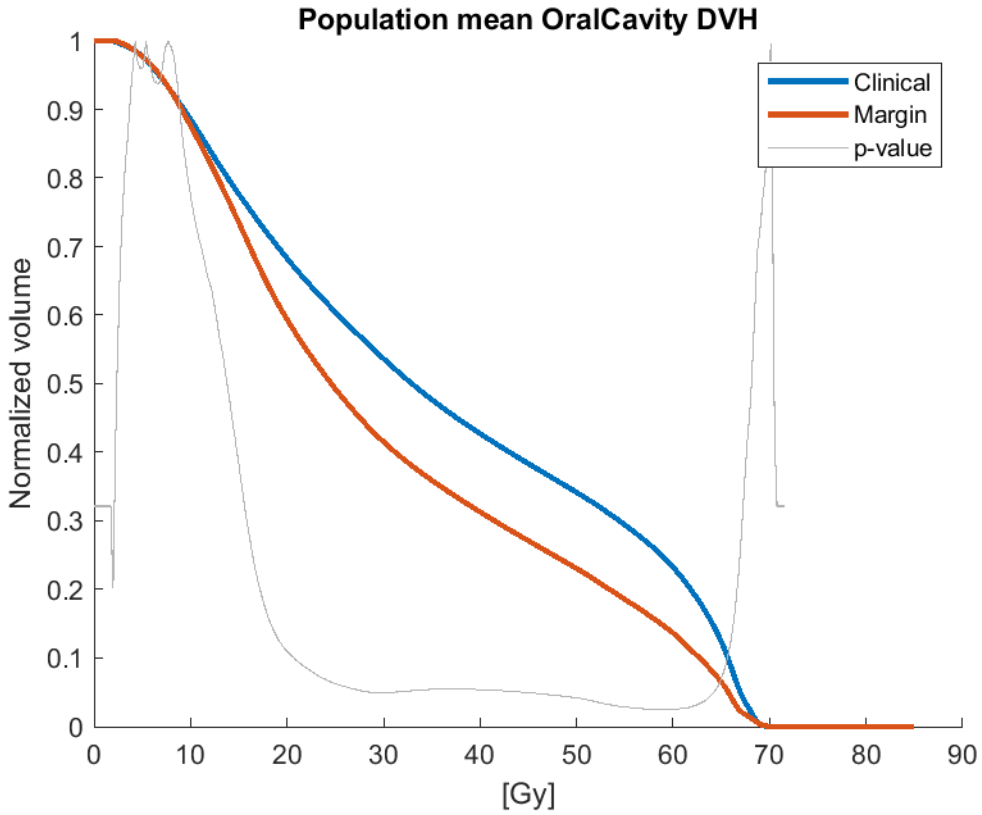


**References**

[1] Zukauskaite R, Kristensen MH, Eriksen JG, Johansen J, Samsøe E, Johnsen L, et al. Comparison of 3-year local control using DAHANCA radiotherapy guidelines before and after implementation of five millimetres geometrical GTV to high-dose CTV margin. Radiother Oncol. 2024;196:110284.
[2] Zukauskaite R, Hansen CR, Grau C, Samsoe E, Johansen J, Petersen JBB, et al. Local recurrences after curative IMRT for HNSCC: Effect of different GTV to high-dose CTV margins. Radiother Oncol. 2018;126:48-55.
[3] Jensen K, Friborg J, Hansen CR, Samsoe E, Johansen J, Andersen M, et al. The Danish Head and Neck Cancer Group (DAHANCA) 2020 radiotherapy guidelines. Radiother Oncol. 2020;151:149-51.
[4] Hansen CR, Bertelsen A, Hazell I, Zukauskaite R, Gyldenkerne N, Johansen J, et al. Automatic treatment planning improves the clinical quality of head and neck cancer treatment plans. Clin Transl Radiat Oncol. 2016;1:2-8.
[5] Hansen CR, Crijns W, Hussein M, Rossi L, Gallego P, Verbakel W, et al. Radiotherapy Treatment plannINg study Guidelines (RATING): A framework for setting up and reporting on scientific treatment planning studies. Radiother Oncol. 2020;153:67-78.
[6] Hansen CR, Jensen K, Smulders B, Holm AIS, Samsoe E, Nielsen MS, et al. Evaluation of decentralised model-based selection of head and neck cancer patients for a proton treatment study. DAHANCA 35. Radiother Oncol. 2023:109812.
[7] Van Den Bosch L, Van Der Schaaf A, Van Der Laan HP, Hoebers FJP, Wijers OB, Van Den Hoek JGM, et al. Comprehensive toxicity risk profiling in radiation therapy for head and neck cancer: A new concept for individually optimised treatment. Radiother Oncol. 2021;157:147-54.

**Impact of Low-Dose Contrast-Enhanced MRI for Glioblastoma Delineation in Adaptive Radiotherapy**

Faisal Mahmood[1,2], Uffe Bernchou[1,2], Frederik Severin Gråe Harboe[3], Anders Bertelsen[1], Anne Bisgaard[1], Rasmus Christiansen[1], Bahar Celik[1], Elisabeth Kildegaard[1], Tine Schytte[2,4], Rikke Hedegaard Dahlrot[2,4]

[1]Laboratory of Radiation Physics, Department of Oncology, Odense University Hospital, Odense, Denmark
[2]Department of Clinical Research, University of Southern Denmark, Odense, Denmark
[3]Department of Radiology, Odense University Hospital, Odense, Denmark
[4]Department of Oncology, Odense University Hospital, Odense, Denmark

**Introduction**

Glioblastomas can change during the course of radiotherapy [1]. MRI-guided radiotherapy using an MRI-linac enables daily adaptation, potentially improving treatment precision. Standard practice involves gadolinium-based contrast agent (GBCA)-enhanced MRI for glioblastoma delineation, but concerns remain regarding GBCA retention and the potential long-term effects of repeated administration [2]. This study investigates the impact of a low-dose GBCA MRI protocol on target definition for adaptive radiotherapy in glioblastoma.

**Materials and methods**

Nine patients eligible for post-operative radiotherapy were enrolled in the MOMENTUM study [3] and treated with hypofractionated radiotherapy (34 Gy in 10 fractions, 5 days per week) using a 1.5 T MRI-linac. Daily imaging included a clinical T1-weighted 3D gradient-echo scan, with gadobutrol (GBCA) administered according to the following dosing scheme: F(1)-N(2)-H(3)-N(4)-F(5)-N(6)-H(7)-N(8)-F(9)-N(10), where F = full-dose (0.1 mmol/kg), H = half-dose (0.05 mmol/kg), and N = no-dose; fraction numbers are indicated in parentheses. In the on-line workflow, the gross tumour volume (GTV) was adapted by an oncologist for fractions where full- or half-dose GBCA was administered. The updated plan was then used as a reference for the subsequent non-contrast fraction, where the GTV was transferred rigidly without modification.

In this retrospective analysis, all 45 MRI scans (9 patients, 5 fractions each) acquired with either full- or half-dose GBCA were presented in random order to a blinded neuroradiologist (FSGH) for GTV delineation. To account for potential longitudinal tumour volume changes, delineations from full-dose scans were averaged across adjacent time points before comparison with half-dose scans. Specifically, the mean GTV volume from fractions 1 and 5 was compared with fraction 3; similarly fractions 5 and 9 compared with fraction 7. (Objective threshold-based semi-automated delineation and 5-point likert quationnaire were also perfomed, but not presented in this abstract).

**Results**

Results indicate a systematic underestimation of GTV with half-dose contrast, suggesting a consistent reduction in tumour volume delineation compared to the full-dose reference (Figure 1A). Furthermore, smaller tumours tend to have greater variability and larger percentage discrepancies, potentially reflecting reduced lesion conspicuity in half-dose scans. In one half-dose scan a small lesion was completely missed
(Figure 1B).

**Conclusions**

GBCA-enhanced MRI is essential for adaptive MRI-guided radiotherapy of glioblastoma. While half-dose MRI may suffice for monitoring, full-dose is preferred for adaptation, especially in small lesions. A feasible low-dose workflow could include full-dose MRI at the first fraction and mid-treatment, with optional half-dose imaging near the end. For small tumours, frequent full-dose imaging is recommended.

References


[1] Bernchou U et al. Evolution of the gross tumour volume extent during radiotherapy for glioblastomas. Radiother Oncol. 2021, PMID: 33848564

[2] Tweedle MF. Gadolinium Retention in Human Brain, Bone, and Skin. Radiology. 2021, PMID: 34128728

[3] de Mol van Otterloo SR et al. The MOMENTUM Study: An International Registry for the Evidence-Based Introduction of MR-Guided Adaptive Therapy. Front Oncol. 2020, PMID: 33014774


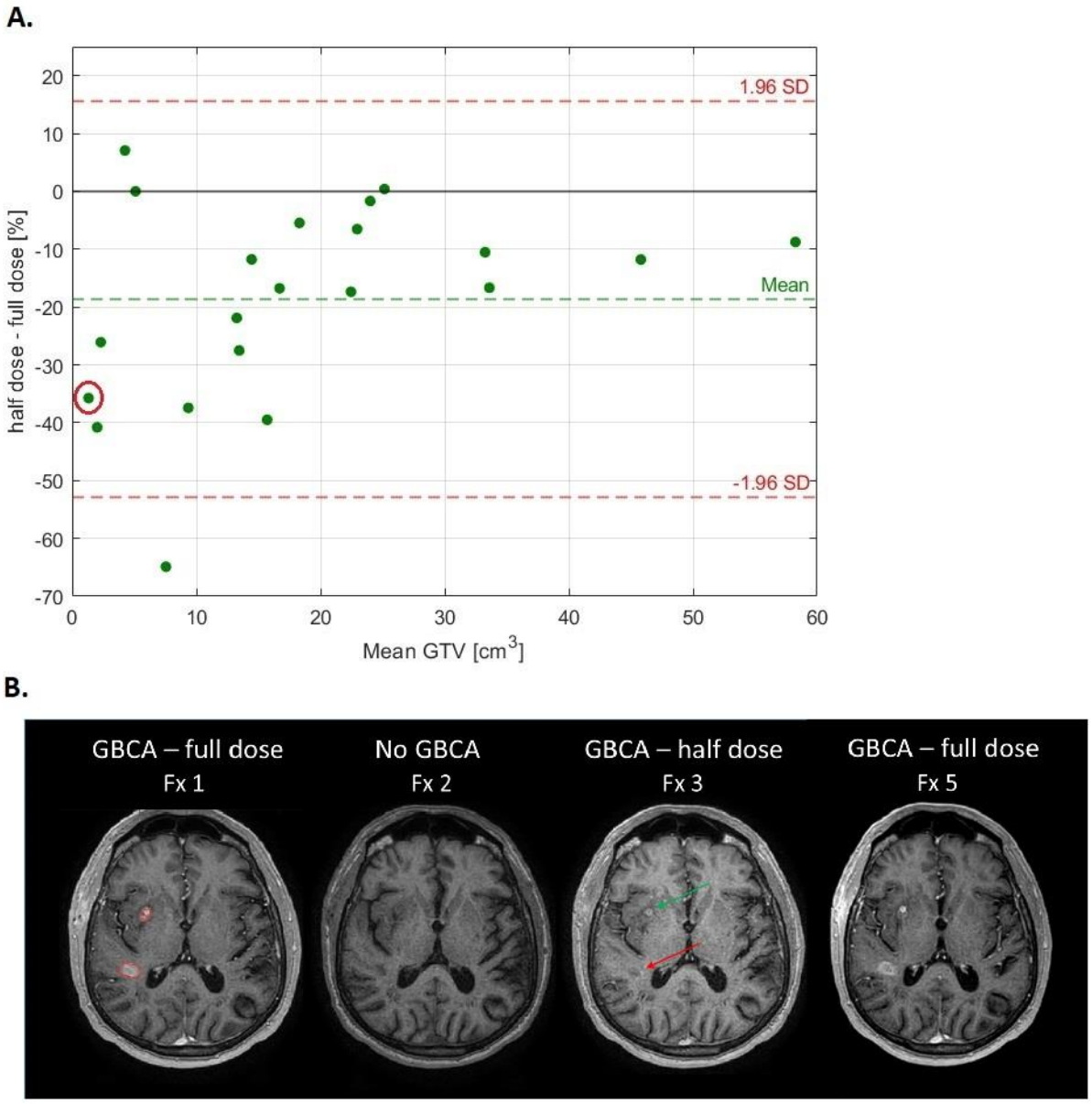


*Figure 1: **A**. The Bland-Altman plot illustrates the agreement between half-dose and full-dose GBCA-enhanced MRI for delineated GTV volume. The y-axis represents the percentage difference in GTV volume between half-dose and full-dose scans, while the x-axis shows the mean GTV volume between the two methods. The limits of agreement, defined as ±1.96 standard deviations (red dashed lines), show a wide spread, with differences ranging from approximately -65% to +15%. **B.** This patient had two small lesions, one of which was missed (red arrow) by the radiologist on the half-dose scan from fraction 3 due to low contrast enhancement. This was not related to actual tumour reduction, later confirmed with full-dose image at fraction 5. The second comparison with half-dose sat fraction 7 is indicated with a red circle in the Bland-Altman plot.*

**Partial tumor boosting in definitive radiotherapy of soft tissue sarcoma**

Scott Grov Diesen[1,2*], Sander Ellefsen[1,2*], Jonas Asperud[3], Taran Paulsen Hellebust[3], Tord Hompland[2,4], Kjetil Boye[5], Ivar Hompland[5], Eirik Malinen[1,2†]

*1: Department of Radiation Biology, Institute for Cancer Research, Oslo University Hospital, Norway*

*2: Department of Physics, University of Oslo, Norway*

*3: Department of Medical Physics, Oslo University Hospital, Norway*

*4: Department of Core Facilities, Institute for Cancer Research, Oslo University Hospital, Norway*

*5: Department of Oncology, Oslo University Hospital, Norway*

*† eirik.malinen@fys.uio.no*

**Shared first authorship*

**Introduction**
Proton therapy (PT) offers superior normal tissue sparing compared to conventional X-ray therapy (XRT) and may be advantageous for patients with soft tissue sarcoma (STS). However, achieving local control in inoperable cases requires very high doses that exceed normal tissue tolerance when using a homogeneous target dose prescription. This highlights the need for more advanced delivery strategies in definitive radiotherapy for STS. Here, we explore a new, hypofractionated partial boost strategy that may increase local control in STS patients.

**Materials and methods**
Local control data from six STS radiotherapy trials and published radiosensitivity data were used to develop and calibrate a tumor control probability (TCP) model, which was then applied to evaluate the new strategy. Treatment plans for 10 inoperable STS patients were retrospectively collected, including clinical target volume (CTV) and gross tumor volume (GTV). A boost volume (BV) was defined applying by a 1 cm inverse margin from the GTV. The CTV dose followed a standard 2 Gy x 33 fraction schedule, while GTV and BV doses were escalated to 1.2x and 1.5x CTV dose based on TCP optimization and clinical considerations. PT and XRT plans were optimized for 20 fractions including QUANTEC-based normal tissue constraints in RayStation (RaySearch Laboratories AB, Sweden).

**Results**
Tumor sites in the selected patients included the thorax, abdomen, and pelvis, with tumor volumes ranging from 40 to 2100 $cm^3$. The estimated mean TCP from the standard treatment and the boost strategy was 0.53 and 0.84, respectively. Treatment planning confirmed that the prescribed target dose levels were achievable in all patients using both PT and XRT (Figure 1), though XRT exhibited poorer target dose conformity. PT had a higher mean gradient index (0.42 vs. 0.3) and delivered lower doses to most organs at risk, though site heterogeneity limited systematic dose-volume comparison with XRT.

**Conclusions**
The proposed partial boosting strategy may be effectively implemented with the desired criteria and is expected to increase local control in patients with inoperable STS. PT appears to offer superior treatment plans, but the new strategy may generally require careful image guidance and

monitoring to ensure that the boost does not impact critical tissues. We plan to evaluate the boost strategy in a clinical trial, aiming to start within 2025.

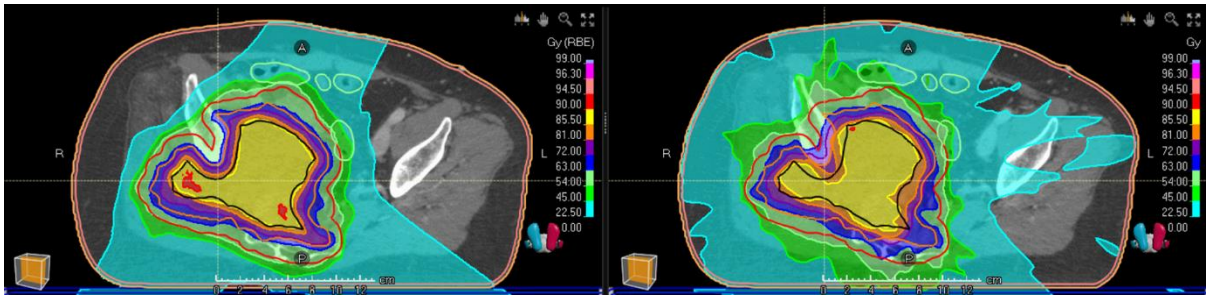


***Figure 1**: Proton (left)- or X-ray (right; VMAT) therapy including partial tumor boosting for a patient with inoperable STS. The proton plan yields high target conformity and a greater dose fall-off compared to the X-ray plan.*

**Simulation-free online adaptive radiotherapy for patients with metastatic spinal cord compression – a feasibility study**

Sandt LJ (1), Åström LM (1), Nielsen AM (1), Giannoulis E (2), Rechner LA (1), Edmund J (1), Persson GF (1,3).
E-mail: Lisette.Juul.Sandt@regionh.dk

(1) Department of Oncology, Copenhagen University Hospital – Herlev and Gentofte, Copenhagen, Denmark.
(2) Department of Health Technology, Technical University of Denmark, Roskilde, Denmark.
(3) Department of Clinical Medicine, Faculty of Health Sciences, University of Copenhagen, Copenhagen, Denmark.

**Introduction:** Metastatic spinal cord compression (MSCC) affects one in ten patients with spinal metastases and requires urgent treatment. Palliative radiotherapy aims to relieve pain and prevent the progression of neurological symptoms. Acquisition of the planning CT for target contouring and dose planning often involves lengthy stays and return visits, which can be exhausting for frail patients. A simulation-free approach, using the patient's diagnostic CT for treatment planning, eliminates the need for a separate planning CT. Combined with cone-beam CT (CBCT)-guided online adaptive radiotherapy (oART), this allows real-time adjustment of the treatment plan by accounting for daily changes in position and anatomy.

The study aimed to evaluate the feasibility and time consumption of different simulation-free oART workflows for patients with MSCC to identify the most suitable option for clinical implementation.

**Materials and methods:** 27 patients previously treated for MSCC were included in the study. Diagnostic CTs (dCT) from the patients were used for initial treatment planning. A total of 120 simulation-free treatments (based on 27 patients with 30 target sites) were simulated in the Ethos emulator, a virtual copy of the clinical Ethos treatment system. Four simulation-free workflows with different contour propagation methods were analyzed: rigid supervised (RSCP), rigid unsupervised (RUCP), deformable supervised (DSCP), and deformable unsupervised (DUCP). No manual edits of the target were performed in the unsupervised workflows. CTV structures from the dCTs were compared to those from each workflow using the Dice Similarity Coefficient (DSC). Additionally, dose distribution and time consumption of the adaptive process were analyzed to evaluate the feasibility of each workflow.

**Results:** Median time consumption of the adaptive process for the RSCP workflow was 7.49 min., significantly exceeding the 6.57 min of the DSCP workflow ($p<0.005$). The DUCP workflow demonstrated a significantly lower median time consumption of 3.27 min., compared to the RUCP workflow of 4.53 min. ($p<0.005$) (Figure 1). The highest and lowest median DSC scores were observed for the DSCP (0.91) and RUCP workflows (0.66). All adaptive treatment plans from the four workflows met all clinical goals for dose coverage.

**Conclusion:** The unsupervised workflows demonstrated superior speed compared to the supervised workflows. Despite an overall good similarity in contouring, significant

differences were still observed in a few cases, such as variations in target positioning. Therefore, further investigation is necessary to assess the safety and potential of an unsupervised workflow. The DSCP workflow was found to be the most optimal for clinical implementation.

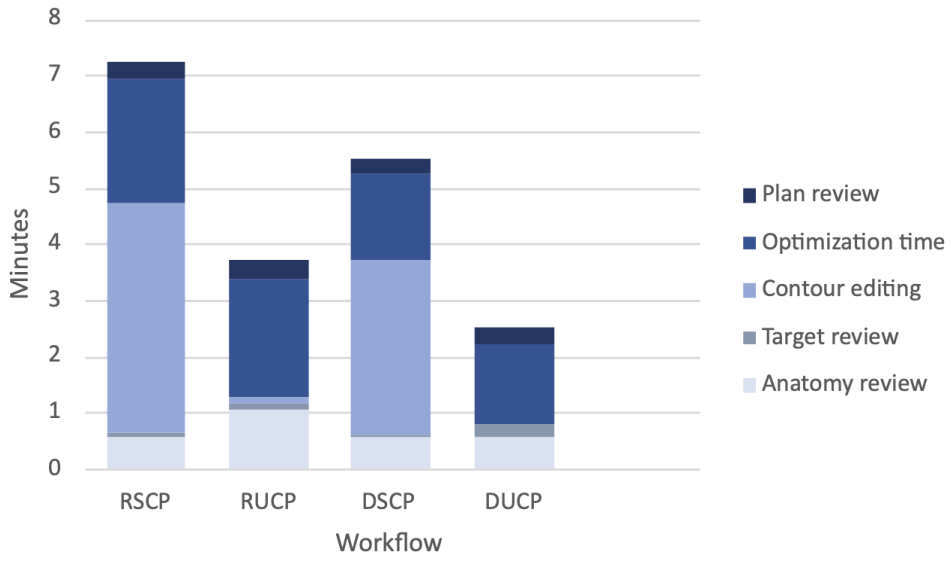


**Figure 1.** Median duration of each five steps (Anatomy review, Target review, Contour editing, Optimization time, and Plan review) in the adaptive workflow for the Rigid Supervised Contour Propagation (RSCP), Rigid Unsupervised Contour Propagation (RUCP), Deformable Supervised Contour Propagation (DSCP), and Deformable Unsupervised Contour Propagation (DUCP).

# Correction of IGRT and Intra-fraction movement using ExacTrac Dynamic for Head and Neck Cancer Patients

Simona I. Holst[1,2)], Maria Andersen[2)], Annette R Jakobsen[1,2)], Martin S Nielsen[1,2,3)]

1) Department for Medical Physics, Aalborg University Hospital, Denmark

2) Department of Oncology & Clinical Cancer Research Center, Aalborg University Hospital, Denmark

3) Department of Clinical Medicine, Aalborg University, Denmark

## Introduction

Radiotherapy for head and neck cancer can be administered using daily Cone Beam Computed Tomography (CBCT) as Image-Guided Radiotherapy (IGRT) with translations only or using 6-Degree Of Freedom (6DOF). Concerns have been raised that the use of rotations can lead to patient movement as they could tend to compensate for the applied tilt. Additional IGRT could be used to verify and correct unwanted movement, while Surface-Guided Radiotherapy (SGRT) could monitor the patient during treatment. This study aimed to model the corrections needed to adjust 6DOF CBCT. Secondary, to quantify the frequency and magnitude of intra-fraction movement detected by combined SGRT and X-ray-based IGRT.

## Materials and methods

Data were collected from 20 patients with a prescribed dose of 66-68 Gy, 33-34 sessions. Each session included IGRT using 6DOF couch shifts including Couch rotations, Roll and Pitch with limits of 3 degrees. The IGRT was initially applied by CBCT followed by corrections with ExacTrac Dynamic (ETD) using volume of interest covering the columna cervicalis. The couch shifts for the following ETD corrections were modelled using linear regression of the form ~ $p_1X+ p_2$ (in [mm] with 95 CI), where predictor variable X represents the Roll ($X_{Roll}$) or Pitch ($X_{Pitch}$) from CBCT. During treatment ETD surface guidance monitored patient movement with a beam hold using 2mm tolerance. Exceeding tolerances triggered verification images with corresponding applied couch shifts.

## Results

Including all sessions the ETD based IGRT corrections, following the initial CBCT, were within submillimeter. The applied model for prediction between applied rotations (Roll and Pitch) from CBCT and the following needed corrections in Lat, Lng and Vrt presented parameters for regression of Lat ($X_{Roll}$) $p_1$ = -0.98(-1.06; -0.90) & $p_2$ = 0.06(-0.05; 0.17), Lng ($X_{Pitch}$) $p_1$ = 0.49(0.43; 0.55) & $p_2$ = 0.27(0.18; 0.37) and Vrt ($X_{Pitch}$) $p_1$ = -0.24(-0.32; -0.16) & $p_2$ = 0.07 (-0.06; 0.20).

SGRT triggered repositioning were documented in 100 out of 669 sessions (15% of the sessions). 52 sessions confirmed that the SGRT threshold (2 mm) was exceeded, Figure 1.

## Conclusions

Translational misalignment can occur when using 6DOF for IGRT procedures if no additional correction images are acquired. The effects were more pronounced in lateral and longitudinal directions, with up to 3 mm for applied Roll or Pitch of 3 degree. The study showed that SGRT intra-fraction movements were observed in 15% of the treatment sessions, of which more than 50% confirmed movement exceeding the 2 mm tolerance.

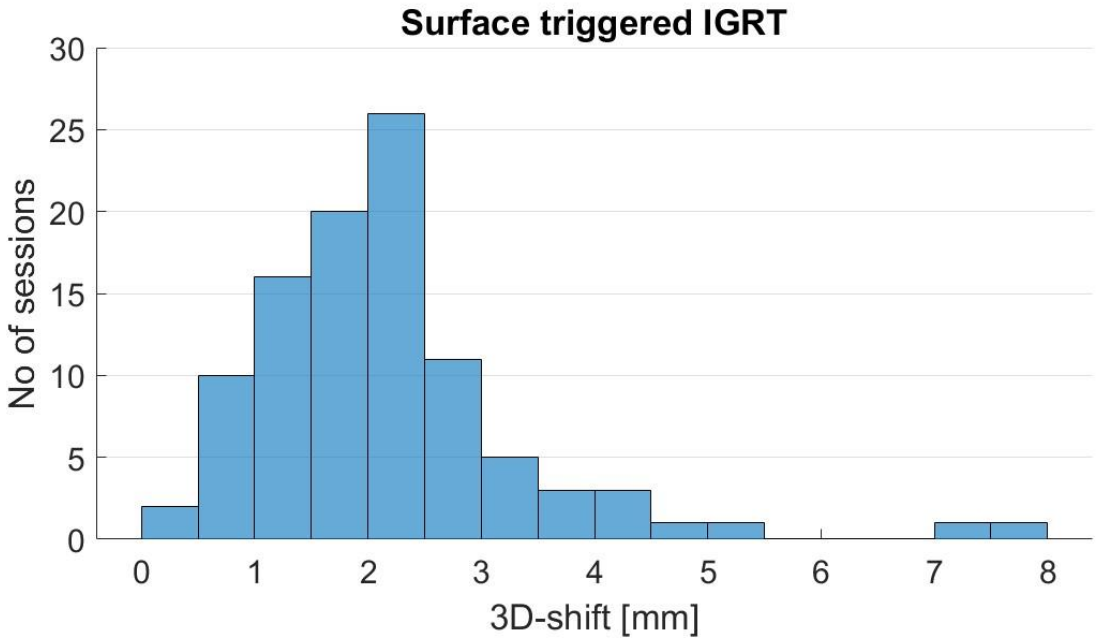


*Figure 1: Intra-fraction correction triggered by Surface Guidance using a 2 mm tolerance.*

**Dosimetric Impact of Respiratory and Anatomical Changes in Proton vs. Photon Therapy: Insights from the European PROTECT Trial on Locally Advanced Esophageal Cancer**

Eckholdt S[1,2], Mortensen HR[1,2], Appelt AL[3], Byskov CS[4], Defraene G[5], Ehmsen ML[1], Haustermans K[5,6], Jensen MF[1], Møller DS[2,4], Nordsmark M[4], Populaire P[5,6], Thing RS[7], Hoffmann L[2,4].

[1] Danish Centre for Particle Therapy, Aarhus University Hospital, Aarhus, Denmark.
[2] Department of Clinical Medicine, Faculty of Health Sciences, Aarhus University, Denmark.
[3] Leeds Institute of Medical Research, University of Leeds, Leeds, United Kingdom.
[4] Department of Oncology, Aarhus University Hospital, Aarhus Denmark.
[5] KU Leuven – University of Leuven – Department of Oncology – Laboratory of Experimental Radiotherapy, Leuven, Belgium.
[6] University Hospitals Leuven, Department of Radiation Oncology, Leuven, Belgium.
[7] Department of Oncology, Vejle Hospital, University Hospital of Southern Denmark, Vejle, Denmark.

**Introduction:**
Patients with locally advanced esophageal cancer are randomized to receive proton (PT) or photon (XT) radiotherapy before surgery in the European phase III PROTECT trial. The robustness of target coverage against setup and range uncertainties and respiration was assessed on planning CT (pCT) and weekly control CTs (cCTs) for the initial 25 patients enrolled at a single study site. The accumulated target dose coverage was obtained using daily cone-beam CT (CBCT) imaging.

**Materials and methods:**
Randomization allocated patients to PT (n=11) or XT (n=14). Patients received 50.4Gy(RBE) in 28 fractions. The clinical target volume accounting for respiratory motion (iCTV) should be $V95\%_{iCTV}$>99% for the nominal plan. Robustness of treatment plans was assessed against setup (5mm), range (3.5%, for PT only) in 14 (PT) and six (XT) scenarios, and respiration ($V95\%_{iCTV}$>97%). To evaluate target coverage, the pCT plan was recalculated on weekly cCT scans; if dosimetric deviations were detected, adaptive re-planning (rCT) was performed. While weekly cCT was performed for the initial eight XT patients, subsequent patients underwent daily dose evaluation using CBCT scans, enabling a continuous assessment of potential dose deviations requiring adaptation. Additionally, treatment plan robustness towards respiration and setup uncertainty (PT:2mm/3.5%, XT:2mm) was examined on cCTs with acceptance criteria adjusted throughout the treatment: stringent in early fractions and gradually less restrictive ($V95\%_{iCTV}$>[96%-94%]).

Using synthetic CT models (RaySearch Laboratories) for PT and calibrated CBCT electron density curves (MIM Software) for XT, daily CBCT facilitated the evaluation of the daily delivered dose. Accumulation of the calculated daily dose distributions was performed on pCT.

**Results:** The pCT demonstrated V95%$_{iCTV}$>99% in all nominal plans. The robustness evaluation of recalculated treatment plans on cCTs confirmed acceptable dose coverage in ten PT and 14 XT patients (Figure 1A). One PT patient (pt2) exhibited V95%$_{iCTV}$ underdosage in the range and setup evaluation on a single cCT and underwent adaptive re-planning.

The accumulated CBCT doses showed V95%$_{iCTV}$>99% in all patients (Figure 1B). Except for PT pt2, who required adaptive re-planning due to underdosage on one cCT, deviations between the accumulated and nominal doses on pCT, cCT, and rCT were <1%.

**Conclusion:** Among 25 PROTECT trial patients, robustness evaluation on weekly cCT scans revealed acceptable target coverage in 24 patients, while 1 patient required re-planning. The accumulated daily CBCT doses confirmed iCTV coverage >99% in all patients, reinforcing the importance of weekly cCT imaging and adaptive radiotherapy for maintaining full target dose.

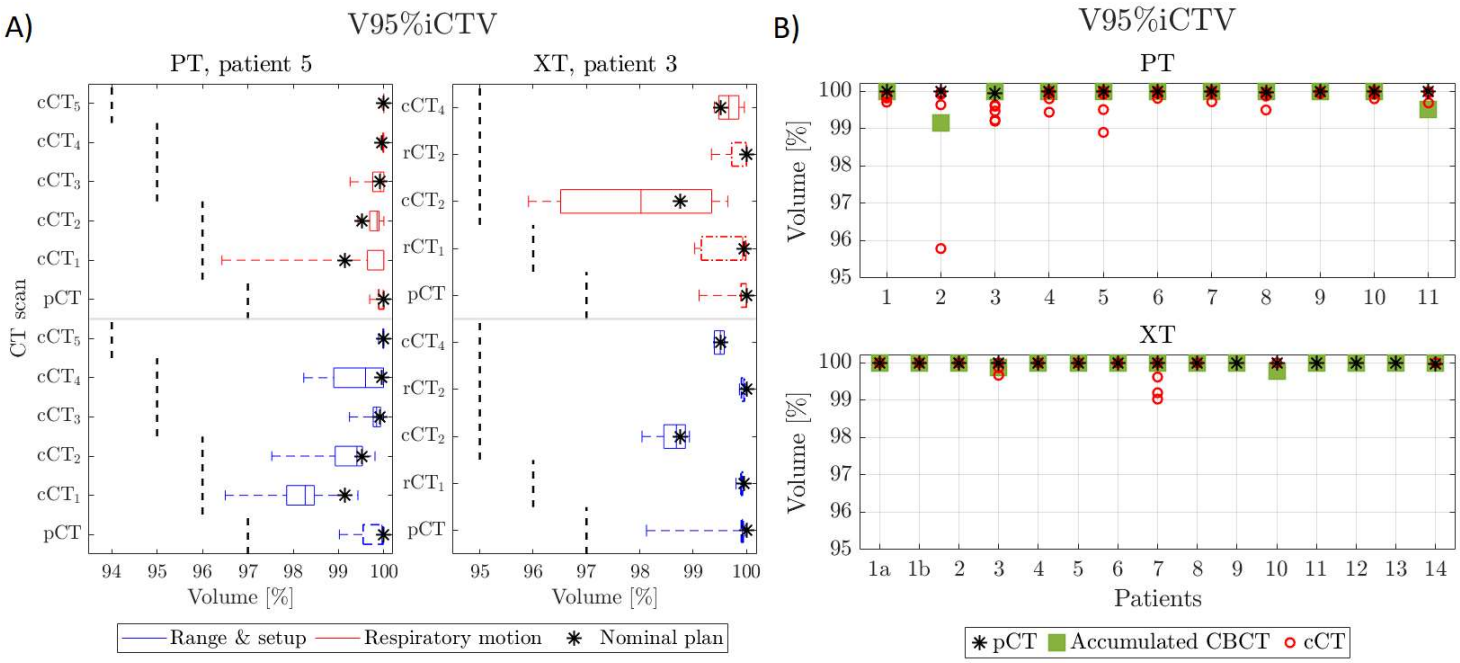


Figure 1: A) V95%$_{iCTV}$ robustness evaluation for one PT and XT patient. Blue and red boxplots represent robustness towards setup and range, and respiration, respectively. Black stars indicate the nominal plan values derived from pCT, cCT or rCT scans, with the dashed line marking the fraction-dependent acceptance criteria. B) V95%$_{iCTV}$ evaluation of the accumulated dose across PT and XT patients. Black stars denote nominal pCT values, while green squares represent the accumulated CBCT dose. Red circles indicate nominal recalculated cCT values. For XT patient 1, separate treatment plans were implemented for cranial and caudal targets.

**Shortening proton therapy treatment time of high-risk prostate cancer patients using laxatives and CBCT guidance**

Stine E. Petersen[a], Vicki T. Taasti[a], Anne Juel Christensen[b], Anne Vestergaard[a], Christine V. Madsen[c], Heidi S. Rønde[a], Jimmi Søndergaard[d], Lasse Bassermann[a], Liliana Stolarczyk[a], Morten Høyer[a], Lise Bentzen[c], Ludvig P. Muren[a]

[a]Danish Centre for Particle Therapy, Aarhus University Hospital, Aarhus, Denmark
[b]Department of Clinical Oncology, Zealand University Hospital, Køge, Denmark
[c]Department of Oncology, Vejle Hospital, University Hospital of Southern Denmark, Vejle, Denmark
[d]Department of Oncology, Aalborg University Hospital, Aalborg, Denmark

Presenting author: Stine E. Petersen, email: stinpete@rm.dk

**Introduction**

Proton therapy of prostate cancer patients can be challenging due to daily changes in bladder filling and changes of gas/feces in the rectum and bowel. These changes may shift the target compared to the position seen on the planning CT (pCT). Consequently, patient repositioning including emptying of the rectum/bowel may be needed before the treatment can be delivered. This study assessed the treatment time and number of cone-beam CTs (CBCTs), before and after introducing a CBCT evaluation scheme and prescription of daily laxatives.

**Materials and methods**

Thirty-five high-risk prostate cancer patients treated with proton therapy within the Danish national randomized PROstate PROTON Trial were included in the study. Twenty-three patients were treated before, and twelve patients were treated after initiation of the new CBCT evaluation scheme (Figure 1) and prescription of oral laxatives. All patients received 78 Gy(RBE) to the prostate with/without the seminal vesicles in 39 fractions, and 56 Gy(RBE) to the elective pelvic lymph nodes delivered using a simultaneous integrated boost technique. All patients followed a drinking protocol before the pCT and before each fraction. No patients were treated with a rectal balloon or rectal spacer. Our daily image guided radiotherapy (IGRT) strategy included a 6D match of the daily CBCT to the pCT based on bony anatomy followed by a 3D match on implanted fiducials markers in the prostate gland. The introduced CBCT evaluation scheme consists of visual evaluation of the position of high-density structures like fiducials and bones in comparison to the delineated structures from the pCT. In this study, treatment time (defined as time from start of the first CBCT to the end of the last treatment field) and preparation time (defined as time from start of the first CBCT to start of the first treatment field) were recorded for all fractions, as well as the number of CBCTs acquired before start of each treatment fraction.

**Results**

The median treatment time per fraction was reduced from 17:15 to 16:32 minutes, resulting in a reduction of 28 minutes over the full treatment course, and the preparation time was reduced from 9:15 to 7:41 minutes after initiating the CBCT evaluation scheme and the laxatives. The median number of CBCTs before start of treatment over the full treatment course went from 60 to 49 CBCTs.

**Conclusion**

The treatment time, preparation time, and number of CBCTs were reduced after introducing the CBCT evaluation scheme and prescription of laxatives.

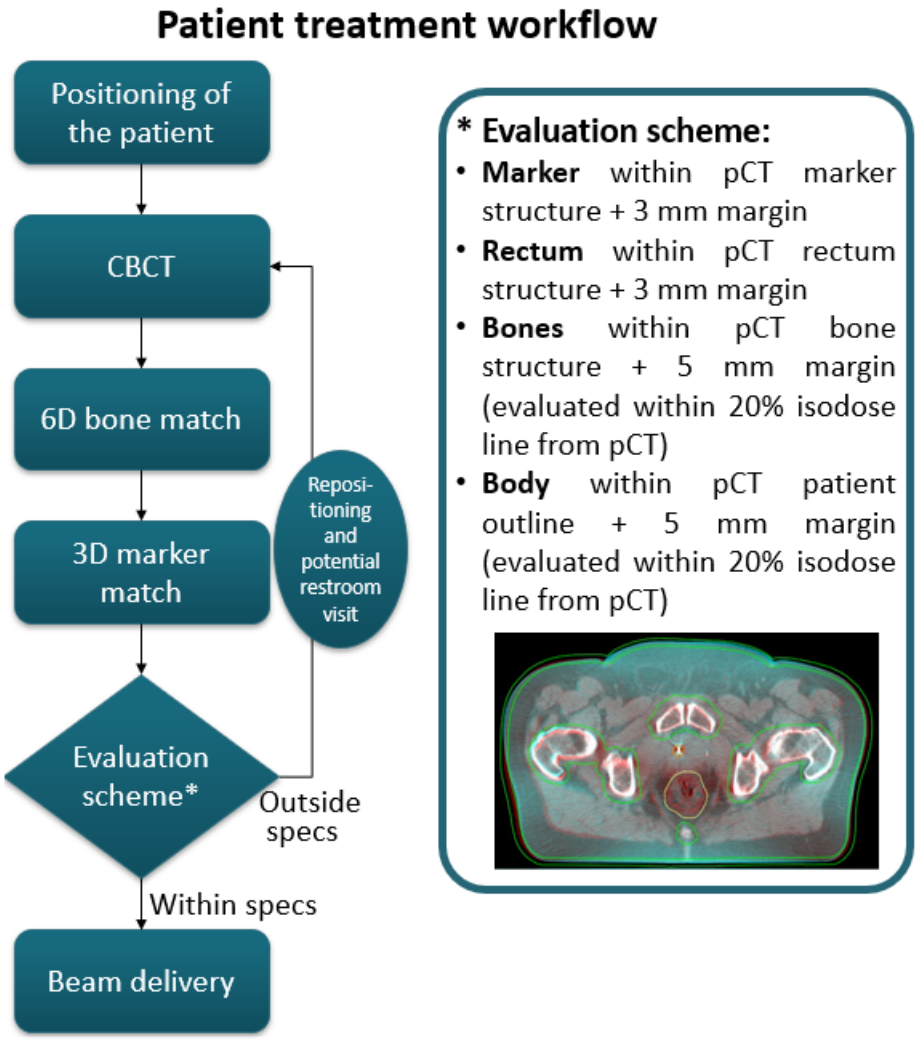


**Figure 1:** Patient treatment workflow. The daily cone-beam CT (CBCT) is registered to the planning CT (pCT), first by a six degree (6D) freedom bone match followed by a 3D match on the implanted gold markers. Then it is checked visually if the markers, bones, rectum and body outline seen on the CBCT are within structures created on the pCT. If this is the case, the plan is delivered, else the patient is repositioned or send to the restroom if bladder or rectum filling is unacceptable.

**Measurement-less patient-specific QA in proton therapy: DCPT experience**

*Liliana Stolarczyk[1*], Sarah Eckholdt[1], Maiken Haislund Guldberg[1], Simon Skouboe[1], Niels Bassler[1], Ulrik Vindelev Elstrøm[1], Ole Nørrevang[1], Heidi S. Rønde[1], Line Bjerregaard Stick[1], Jakob Borup Thomsen[1], Maria Fuglsang Jensen[1]*

* lilsto@rm.dk
[1]Danish Centre for Particle Therapy (DCPT), Denmark

**Introduction:**
Measurement-based patient-specific QA (PSQA) in pencil beam scanning proton therapy is a time-consuming process. The 2023 ESTRO Physics Workshop on PSQA in proton therapy, attended by 33 participants from over 20 centers, focused on defining a path towards measurement-less PSQA, exploring alternatives such as log-file-based QA and independent dose calculations (IDC). In line with the workshop recommendations, DCPT implemented an IDC-based PSQA workflow using a TOPAS Monte Carlo (MC) beam model to reduce the measurement burden while maintaining treatment accuracy.

**Methods and Materials:**
DCPT's measurement-less PSQA workflow begins with recalculating the patient plan on a virtual solid water phantom in the Eclipse treatment planning system (TPS), a step common to standard PSQA. The plan is then exported to a TOPAS MC server, where IDC are performed automatically. The resulting dose distributions are imported back into the TPS and analysed using in-house Gamma Index (GI) evaluation scripts. IDC were validated against measurements performed in a solid water phantom using an ionization chamber array (Matrix PT, IBA Dosimetry). The IDC workflow was integrated into the clinical environment within Eclipse TPS, allowing direct comparison between IDC, TPS dose distributions, and measured data. Criteria were established for IDC acceptance, with additional measurements required for plans failing these criteria.

**Results:**
IDC validation against measurements showed that the average passing rate for 140 tested fields was 98.7% (2D GI (3%, 2mm)). Based on these results, DCPT established pass criteria for comparison of TPS calculations and IDC: 90% for 3D GI (1%, 2mm) and 98% for 3D GI (3%, 2mm). Currently, 86% of all fields meet these criteria. Outliers undergo detailed analysis, including profile comparisons between IDC and Eclipse calculations, with measurements performed if necessary. Since implementing IDC-based PSQA at DCPT in the beginning of 2024, 410 patient plans have been evaluated using the workflow. In 93% of the plans, IDC was sufficient without additional measurements, while 7% required verification due to complex geometry, high dose gradients, uncertainties in range or noise in MC simulations.

**Conclusions:**
DCPT's transition to IDC-based PSQA demonstrates that measurement-less approaches can be effectively integrated into clinical practice. While measurements remain necessary for select cases, IDC has significantly streamlined the PSQA process, reducing the need for routine measurements. This shift aligns with the broader trend in the proton therapy community toward efficient, standardized, and evidence-based QA practices in PSQA.

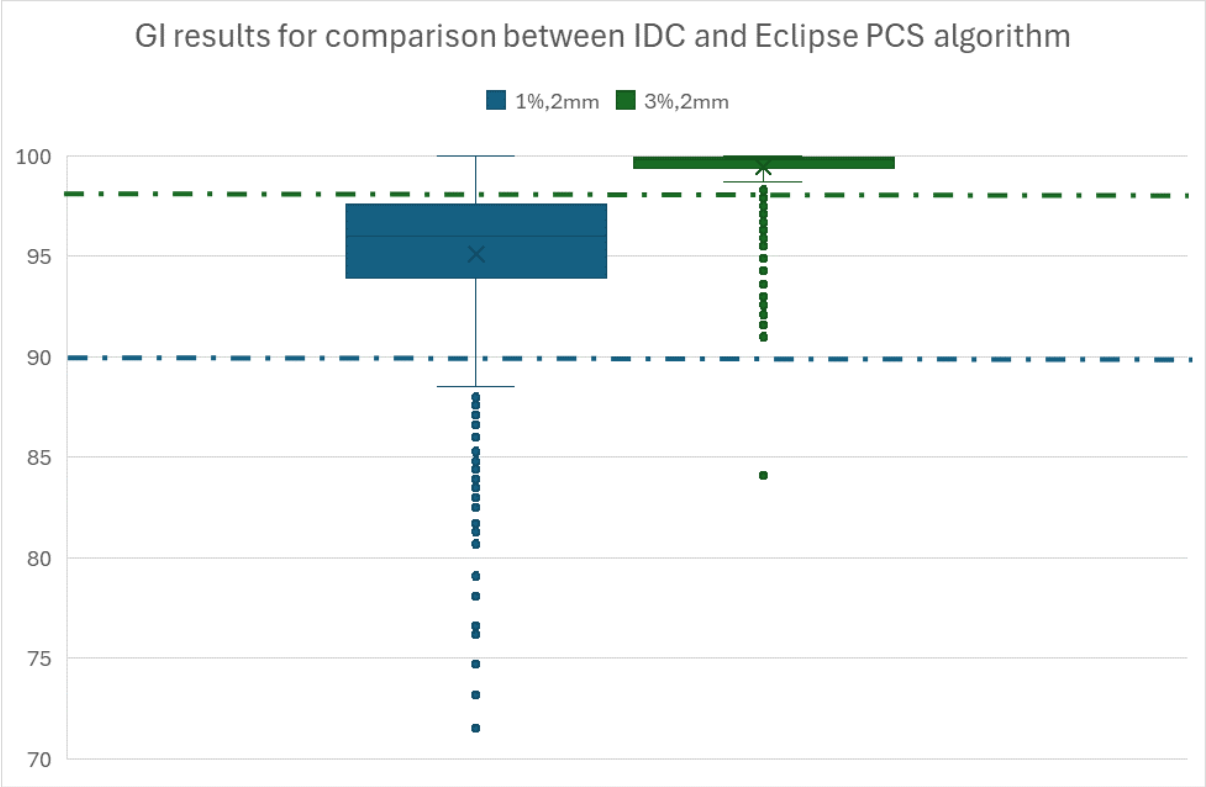


**Figure 1**: Gamma Index (GI) pass rates for secondary dose calculations at DCPT. Dashed lines are showing 90% for 3D GI (1%, 2mm) and 98% for 3D GI (3%, 2mm) pass criteria for comparison of TPS calculations and IDC.

# Quantification of proton stopping-power ratios for photon-counting computed tomography

Lasse Bassermann[1*], Jens Edmund[2], Weronika Elżbieta Olech[3], Michael Brun Andersen[3], Stine Elleberg Petersen[1], Ludvig Paul Muren[1], Vicki Trier Taasti[1]

[1]Danish Centre for Particle Therapy, Aarhus University Hospital, Aarhus, Denmark
[2]Department of Oncology, Herlev and Gentofte University Hospital, Herlev, Demark
[3]Department of Radiology, Herlev and Gentofte University Hospital, Herlev, Demark
[*]lasbas@rm.dk

## Introduction

Computed tomography (CT) scans are used to estimate stopping-power ratios (SPRs) for dose calculations in proton therapy treatment planning. Photon-counting CT (PCCT) has potential to improve the SPR accuracy, and previous studies have indicated a reduced influence of phantom size on SPR estimations for PCCT. The aim of this study was to quantify the accuracy of size-specific SPR estimations based on PCCT scans.

## Materials and methods

PCCT scans were acquired of the Gammex Advanced Electron Density phantom, which has a small and large size simulating the head and abdomen of an adult. Various soft-tissue and bone insert configurations were scanned. For all scans, virtual monoenergetic images (VMIs) were created. These were used to estimate SPRs of the inserts. The highest SPR accuracy was found using a VMI pair of 40 and 160 keV, which was used for further evaluations. Separate SPR fits were created for the small and large phantom. The SPR accuracy was calculated as the difference between the fitted and expected SPR for all inserts, in each configuration. Positional effects on the SPR accuracy were evaluated for bone inserts placed at the centre of the large and small phantom, and at the periphery of the large phantom (Figure 1a). The CIRS anthropomorphic head phantom was scanned, and the SPR was estimated for the brain. The range for a 100 MeV proton beam into the head phantom for a simple and complex (Figure 1b) line profile was estimated based on the SPR fits for the small and large phantom.

## Results

The SPR accuracy was highest when estimated with the fit for the corresponding configuration (Figure 1c-h), indicating a size-dependency. The median SPR deviation for the small phantom was 0.2% (0.3% for bones, 0.1% for soft tissue inserts) and 0.3% for the large phantom (0.4% for bones, 0.2% for soft tissue inserts). For bones in the periphery of the large phantom with the large-phantom fit, the median SPR deviation was -0.5%. For brain tissue in the head phantom, the median SPR deviation for the small-phantom fit was -0.1%. The estimated proton range of a beam into the head with a small-phantom fit was 73.6 mm for the simple and 75.5 mm for the complex line profile. For a large-phantom fit, the ranges were 73.4 mm and 75.4 mm.

## Conclusions

In this study, the importance of using size-specific SPR estimation to obtain precise dose calculations for PCCT scans was shown.

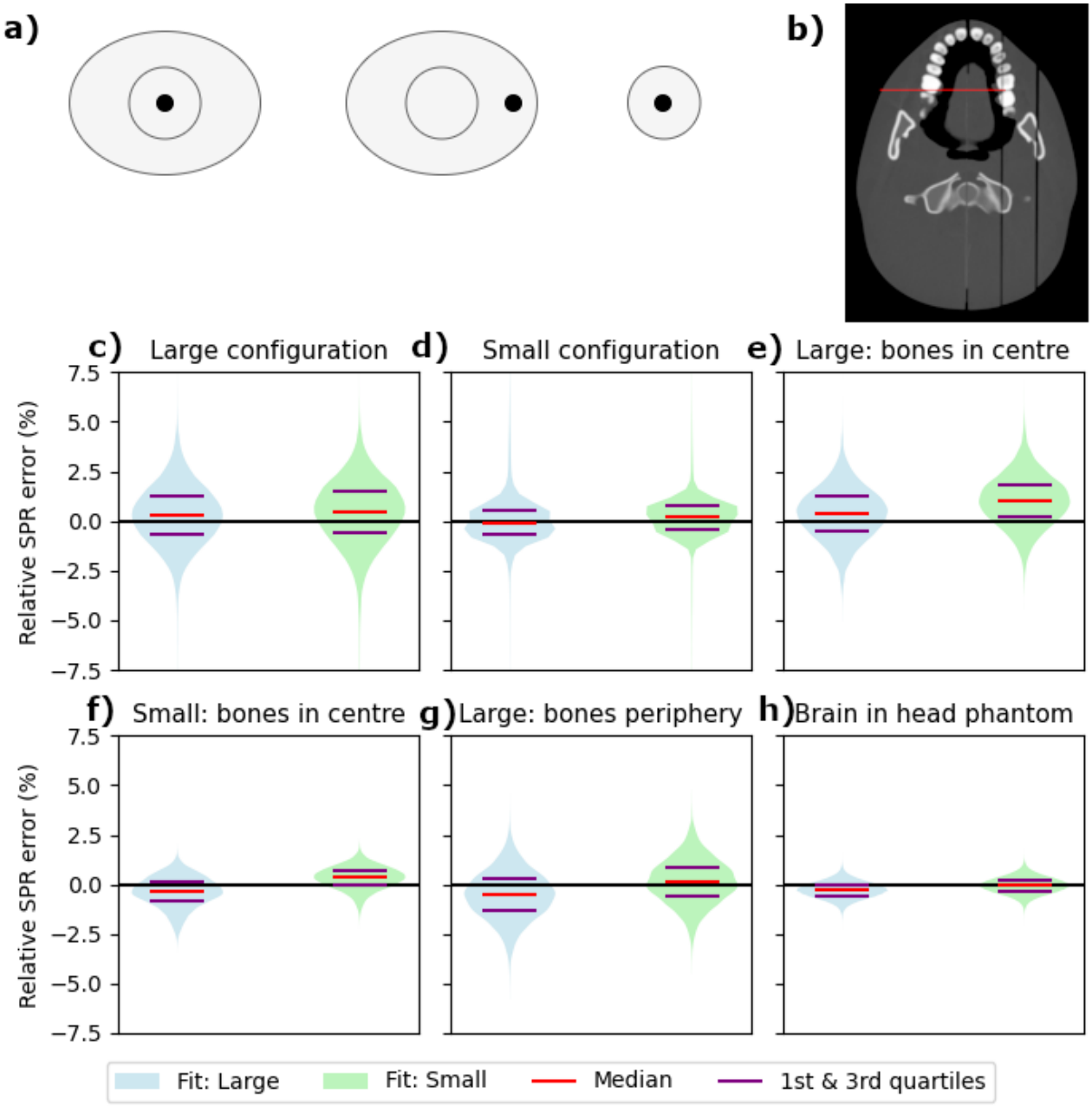


**Figure 1:** Stopping-power ratio (SPR) evaluations. (a) The different positions for the bone inserts to evaluate the influence of the position and size on the SPR estimation. The bone inserts were placed in the centre and periphery of the large phantom, and in the centre of the small phantom. (b) Position of the complex line profile through the head phantom. (c) SPR deviation between the fitted and expected SPR for all inserts in the large and (d) small phantom configuration. (e) SPR deviation for the bone inserts in the centre of the large configuration, (f) the centre of the small configuration, (g) and for the bone inserts in the periphery of the large configuration. (h) SPR deviation for brain tissue in the head phantom.

**The impact of anatomical variations and RBE uncertainties on proton therapy dose delivery within a randomized clinical trial for high-risk prostate cancer**

Maria CW Heisel (1), Stine Elleberg Petersen (1), Liliana Stolarczyk (1), Rasmus Klitgaard (1,2), Anne Vestergaard (1,2), Sarah Eckholdt Jensen (1,2), Sofie Tilbæk (1,2), Heidi S. Rønde (1), Lise N. Bentzen (3), Jimmi Søndergaard (4), Morten Høyer (1,2) and Ludvig P Muren (1,2)

(1) Danish Centre for Particle Therapy, Aarhus University Hospital, Aarhus, Denmark

(2) Department of Clinical Medicine, Aarhus University, Aarhus, Denmark

(3) Aarhus University, Denmark

(4) Department of Oncology, Aalborg University Hospital, Aalborg, Denmark

## Introduction

The localized dose delivery of spot-scanning proton therapy (PT) is challenged by inter-fractional variations in anatomy and by uncertainties in relative biological effectiveness (RBE). For high-risk prostate cancer patients, inter-fractional anatomical variations may compromise the planned target and normal tissue doses. The proton RBE is in current clinical practice assumed to be constant but is likely to vary with the linear energy transfer (LET), influencing in particular RBE-corrected normal tissue doses. The aim of this study was therefore to study dose/volume variations caused by anatomical changes and RBE uncertainties during PT for prostate cancer, assessed by fulfilment of clinically applied dose/volume constraints.

## Materials and methods

Seven high-risk prostate cancer patients included in the pilot phase of the national PROstate PROTON Trial 1 were evaluated. They received 78 Gy to prostate +/- seminal vesicle (CTVp) and 56 Gy to the elective lymph node volume (CTVe) in 39 fractions, using four beams. Clinical treatment plans (convolution superposition algorithm; Eclipse) were optimized to meet clinical dose/volume constraints for the target and organs at risk (OAR). For each patient, weekly control CT (cCT) scans (6-8 scans, 53 in total) were used to re-calculate dose and calculate LET distributions over a full treatment with TOPAS Monte Carlo. RBE-weighted dose metrics were calculated on the basis of three variable LET-dependent RBE models including two phenomenological and one linear model. The impact of RBE variations on constraints were analyzed using error propagation. Dose/volume metrics on the cCTs was labeled as ‘outside’ the constraint level if any RBE-weighted dose/volume interval violated the constraint.

## Results

The high-dose target (CTVp) coverage constraints were met in the dose re-calculations for all 53 cCTs also when accounting for RBE uncertainty. For the low-dose CTVe, RBE uncertainty inclusive dose re-calculations were outside clinical constraints in 29 of 53 cCTs, compared to 9 cCTs if RBE uncertainty was not accounted for. For the rectum, the V75 Gy dose/volume metrics were outside the constraints in 43 of 53 cCTs if accounting for RBE uncertainty, but mostly within at lower dose levels (Fig 1). For the bladder, the V80 Gy dose/volume metrics were outside the constraints for 6 of 53 cCTs when accounting for RBE uncertainty, all for one patient.

**Conclusion**

Both inter-fractional anatomical changes and RBE uncertainties influenced fulfilment of clinical dose/volume constraints, in particular at V75 Gy for the rectum. The high-dose target coverage was robust to both anatomical variations and RBE uncertainties.

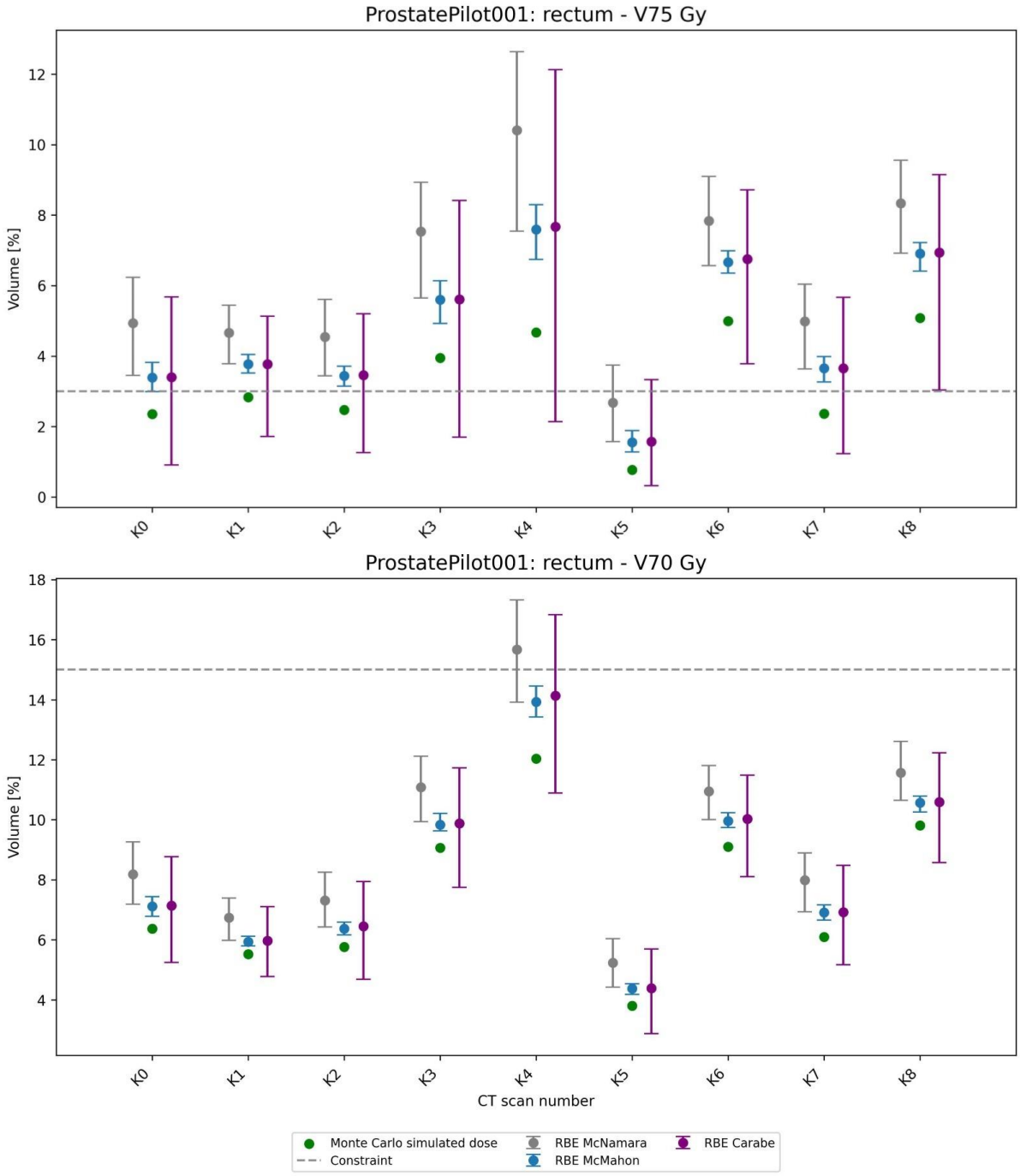


*Figur 1. Constraint V75 Gy and V70 Gy evaluations for rectum across cCT scans during treatment for one prostate patient. Colored points represent results from Monte Carlo simulated dose (RBE = 1.1) (green) and three different RBE-weighted biological doses with error bars for model uncertainty (blue, grey, purple). The dashed gray line marks the constraint threshold. If at least one of the RBE models predicted biological dose exceeded the constraint, it was counted as an RBE model variation falling outside the constraints. The x-axis denotes CT scan numbers, and the y-axis shows structure volume (%).*

# Micro-Dosimetric Measurement of Secondary Particles Generated in Bolus and Collimator for Passive Scattering Systems in Carbon Ion Therapy

Villads L. Jacobsen[1,2], James Vohradsky[3], Vladimir Pan[3], Linh T. Tran[3], Daniel Bennett[3], Niels Bassler[1,2], Anatoly B. Rosenfeld[3]

[1] Department of Clinical Medicine, Aarhus University Hospital, Aarhus, Denmark. villads.lundsteen@clin.au.dk
[2] Danish Centre for Particle Therapy, Aarhus University Hospital, Aarhus, Denmark.
[3] Centre for Medical and Radiation Physics, University of Wollongong, Wollongong, NSW, Australia.

**Introduction:** Currently, 14 carbon ion therapy clinics are operating worldwide, with 12 employing either passive scattering systems alone or a combination of passive and pencil beam scanning systems. In treatments using passive scattering beams, a plastic bolus and brass collimator are commonly used to shape the beam to the target region. However, there is limited research on the secondary particles produced in the bolus and collimator, and their potential impact on treatment outcomes remains unclear. This study presents microdosimetric spectra obtained from 42 distinct positions within a spread-out Bragg peak (SOBP) carbon beam, measured at the Heavy Ion Medical Accelerator in Chiba (HIMAC). These measurements are further complemented by Monte Carlo simulations, providing spectral particle decomposition data for isolating secondary particles produced in the bolus and collimator.

**Methods:** A 10 × 10 cm² carbon beam with a SOBP ranging from 8 cm to 14 cm was used for irradiation. The beam first passed through a previously utilized patient-specific collimator and bolus before reaching the silicon-on-insulator (SOI) microdosimeter. Measurements were performed at three depths within the SOBP using range shifters (RS): the beam entrance (0 mm RS), the SOBP entrance (79.58 mm RS), and the central SOBP (109.66 mm RS). At each depth, two SOI microdosimeters with a 10 µm SV thickness were positioned—one at the lateral center of the beam and the other 40 mm above. The detectors were then laterally shifted by ±15 mm, 30 mm, or 40 mm to the left or right within the field. Monte Carlo simulations were conducted using OpenTOPAS, including a geometrically accurate fixed-gantry setup and detector geometry [1].

**Result:** Preliminary results show good agreement between the measured microdosimetric spectra and simulations, as shown in Figure 1. The central peak for primary carbon ion particles is 3 keV/µm lower in the simulation than in the measurements, with both having a similar FWHM of ~10.9 keV/µm. However, a notable discrepancy exists below the main peak, where a 7 keV/µm feature appears in the measurements but not in the simulations. This difference is speculated to arise from secondary particle production.

**Conclusion:** Simulated microdosimetric spectra and measurements showed good agreement at the primary particle peak, but discrepancies were observed in the lower energy regions, where fragmentation products dominate according to simulations. Ongoing investigations focus on the nuclear fragmentation models, particularly the fragments generated in the bolus and collimator.

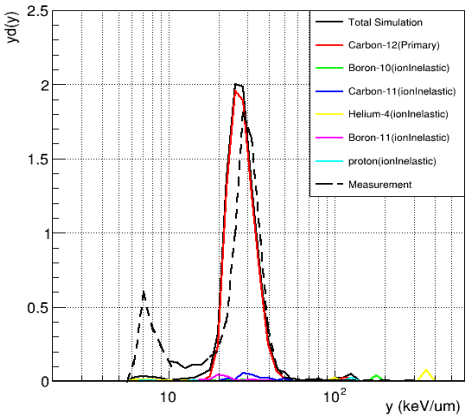


Figure 1. Measurement and simulation of microdosimetric spectra in silicon of the central position..

**References:**

1. Bolst, David, et al. "Modelling the biological beamline at HIMAC using Geant4." *Journal of Physics: Conference Series*. Vol. 1154. No. 1. IOP Publishing, 2019.

**Quantifying specific proton range uncertainty for pediatric cancer patients**

Kyriakos Fotiou[1] (kyriakos.fotiou@rm.dk), Lasse Bassermann[1], Maria Fuglsang Jensen[1], Klaus Seiersen[1], Stine Elleberg Petersen[1], Yasmin Lassen-Ramshad[1], Ludvig Muren[1], Vicki Trier Taasti[1]

[1]Danish Centre for Particle Therapy, Aarhus University Hospital, Aarhus, Denmark

**Introduction**

Stopping-power ratio (SPR) uncertainty in proton therapy is conventionally estimated from CT scans of adult-sized head and body phantoms and applied universally across all patients. However, this approach may overestimate the SPR uncertainty for pediatric brain cancer patients since beam hardening effects are lower for smaller sizes. This study aimed to quantify SPR uncertainty specifically for pediatric brain cancer patients, compare it to adult-based estimates, and assess its impact on dose deposition in surrounding organs-at-risk (OARs).

**Materials and methods**

A modular ring phantom (Sun Nuclear) with diameters of 10, 20, 30, 40 cm was scanned with a twin-beam dual-energy CT scanner (Somatom Definition Edge, Siemens Healthineers), generating virtual monoenergetic images (VMI) at 90 keV. SPR uncertainty was estimated separately for pediatric and adult approaches. The pediatric SPR uncertainty was derived using only the relevant phantom sizes (10-20 cm), whereas the adult approach followed the conventional head-body method utilizing the 20 and 40 cm phantoms. Total SPR uncertainty was evaluated as a combination of beam hardening uncertainty (CT number variations due to phantom size and insert position), modeling uncertainty (differences between measured and modeled CT numbers), and inherent uncertainty (variations in tissue composition and density). To evaluate the clinical impact of pediatric and adult SPR uncertainties, a proton treatment plan was created for the virtual anthropomorphic ICRP 1-year-old phantom. The brainstem and an adjacent tumor were delineated, and a nominal proton plan was constructed to deliver 60 Gy to the target. The nominal dose distribution was re-evaluated under the influence of pediatric and adult SPR uncertainties. Shifts in the dose distribution were analyzed, and the resulting dose deposited to the brainstem was evaluated under the pediatric and adult uncertainties

**Results**

Applying the conventional adult head-body method to estimate the SPR uncertainty resulted in 2.4% proton range uncertainty, while correctly accounting for pediatric sizes, the uncertainty was reduced to 1.5%. The lowered range uncertainty translated into a lower brainstem dose (Figure 1). For the nominal plan, the brainstem $D_{0.03cc}$ was 40.7 Gy. Adding the adult range uncertainty, the high dose region overshot into the brainstem increasing $D_{0.03cc}$ to 44.9 Gy, which was reduced to 42.7 Gy for the pediatric-based uncertainty.

**Conclusions**

Adult-based range uncertainties overestimated the uncertainties seen for pediatric patients, due to the reduced beam hardening for small patient sizes. Correctly accounting for the decreased sizes of children, enables the sparing of OARs adjacent to the tumor.

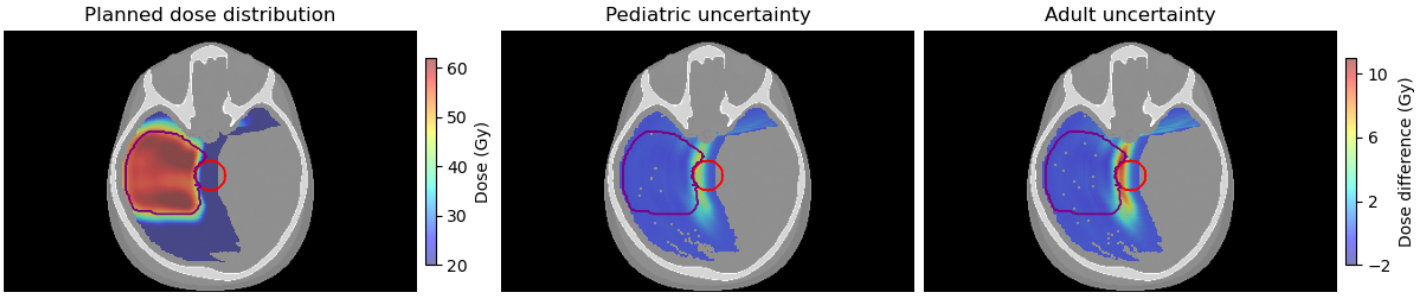


**Figure 1:** Proton dose distribution for a pediatric brain treatment plan. The left image displays the planned proton dose distribution, with the tumour delineated in purple and the brainstem in red. The middle image depicts the dose difference between the planned nominal dose and the dose distribution when introducing the pediatric range uncertainty, while the right image illustrated the dose difference when introducing adult range uncertainty. Dose difference was calculated by subtracting the nominal dose distribution from those including uncertainties.

**Evaluating stopping-power ratio accuracy for proton therapy planning of brain cancer patients applying two dual-energy CT approaches, including metal implant considerations**

*Ivanka Sojat Tarp[1] (ivatar@rm.dk), Vicki Trier Taasti[1], Maria Fuglsang Jensen[1], Ludvig Paul Muren[1], Kenneth Jensen[1]*
[1]Danish Centre for Particle Therapy, Aarhus University Hospital, Aarhus, Denmark

**Introduction**

Accurate stopping-power ratio (SPR) estimation is essential for proton therapy planning. Patients undergoing postoperative proton therapy for brain cancer treatment may have surgically implanted metal fixation clips, which can potentially compromise the precision of SPR estimation. The SPR is usually estimated from a computed tomography (CT) scan of the patient using a Hounsfield look-up table (HLUT), utilizing an empirical linear relationship between CT numbers and SPRs. Previous studies have shown that dual-energy CT (DECT) can reduce beam hardening by creating virtual monoenergetic images (VMIs) or even improve the accuracy of proton range estimation by estimating SPR directly. The aim of this study was to examine the consistency between HLUT-based SPR estimation from VMIs and direct DECT-based SPR estimation in patients with brain cancer.

**Materials and methods**

DECT scans were acquired for ten brain cancer patients treated clinically with proton therapy. Two SPR maps were generated for each patient based on the DECT scan. The first SPR map was created using a VMI at 90 keV and by applying a calibration curve based on the established consensus guideline. The second SPR map was created using the commercial DirectSPR algorithm (Siemens Healthineers) directly on the DECT scan. First, the clinical proton treatment plan was recalculated on both SPR maps and the resulting dose distributions were compared based on relevant dose-volume histogram parameters. Next, a voxel-wise comparison was performed between the two different SPR maps. A separate comparison was performed for metal implants.

**Results**

Dose differences in organs-at-risk were minimal between the two SPR methods, with no meaningful difference in mean or near-maximum ($D0.03cm^3$) doses. SPR values from DirectSPR showed strong agreement with consensus guideline-based VMI at 90 keV for CT numbers up to approximately 1500 Hounsfield Units (HU) (Figure 1). However, for CT numbers exceeding 1500 HU, discrepancies became increasingly evident, particularly in regions containing metallic implants, where DirectSPR gave higher SPR values than the HLUT. Note that the applied HLUT was adjusted in the high-density region to match the SPR of titanium; a similar CT number threshold might need to be considered when using DirectSPR.

**Conclusion**

Our findings indicated that DirectSPR provided consistent SPR values up to 1500 HU, beyond which deviation occurred, particularly in areas containing metal. However, these deviations had a limited effect on dose distribution. Nevertheless, special consideration should be given to high-density materials when beams pass through the metal implants.

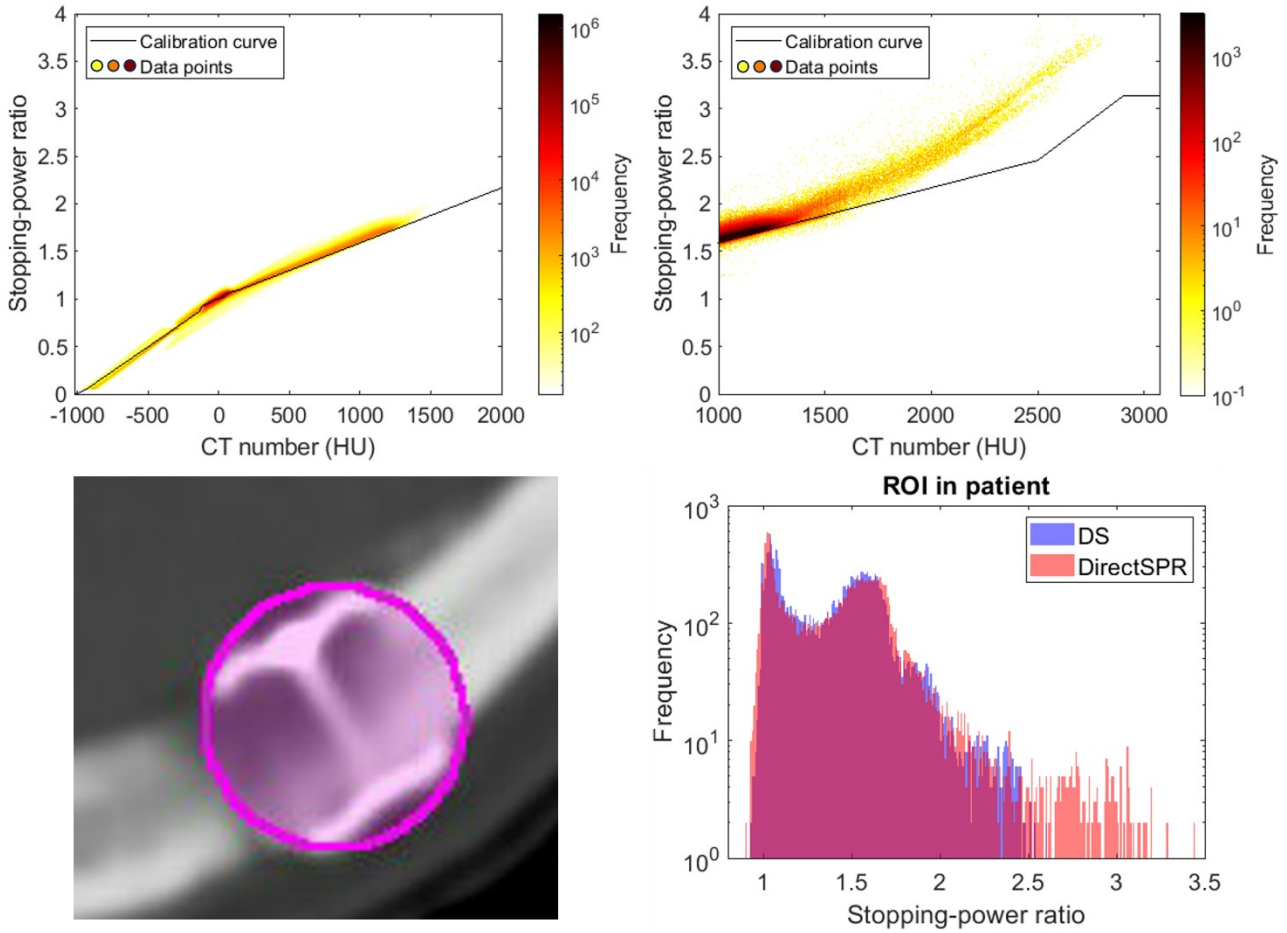


**Figure 1.** *Top:* Frequency distribution of voxel-wise relationship between the CT numbers for the virtual monoenergetic image (VMI) at 90 keV and the DirectSPR for all voxels within the body structure for all patients (N=10). The entire CT number range is shown in the left figure, while the right figure shows the high-density region including metal implants. The colour scale represents the frequency on a logarithmic scale. *Bottom: Left* – Section of a patient CT image with the highlighted region of interest (ROI) containing CranioFix® metal clips. *Right* – Histogram of SPR values for the ROI from the bottom left figure compares the VMI HLUT-based SPR and the DirectSPR for patients with metal implants (N=6).

**Proton treatment planning guidelines to reduce radiation-induced image changes in gliomas**

Anne Vestergaard[1], Jesper Kallehauge[1], Aida Muhic[2,1], Slavka Lukacova[3], Rikke Dahlrot[4,5,1], Charlotte Haslund[6], Bob Smulders[2,1], Yasmin Lassen[1], Morten Høyer[1]

1. Danish Centre for Particle Therapy, Aarhus University Hospital, Aarhus, Denmark
2. Department of Oncology, Rigshospitalet, Copenhagen, Denmark
3. Department of Oncology, Aarhus University Hospital, Aarhus, Denmark
4. Department of Oncology, Odense University Hospital, Odense, Denmark
5. Institute of Clinical Research, University of Southern Denmark, Odense, Denmark
6. Department of Oncology, Aalborg University Hospital, Aalborg, Denmark

**Introduction:** Radiation-induced image changes (RICE) on MRI have been observed after proton therapy of gliomas. RICE often occur in the brain tissue near the ventricles, the periventricular zone (PVZ). Eulitz et al. [1] found that generalized equivalent uniform dose (gEUD, a=11) for PVZ correlated with the risk of RICE. Similarly, Niyazi et al. [2] found that gEUD(a=9) for Brain-GTV-Brainstem correlated with the risk of grad ≥ 2 RICE. This study aims to evaluate the change in dose metrics of Brain-GTV-Brainstem and PVZ in two cohorts of gliomas treated before and after a revision of treatment planning guidelines.

**Materials and methods**: Two cohorts of patients with WHO grade 3 gliomas were treated to a prescription dose of 59.4 Gy (RBE) in 33 fractions using Pencil Beam Scanning, 3-4 beams, and multi-field optimization. Cohort 1: 62 patients treated between 2019 and 2021. Cohort 2: 40 patients treated from 2023 to 2024. PVZ was defined as a 4 mm wall around the ventricles. In February 2023 PVZ was introduced as an organ at risk. To reduce the risk of RICE, the near-max dose (D0.03cc) was stepwise reduced, first to 103% of 59.4 Gy (RBE) and later to 59.4 Gy (RBE). The dose metrics for PVZ were D1cc, D5cc, and gEUD(a=11) and the Brain-GTV-Brainstem metrics D1cc, D5cc, and gEUD(a=9) were calculated. The NTCP model from Niyazi et al. was used and the parameters from the two cohorts were compared using the Wilcoxon-Rank sum-test (α=0.05).

**Results**: The dose metrics for PVZ were all lower in cohort 2 compared to cohort 1. The reductions of D1cc and D5cc were both statistically significant, whereas the reduction of gEUD(a=11) was marginally significant($p=0.06$). For Brain-GTV-Brainstem, all investigated parameters were statistically significantly reduced ($p<0.01$). The mean NTCP decreased from 12% in cohort 1 to 9.6% in cohort 2 ($p=0.02$).

**Conclusions**: Based on dose metrics, a reduction in the risk of RICE is expected in cohort 2. Clinical and MRI follow-up is needed to confirm that this reduction translates into reducing the risk of symptomatic and/or asymptomatic RICE after proton therapy for WHO grade 3 gliomas.

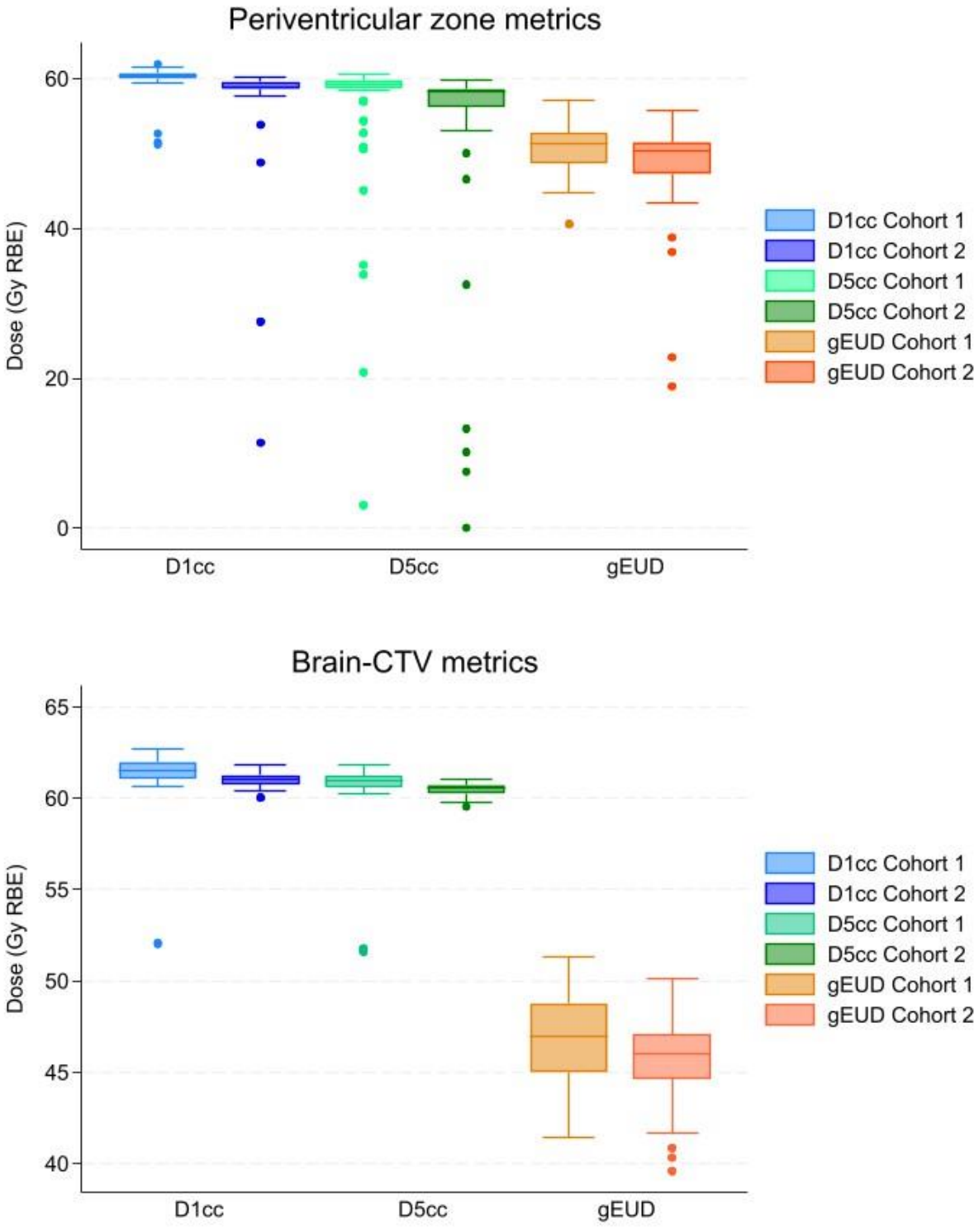


Figure: The upper panel shows the metrics D1cc, D5cc, and gEUD(a=11) for PVZ for the two cohorts treated before and after the change in treatment planning guidelines. The lower panel shows the metrics D1cc, D5cc, and gEUD(a=9) for Brain-GTV-BS. All dose metrics decreased for cohort 2 compared to cohort 1 with p-values ranging from below 0.01 to 0.06.

[1] Eulitz J, E GCT, Klunder L, Raschke F, Hahn C, Schulz E*, et al.* Increased relative biological effectiveness and periventricular radiosensitivity in proton therapy of glioma patients. Radiother Oncol. 2023;178:109422.
[2] Niyazi M, Niemierko A, Paganetti H, Sohn M, Schapira E, Goldberg S*, et al.* Volumetric and actuarial analysis of brain necrosis in proton therapy using a novel mixture cure model. Radiother Oncol. 2020;142:154-61.

# Clinical implementation of Intensity Modulated Proton Therapy (IMPT) for testicular seminoma – result for treatment of the first 30 patients.

**Corresponding author**
Heidi S. Rønde; heidre@rm.dk
Danish Centre for Particle Therapy, Aarhus University Hospital, Aarhus, Denmark

**Authors and affiliations**
Rønde HS[1], Kallehauge JF[1], Høyer M[1], Als AB[2], Agerbæk M[2], Lauritsen J[3], Petersen PM[3], Dysager L[4], Kronborg CJS[1]

1 Danish Centre for Parcle Therapy, Aarhus University Hospital, Aarhus, Denmark
2 Department of Oncology, Aarhus University Hospital, Aarhus, Denmark
3 Department of Oncology, Rigshospitalet, Copenhagen, Denmark
4 Department of Oncology, Odense University Hospital, Odense, Denmark

## Introduction

Proton therapy reduces the mid- and low-dose bath to surrounding tissues. We previously demonstrated that this reduces the estimated secondary cancer risk, which is vital for younger seminoma patients with favourable prognosis (Rønde et al. 2023). Here, we present dosimetric results for implementing Intensity Modulated Proton Therapy (IMPT) as a national standard for seminoma treatment.

## Materials and methods

The initial 30 patients with stage IIa seminoma treated with IMPT were included. Twenty-one patients had 20 Gy (RBE) in 10 fractions and 9 had 24 Gy (RBE) in 12 fractions to the elective clinical target volume (CTV-E) according to national guidelines. For the boost to the positive lymph node (CTV-T) doses ranged from 10-12 Gy (RBE). Plans were robustly (14 scenarios) multi field optimised (MFO) in Eclipse (Varian Medical Systems) on the planning CT. Plans used five fields: three posterior covering the entire target length and two anterior covering only the most caudal region. Organs at risk (OAR) were delineated according to RTOG guidelines. Control CTs were performed routinely, on average 1.5 times per patient (range: 1-3), during treatment to recalculate the dose to ensure target coverage.
A standard IGRT strategy using two Cone-Beam CTs (CBCTs) was developed due to the targets extending beyond the CBCT field of view. Four match structures were used. The first 16 patients were 'hand-held' before implementing a standard adaptive scheme.

## Results

The median CTV-E length in the cranio-caudal direction was 26.9 cm (21.8–32.0) with a median volume of 551.4 $cm^3$ (365.4-805.4). Target coverage of V95%=100% for the nominal plan and V95%>98% for worst-case scenarios were fulfilled for all plans. Likewise, the worst-case scenario was fulfilled for all dose plans recalculated on the 46 control CT scans.

A full list of all OAR results is summarised in Table 1.
The number of replans was four in three patients. The median time for our IGRT strategy was 14:07 minutes (06:50–48:00) across all patients with two CBCTs.

**Conclusions**

We have demonstrated a low OAR dose with clinical implementation of IMPT for seminoma, which has the potential to decrease the risk of secondary cancers, and toxicities such as nausea. The result is in line with the findings in our previous study. Furthermore, we have established a robust setup for treatment planning, IGRT strategy, treatment delivery, and responses to replans when needed. On this basis, we suggest considering IMPT for testicular seminoma when proton therapy is available.

**Table 1.** Results - Median (range)

| OAR | Dose metric | IMPT - 20Gy | IMPT - 24 Gy |
|---|---|---|---|
| Body Outline | Mean [Gy] | 1.5 (1.2 - 2.1) | 1.8 (1.5 - 3.0) |
| Bladder | v15Gy [%] | 1.2 (0 - 7.8) | 1.5 (0 - 15.1) |
| Duodenum | v15Gy [$cm^3$] | 35.9 (1.1 - 84.8) | 44.4 (25.5 - 80.5) |
| Pancreas | v15Gy [%] | 32.3 (0 - 63.1) | 34.9 (0.0 - 70.5) |
| Stomach | v15Gy [$cm^3$] | 0.0 (0.0 - 3.7) | 0.0 (0.0 - 8.1) |
| Bowel Bag | v15Gy [$cm^3$] | 428.9 (194.1 - 614.5) | 462.2 (310.1 - 697.7) |
| Spinal Cord | near max [0.03 $cm^3$] | 12.9 (9.8 - 18.2) | 13.2 (11.8 - 19.9) |
| Kidney L | v17Gy [%] | 0.0 (0.0 - 6.1) | 0.4 (0.0 - 2.6) |
| Kidney L | Mean [Gy] | 1.8 (0.5 - 4.1) | 2.4 (0.0 - 2.6) |
| Kidney R | v17Gy [%] | 0.6 (0.0 - 3.0) | 2.2 (0.0 - 5.0) |
| Kidney R | Mean [Gy] | 2.2 (0.8 - 5.6) | 2.6 (1.3 - 5.7) |

# Linear energy transfer inclusive normal tissue complication probability modelling for late rectal and urinary morbidity following proton therapy

Rasmus Klitgaard[1,2], Stine Elleberg Petersen[1], Perry B. Johnson[3], Mark Artz[3], Curtis Bryant[3], Andreas Havsgård Handeland[4,5], Camilla Hanquist Stokkevåg[4,5], Nancy Price Mendenhall[3] and Ludvig Paul Muren[1,2]

[1]*Danish Centre for Particle Therapy, Aarhus University Hospital, Aarhus, Denmark.* [2]*Dept of Clinical Medicine, Aarhus University, Aarhus, Denmark.* [3]*Dept of Radiation Oncology, University of Florida Health Particle Therapy Institute, Jacksonville, Florida.* [4]*Dept of Physics and Technology, University of Bergen, Bergen, Norway.* [5]*Cancer Clinic, Haukeland University Hospital, Bergen, Norway*

**Introduction:** Normal tissue complication probability (NTCP) modelling for late gastro-intestinal (GI) and genito-urinary (GU) morbidities following proton therapy (PT) of prostate cancer can be used to evaluate the risk of complications ahead of PT. Biological effects from PT depends on the relative biological effectiveness (RBE), which has been shown to vary with the physical entity linear energy transfer (LET). However, previous NTCP models for PT in prostate cancer have not explicitly accounted for this variation. The aim of this study was therefore to develop LET-inclusive NTCP models predicting late GI and GU morbidity following PT of prostate cancer.

**Materials and methods:** Dose and LET was calculated using the FLUKA Monte Carlo code for a cohort of 860 patients previously treated for prostate cancer using PT. Morbidities were scored prospectively using the physician-graded Common Terminology Criteria for Adverse Events (CTCAE) and the patient-reported Expanded Prostate Cancer Index Composite (EPIC), and subsequently included in a multivariate logistic regression. The area under the receiver operating characteristic curve (AUC) was used to evaluate models for four CTCAE endpoints and nine EPIC endpoints, each for volume vs wall metrics.

**Results:** The most selected predictors for all morbidities included age and anti-coagulant use, as well as high-dose/LET volumes and LET-constrained equivalent uniform dose measures for LET above 2 keV/µm for GI morbidities and above 2.5 keV/µm for GU morbidities (Fig. 1). AUC values were between 0.52 and 0.80 across all models. Models based on rectum and bladder volume metrics were similar to models based on rectal and bladder wall metrics.

**Conclusions:** NTCP models predicting late GI and GU morbidities were dependent on age, anti-coagulant use and for GI models also high-dose levels delivered at LET values above 2 keV/µm. Late GU morbidity models included low, intermediate and high doses delivered at LET values above 2.5 keV/µm, but volumes with LET levels above 6 keV/µm without dose constraints were also identified as predictive.

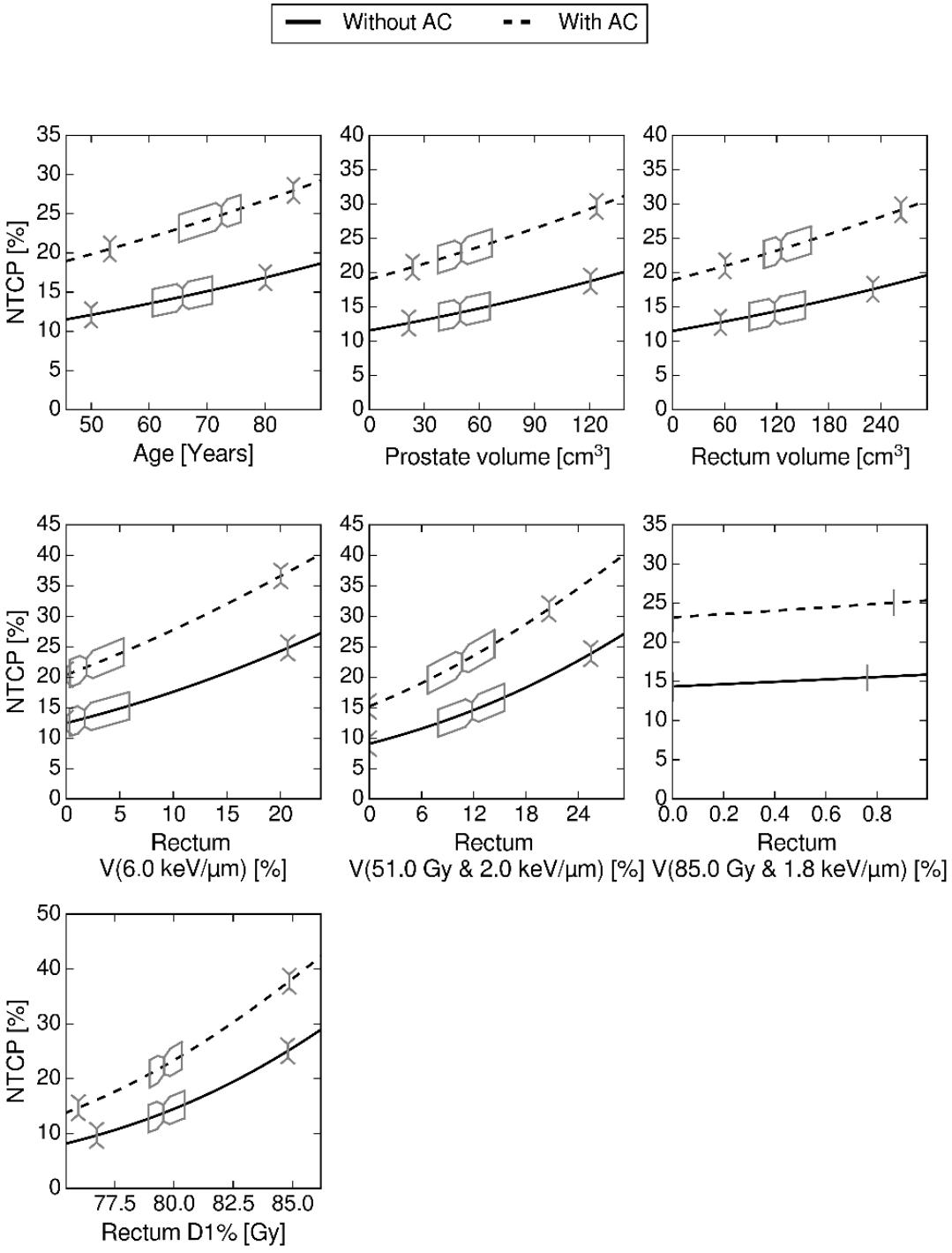


Figure 1: GI Grade 2+ NTCP model based on rectum metrics. For each panel, all other parameters are fixed at their mean value. The horizontal box-plots on the curves indicates the parameter values in the total cohort, both for patients with AC usage (dotted lines) and those without AC usage (solid lines). The boxplot ticks are 2.5% percentile, 25 percentile, median (notch), 75% percentile and 97.5% percentile.

# 3D Swin Transformer for Patient-Specific Proton Dose Prediction of Brain Cancer Patients

Anne Haahr Andresen[1,2], Yasmin Lassen[2], Slávka Lukacova[3], Christian Rønn Hansen[2,4,5], Jesper Folsted Kallehauge[1,2]

[1] Department of Clinical Medicine, Aarhus University, Aarhus, Denmark
[2] Danish Centre for Particle Therapy, Aarhus University Hospital, Aarhus, Denmark
[3] Department of Oncology, Aarhus University Hospital, Aarhus, Denmark
[4] Department of Oncology, Odense University Hospital, Odense, Denmark
[5] Institute of Clinical Research, University of Southern Denmark, Odense, Denmark

## Introduction

Deep Learning (DL) models have been investigated extensively to mimic clinically relevant photon doses for a wide variety of clinilcal treatment sites. Contrarily, proton dose prediction has seen slower progress, potentially, due to the fact that tradiational U-Net approaches with local receptive fields being unable to capture the long range unique dose fall off of proton therapy. This study aimed to evaluate the performance of a novel DL approach for proton dose prediction in the brain.

## Method and Materials

A dataset of 191 patients with corresponding CT scans, clinically approved proton treatment plans, and all relevant structures including target and organs at risk (OAR) was used. Of the 191 dose plans, 181 were used for training and 10 for final evaluation. The 3D shifted window transformer (Swin-Transformer) was trained for 50 Epochs, batch size of 1, and using ADAM optimizer on a NVIDIA A40 GPU. The final prediction was mean normalized to CTV prescribed dose of the references plans. Comparison to clincal ground truth was evaluated using, Gamma analysis (3%, 3 mm) and global Mean Absolute Error (MAE), to evaluate dose accuracy and structural similarity index measure (SSIM) to assess structural and perceptual similarity between predicted and ground truth.

## Results

The 3D Swin transfomer proton dose prediction model achieved a median Gamma(3%,3mm) pass rate of 63.7% (42.5% - 74.6%), global median MAE of 0.45 Gy (0.27-1.30) Gy and median SSIM of 0.93 (0.90-0.97). Graphic example of proton dose prediction performance is given in figure 1 along with comparison of relevant dose volume histograms (DVH).

**Conclusion**

The evaluated performance parameters highlights the potential of the 3D Swin transformer as interesting candidate for the proton dose prediction in the brain. Systematic hyperparameter tuning and physics-informed constraints could potentially further improve the model performance and its future clinical use.

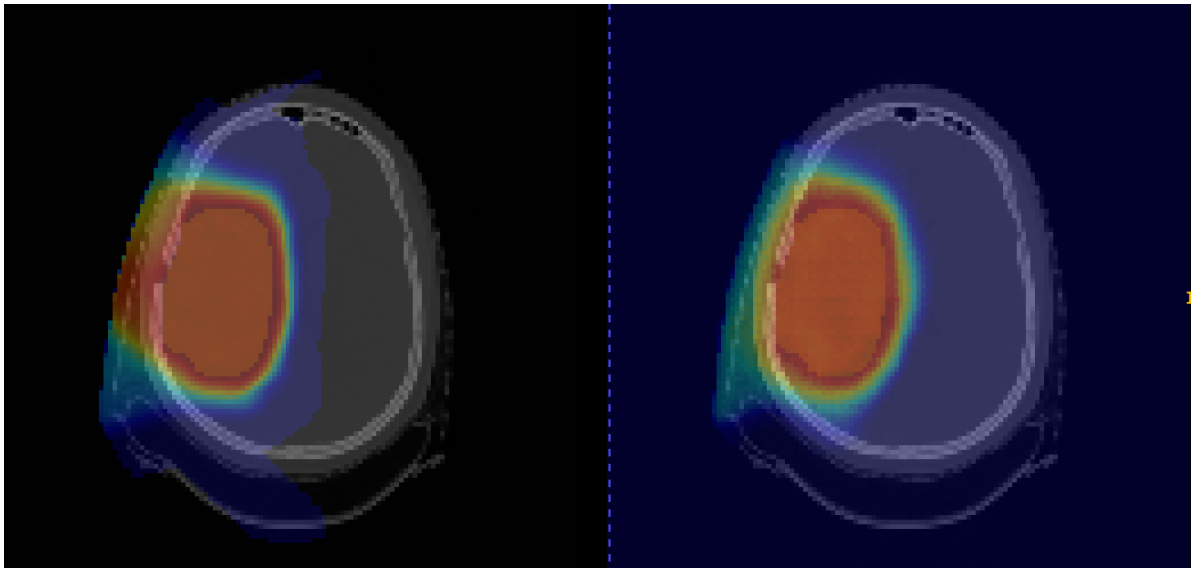

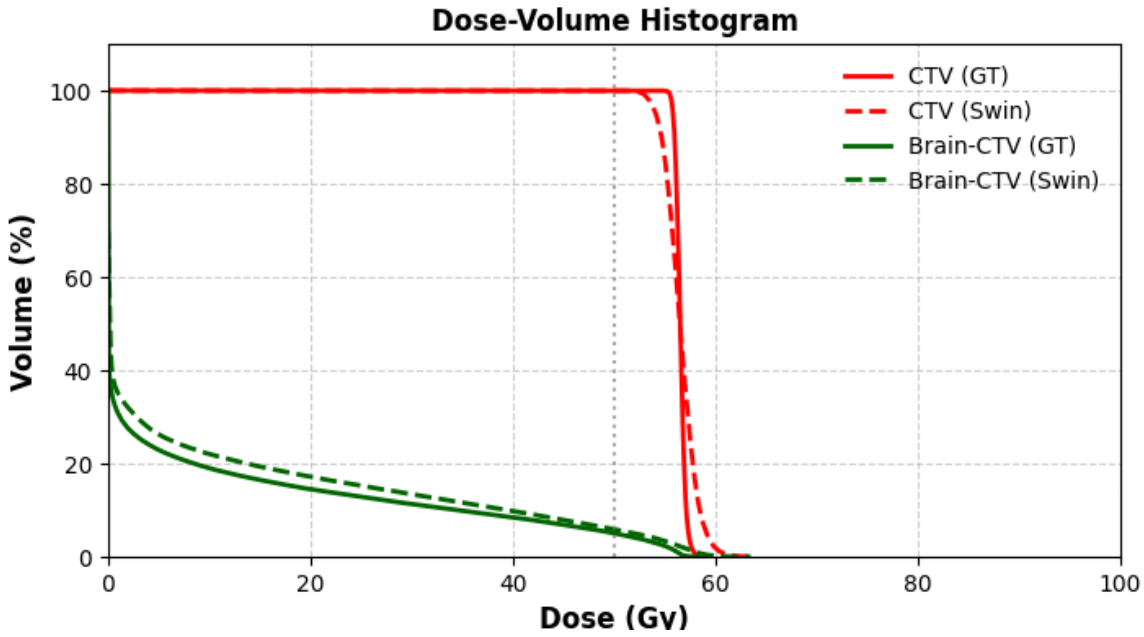


Figure 1: Comparison of dose distributions from ground truth (top left) and Swin-Transformer (top right). The DVH (bottom) illustrates good agreement to ground truth for CTV (red) and Brain-CTV (green).

**Determining the effects of hyperthermia on the tumor and acute normal tissue response of electron FLASH radiotherapy**

Sinha PM[1], Kristensen L[1,2], Folefac CA[1], Præstegaard LH[3], Hoffmann L[3], Poulsen PR[2], Horsman MR[1], Sørensen BS[1,2]

[1]Experimental Clinical Oncology-Department of Oncology, [2]Danish Centre for Particle Therapy, [3]Department of Oncology, Aarhus University Hospital,DK-8200, Aarhus, Denmark

**Introduction:** The normal tissue-sparring potential of ultra-high dose rate (FLASH) radiation is an emerging area of research in radiation oncology, as radiation delivered in extremely short durations (within milliseconds), has shown to significantly reduce normal tissue toxicity in comparison to conventional radiation, while maintaining the same tumor response. However, there is no previous indication of how mild hyperthermia – a potent radiosensitiser – would influence this unique proposition of FLASH radiotherapy. Hence, this study was designed to investigate the potential of combining FLASH radiation with hyperthermia in tumors as well as normal tissues.

**Materials and Methods:** Experiments were conducted using unanaesthetised female C3D2F1 mice, in which C3H tumors were implanted in the right hind leg. Treatments were initiated when tumors reached approximately 200 $mm^3$. The tumor-bearing leg was restrained and irradiated with a single dose of electron radiation at either a conventional dose rate (CONV; ~0.17 Gy/s) or an ultra-high dose rate (FLASH; ~233 Gy/s), administered alone or in combination with hyperthermia (42.5°C for 60 minutes, given 30 minutes after radiation). For normal tissue studies, the same mouse model and experimental setup were used, but with non-tumor-bearing mice.

In tumor studies, the endpoint was the time required for the tumor volume to reach three times its initial treatment size ($TGT_3$). With this, the area under the dose-response curve (AUC) was calculated to assess efficacy. For normal tissue studies, the responders for moderate moist desquamation and leg deformities, was determined. These were then further analysed using logistic regression to evaluate their correlation with applied treatments.

**Results:** In our experiments, FLASH radiation was ~1400 times faster than CONV radiation. The radiation induced tumor and acute normal tissue studies are summarised on table 1.

**Table 1:** Summary showing the dose rate-effects and hyperthermic radiosensitaisation in tumors and acute normal tissues.

| | **Tumor Studies** | | **Acute Normal tissue Studies** | |
|---|---|---|---|---|
| **Groups** | **AUC (95% CI)** | **dDMF (95% CI)** | **$MDD_{50}$ (95% CI)** | **dDMF (95% CI)** |
| **CONV** | 238.12 (203.43 - 273.82) | **1.11 (0.84 - 1.46)** | 30.13 (29.10 - 31.20) | **1.53 (1.46 - 1.61)** |
| **FLASH** | 264.53 (205.77 - 323.30) | | 45.67 (43.87 - 47.55) | |
| **CONV + heat** | 390.64 (314.37 - 466.91) | **1.01 (0.82 - 1.27)** | 23.36 (22.11 - 24.67) | **1.45 (1.34 - 1.56)** |
| **FLASH + heat** | 394.56 (348.71 - 440.41) | | 34.24 Gy (32.76 - 35.79) | |

**AUC**: Area under the dose response curve (Gy*days); **CONV**: Conventional radiation (~0.17 Gy); **dDMF**: dose-rate Dose modifying factor: (FLASH / CONV); **FLASH**: ultra-high dose rate radiation (~233 Gy); **heat**: Hyperthermia (42.5°C for 1 hour, given 30 minutes after radiation); **$MDD_{50}$**: Dose required to induce an acute skin response in 50% of the treated mice (Gy).

**Conclusion:** Tumor response remained comparable between CONV and FLASH radiation, even when heat is applied. FLASH radiation demonstrated an acute normal tissue protection when compared to CONV radiation, and both FLASH and CONV radiation response was enhanced to a similar level when heated.

**Fractionation reduces FLASH-sparing in an acute skin murine model**

**Line Kristensen,** line.kristensen@clin.au.dk, Danish Centre for Particle Therapy & Department for Experimental Clinical Oncology, Aarhus University Hospital, Aarhus, Denmark.

**Line Kristensen**[a,b,c], Jacob Graversen Johansen[a,c], Sky Rohrer[a,c], Anna Holtz Hansen[b,c], Lars H Præstegaard[d], Lone Hoffmann[c,d], Per Rugaard Poulsen[a,c], Brita Singers Sørensen[a,b,c]

[a] Danish Centre for Particle Therapy, Aarhus University Hospital, Aarhus, Denmark
[b] Department of Experimental Clinical Oncology, Aarhus University Hospital, Aarhus, Denmark
[c] Department of Clinical Medicine, Aarhus University, Aarhus, Denmark
[d] Department of Oncology, Aarhus University Hospital, Aarhus, Denmark

**Introduction:** A favourable normal tissue-sparing effect of FLASH irradiations with ultra-high dose rates has been shown in several preclinical studies. Most studies report single-dose irradiations and do not include a fractionated irradiation scheme. The clinical standard is fractionated radiotherapy, and therefore the interplay between fractionation and FLASH sparing is of high relevance. This study quantified the tissue-sparing effect of FLASH on acute skin toxicity with a single dose, four-fraction and eight-fraction scheme.

**Materials and methods:** Acute skin toxicity after conventional dose rate (CONV, 0.16 Gy/s) and FLASH (mean±sd 247±10 Gy/s) irradiation was assessed in female CDF1 mice. The right hindleg of unanaesthetised mice was irradiated using either a single dose, one daily dose for four consecutive days or two daily doses with a 6-hour interval for four consecutive days with 6 - 12 mice per dose. A FLASH-enabled Varian TrueBeam accelerator delivered irradiation with a 16 MeV electron beam. Acute skin toxicity was quantified by hair loss, moist desquamation and toe separation and was monitored daily from 9 to 25 days post-treatment.

**Results:** The comparison of CONV to FLASH irradiated mice indicated a tissue-sparing effect of FLASH for single-irradiation, which was partly lost for 4-fractions and fully lost for 8 fractions (Figure 1). Single-dose irradiations provided a mean dose modification ratio of 1.42 (Figure 1A). In contrast, 4 fractions provided a lower mean FLASH protection ratio of 1.20 (Figure 1B). For 8 fractions, the protection ratio was reduced to 1.05 with overlapping 95% confidence intervals (Figure 1C).

**Conclusion:** Fractionation reduced the acute skin-sparing effect seen in single-fraction FLASH studies. However, a tissue-sparing effect of 20% was still present at 4 fractions. When moving to 8 fractions, the protective effect of FLASH was lost. Thus, the FLASH tissue-sparing was increasingly reduced in the investigated fractionation schemes.

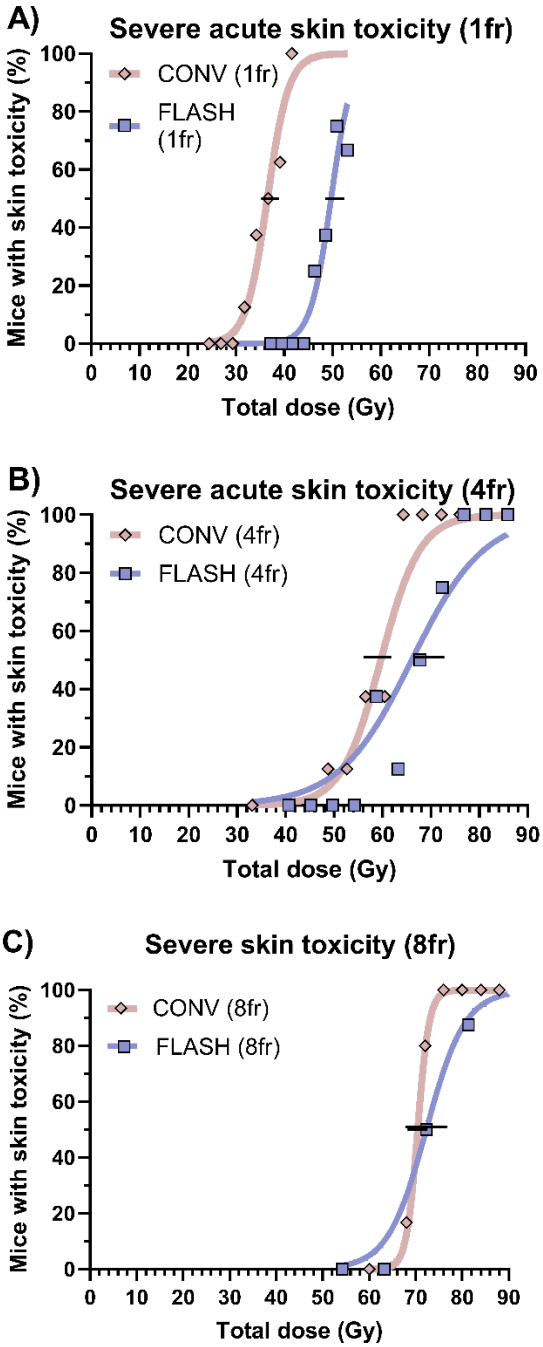


**Figure 1: Dose-response curve for acute skin toxicity after electron irradiation.** Percentage of mice developing severe skin toxicity as a function of dose within 25 days after exposure with a conventional (CONV) dose rate (pink diamonds) or ultra-high dose rate (FLASH, blue squares), and their logistic regression model outcomes (CONV pink line, FLASH blue line). Black lines indicate 95% CI at 50% toxicity for each dose-response curve.
A) Response to single dose (1 fraction) irradiation.
B) Response to 4-fraction irradiations.
C) Response to 8-fraction irradiations.

**Mild hypoxia reduces FLASH skin-sparing in a murine model**

**Line Kristensen,** line.kristensen@clin.au.dk, Danish Centre for Particle Therapy & Department for Experimental Clinical Oncology, Aarhus University Hospital, Aarhus, Denmark.

**Line Kristensen**[a,b,c], Jacob Graversen Johansen[a,c], Sky Rohrer[a,c], Cathrine Overgaard[b,c], Anna Holtz Hansen[b,c], Per Rugaard Poulsen[a,c], Brita Singers Sørensen[a,b,c]

[a] Danish Centre for Particle Therapy, Aarhus University Hospital, Aarhus, Denmark
[b] Department of Experimental Clinical Oncology, Aarhus University Hospital, Aarhus, Denmark
[c] Department of Clinical Medicine, Aarhus University, Aarhus, Denmark
[d] Department of Oncology, Aarhus University Hospital, Aarhus, Denmark

**Introduction:** The FLASH effect, where ultra-high dose rate (UHDR) elicits a favourable normal tissue-sparing, has been shown in several preclinical in vivo studies. The degree of tissue-sparing is debated, in part because it seems to be tissue-type dependent. Furthermore, differences in study setups might cause significant changes to the investigated system. Factors such as the fixation method of in vivo models could influence irradiation response, as it changes blood supply, which in turn changes e.g. oxygen levels. This study investigated the acute skin sparing effect of FLASH after single-dose irradiation under two different fixation methods: a glued fixation with minimum blood supply restriction and a taped fixation with slight blood supply restraint to the skin.

**Materials and methods:** The radiation-induced acute skin toxicity of 307 female CDF1 mice was assessed. Mice were treated on their right hindleg with a single-dose irradiation between 19 - 58 Gy with either conventional (CONV, 0.16 Gy/s) or FLASH (247±10 Gy/s) irradiation. The leg was fixated with either glue or tape. Mice in the glue-fixation arm were taped during the gluing procedure and had a 10-minute period afterwards without tape restraint to restore blood supply to the leg. Mice in the tape-fixation arm were taped on their toes shortly before and throughout the irradiations. Irradiations were performed with a FLASH-enabled Varian TrueBeam accelerator using a 16 MeV electron beam. Acute skin toxicity was quantified by hair loss, moist desquamation and toe separation and was monitored daily from 9 to 25 days post-treatment. A dose-modification factor (DMF) was found from CONV compared to FLASH for each fixation method.

**Results:** A FLASH skin-sparing effect was found for both glued and taped mice compared to CONV irradiated mice (Figure 1). The DMF was 54% for glue-fixated mice and 37% for tape-fixated mice. The dose-response curves revealed this difference in DMF to be entirely due to a shift in radiosensitivity for CONV-treated mice (Figure 1). CONV-treated tape-fixated mice were more radioresistant than the glue-fixated mice, consistent with the expected response to mild hypoxia. Meanwhile, the fixation method did not affect the mice treated with FLASH.

**Conclusion:** Blood supply modulation due to the fixation method, and thus possibly oxygen modulation, influenced the radiation-induced acute skin toxicity for CONV-treated mice but did not affect FLASH-treated mice. These observations support the impact of blood supply and in turn oxygen level in the mechanism behind the FLASH tissue-sparing effect.

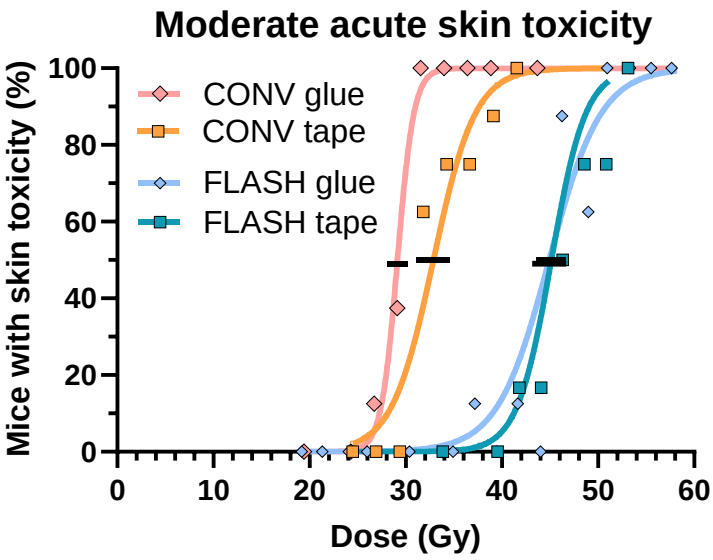


**Figure 1**: Dose-response relationship for conventional dose rate (CONV) irradiations (red nuances) compared to FLASH irradiations (blue nuances) for mice fixated with glue (diamonds) compared to tape (squares). Black lines depict 95% confidence intervals. For each curve, n=68-114 mice.

# How is the FLASH effect influenced by oxygen deprivation in a murine model?

**Anna Holtz Hansen anho@oncology.au.dk**

Anna Holtz Hansen[a,b,c,], Line Kristensen[a,b,c], Lone Hoffmann[c,b], Lars H Præstegaard[b], Jacob Graversen Johansen[a,c], Michael Robert Horsman[b,c], Per Rugaard Poulsen[a,c], Brita Singers Sørensen[a,b,c,]

[a] Danish Centre for Particle Therapy, Aarhus University Hospital, Aarhus, Denmark
[b] Department of Oncology, Experimental Clinical Oncology, Aarhus University Hospital
[c] Department of Clinical Medicine, Aarhus University, Aarhus, Denmark

**Background:** FLASH-Radiotherapy (FLASH-RT) has gained increasing attention for its potential to reduce normal tissue toxicity while preserving tumor control effectiveness similar to conventional dose rate (CONV) radiotherapy. However, the cellular mechanism behind FLASH is still unknown. One hypothesis for the effectiveness of FLASH-RT suggests that the induction of radiolytic oxygen depletion (ROD) causes radiation protection of normal tissues. This study provides experimental data to elucidate aspects of the ROD hypothesis by comparing the FLASH skin sparing effect between normoxic and hypoxic conditions in an established radiobiological setup for in vivo irradiation of mice legs.

**Methods:** The experimental setup involved four treatment groups of unanesthetized female C3H/HeNRj mice, exposed to either conventional dose rate (0.16 Gy/s) or UHDR (ultra high dose rate) (233 Gy/s) electron beam irradiation under normoxic or oxygen deprived conditions. A FLASH-enabled TrueBeam accelerator (Varian) delivered irradiation with a 16 MeV electron beam. Oxygen deprivation was induced by clamping the irradiated hindleg with tourniquets to restrict blood supply prior to and during irradiation. The acute biological response to radiation was quantified using full dose response curves for an acute skin toxicity assay, with skin damage scored on a scale from mild to severe. The scoring system assessed hair loss, moist desquamation area, lack of toe separation, and skin redness over the 28-day period following irradiation.

**Results:** Restricting oxygen supply by clamping the hindleg during irradiation resulted in a general shift of the dose-response curves, requiring higher doses for both CONV and FLASH irradiation to achieve the same level of skin toxicity. However, while FLASH required approximately 50% higher doses than CONV to induce equivalent toxicity under normal oxygen conditions, under clamped conditions, the dose-response curves for FLASH and CONV were no longer statistically distinct. The lack of normal-tissue sparing under hypoxia indicates that oxygen plays a key role in the normal tissue-sparing effect of FLASH

**Conclusion:** This study showed that the presence of oxygen is crucial to obtain the FLASH sparing effect. The observed lack of FLASH sparing under oxygen deprived conditions would be expected if the FLASH effect is partly caused by or amplified by ROD.

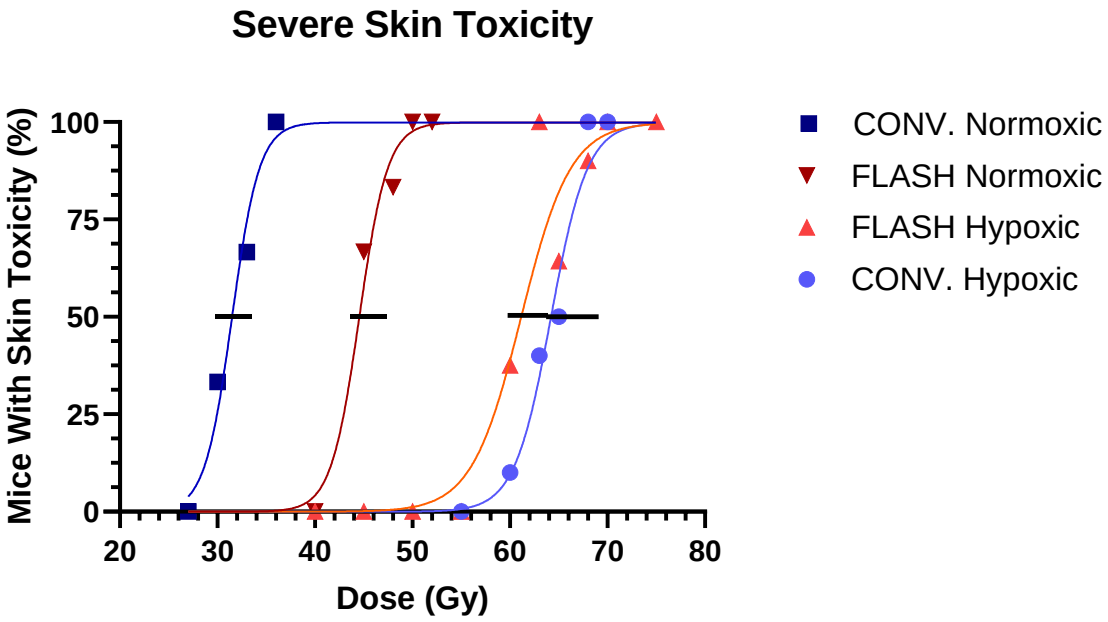
Severe Skin Toxicity
Mice With Skin Toxicity (%)
100
75
50
25
0
20
30
40
50
60
70
80
Dose (Gy)
CONV. Normoxic
FLASH Normoxic
FLASH Hypoxic
CONV. Hypoxic

**A Quantitative Approach to Image Quality Assessment for Delineation in Radiotherapy**

Cecilie Valet Henneberg[1,2,*], Weronika E. Olech[3], Mathias Dreyer Teller[1,4], Gitte Fredberg Persson[1,4], Michael Brun Andersen[3], Felix Christoph Müller[3], Claus P. Behrens[1,2], Henriette Klitgaard Mortensen[1], Jens M. Edmund[1]

[1]*Department of Oncology, Copenhagen University Hospital - Herlev and Gentofte, Copenhagen, Denmark;* [2]*Department of Health Technology, Technical University of Denmark, Kgs. Lyngby, Denmark;* [3]*Department of Radiology, Copenhagen University Hospital - Herlev and Gentofte, Copenhagen, Denmark;* [4]*Department of Clinical Medicine, University of Copenhagen, Copenhagen, Denmark*

**Introduction**: High-quality imaging is crucial for accurate tumor and organs-at-risk (OARs) delin-eation, directly impacting the effectiveness of radiotherapy (RT). Qualitative assessments of CT image quality by clinicians can be time-consuming and prone to bias. This study uses the contrast-to-noise ratio (CNR) as a quantitative surrogate for clinical image quality assessment in photon-counting CT (PCCT).

Materials and Methods: 140 kVp PCCT scans of a (semi-)anthropomorphic abdomen phantom (QRM) and two patients were acquired. The CNR was calculated between an iodine insert (2 mg/cm³) and solid water for the phantom, and between the prostate and bladder for the patients. Two regions of interest

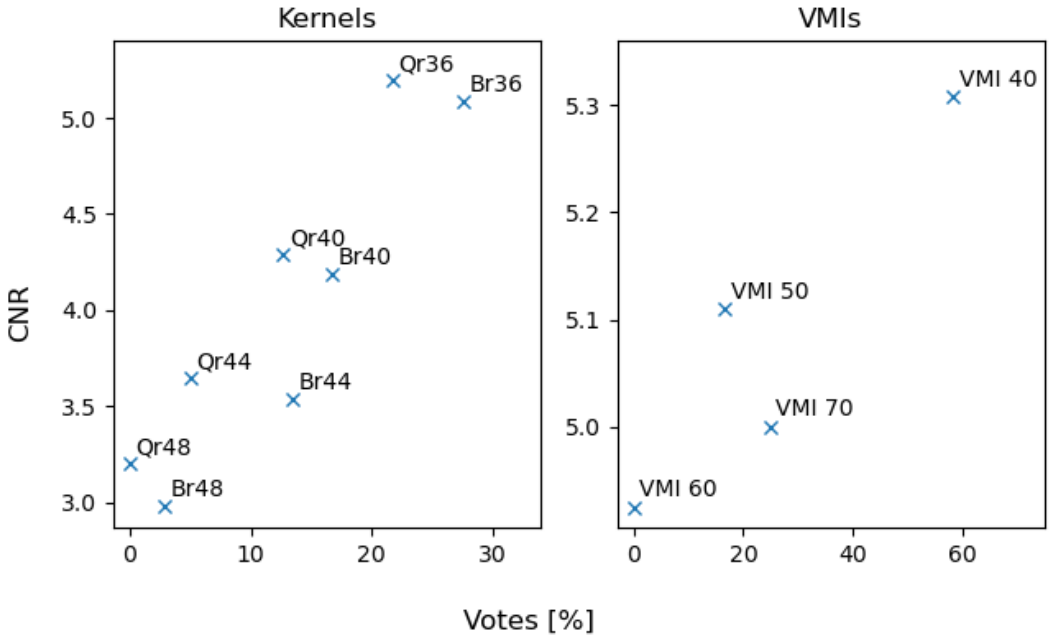


Figure 1: The left plot shows CNR as a function of vote percentage for eight kernels, averaged over VMI 40, 50, 60, and 70 keV, as well as two patients. The right plot presents CNR as a function of vote percentage for four VMIs, using Br36 and averaged over the same two patients. To assess clinical usability, experts evaluated key structures such as the prostate/bladder and prostate/rectum borders. In a 'choose best' setting, they selected the optimal kernel for each reconstruction and the best reconstruction for their preferred kernel. The collected votes were then converted into percentages and averaged across reconstructions and patients to identify trends in expert preferences.

*cecilie.valet.henneberg@regionh.dk

(ROIs) were manually positioned on the scans and the CNR was calculated as

$$CNR = \frac{|HU_1 - HU_2|}{\sqrt{SD_1^2 + SD_2^2}} \quad (1)$$

where $HU_{1/2}$ and $SD_{1/2}$ are the mean and standard deviation of ROIs 1 and 2, respectively. For the patient scans, the prostate ROI was placed near the gold markers to ensure coverage within the gland, while minimizing the impact of metal artifacts and calcium deposits. Identical ROIs were used across various kernels (Qr/Br/Bv/Hr/Hv 36-72) and reconstructions (virtual monoenergetic images, VMI 50-170 keV) to eliminate variability from placement differences. A blinded, multidisciplinary expert panel consisting of oncologists, radiologists, and radiographers (5-7 in total) assessed the clinical image qual-ity of different kernel/VMI combinations through individual voting. The Spearman correlation between CNR and expert assessments was calculated to determine alignment with clinical preferences.

**Results**: Both phantom and patient studies showed that softer kernels (Qr/Br ≤ 48) and VMIs ≤ 70 keV resulted in higher CNR. Expert votes favored these soft kernels but showed inconsistencies in VMI preferences (Figure 1). While CNR suggested improved quality at lower VMIs, experts were divided between these and VMI 70, which is equivalent to standard CT quality. This discrepancy could reflect either bias or limitations in using CNR alone to fully capture clinical usability. The Spearman test confirmed a strong correlation between CNR and kernel preferences (r=0.83, p=0.01) but no clear correlation between CNR and VMI preferences (r=0.8, p=0.2), suggesting additional factors influence expert decision-making in addition to CNR.

**Conclusion**: A CNR-based quantitative approach can effectively guide kernel selection for PCCT in RT but has limitations for VMI. The lack of significant correlation between CNR and VMI preference suggests that additional image quality metrics may be necessary, although a trend toward low VMIs was observed. Future work will explore additional image quality metrics based on clinicians' assessments to improve the method's clinical relevance.

# A prospective observational study on the clinical utility of photon-counting and dual-energy CT for prostate cancer delineation


## Author names and affiliations

Teller LMD[a+b], Henneberg CV[a+c], Lindberg H[a], Løgager V[d], Petersen SE[e], Taasti VT[e], Bassermann L[e], Olech WE[d], Mortensen HK[a], Søndergaard J[g], Madsen CV[h], Yakymenko D[i], Jakobsen CB[f], Behrens CP[a+c], Müller F[d], Andersen MB[d+b], Persson GF[a+b], Edmund J[a].

*[a] Department of Oncology, Copenhagen University Hospital, Herlev and Gentofte, Herlev, Denmark, DK; [b] Dept of Clinical Medicine, University of Copenhagen, Copenhagen, DK; [c] Department of Health Technology, Technical University of Denmark, Kgs.Lyngby, Denmark. [d] Department of Radiology, Copenhagen University Hospital, Herlev and Gentofte, Herlev, Denmark, DK; [e] Danish Centre for Particle Therapy, Aarhus University Hospital, Aarhus, DK; [f] Department of Oncology, Copenhagen University Hospital - Rigshospitalet, Copenhagen, DK; [g] Department of Oncology, Aalborg University Hospital, Aalborg, DK; [h] Department of oncology, Vejle Hospital, Vejle, DK; [i] Department of oncology, Næstved Hospital, Næstved, DK.*


## Introduction

Single-energy CT (SECT) has limited soft tissue contrast, making it inferior to MRI for delineating and staging prostate cancer. Photon-counting CT (PCCT) offers improved spatial resolution, higher contrast-to-noise ratio (CNR), and elimination of electronic noise. Additionally, PCCT enables virtual monoenergetic images (VMI) and iodine mapping, enhancing contrast and reducing inter-observer variability.

This prospective observational study evaluates DECT and PCCT for improving radiotherapy (RT) delineation accuracy and reducing MRI registration uncertainties compared to the standard radiotherapy delineation setup (SECT+MRI). It consists of two phases: Phase 1, developing a delineation DECT- and PCCT-based prostate atlas and Likert scale. Phase 2: Multicentre delineation and subjective image quality rating performed by six radiotherapy departments (Figure 1), set to begin Q3 2025. This abstract presents Phase 1 results.

We propose a standardized workflow for evaluating new imaging modalities in RT, supporting delineation studies, and facilitating clinical implementation. While demonstrated for PCCT in prostate cancer, this ap-proach is applicable to other modalities and cancer types.

## Materials and methods

Phase 1: Five prostate cancer patients underwent MRI, contrast-enhanced (CE) PCCT, and CE-DECT at Herlev Hospital. SECT-equivalent images were generated from DECT. Potential candidates for optimal reconstruction kernels and VMIs combinations were pre-selected based on CNR measurements from an anthropomorphic phantom study.

A multidisciplinary workshop (oncologists, radiologists, a radiation therapist, and a diagnostic radiographer) identified the most suitable reconstruction kernel and VMIs for prostate and seminal vesicle delineation. For each VMI, participants viewed eight images with two reconstruction kernels and performed a blinded vote, selecting the most optimal for delineation. The voting results guided the development of a delineation atlas to standardize procedures and reduce inter-observer variability. A five-point Likert scale (1 = delineation not possible, 5 = excellent) was designed to assess the clinical utility of selected images in Phase 2.


Louis Mathias Dreyer Teller, e-mail: louis.mathias.dreyer.teller@regionh.dk

## Results

The workshop identified VMI 70keV, VMI 40keV, and iodine maps as optimal PCCT image sets, with BR36 as the preferred reconstruction kernel. A delineation atlas incorporating selected images was developed to opti-mize prostate delineation. A Likert scale was created to assess subjective image quality rating for RT planning, providing structured feedback on the potential clinical benefits of individual images.

## Conclusion

We have established a structured workflow for assessing the clinical feasibility of novel imaging modalities compared to current practice (Figure 1). This method ensures an approach to systematically evaluating and integrating novel imaging into radiotherapy planning, facilitating its potential adoption across various cancer types.

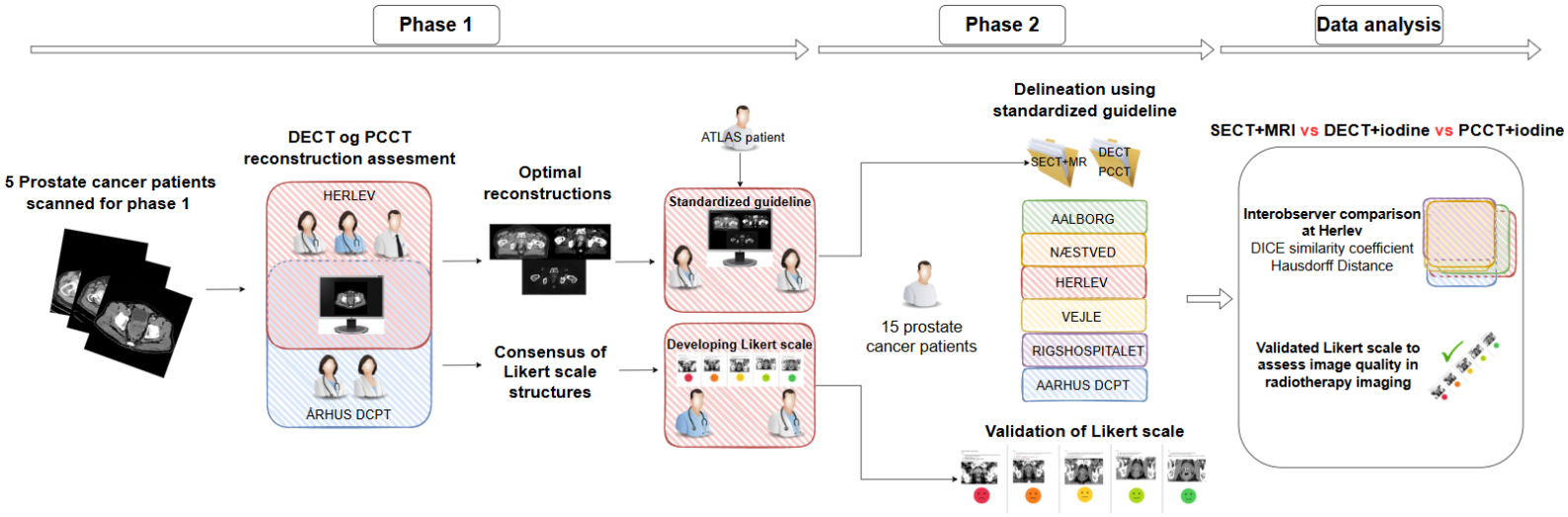


**Figure 1** *Overview of the proposed standardized workflow.*
Phase 1: Development of a DECT- and PCCT-based prostate delineation atlas and a Likert scale. Phase 2: Patient inclusion, multicenter delineation, and subjective image quality assessment. Data analysis includes inter-observer variability (Dice similarity coefficient and Hausdorff distance).

**Accurate Dose Calculation in Combined Single- and Dual-Energy CT Workflows in Radiotherapy**

Hella Sand, hmbs@rn.dk, Department of Medical Physics, Aalborg University Hospital, Aalborg, Denmark

**Authors**

Hella Sand[1,2], Jens Edmund[3], Ane Appelt[4], Jimmi Søndergaard[5], Laurids Østergaard Poulsen[2,5], Martin Skovmos Nielsen[1,2]

[1]Department of Medical Physics, Aalborg University Hospital, Aalborg, Denmark
[2]Department of Clinical Medicine, Aalborg University, Aalborg, Denmark
[3]Department of Oncology, Radiotherapy Research Unit, Copenhagen University Hospital - Herlev and Gentofte, Herlev, Denmark
[4]Leeds Institute of Medical Research, University of Leeds, Leeds, UK
[5]Department of Oncology, Aalborg University Hospital, Aalborg, Denmark

**Introduction**

Dual-energy CT (DECT) is gaining prominence in radiotherapy due to its ability to enhance contrast, reduce artifacts, and provide material characterization, including relative electron density (RED) and perfusion maps. This development will naturally lead to mixed clinical workflows within the same department, where patients are scanned with either single-energy CT (SECT) or DECT. Accurate dose calculation requires a Hounsfield lookup table (HLUT) to convert Hounsfield units (HU) to electron or mass densities, which depend on both scan energy and reconstruction method. This study aims to create a fail-safe approach for the use of a single HLUT for both SECT and DECT workflows.

**Materials and methods**

A head/body-phantom (Gammex, Sun Nuclear) with nine density inserts (0.525–1.924g/cc) was scanned using SECT (120kVp) and DECT (head mode: 80kVp/Sn140kVp, body mode: 100kVp/Sn140kVp). DirectDensity (Siemens) reconstructs mass (DDm) or RED images (DDe) independent of SECT tube potential. SECT reconstructions included standard, DDm, and DDe. DECT reconstructions included virtual monoenergetic images (VMIs), RED, and DDm/DDe from the high-energy spectra (Sn140kVp).

HLUTs were generated for all SECT and DECT reconstructions. Matching DECT-HLUT for each SECT-HLUT was identified based on minimal root mean square error (RMSE).

To validate the proposed approach in a clinical-like setting, a whole-body anthropomorphic phantom (PBU-60) was SECT and DECT scanned as above. SECT standard, DDm and DDe based treatment plans were re-calculated on the matching DECT reconstructions, and dose differences were evaluated for voxels receiving >10% of prescribed dose (Th10%) in head (20Gy/4Fx), thorax (66Gy/33Fx), and pelvis (37.5Gy/3Fx).

**Results**

HLUT matching *(Figure 1)*: The DECT VMI 71keV yielded the lowest RMSE (4HU) for the SECT standard (Method1). A DDm from the Sn140kVp DECT best matched the corresponding SECT DDm (RMSE=5HU) (Method2). The DECT RED showed closest agreement with the corresponding SECT DDe (RMSE=6HU) (Method3).

Dose differences *(Figure 1, insert)*: For Method1, >98% of voxels were within 0.8%, 1.0% and 0.3% of prescribed dose for the head, thorax and pelvis, respectively. For Method2, >98% of voxels were within 1.5% (head), 1.5% (thorax), and 1.0% (pelvis). For Method3, >98% of voxels were within 4.0% (head), 1.3% (thorax), and 1.8% (pelvis).

**Conclusion**

For Method1 and Method2, a shared HLUT enables accurate dose calculations with clinically acceptable dose differences (0.3–1.5%). In contrast, Method3 results in dose differences up to 4.0%, challenging acceptability. Thus, shared HLUTs are feasible for selected reconstruction methods, supporting a more flexible and robust clinical workflow for DECT implementation in radiotherapy.

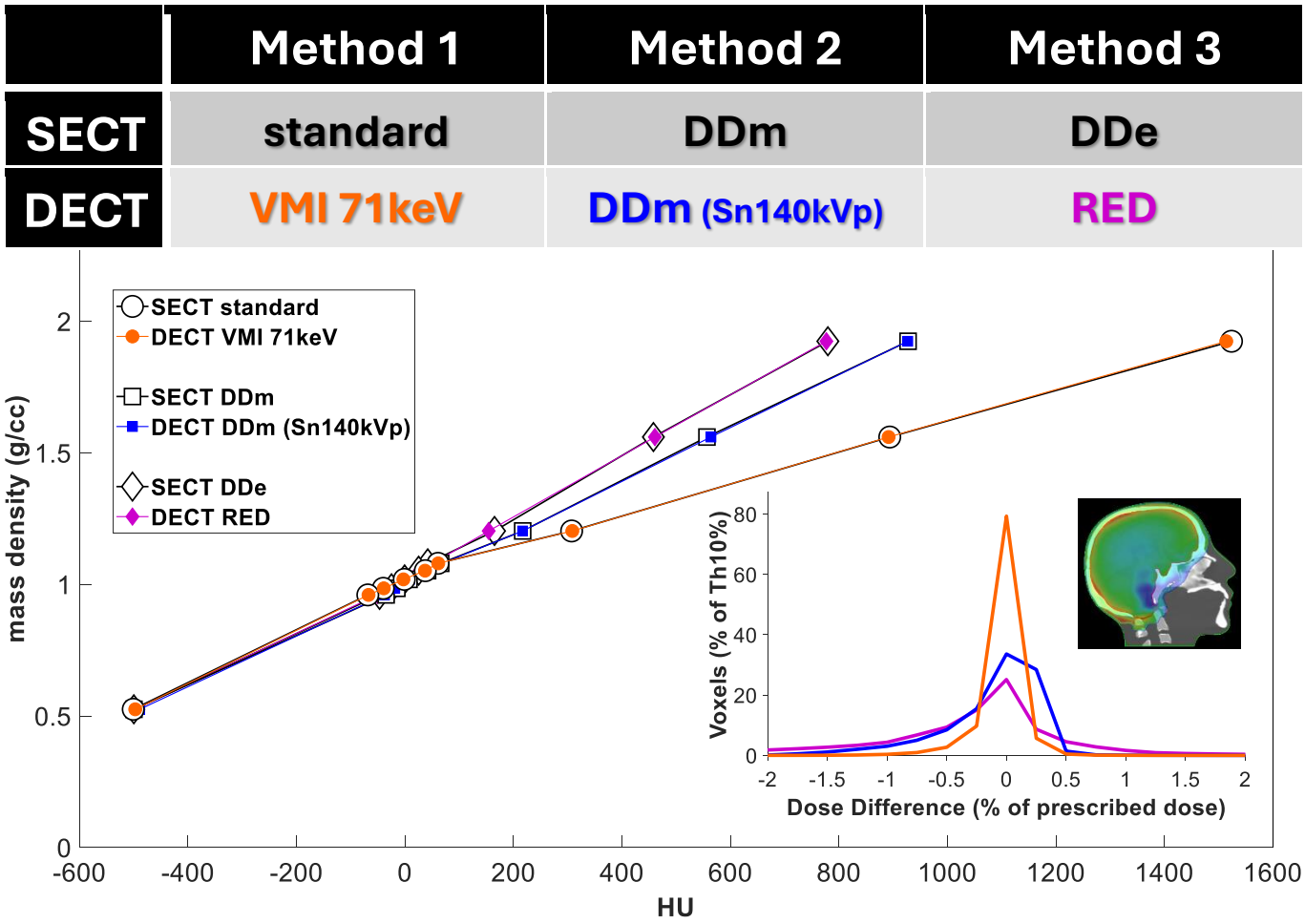


***Figure 1.*** HLUT curves for SECT and DECT across all three methods. *Insert, lower right corner:* Voxel dose differences (for voxels receiving >10% of prescribed dose) expressed as a percentage of the prescribed dose for dose calculations in the head region.

**Influence of b-value combination in quantitative diffusion weighted MRI of rectal cancer**

Johanna A. Hundvin[1,2], Marius Bornstein[3], Anne Negård[4,5], Stein H. Holmedal[4], Sebastian Meltzer[3], Anne H. Ree[3,5], Sara Pilskog[1,2], Kathrine R. Redalen[6]
johanna.austrheim.hundvin@helse-bergen.no

[1]*Cancer Clinic, Haukeland University Hospital, Bergen, Norway;*
[2]*Institute of Physics and Technology, University of Bergen, Bergen, Norway;*
[3]*Department of Oncology, Akershus University Hospital, Lørenskog, Norway;*
[4]*Department of Radiology, Akershus University Hospital, Lørenskog, Norway;*
[5]*Institute of Clinical Medicine, University of Oslo, Oslo, Norway*
[6]*Department of Physics, Norwegian University of Science and Technology*

**Introduction:** Diffusion weighted MRI (DWI) is routinely performed in the clinic to qualitatively aid investigation of rectal cancer and local lymph nodes. Quantitative analysis can be assessed using the apparent diffusion coefficient (ADC), commonly calculated by a mono-exponential model from DWI acquisitions with at least two degrees of diffusion-weighting set by *b*-values. Still, quantitative utilisation is not yet clinically established due to considerable variation in reported ADC values. Recognising the lack of consensus on optimal *b*-value selection for ADC calculation in rectal cancer, the aim of this study was to examine how different b-value combinations affect the resulting ADC.

**Materials and methods:** DWI with seven *b*-values (b = 0, 25, 50, 100, 500, 1000 and 1300 s/mm$^2$) was acquired from 25 rectal cancer patients enrolled in the prospective biomarker study OxyTarget (NCT01816607) on a 1.5T Philips Achieva MRI scanner. Whole-tumour regions-of-interests were contoured by two radiologists and ADCs were calculated from 16 different b-value combinations using the mono-exponential model. For reference, the ADC was also calculated using the bi-exponential model including all *b*-values.

**Results:** Significant variability in tumour ADCs was detected for the different *b*-value combinations. When excluding low b-values (b ≤ 100 s/mm$^2$) the ADCs were significantly reduced (Figure). The *b* = 0 s/mm$^2$ is commonly included in ADC calculation; this study shows its inclusion results in a substantial overestimation. The combination of b = 500, 1000 and 1300 s/mm$^2$ in the mono-exponential model resulted in a deviation of only 0.5% compared to the bi-exponential reference.

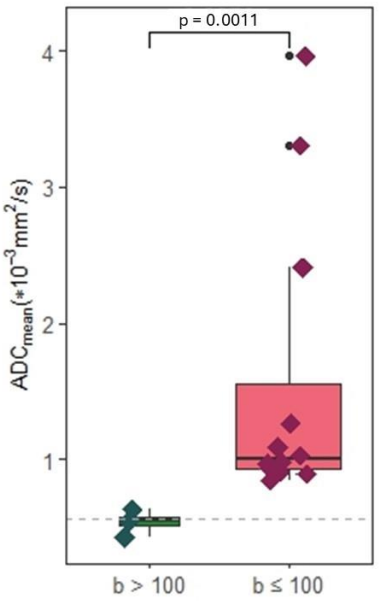


*Figure: Mean tumour ADC values calculated using the mono-exponential model, grouping by the inclusion of b-values above (left, four combinations) or below (right, twelve combinations) 100 s/mm$^2$. The dotted line shows the reference mean calculated by the bi-exponential model.*

**Conclusions:** In rectal cancer, tumour ADC calculated using the mono-exponential model is strongly influenced by the choice of *b*-values. By eliminating the contribution from perfusion (b ≤ 100 s/mm$^2$) the uncertainty in the calculations is significantly reduced. Quantitative inter- and intratumour comparisons should not be performed if ADCs are calculated using DWI with different *b*-value combinations.